# HIGHWAY RESEARCH RECORD

**Number 189**

# Design, Performance and Surface Properties of Pavement

9 Reports

Subject Area

25 Pavement Design
26 Pavement Performance



HIGHWAY RESEARCH BOARD
DIVISION OF ENGINEERING NATIONAL RESEARCH COUNCIL
NATIONAL ACADEMY OF SCIENCES—NATIONAL ACADEMY OF ENGINEERING

Washington, D.C., 1967

Publication 1520

Price: $5.00

Available from

Highway Research Board
National Academy of Sciences
2101 Constitution Avenue
Washington, D.C. 20418

# *Department of Design*

W. B. Drake, Chairman
Assistant State Highway Engineer for Planning, Research and Materials
Kentucky Department of Highways, Lexington

HIGHWAY RESEARCH BOARD STAFF

L. F. Spaine, Engineer of Design

PAVEMENT DIVISION

Milton E. Harr, Chairman
Professor of Soil Mechanics, School of Civil Engineering
Purdue University, Lafayette, Indiana

COMMITTEE ON RIGID PAVEMENT DESIGN
(As of December 31, 1966)

F. H. Scrivner, Chairman
Pavement Research Engineer
Texas Transportation Institute
Texas A & M University, College Station

W. Ronald Hudson, Secretary
Research Engineer and
Assistant Professor of Civil Engineering
Department of Civil Engineering
The University of Texas, Austin

Henry Aaron, Chief Engineer, Reinforced Concrete Pavement Division, Wire Reinforcement Institute, Washington, D. C.
Phillip P. Brown, Consultant, Soils, Mechanics and Paving, Bureau of Yards and Docks, Department of the Navy, Washington, D. C.
Harry D. Cashell, Deputy Chief, Structural Research Division, U. S. Bureau of Public Roads, Washington, D. C.
B. E. Colley, Manager, Paving Development Section, Portland Cement Association, Skokie, Illinois
E. A. Finney, Director, Research Laboratory Division, Michigan Department of State Highways, Lansing
Phil Fordyce, Supervising Engineer, Pavement Engineering, Portland Cement Association, Chicago, Illinois
W. S. Housel, University of Michigan, Ann Arbor
F. N. Hveem, Consultant, Sacramento, California
W. H. Jacobs, Executive Secretary, Rail Steel Bar Association, Chicago, Illinois
C. D. Jensen, Director of Research and Testing, Pennsylvania Department of Highways, Harrisburg
Wallace J. Liddle, Engineer of Materials and Research, Utah State Department of Highways, Salt Lake City
Phillip L. Melville, Civil Engineering Branch, Engineering Division, Military Construction, Office, Chief of Engineers, Department of the Army, Washington, D. C.
Ernest T. Perkins, Executive Director, East Hudson Parkway Authority, Pleasantville, N. Y.
Thomas B. Pringle, Chief, Civil Engineering Branch, Engineering Division Military Construction, Office of Chief of Engineers, Department of the Army, Washington, D. C.
M. D. Shelby, Research Engineer, Texas Transportation Institute, Texas A & M University, College Station
W. T. Spencer, Assistant Chief, Division of Materials and Tests, Indiana State Highway Commission, Indianapolis

Otto A. Strassenmeyer, Associate Highway Engineer—Research and Development, Connecticut State Highway Department, Wethersfield
William Van Breemen, Consultant, Trenton, N. J.
K. B. Woods, Goss Professor of Engineering, School of Civil Engineering, Purdue University, Lafayette, Indiana

## COMMITTEE ON FLEXIBLE PAVEMENT DESIGN

(As of December 31, 1966)

Stuart Williams, Chairman
Highway Research Engineer
U.S. Bureau of Public Roads
Washington, D.C.

A. C. Benkelman, Altamonte Springs, Florida
John A. Bishop, Director, Soils and Pavement Division, U.S. Naval Civil Engineering Laboratory, Port Hueneme, California
Thomas L. Bransford, Professor of Civil Engineering, Auburn University, Auburn, Alabama
W. H. Campen, Consultant, Omaha Testing Laboratories, Omaha, Nebraska
Bonner S. Coffman, Associate Professor of Civil Engineering, Ohio State University, Columbus
Robert A. Crawford, Assistant Research Engineer, South Dakota Department of Highways, Pierre
George H. Dent, Benjamin E. Beavin Company, Baltimore, Maryland
James M. Desmond, State Materials Engineer, Wyoming State Highway Commission, Cheyenne
Charles R. Foster, Coordinator of Research, National Asphalt Pavement Association, Texas A&M University, College Station
J. E. Gray, Engineering Director, National Crushed Stone Association, Washington, D.C.
John M. Griffith, Director of Research and Development, The Asphalt Institute, University of Maryland, College Park
Frank B. Hennion, Assistant Chief, Civil Engineering Branch, Engineering Division, Military Construction, Office, Chief of Engineers, Department of the Army, Washington, D.C.
Raymond C. Herner, Consulting Engineer, Indianapolis, Indiana
W. S. Housel, University of Michigan, Ann Arbor
Charles W. Johnson, Engineer of Construction, New Mexico State Highway Department, Santa Fe
Wallace J. Liddle, Engineer of Materials and Research, Utah State Department, Highways, Salt Lake City
R. E. Livingston, Consultant, Denver, Colorado
Alfred W. Maner, Staff Engineer, The Asphalt Institute, University of Maryland, College Park
Chester McDowell, Supervising Soils Engineer, Texas Highway Department, Austin
C. E. Minor, Assistant Director for Planning Research and Materials, Washington State Department of Highways, Olympia
Carl L. Monismith, University of California, Berkeley
A. O. Neiser, Assistant State Highway Engineer, Kentucky Department of Highways, Frankfort
Frank P. Nichols, Jr., Associate Engineering Director, National Crushed Stone Association, Washington, D.C.
R. L. Peyton, Assistant State Highway Engineer, State Highway Commission of Kansas, Topeka
E. G. Robbins, Portland Cement Association, Chicago, Illinois

George B. Sherman, Supervising Highway Engineer, California Division of Highways, Sacramento
Rollin J. Smith, Shawnee Mission, Kansas
Fred Sternberg, Senior Highway Engineer—Research, Connecticut State Highway Department, Hartford
John H. Swanberg, Chief Engineer, Minnesota Department of Highways, St. Paul
B. A. Vallerga, Director of Engineering, Materials Research & Development, Woodward-Clyde-Sherard & Associates, Oakland, California

## COMMITTEE ON SURFACE PROPERTIES—VEHICLE INTERACTION

(As of December 31, 1966)

David C. Mahone, Chairman
Highway Research Engineer
Virginia Council of Highway Investigation and Research, Charlottesville

M. D. Armstrong, Director of Research, Ontario Department of Highways, Toronto, Ontario, Canada
Joseph E. Bell, Division of Materials, Development and Research, D. C. Department of Highways and Traffic, Washington, D. C.
A. D. Brickman, Department of Mechanical Engineering, Pennsylvania State University, University Park
W. F. R. Briscoe, Manager, Tire Reliability, Product Development, United States Rubber Company, Detroit, Michigan
John E. Burke, Engineer of Research and Development, Illinois Division of Highways, Springfield
William C. Burnett, Associate Civil Engineer, Bureau of Physical Research, New York State Department of Public Works, Albany
A. Y. Casanova III, Highway Research Engineer, Structures and Applied Mechanics Division, U. S. Bureau of Public Roads, Washington, D. C.
John H. Cox, Manager, Fleet and Commercial Testing, Firestone Tire and Rubber Company, Akron, Ohio
Louis F. DiNicola, III, Division of Research, New Jersey State Highway Department, Trenton
Blaine R. Englund, Assistant Plant Engineer, General Motors Proving Ground, Milford, Michigan
E. A. Finney, Director, Research Laboratory Division, Michigan Department of State Highways, Lansing
William Gartner Jr., Materials, Research and Training Engineer, Florida State Road Department, Gainesville
B. G. Hutchinson, Department of Civil Engineering, University of Waterloo, Waterloo, Ontario, Canada
Robert N. Janeway, President, Janeway Engineering Company, Detroit, Michigan
Upshur T. Joyner, Landing and Impact Branch, Dynamic Loads Division, National Aeronautics and Space Administration, Langley Research Center, Hampton, Virginia
H. W. Kummer, Research Assistant, Department of Mechanical Engineering, Pennsylvania State University, University Park
Samuel I. Lipka, Singapore, Malaysia
B. Franklin McCullough, Supervising Design Research Engineer, Texas Highway Department, Austin
Robert B. McGough, Consultant, Department of the Air Force, Headquarters United States Air Force, Washington, D. C.
W. E. Meyer, Professor of Mechanical Engineering, Department of Mechanical Engineering, Pennsylvania State University, University Park
Desmond F. Moore, Dublin, Eire

Ralph A. Moyer, Research Engineer and Professor Emeritus, Institute of Transportation and Traffic Engineering, University of California, Richmond
F. William Petring, Principal Engineer, Vehicle Systems, Automotive Safety Research Engineering Staff, Ford Motor Company, Dearborn, Michigan
Rolands L. Rizenbergs, Research Engineer, Kentucky Department of Highways, Lexington
Richard K. Shaffer, Research Coordinator, Pennsylvania Department of Highways, Harrisburg
W. E. Teske, Paving Engineer, Portland Cement Asociation, Chicago, Illinois
E. A. Whitehurst, Director, Tennessee Highway Research Program, University of Tennessee, Knoxville
Ross G. Wilcox, Executive Secretary, Safe Winter Driving League, Chicago, Illinois
Dillard D. Woodson, The Asphalt Institute, University of Maryland, College Park

## COMMITTEE ON PAVEMENT CONDITION EVALUATION

(As of December 31, 1966)

Malcolm D. Graham, Chairman
Director, Bureau of Physical Research
New York State Department of Public Works, Albany

Robert F. Baker, Director, Office of Research & Development, U. S. Bureau of Public Roads, Washington, D. C.
Frederick E. Behn, Assistant Engineer of Specifications and Development, Ohio Department of Highways, Columbus
A. Y. Casanova, III, Highway Research Engineer, Structures and Applied Mechanics Division, U. S. Bureau of Public Roads, Washington, D. C.
W. B. Drake, Assistant State Highway Engineer for Planning, Research and Materials, Kentucky Department of Highways, Lexington
Karl H. Dunn, Materials Research Engineer, State Highway Commission of Wisconsin, Madison
Leroy D. Graves, Associate Professor of Civil Engineering, Notre Dame University, Notre Dame, Indiana
W. S. Housel, University of Michigan, Ann Arbor
W. Ronald Hudson, Research Engineer and Assistant Professor of Civil Engineering, Department of Civil Engineering, The University of Texas, Austin
Louis C. Lundstrom, Director of Automotive Safety Engineering, General Motors Technical Center, General Motors Corporation, Warren, Michigan
Alfred W. Maner, Staff Engineer, The Asphalt Institute, University of Maryland, College Park
Phillip L. Melville, Civil Engineering Branch, Engineering Division, Military Construction, Office, Chief of Engineers, Department of the Army, Washington, D. C.
A. B. Moe, Manager, Maintenance Branch, Bureau of Yards and Docks, U. S. Navy, Washington, D. C.
Frank P. Nichols Jr., Associate Engineering Director, National Crushed Stone Association, Washington, D. C.
Bayard E. Quinn, Mechanical Engineering School, Purdue University, Lafayette, Indiana
Foster A. Smiley, Maintenance Engineer, Iowa State Highway Commission, Ames
Elson B. Spangler, General Motors Corporation, Warren, Michigan
Bertram D. Tallamy, Consulting Engineer, Washington, D. C.
W. E. Teske, Paving Engineer, Portland Cement Association, Chicago, Illinois
Frank Y. Wilkinson, Federal Aviation Agency, Atlanta, Georgia
Eldon J. Yoder, Joint Highway Research Project, Purdue University, Lafayette, Indiana

# Foreword

The nine papers in this RECORD cover a variety of subjects dealing with the design, performance and surface properties of pavements. The first paper presents the results of a Portland Cement Association laboratory investigation of the ability of interlocking aggregate to transfer load across concrete pavement joints. The repetitive action of tandem truck wheels across a joint was simulated, and the validity of the simulation was confirmed by field tests. Effectiveness of load transfer across joints was found to be dependent on load intensity and duration, slab thickness, joint width, subgrade bearing value and aggregate angularity. The second paper by the same laboratory reports on an investigation to determine the contribution of cement-treated subbases to the load-carrying capacity of concrete pavement. Laboratory results are compared with the theoretical behavior of concrete slabs on clay subgrades. The study included the investigation of the value of bond between the concrete and the cement-treated subbase and the adaptability of current design methods to this type of construction.

The introduction of the equivalent wheel load concept of the AASHO Road Test has prompted the Texas Highway Department to explore methods of obtaining the magnitude and number of repetitions of all axle loads on highway pavement. The third paper reports on a study of three procedures for estimating an axle weight distribution for any given highway location in the state.

The California Division of Highways has been engaged in a research project with the objectives of measuring and allowing for resilient behavior of soils in a flexible pavement system. The fourth paper reports on the development of a laboratory testing device to measure resilience properties of roadway materials and on the results of qualitative tests on the main types of soils encountered in roadway construction. A comparison of field deflections with laboratory resilience tests indicates that a proposed resilience design procedure is generally consistent and effective in isolating potential resilience problems.

The fifth paper reports on the development by West Virginia University of a high-capacity rolling load testing machine and on the results of tests performed with it. The purpose of the machine is to provide an economical and accelerated program for the evaluation of highway base-course materials.

A study has been conducted by the Kentucky Department of Highways to evaluate the theoretical and practical aspects of using an automobile as a testing device for the measurement of pavement slipperiness. Twenty-five skid resistance values are compared and correlated. The measurement of time in the velocity increment between 30 mph and 20 mph has been selected as an interim standard test.

The next two papers concern the subject of measurement of pavement roughness profiles. One paper describes the basic mechanical and electrical features of the automobile-installed Portland Cement Association Road Meter. The physical limitations of the instrument are defined and results of correlation tests with the CHLOE Profilometer are presented. The second study by the University of Texas Center for Highway Research seeks to evaluate the feasibility of utilizing recent developments in the field of electronics and directional control instrumentation in the development of high-speed road profile measuring equipment. The author discusses profile measurement parameters, the techniques for evaluating these parameters, the need for high-speed measurement and the equipment and techniques available for the measurement.

The final paper reports on the problems encountered in using elevation power spectra, calculated from highway elevation measurements, as a criterion of pavement condition. The author points out the need for a standardized procedure for obtaining elevation measurements and for making power spectra calculations if pavement condition criteria comparable to BPR roughometer ratings are to obtained.

# Contents

AGGREGATE INTERLOCK AT JOINTS IN CONCRETE PAVEMENTS

B. E. Colley and H. A. Humphrey . . . . . 1

CEMENT-TREATED SUBBASES FOR CONCRETE PAVEMENTS

L. D. Childs . . . . . 19

ESTIMATING THE DISTRIBUTION OF AXLE WEIGHTS FOR SELECTED PARAMETERS

Kenneth W. Heathington and Paul R. Tutt . . . . . 44

A RESILIENCE DESIGN PROCEDURE FOR FLEXIBLE PAVEMENTS

Ernest Zube and Raymond Forsyth . . . . . 79

Discussion: W. H. Campen; Ernest Zube and Raymond Forsyth . . . . . 102

LABORATORY TESTS WITH A HEAVY-DUTY ROLLING LOAD MACHINE

R. R. Haynes and D. T. Worrell . . . . . 105

SKID TESTING WITH AN AUTOMOBILE

Rolands L. Rizenbergs and Hugh A. Ward . . . . . 115

DEVELOPMENT OF THE PCA ROAD METER: A RAPID METHOD FOR MEASURING SLOPE VARIANCE

M. P. Brokaw . . . . . 137

HIGH-SPEED ROAD PROFILE EQUIPMENT EVALUATION

W. Ronald Hudson . . . . . 150

Discussion: Paul Milliman . . . . . 164

PROBLEMS ENCOUNTERED IN USING ELEVATION POWER SPECTRA AS CRITERIA OF PAVEMENT CONDITION

B. E. Quinn and K. Hagen . . . . . 166

# Aggregate Interlock at Joints in Concrete Pavements

B. E. COLLEY and H. A. HUMPHREY
Respectively, Manager, and former Senior Development Engineer, Paving Development Section, Research and Development Laboratories, Portland Cement Association

Load transfer across joints in concrete pavements through shear developed by interlocking aggregate was investigated in the laboratory by simulating the repetitive motion of tandem truck wheels across a joint.

Effectiveness of load transfer was found to depend on load magnitude, number of repetitions, slab thickness, joint opening, subgrade bearing value, and aggregate angularity. A summary statistic called "endurance index" is used to relate the significant variables to test performance.

•TRANSVERSE contraction joints are constructed in concrete pavements to relieve tensile stresses, and when properly spaced they control the location of transverse cracks. Proper spacing is determined principally by three factors: (a) the presence or absence of steel, (b) the environment, and (c) the properties of the aggregates.

Contraction joints are most frequently constructed by sawing or forming a narrow groove in the pavement to the depth required to produce a plane-of-weakness. For highway pavements the minimum depth of the groove is generally one-sixth the slab thickness; sawed joints should meet the additional requirement that the depth be not less than the diameter of the maximum size aggregate. At the plane-of-weakness, restrained contraction forces produce a crack below the groove.

Load transfer across the crack is developed either by the interlocking action of the aggregate particles at the faces of the joint (aggregate interlock) or by a combination of aggregate interlock and mechanical devices such as dowel bars. When load transfer is adequate, load stresses and deflections in the vicinity of a joint are low, and the riding quality of the pavement is maintained.

To analyze the factors that influence the load transfer characteristics of aggregate interlock joints, a research program was inaugurated in the laboratory with equipment that permitted control of significant variables. Laboratory results were compared with data from field tests on highway pavements.

The objective of the program was to evaluate the effectiveness and endurance of load transfer developed by aggregate interlock under loading conditions simulating in-service concrete pavements.

Five variables considered significant to the performance of joints were selected for study: (a) width of joint opening, (b) thickness of concrete slab, (c) magnitude of load, (d) foundation support, and (e) shape of aggregate. For this investigation, maximum size of aggregate was held constant. Future studies will consider this important aspect of joint design.

## FACILITIES AND INSTRUMENTATION

### Facilities for Laboratory Study

A testing device was developed to apply repetitive loads of known magnitude in a manner closely simulating the action on a pavement as a vehicle passes over the joint.

Paper sponsored by Committee on Rigid Pavement Design and presented at the 46th Annual Meeting.

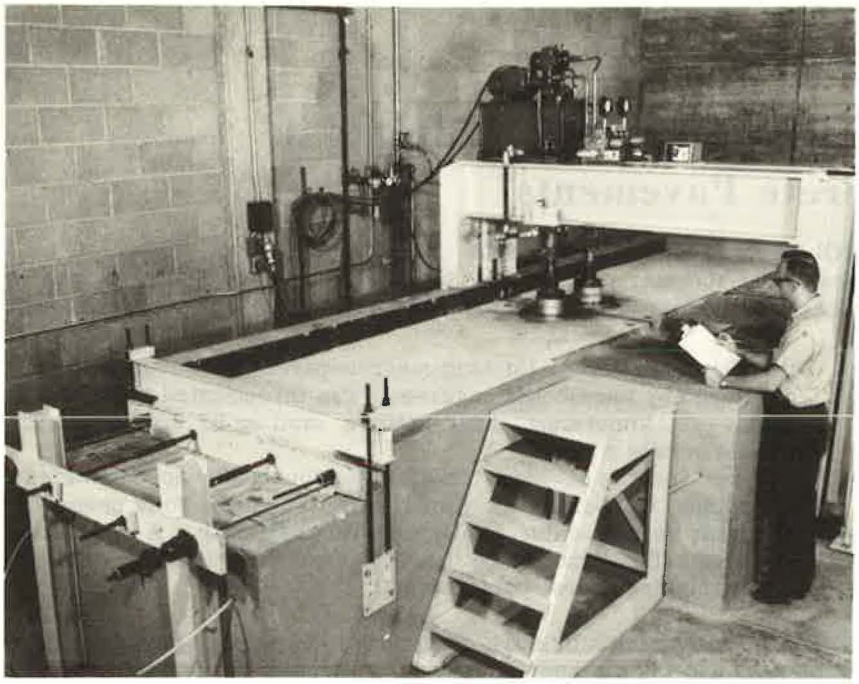

Figure 1. Load transfer test equipment.

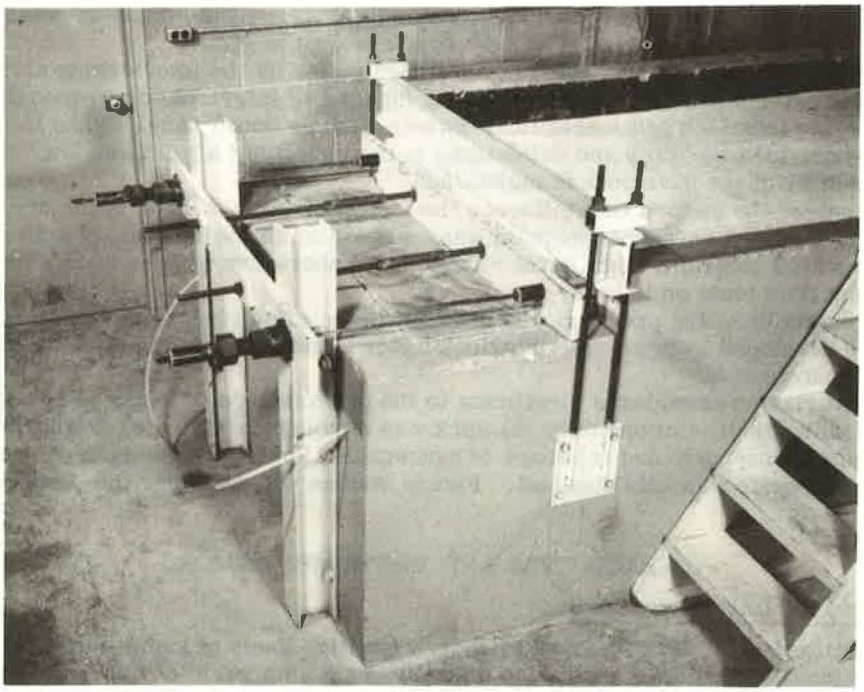

Figure 2. Joint-width control system.

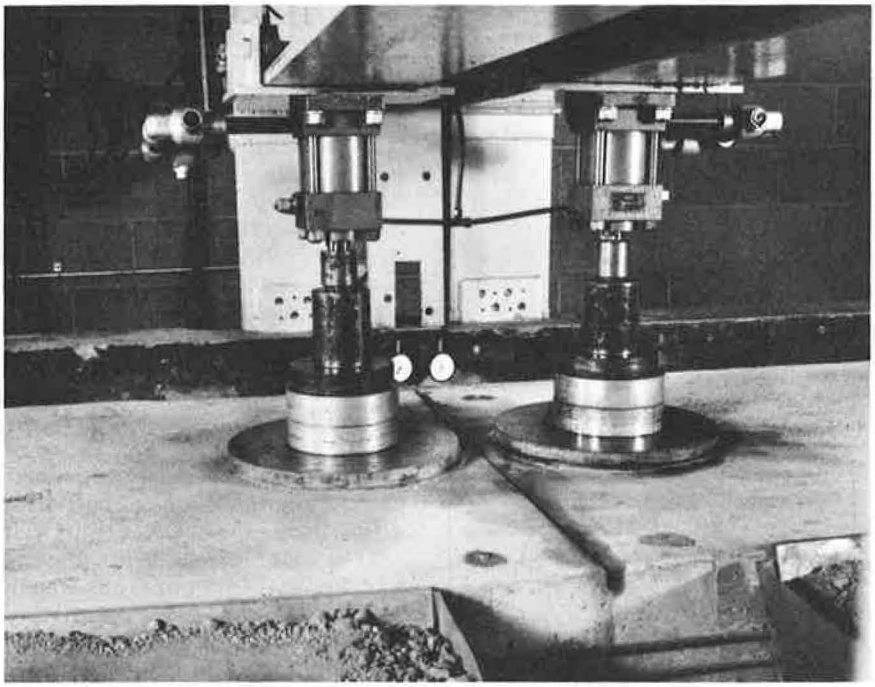

Figure 3. Load application equipment.

Two devices were constructed. They are housed in an air-conditioned area where the temperature is maintained at 72 F throughout a test to permit the joint width to be held constant while the effects of other variables are studied.

The device shown in Figure 1 consists of three basic components: (a) a base box which contains the subgrade, subbase, and concrete slab and also acts as support for the load application equipment; (b) a joint width control system; and (c) the repetitive loading apparatus and reaction frames.

Base Box—The base box of reinforced concrete is 4 ft high, 6 ft wide, and 22 ft long. The center section of the box is wider on one side to provide an area 3 ft wide and 8 ft long for future studies of the performance of shoulders. The walls and floor of the box are waterproofed to prevent excessive loss of moisture from the subgrade and subbase materials. Silty-clay soil was compacted in the box to a depth of $2\frac{1}{2}$ ft to serve as a subgrade upon which various combinations of type and thickness of subbase and pavement slabs are constructed and tested.

Joint Opening Control—The system for controlling joint opening permits adjustment of the width and maintenance of that width for the duration of the test. Equipment developed for this operation is shown in Figure 2. To open the joint, two steel rods anchored in the concrete are connected through threaded couplings to crossbars at the ends of the box. By tightening the couplings the slabs are pulled apart, thus opening the joint. To close the joint, two steel strands are employed along each side of the slab. One strand on each side is anchored to the left end of the slab and the right crossbar. The other strand is anchored in a similar manner to the right end of the slab and the left crossbar. By applying tension to the four strands the slabs are pulled together, thus reducing the opening. The combined use of these systems and control of the temperature maintained joint openings to within 0.001 in. of the desired value throughout a test.

The transverse beam shown on the end of the slab in Figure 2 prevents upward movement of the slab ends when the joint is loaded. With the slab restrained, the movement of a joint under test is similar to that of a transverse joint between full length slabs.

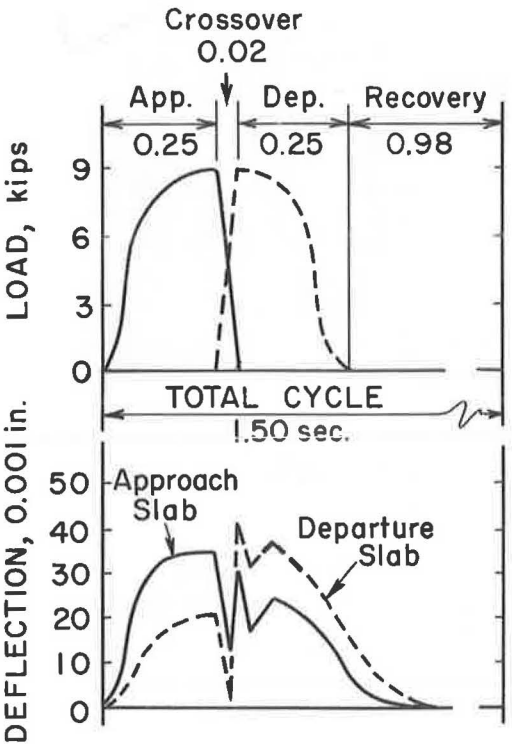


Figure 4. Loading cycle.

Repetitive Loading Apparatus—The hydraulic rams shown in Figure 3 react against a steel frame that is fastened to the base box. Loads are transmitted to the pavement by a pair of 16-in. diameter steel bearing plates resting on ¼-in. solid rubber pads. The plates are positioned on each side with their centers 9 in. from the joint and on the longitudinal centerline of the slab. Between each plate and the hydraulic jack are a series of spacer plates and a load cell.

The load application equipment is an electrically operated air-hydraulic system that alternately pulses the rams on either side of the joint to produce loads up to a maximum of 12,000 lb. Details of the controls for the sequence of loading and rate of load application have been described in a previous report (1).

The loading sequence closely simulates a continuous train of truck wheels traveling across the joint at approximately 30 mph. The magnitude of load, sequence and rate of loading may be varied to represent load patterns imposed by different types of traffic.

The rate of loading together with the corresponding joint deflection for a loading cycle are shown in Figure 4. To simulate a wheel approaching a joint, the load applied to the approach slab is increased from zero to full load in ¼ sec. The load on the approach slab is then released to zero and simultaneously the load on the departure slab increased from zero to full load in 0.02 sec. This interval would permit a tire making a 10-in. print and traveling 30 mph to move completely across the joint. To simulate a wheel moving away from the joint the load on the departure slab is reduced to zero in

Figure 5. Field test equipment.

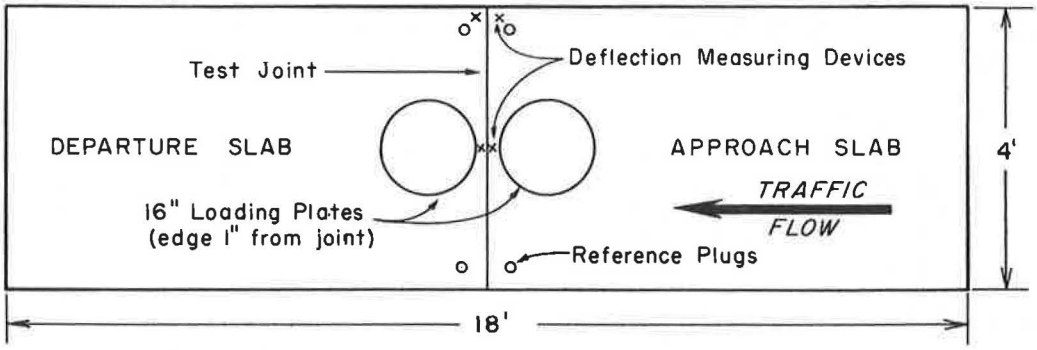


Figure 6. Plan of test slab and instrumentation.

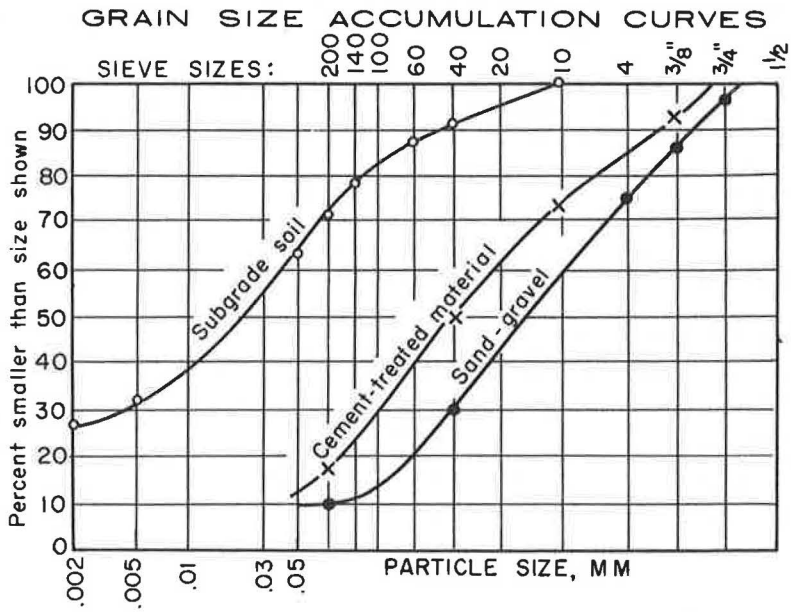


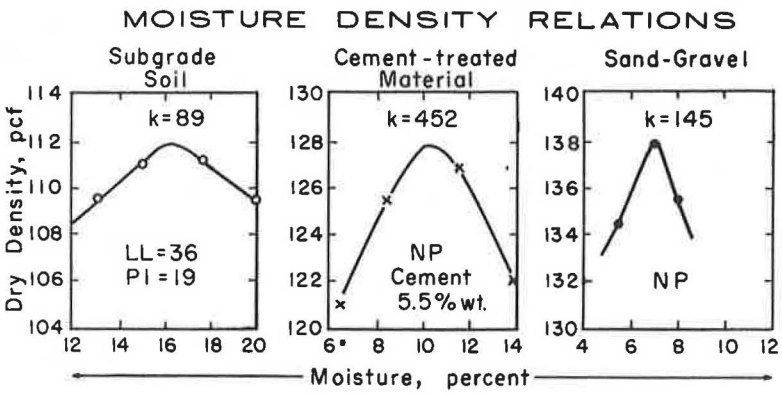


Figure 7. Foundation materials.

¼ sec. This action is followed by an interval of approximately 1 sec. when there is no load on either ram and the slabs return to a no-load position. A joint under test receives about 50, 000 of the 1. 5-sec loading cycles per day.

### Facilities for Field Tests

Tests on existing pavements were made with moving loads of known weight in assigned paths across selected joints. The control vehicle was a tractor-semitrailer with variable wheelbase. Auxiliary equipment included a utility vehicle and house-trailer type mobile laboratory (Fig. 5). A more complete description of the equipment and its potential is given by Nowlen (2).

### Instrumentation of Laboratory Slabs

Test slabs were instrumented for measurements of joint openings and deflections. In addition, devices were installed to measure the magnitude and rate of load repetitions. Automatic recordings of slab deflections and load magnitude were obtained at regular intervals. The instrumentation plan is shown in Figure 6.

Joint opening was measured using brass reference plugs and a Whittemore strain gage. Initial measurements were made before the slab was cracked to form the joint, so that reported joint openings are actual distances between the fractured faces of the concrete.

To evaluate load transfer, deflections on each side of the joint were measured with 0. 001-in. dial indicators for static loading, and with electronic deflectometers for dynamic loading. The dials and deflectometers were supported by brackets attached to the base box.

The magnitude of load applied to the slab was measured with load cells placed below each ram. These strain-sensed cells were connected electrically to a strain indicator for static measurements, and to an automatic recorder to measure the rate of load application and magnitude of repetitive load.

### Instrumentation of Field Pavements

Pavement joints were instrumented in a manner similar to the laboratory slabs to measure deflection as the vehicle approached, crossed, and departed from the joint. Pavement joint openings were measured in the manner described for laboratory slabs. On pavements that had been in service before testing, the first caliper measurement between joint plugs was not made at zero opening. Distances between joint faces at this initial reading were determined by an optical comparator.

## MATERIALS

### Foundation for Laboratory Slabs

Subgrade—To provide a subgrade for the specimen pavement slabs, a silty-clay soil was compacted in each base box to a depth of 2½ ft. Gradation and moisture-density relations of the subgrade soil are shown in Figure 7. The soil was compacted in 6-in. lifts to standard conditions, as determined by AASHO Method T99 or ASTM Method D 698. Each time a new subbase and slab was placed, the subgrade was reprocessed, thus assuring a uniformly low bearing value subgrade for each test. The average bearing value, k, measured with a 24-in. diameter plate at 0. 05-in. deflection, was 89 lb/sq in./in. (pci). The prepared subgrade was covered with a sheet of polyethylene to restrict loss of moisture.

Subbase—Two types of subbase were used, a sand-gravel and a cement-treated material. The gradations and moisture-density relations of these materials are shown in Figure 7.

The subbase materials were mixed in a pug mill. The nonplastic sand-gravel was placed at standard conditions as specified by AASHO Method T99 or ASTM Method D 698. The cement-treated material was mixed with 5. 5 percent cement by weight and 11 percent water. The cement requirement was determined using ASTM Procedures

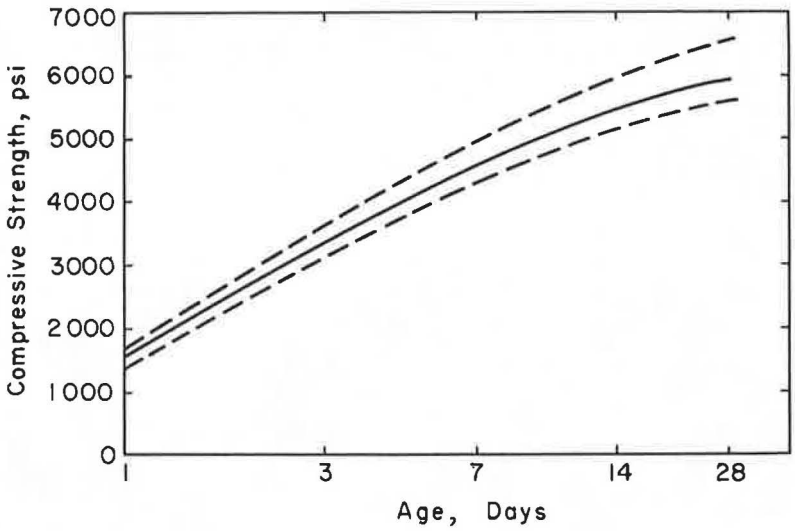


Figure 8. Concrete strength.

D559 and D560 and the Portland Cement Association criteria for weight loss (3). The moisture-density relationship was determined using ASTM Method D558.

The subbase materials were compacted to 100 percent of standard density using a mechanical tamper and a vibrating sled. All subbases had a compacted thickness of 6 in. and, to restrict moisture loss, were covered with a sheet of polyethylene. This also reduced friction on the foundation and aided in adjusting joint width.

The bearing value, k, was measured using a 24-in. diameter plate. The average bearing value of the sand-gravel subbase was 145 pci and that of the cement-treated subbase measured at age seven days was 452 pci.

## Laboratory Pavements

Concrete Slabs—The slabs were 46 in. wide and 18 ft long with a transverse joint at the midpoint. The maximum aggregate size in the concrete was 1½ in., the cement factor was 6 sk per cu yd, water-cement ratio 0.50, slump 2.5 to 3.5 in., and air content 4 to 5 percent. Prior to load testing, the concrete was cured for 14 days under polyethylene sheets. The 14-day compressive strength of the concrete averaged 5,500 psi. In Figure 8 the average age-strength relationship of the concrete is shown by the solid line and the dashed lines represent the range of extreme values.

Two aggregates were used in the concrete. One was a natural gravel with subrounded to rounded particles. It consisted of about 55 percent siliceous materials that

TABLE 1

PHYSICAL CHARACTERISTICS OF CONCRETE AGGREGATES

| Test | Natural Gravel | Crushed Stone |
|---|---|---|
| Absorption (24 hr), percent | 2.0 | 2.4 |
| Bulk, specific gravity (s. s. d.)[a] | 2.67 | 2.65 |
| Unit wt (dry rodded), lb/cu ft | 107 | 105 |
| Abrasion (L. A. method)[b], percent | 28 | 24 |

[a]Saturated, surface dry.
[b]ASTM designation C 131.

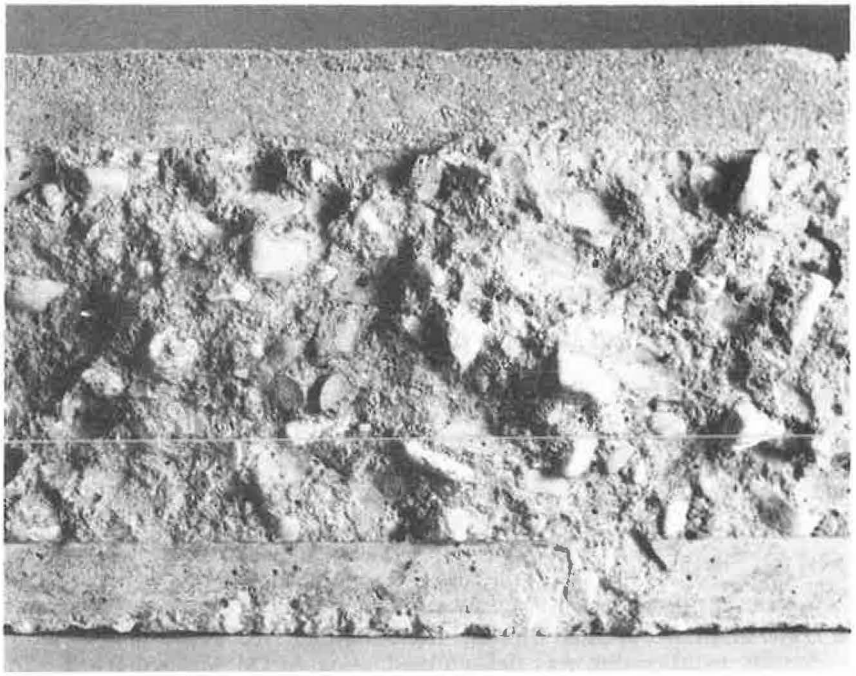

Figure 9. Joint interface.

include quartzite, feldspar, and a variety of igneous and metamorphic rock types. This material was crushed and recombined to the same gradation as the natural gravel for a study of the effect of particle shape.

The second aggregate was a crushed stone with angular particles that consisted of 65 percent dolomite and 35 percent siliceous materials. Both aggregates had the same gradation. Physical characteristics of the aggregates are given in Table 1.

Test Joints—Joints were of the plane-of-weakness type where load transfer is achieved solely by aggregate interlock. A removable parting strip of 20-gage galvanized metal of 1-in. height was supported transversely on the foundation at the joint location. While the concrete was plastic, a groove 1 in. in depth was formed in the surface of the slab directly over the metal strip. Thus a vertical joint was assured and angle of fractured face was not a variable. The slab was cracked in the weakened plane to its full depth with minimum disturbance to the foundation the day after casting by loading at the joint while applying tension to the slab ends. This method of making a joint produced a roughened interface depth of 5 in. for the 7-in. thick slabs, and 7 in. for the 9-in. thick slabs. The depth of fractured face was slightly less than that usually formed in highway pavements. The texture of a joint interface after completion of testing is shown in Figure 9.

## TEST PROCEDURES

### Program and Measurements for Laboratory Study

Specimens were prepared for testing by setting the selected joint opening, seating the rams on the loading plates, and programming the load application equipment to apply the desired repetitive load. Data obtained prior to the start of repetitive loading and at regular intervals throughout the test were: (a) joint opening; (b) deflections of both the loaded and unloaded slabs produced by a static load of 9 kips applied successively to the approach and departure slabs; and (c) deflections of the slabs produced by applying a dynamic loading cycle of the programmed magnitude.

TABLE 2

FIELD MEASUREMENTS OF JOINT OPENINGS

| Location | Joint Spacing (ft) | Maximum Opening (in.) |
|---|---|---|
| Michigan | 10 | 0.06 |
| Michigan | 20 | 0.08 |
| California | 15 | 0.03 |
| Oregon | 15 | 0.06 |
| Kentucky | 20 | 0.05 |
| Missouri | 25 | 0.07 |
| Minnesota | 15 | 0.07 |

Repetitive loading was initiated 15 days after the concrete slab was cast. About 50,000 loads were applied daily in a 22-hr period. During the remaining 2 hr, static load test data were obtained and routine maintenance was performed on the equipment. The program of repetitive loading and data recording was continued until deflection data showed no load transfer or until one million cycles had been applied.

A series of special tests was conducted on several of the joints after completion of routine testing. Load-deflection tests were made as the joints were progressively closed in increments of 0.005 in. with 1000 cycles of repetitive load applied at each joint opening. This was continued until no further reduction of joint opening could be obtained.

The tightly closed joint was then progressively opened in increments of 0.01 in. and the sequence of repetitive loading and load-deflection tests repeated at each joint opening. This was continued until effectiveness was reduced to zero or until the width of joint opening was 0.10 in.

The laboratory test procedure subjected a joint to loading conditions more severe than those encountered in the field. The action of the specimen slabs, though similar, did not duplicate the action of concrete pavements in service; deflections measured in the laboratory exceeded deflections measured at similar joints in the field. Principal reasons for the differences were: (a) the specimen slabs, being only 46 in. wide, did not have as large a resisting cross section; (b) the height of roughened interface was about 0.5 in. less for the 7-in. slabs and 0.25 in. less for the 9-in. slabs; (c) joint opening was held constant in the laboratory, whereas in the field there are cycles of opening and closing; (d) laboratory loads were applied at a rate of 40 applications per minute, so that the pavement and foundation had little time to recover between load applications; (e) the age of concrete was less than 60 days for these tests and strengths may have been slightly less than those for pavements of much greater ages; and (f) the subgrade k-value was deliberately low to represent a poor field subgrade condition. Because of these factors it is considered that the laboratory data were conservative.

## Evaluation of Load Transfer

Ability of a slab to carry load is normally evaluated by computing stresses from measured strains. Other suitable responses are subgrade pressure and slab deflection.

When a wheel load at a slab end is resisted in part by an adjacent slab there is asymmetric loading. The slab under the wheel is loaded by direct bearing, while the adjacent slab is loaded by shear in the load transfer mechanism. Therefore, corresponding areas of the two slabs do not experience similar stresses, and readings from symmetrically placed strain gages are not comparable.

Pressure comparisons are likewise unsatisfactory. In addition to the need for meter installation at the time of construction, valid readings can be made only during periods when the slab ends are flat on the subgrade to preclude any downward movement not sensed by the meter.

Ability to transfer load across the joint in this study was evaluated by comparing deflections of the two slabs. As these slabs were in identical environments, temperature and moisture affected each similarly and subgrade reaction modulus also was essentially

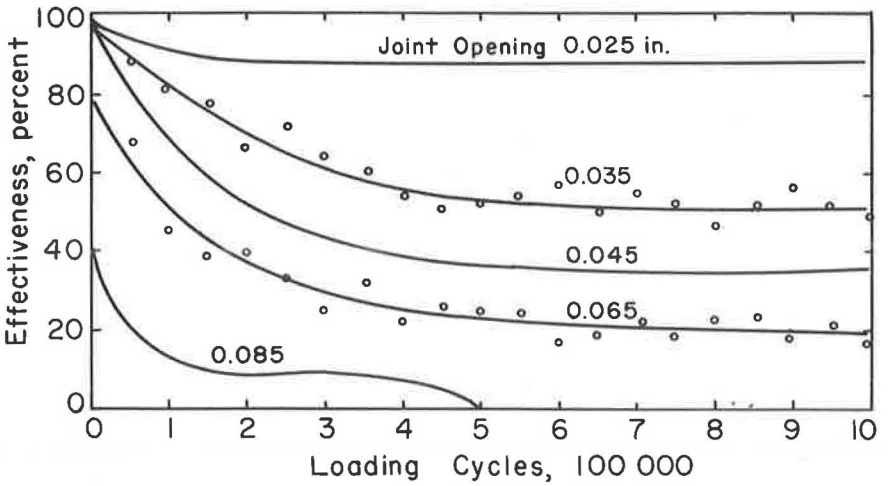


Figure 10. Influence of joint opening on effectiveness, 9-in. concrete slab, 6-in. gravel subbase.

the same. Lack of complete transfer or, in this study, looseness of interlock resulted in larger deflections of the slab under plate load than those of the adjacent slab.

Load transfer effectiveness was rated using a method devised by Teller and Sutherland (4). In this method, joint effectiveness, E, is computed using the formula

$$E\ (\%) = \frac{2d_j'}{d_j + d_j'}\ (100) \qquad (1)$$

where $d_j'$ is the deflection of the unloaded slab and $d_j$ is the deflection of the loaded slab. If load transfer at a joint were perfect, the deflections of the loaded and unloaded slabs would be equal and the effectiveness would be 100 percent. If, however, there were no load transfer at a joint, only the loaded slab would deflect and the effectiveness would be zero. All effectiveness values are computed from measured deflections obtained with a 9-kip static load applied to the approach slab.

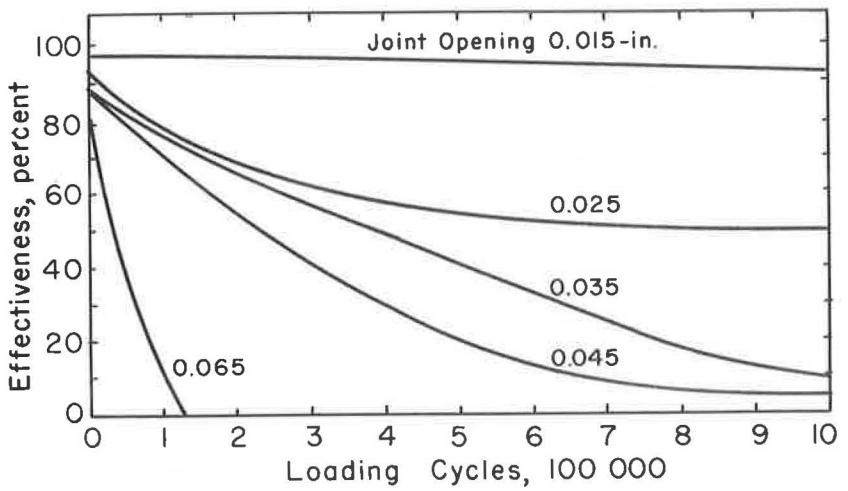


Figure 11. Influence of joint opening on effectiveness, 7-in. concrete slab, 6-in. gravel subbase.

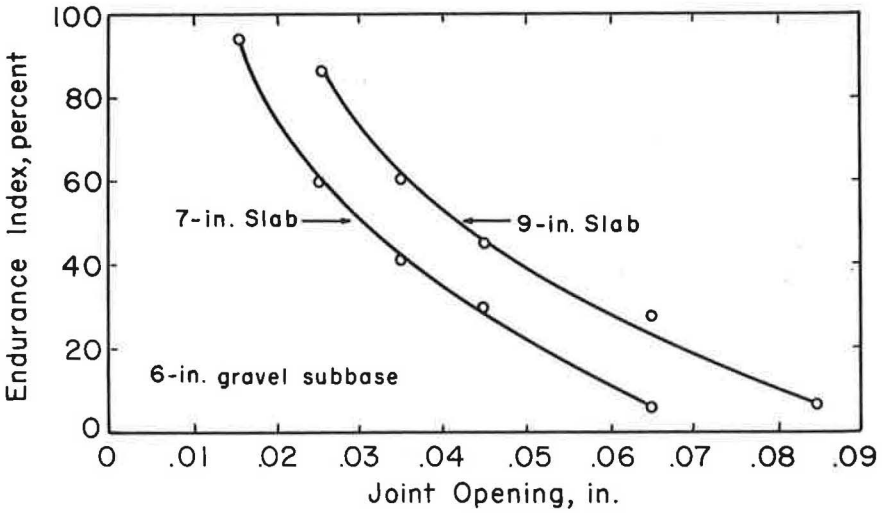


Figure 12. Influence of joint opening on endurance index.

Tests to determine effectiveness were made at intervals of 50, 000 load applications. Data are reported in plots of computed joint effectiveness against number of load cycles. A summary statistic of joint performance called the endurance index (EI) was developed. This index is expressed in percent and is obtained by dividing the area under the curve of effectiveness vs cycles by the area that would be developed if the joint retained an effectiveness of 100 percent throughout one million load applications.

## PRESENTATION AND DISCUSSION OF DATA

Data are presented on the effectiveness and endurance of aggregate interlock as a means of providing load transfer at a joint. Variables evaluated independently are joint opening, strength of foundation, load, and shape of aggregate. The effect of slab thickness on load transfer is included as a portion of the discussions under joint opening and strength of foundation.

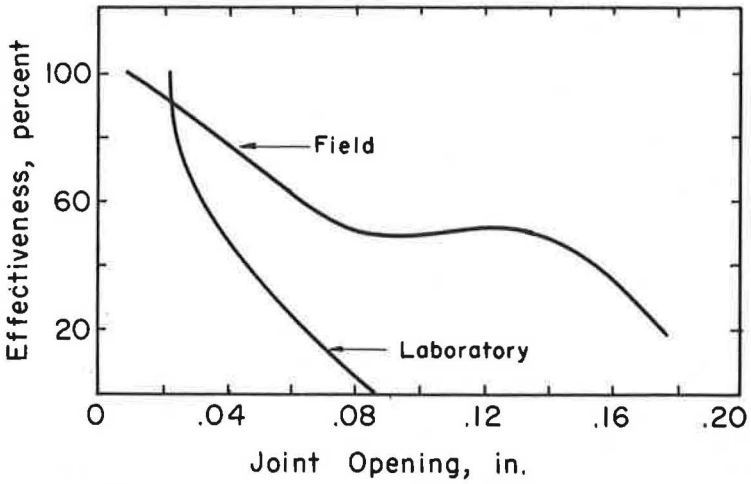


Figure 13. Comparison of field and laboratory data.

Influence of Joint Opening

When expansion joints are used only at structures or are widely spaced, the opening of a contraction joint depends primarily on spacing between joints and environment. Data in Table 2 are measurements on pavements in service of joint openings over a 10-year period (5) showing the relationship between maximum opening, spacing, and geographical location. Based on these data, joint openings selected for test in the laboratory ranged from 0.015 to 0.085 in.

A 9-kip repetitive load was used to evaluate the influence of joint opening on effectiveness. Curves for 9-in. slabs on 6-in. gravel subbases are shown in Figure 10. Data points are shown on the curves for joint openings of 0.035 and 0.065 in. There was only minor scatter in the data and for simplicity the points for remaining curves are omitted. It is seen that effectiveness decreased as the joint opening became wider. Effectiveness also decreased with additional load applications, although more than 90 percent of the decrease occurred during the first 500,000 repetitions. A similar trend is observed for the data in Figure 11 obtained for 7-in. slabs. In Figure 12, these data are summarized as a plot of endurance index vs joint opening. It is seen that the EI decreased as joint opening increased. The effect of slab thickness on effectiveness can be observed by comparing joint openings at equal EI values. For example, at an EI value of 60 percent the openings in the 7- and 9-in. slabs were 0.025 and 0.035 in., respectively, and at an EI of 5 percent the openings were 0.065 and 0.085 in., respectively. This tendency for the difference between openings to increase as the EI decreased was noted throughout the range of testing and demonstrates the advantage of a thicker slab at wider openings.

Deflection data obtained from tests on in-service pavements using the PCA mobile laboratory equipment were reduced in the same manner as those from laboratory studies. The field pavements were from 4 to 21 years old and were located in six states with climatic features varied from Wisconsin to Florida. The pavements were 9 in. thick with joint spacing ranging from 15 to 30 ft and were placed on granular subbases, with k-values ranging from 120 to 190 pci. A comparison of effectiveness ratings between laboratory and field is shown in Figure 13.

The laboratory effectiveness values were taken from Figure 10 at 500,000 load cycles. It should be noted that the plot would not vary significantly if the values selected had been for one million load cycles. Complete traffic records were not available for the field projects but it is reasonable to assume that the pavements had carried between 300,000 and two million applications of a 9,000-lb wheel load. The field data showing openings larger than 0.08 in. were obtained on pavements with 30-ft joint spacing located in an area having large variations in temperature.

The comparison shows that laboratory effectiveness values were considerably less than those obtained from field data. Previously it was indicated that the laboratory loading procedure was more severe than field loading. A portion of the difference in performance is due to daily and seasonal changes in joint openings. For example, a joint that is open 0.08 in. on a winter day may be open only 0.02 to 0.05 in. for a large portion of the year. In this case only a small percentage of the loads would be applied to the joint when the opening was maximum in contrast to the laboratory loading procedure where all loads were applied at the same opening. This aspect of joint design can be considered by applying proper weight factors to traffic and joint opening data for the geographical area under consideration.

The effect of joint opening and closing on the fit between worn aggregate particles in the fractured faces of the joint is also important to load transfer. This factor was investigated by special tests on several laboratory slabs after completion of routine loading. The data in Figure 14 were obtained from a 9-in. slab on a gravel subbase. The slab had received one million 9-kip load applications at a joint width of 0.065 in. At the end of routine testing, joint effectiveness was 19 percent. At this time the opening was closed in increments of 0.01 in. to the smallest width that could be obtained. To aid closing and create wear at the joint, one thousand load applications were applied after each increment of closure. At the smallest opening, effectiveness had increased to 100 percent.

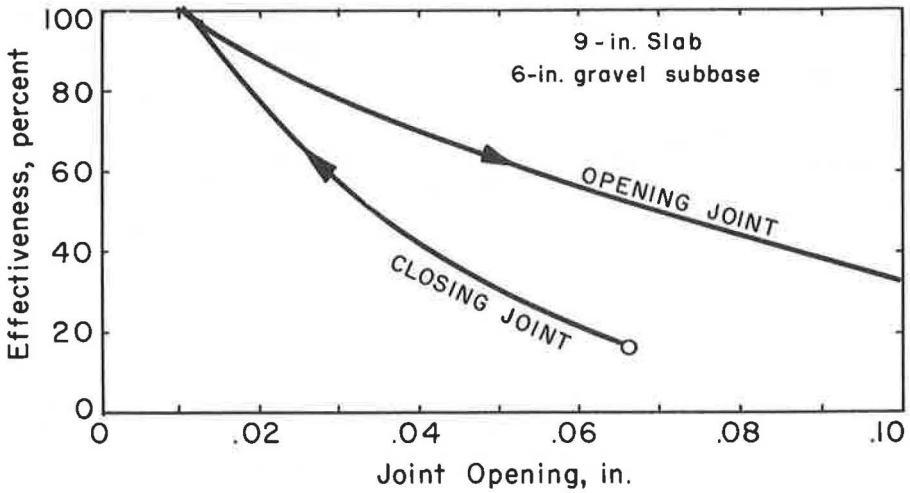


Figure 14. Effect of varying joint opening.

After reaching minimum closure, the same technique was followed as the joint was reopened in increments to a maximum width of 0.1 in. Although effectiveness decreased during reopening, the rate of decrease was low and at an opening of 0.065 in. effectiveness was 52 percent. This is in contrast to 19 percent at the end of routine testing. Furthermore, at an opening of 0.1 in. effectiveness was 32 percent.

## Influence of Foundation Support

Three materials were used to investigate the influence of foundation support on load transfer effectiveness and endurance. The materials were: (a) a clay subgrade with k = 89 pci; (b) a gravel subbase with k = 145 pci; and (c) a cement-treated subbase with k = 452 pci. All slabs were tested with a 9-kip repetitive load. Effectiveness data are shown in Figure 15 for 7- and 9-in. slabs with joint openings of 0.035 in. on clay subgrades. Effectiveness at the end of one million load cycles was 5 and 29 percent, respectively. As a basis of comparison, effectiveness values at this opening on the granular subbases,

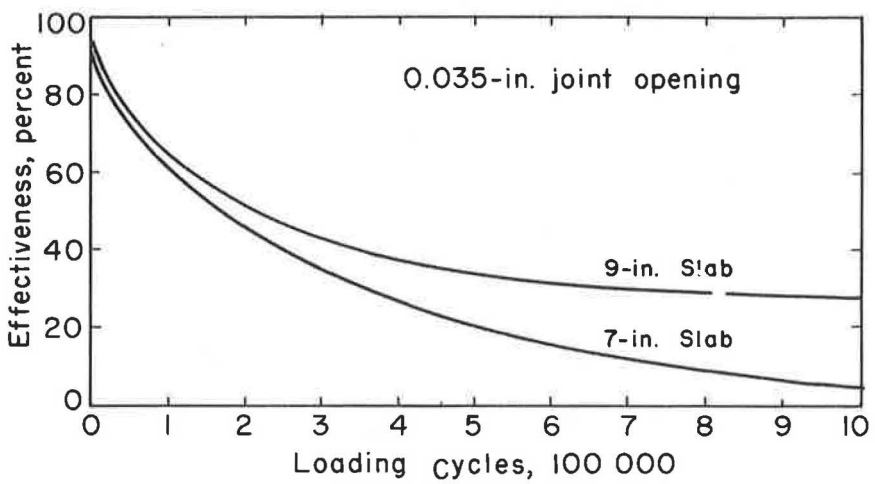


Figure 15. Effectiveness of joints in slabs on clay subgrade.

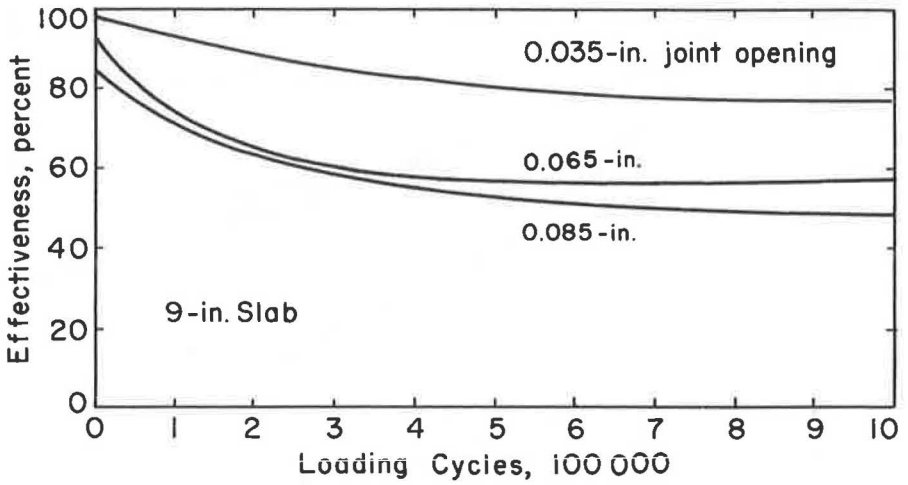


Figure 16. Effect of cement-treated subbase.

reported in Figures 10 and 11 for 7- and 9-in. slabs, were 9 and 50 percent. It is apparent that the added stiffness of the 9-in. slab contributed significantly to the aggregate interlock of the slab on a clay subgrade.

Joint effectiveness was further increased when slabs were placed on a 6-in. cement-treated subbase. This is demonstrated by test results shown in Figure 16. These data are for 9-in. slabs with joint openings of 0.035, 0.065, and 0.085. End values of effectiveness corresponding to these openings were 77, 57 and 50 percent. In contrast, effectiveness values on the granular subbase were 50 and 19 percent, respectively, for the 0.035- and 0.065-in. openings. Furthermore, effectiveness for the 0.085-in. joint opening tested on the gravel subbase was zero after only 500, 000 load cycles.

The test results are summarized in terms of the endurance index in Figure 17. All data are for joint openings of 0.035 in. It is seen that as the k-value of the foundation was increased from 90 to 450 pci, the endurance index was increased about 2.6 times for the 7-in. slabs and about 2 times for the 9-in. slabs.

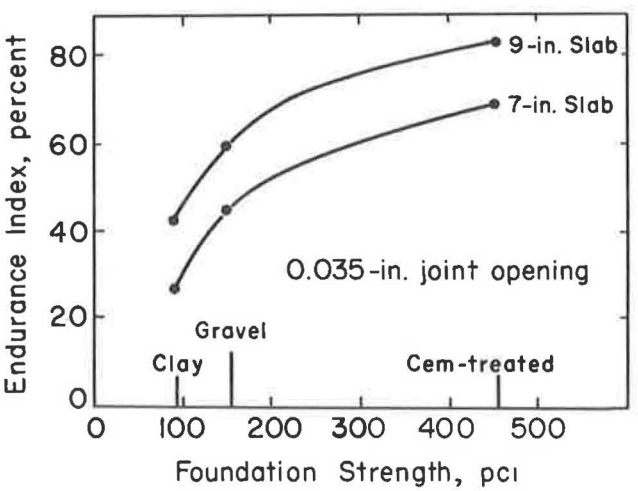


Figure 17. Effect of foundation strength on endurance index.

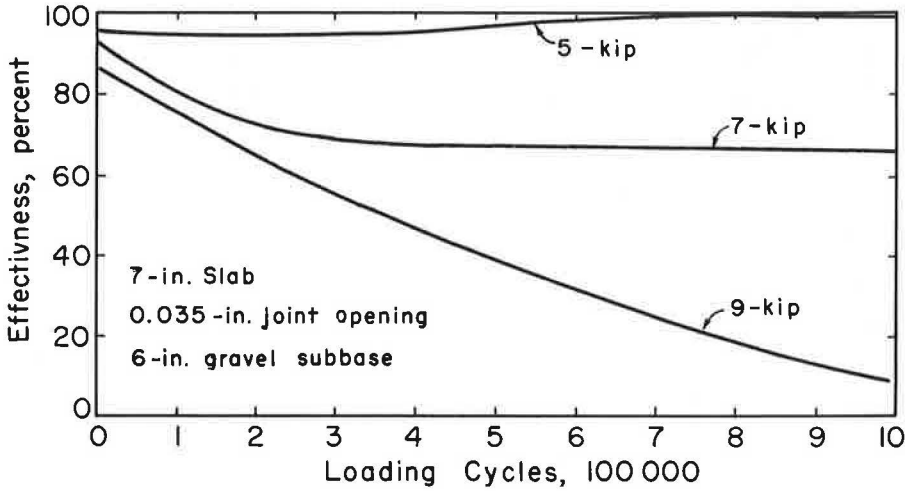


Figure 18. Influence of load on effectiveness.

## Influence of Load Magnitude

The influence of load on joint effectiveness is shown in Figure 18. The data are for 7-in. slabs on gravel subbases with joint openings of 0.035 in. Prior to repetitive loading the effectiveness of the three joints was about the same, ranging from 87 percent to 95 percent.

Significant differences in effectiveness developed under the action of repetitive loading and became more pronounced as the test continued. After 500,000 loading cycles, the effectiveness of the joints tested with the 5-, 7-, and 9-kip repetitive load was 96, 68, and 39 percent, respectively. After one million loading cycles the effectiveness values were 98, 65, and 9 percent. These data indicate that effectiveness decreased as the magnitude of load was increased. At the end of routine testing, one million additional load cycles were applied to the slab tested with the 5-kip load and there was no further change in effectiveness. This is significant as it suggests that light loads cause little or no wear and probably do not need to be considered.

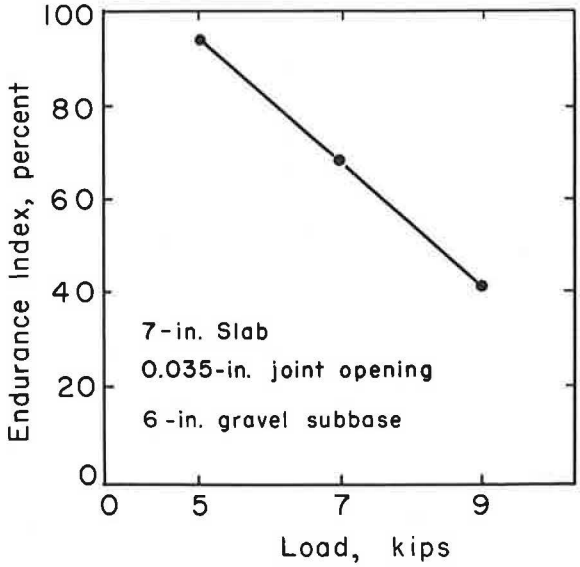


Figure 19. Effect of load on endurance index.

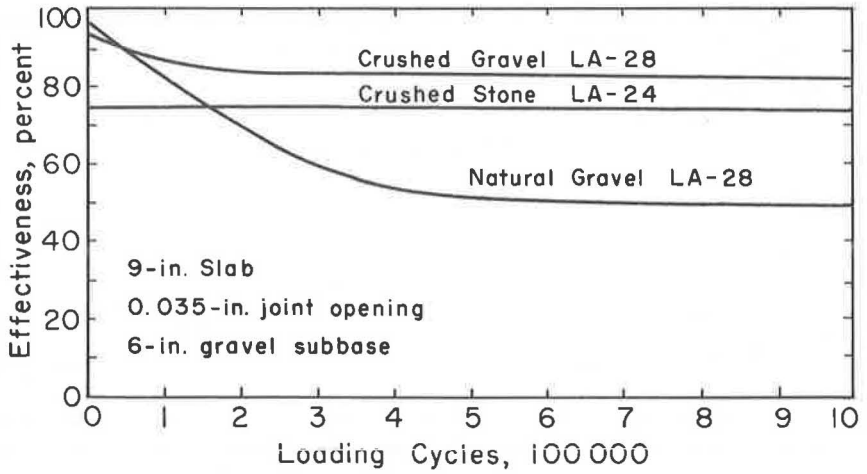


Figure 20. Influence of aggregate shape on joint effectiveness.

As shown in Figure 19, the effect of load on endurance index was linear. The endurance index decreased as the load was increased.

## Influence of Aggregate Shape

The influence of aggregate shape on effectiveness is shown in Figure 20. These curves were obtained from tests on 9-in. slabs with 0.035-in. joint opening placed on gravel subbases.

The data shown in the bottom curve were taken from Figure 10. The coarse aggregate used in this test slab was a rounded natural gravel with a Los Angeles abrasion value of 28. The data shown in the middle curve were obtained from a slab cast with crushed stone coarse aggregate that had a Los Angeles abrasion value of 24. The gradation of the crushed stone was the same as the gradation of the natural gravel. Comparing these data, it is seen that joint effectiveness values for the crushed stone were larger than values for the gravel. Although the two aggregates had slightly different

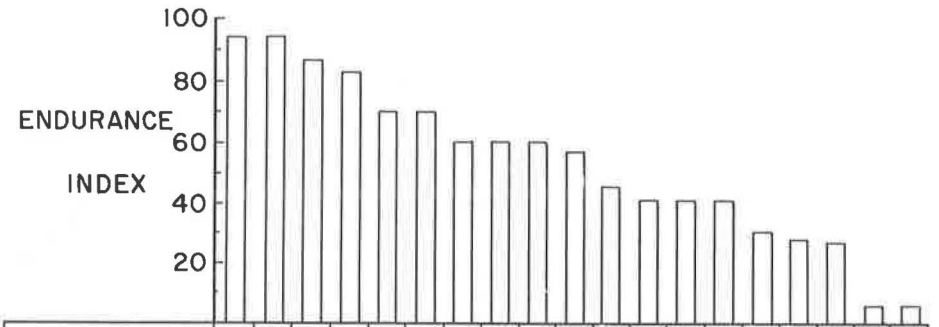


| Joint Opening | 15 | 35 | 25 | 35 | 35 | 35 | 35 | 65 | 25 | 85 | 45 | 35 | 35 | 65 | 45 | 65 | 35 | 65 | 85 |
|---|---|---|---|---|---|---|---|---|---|---|---|---|---|---|---|---|---|---|---|
| Slab Thickness | 7 | 7 | 9 | 9 | 7 | 7 | 9 | 9 | 7 | 9 | 9 | 9 | 7 | 7 | 7 | 9 | 7 | 7 | 9 |
| Foundation | G | G | G | CT | CT | G | G | CT | G | CT | G | C | G | CT | G | G | C | G | G |
| Repetitive Load | 9 | 5 | 9 | 9 | 9 | 7 | 9 | 9 | 9 | 9 | 9 | 9 | 9 | 9 | 9 | 9 | 9 | 9 | 9 |

Figure 21. Equivalence of performance.

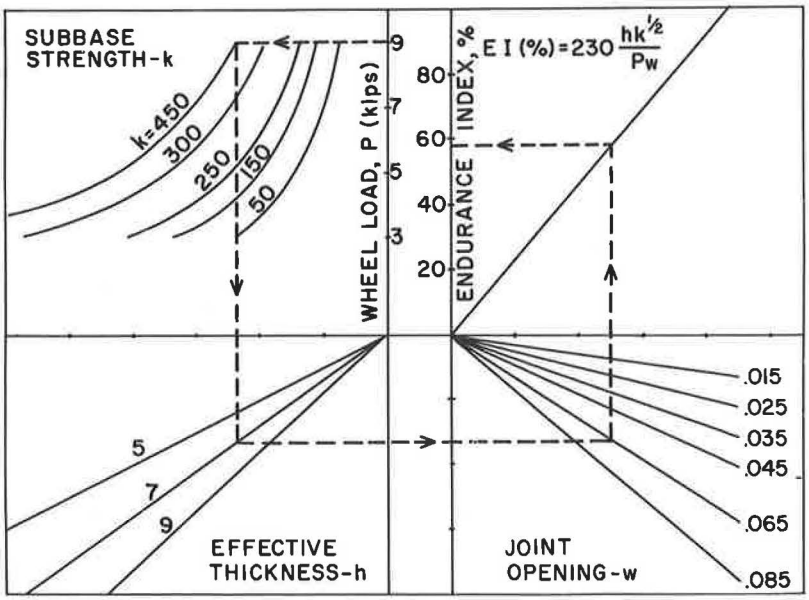


Figure 22. Endurance of joints.

properties, the higher effectiveness of the crushed stone was attributed to its angularity. To check this observation, effectiveness data were obtained for a third slab shown by the top curve. The coarse aggregate for this slab was the natural gravel after being crushed and recombined to its original gradation. In this case the only variable was the shape of the coarse aggregate and joint effectiveness was increased from 50 to 84 percent. Thus, for the same hardness, effectiveness was increased with increased angularity of the coarse aggregate.

## EQUIVALENCE OF PERFORMANCE

Data summarized in Figure 21 can be used to show equivalence of performance. It is seen that bars of equal height indicate slabs with equal endurance index values. The variables are joint opening, slab thickness, type of foundation, and magnitude of load. Under the heading of foundation, designations are G for gravel subbase, CT for cement-treated subbase, and C for clay subgrade.

Two designs were equivalent at an endurance index of 70. Each was a 7-in. slab with a joint opening of 0.035 in. However, one slab was supported on a cement-treated subbase and the other on a gravel subbase. It is seen that the additonal foundation strength provided by the cement-treated subbase increased the load capability of the joint by 2 kips.

Numerous other comparisons can be made; however, to summarize the test results, an equation was developed by regression analysis. This equation relates endurance index to the significant variables included in the test program. It includes only data obtained from the rounded natural gravel. The equation is

$$EI = 230 \frac{h}{Pw} \sqrt{k} \qquad (2)$$

where

h = depth of roughened interface, in.,
k = foundation modulus, pci,
P = wheel load, lb, and
w = joint opening, in.

Figure 22 is a nomograph developed from Eq. 2. A solution by the use of the nomograph is illustrated by following the arrows. Starting with a 9,000-lb wheel load and proceeding horizontally to a k of 450 pci, vertically to an effective thickness of 7 in., and horizontally to a joint opening of 0.065 in., it is seen that the endurance index is 58.

The equation has a standard error of estimate of 9.2 percent and a coefficient of correlation of 90 percent.

## SUMMARY

Load transfer across transverse joints in concrete pavements through shear in the aggregate interlock was investigated. Two laboratory devices applied repetitive loads alternatively on the two slabs separated by the test joint. Load interval and frequency were programmed to simulate the movement of tandem axles of highway vehicles. Validity of simulation was established by field tests with the PCA mobile laboratory.

The ability of a joint to transfer load was established by its effectiveness. The ability to retain this effectiveness under load repetitions was labeled the endurance index.

The following trends were observed:

1. When test load, slab thickness, and subbase were held constant, joint effectiveness decreased as the joint opening was increased.
2. When these conditions prevailed and joint width was held constant also, effectiveness decreased with load applications but the rate of decrease became less with continued repetitions. Usually 90 percent of effectiveness loss occurred during the first 500,000 applications.
3. Effectiveness of a joint at a given opening was improved by closing the joint incrementally while subjecting it to limited repetitions before restoring the width to the stipulated value. This operation to study the effect of aggregate fit and attrition explains in part the good effectiveness values obtained for in-service highway joints that develop wide winter openings.
4. Joint effectiveness improved with foundation bearing value, k. Effectiveness of joints in 7-in. slabs on cement-treated subbases was 2.6 times that for slabs on clay subgrades. Cement-treated subbases doubled the joint effectiveness for slabs on clay subgrades when the concrete was 9 in. thick.
5. Experiments with 7-in. slabs on gravel subbases showed that the effectiveness values at 0.035-in. openings decreased continuously under 9-kip loading, reached a pleateau at 65 percent under 7-kip loadings, and remained close to 98 percent under 5-kip loadings. This is significant as it suggests that for each joint design, effectiveness is not influenced by loads less than a critical value.
6. For the same aggregate or for aggregates of the same hardness, effectiveness increased with increased particle angularity.

Endurance index was established as a suitable criterion for equivalence of joint performance. An empirical relation relating endurance index to slab thickness, subgrade k, load, and joint opening was developed and placed in nomograph form.

## REFERENCES

1. Kapernick, J. W. Equipment for Studying Pavement Joint Performance in the Laboratory. Jour. PCA R&D Labs., Vol. 5, No. 2, May 1963.
2. Nowlen, W. J. Techniques and Equipment for Field Testing of Pavements. Jour. PCA R&D Labs., Vol. 6, No. 3, Sept. 1964; PCA Development Dept. Bull. D83.
3. Soil-Cement Laboratory Handbook. Portland Cement Assoc., Chicago, 1959, p. 34.
4. Teller, L. W., and Sutherland, E. J. A Study of Structural Action of Several Types of Transverse and Longitudinal Joint Design. Public Roads, Vol. 17, No. 7, Sept. 1936.
5. Joint Spacing in Concrete Pavements: 10-Year Reports on Six Experimental Projects. Research Report 17-B, 1956, 159 pp.

# Cement-Treated Subbases for Concrete Pavements

L. D. CHILDS, Principal Development Engineer, Paving Development Section, Portland Cement Association

The contribution of cement-treated subbases to the load-carrying capacity of concrete pavements was investigated. Concrete slabs 3, 5 and 7 in. thick were cast on 3-, 6- and 9-in. cement-treated subbases. Interlayer treatments were sand-cement grout, SS-1 bituminous emulsion and 4-mil polyethylene.

Slab responses to loads were compared with theoretical behavior of concrete slabs on clay subgrades. On the average, 2½ in. of cement-treated subbase was as effective in resisting deflection as 1 in. of concrete. At edges where the subbase was extended 1 ft beyond the concrete slab, 2 in. of cement-treated subbase resisted deflection caused by edge loads as effectively as 1 in. of concrete. Cement-treated subbases also improved load transfer across joints.

Pavements with grout bond resisted deflection as effectively as unbonded designs with an added ½ to 1 in. of concrete thickness. Emulsion produced erratic bond. These pavements on the average, were only slightly stiffer than those without bond. Upward curl and deflections at corners of curled slabs were less for designs with grout bond than for other treatments.

Fatigue studies indicated excellent endurance for all pavements tested. Although pavements were subjected to overloads at edges, no edge failures were produced. Excessive loads at corners caused cracking in some 3- and 5-in. pavements at 200,000 cycles or more, but only one design was considered unserviceable prior to 1 million load applications.

•ROADS have been built with soil-cement for many years, but few subbases for concrete pavements were treated with cement before 1950. In 1938, a 7-mile length of 9-6-9 concrete pavement was built on a 22-ft wide by 6-in. deep soil-cement subbase in Oklahoma (1). Subgrades in this region contained expansive soils and cement treatment was used to reduce soil swell. In 1946, the subbase for a section of the San Diego to Los Angeles freeway (2) was prepared by treating the upper 4 in. with cement. The primary purpose of the treatment was to minimize joint faulting and pumping and to improve the riding quality of the pavement. The treatment was successful and became a general practice in California in 1950.

Other areas of the country became interested in cement-treated subbases, not only to improve the pavement but to reduce the cost of subbases when suitable granular materials were not available locally. This type of subbase, commonly designated as CTS or CTSB, has now been used in 29 of the United States and 2 provinces in Canada.

An important factor in the thickness design of concrete pavements on CTS is the contribution of the stiff subbase to the load-carrying ability of the pavement. Studies of this factor are in progress at the Portland Cement Association Laboratories. Progress was reported to the Highway Research Board in 1964 (3). The laboratory test program has been continued, and this paper extends the scope of the first report.

---

Paper sponsored by Committee on Rigid Pavement Design and presented at the 46th Annual Meeting.

The objectives of this study are: (a) to measure the deflection, strain and pressure response of loaded concrete slabs on cement-treated subbases; (b) to investigate the value of developing full interface friction between the concrete and the cement-treated subbase by establishing interlayer bond; and (c) to study the adaptability of current design methods to concrete pavements on cement-treated subbases.

Supplemental studies developed as the tests progressed are: (a) observations of the effects of small flexural cracks in the cement-treated material on the life of the pavement, and (b) evaluation of the improvement in load capacity achieved by extending the cement-treated subbase beyond the edge of the concrete.

Static load tests on pavement slabs were supplemented by repetitive load tests on slabs to obtain a concept of the endurance that might be expected under traffic. Stress distribution in beams representative of each composite design was also studied.

## NOTATION

Symbols used in this paper in order of their appearance are defined as follows:

- $k$ = Modulus of foundation reaction, psi per in. (pci)
- CTS = Cement-treated subbase
- $f_c$ = Compressive strength, psi
- MR = Modulus of rupture, psi (subscripts indicate material)
- E = Modulus of elasticity, psi (subscripts indicate material)
- D. G. = Dense graded
- O. G. = Open graded
- PCC = Portland cement concrete
- $d_i$ = Deflection, in., of interior of pavement due to interior load
- P = Applied load, lb
- h = Thickness of concrete, in.
- $\mu$ = Poisson's ratio for concrete
- r = Radius of loaded area, in.
- $d_e$ = Deflection of pavement edge due to edge load
- t = Thickness, in., of CTS
- $d_c$ = Deflection, in., of pavement corner due to corner load
- $d_1$ = Deflection of loaded side of joint
- $d_2$ = Deflection of side of joint opposite load, in.
- c = Distance from CTS bottom surface to neutral plane, in.
- $\epsilon_1$ = Theoretical strain in concrete extreme fibers, millionths
- $\epsilon_2$ = Theoretical strain in CTS extreme fibers, millionths
- S = Section modulus (I/c) where I is moment of inertia
- $\sigma_c$ = Compressive stress in top concrete surface at beam cracking, psi
- $M_f$ = Moment to cause flexural crack in CTS, lb-in.
- $M_u$ = Moment to cause crack in upper layer of concrete, lb-in.
- y = Calculated midspan deflection of beam, in.
- n = Ratio of elastic moduli ($E_{conc.}/E_{CTS}$)
- w = Measured beam deflection, in.
- $\epsilon_C$ = Measured compressive strain, in.
- $\epsilon_T$ = Measured tensile strain, in.
- $\sigma_{max}$ = Stress due to maximum repetitive load
- $\sigma_g$ = Upper stress to cause fatigue from Goodman diagram.

## MATERIALS AND SPECIMENS

The subgrade, subbase and surfacing materials were the same as those described in previous publications (3). The essential properties are reviewed here.

### Subgrade

A silty-clay soil with 70 percent passing a No. 200 sieve, a liquid limit of 36, and a plasticity index of 19 was compacted to a depth of 4 ft in a waterproof pit. Compacted density and moisture content were approximately at standard conditions of 112 pcf

TABLE 1

COMPONENTS AND FOUNDATION MODULI

| Identity Symbol[a] | Layer Thickness (in.) | | Interlayer Treatment | Modulus k (pci) | |
|---|---|---|---|---|---|
| | Concrete | CTS | | Subgrade | Subbase |
| 3N3 | 3 | 3 | Polyeth. | 68 | 190 |
| 3S6 | 3 | 6 | Asphalt | 71 | 345 |
| 3N9 | 3 | 9 | Polyeth. | 75 | 540 |
| 3S9 | 3 | 9 | Asphalt | 89 | 530 |
| 5S3 | 5 | 3 | Asphalt | 85 | 210 |
| 5S6 | 5 | 6 | Asphalt | 74 | 420 |
| 5B6 | 5 | 6 | Grout | 79 | 435 |
| 5S9 | 5 | 9 | Asphalt | 100 | 560 |
| 5B9 | 5 | 9 | Grout | 70 | 580 |
| 7N3 | 7 | 3 | Polyeth. | 75 | 210 |
| 7S3 | 7 | 3 | Asphalt | 90 | 200 |
| 7S6 | 7 | 6 | Asphalt | 102 | 420 |
| 7B6 | 7 | 6 | Grout | 71 | 380 |
| 7N9 | 7 | 9 | Polyeth. | 98 | 550 |
| 7S9 | 7 | 9 | Asphalt | 85 | 515 |
| 7B9 | 7 | 9 | Grout | 93 | 535 |

[a]The first number refers to concrete thickness, the letter to interlayer treatment, and the last number to CTS thickness.

TABLE 2

SPECIMEN PROPERTIES AT 28 DAYS

| Pavement | Cement-Treated Material | | | Concrete at 28 Days | | |
|---|---|---|---|---|---|---|
| | $f_c$ (psi), 2.8 × 5.6-in. Cylinder | MR (psi), 3 × 3-in. Beam | E ($10^6$ psi), 3 × 3-in. Beam | $f_c$ (psi), 6 × 12-in. Cylinder | MR (psi), 6 × 6-in. Beam | E ($10^6$ psi), 6 × 12-in. Cylinder |
| 3N3 | 530 | 105 | 1.0 | 4480 | 530 | 5.0 |
| 3S6 | 480 | 110 | 1.4 | 5870 | 710 | 5.9 |
| 3N9 | 430 | 95 | 1.3 | 5660 | 760 | 5.4 |
| 3S9 | 460 | 100 | 1.3 | 5280 | 680 | 5.4 |
| 5S3 | 520 | 133 | 1.4 | 5430 | 740 | 5.3 |
| 5S6 | 610 | 125 | 1.5 | 4960 | 705 | 5.3 |
| 5B6 | 505 | 120 | 1.3 | 5050 | 660 | 5.1 |
| 5S9 | 480 | 135 | 1.4 | 5230 | 690 | 5.2 |
| 5B9 | 430 | 110 | 1.5 | 5310 | 735 | 5.1 |
| 7N3 | 465 | 125 | 1.3 | 4950 | 715 | 5.6 |
| 7S3 | 650 | 85 | 1.4 | 6020 | 780 | 6.0 |
| 7S6 | 580 | 120 | 1.3 | 5330 | 710 | 5.6 |
| 7B6 | 450 | 90 | 1.1 | 5200 | 695 | 5.3 |
| 7N9 | 440 | 115 | 1.5 | 4210 | 590 | 5.0 |
| 7S9 | 485 | 105 | 1.3 | 4920 | 630 | 5.1 |
| 7B9 | 500 | 110 | 1.4 | 5140 | 650 | 5.1 |

(dry density) and 16.5 percent moisture. It was necessary to rework the top foot of subgrade before placing each new subbase. Reaction modulus tests with a 30-in. diameter plate at 0.05 in. deflection averaged 81 pci. The k-value for each foundation is given in Table 1. The slabs are identified by a 3-character designation that lists the concrete thickness followed by a letter denoting the type of interlayer treatment and a final number giving the subbase thickness.

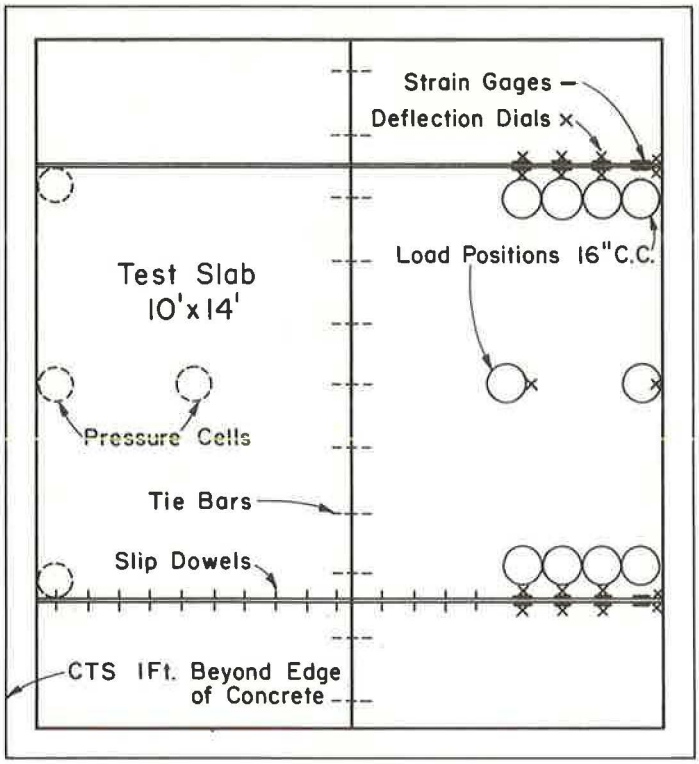


Figure 1. Load positions and instrumentation.

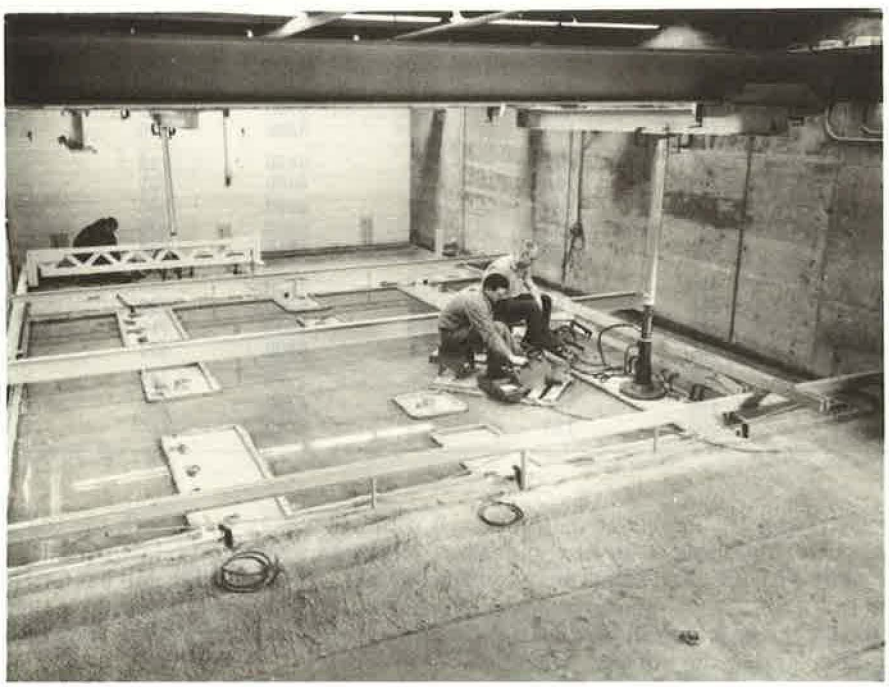

Figure 2. Test slabs flooded to prevent curl.

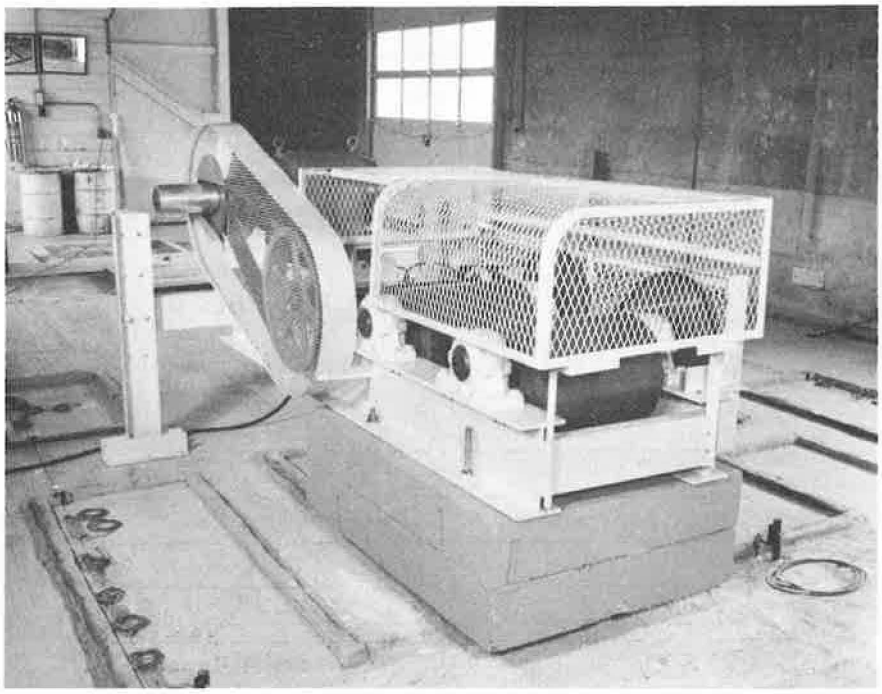

Figure 3. Two-mass oscillator for repetitive loading.

## Cement-Treated Material

A nonplastic soil with 50 percent passing the No. 40 sieve was mixed with 5.5 percent cement and 11 percent water by weight to make the cement-treated subbase. The cement requirement was determined by ASTM Standard methods and the Portland Cement Association criterion for brush loss. This material was compacted to densities close to the standard value of 125 pcf (dry) and 10.5 percent moisture. For unbonded and grout-bonded pavements the CTS was cured 14 days under polyethylene. Emulsion was applied immediately after CTS compaction on those subbases placed for the bituminous interlayer study.

The subbase, as originally constructed, extended 1 ft beyond the edge of the concrete. After load testing the flat slabs with bituminous interlayer, the extended ledge was removed and tests repeated to compare the responses of the wide subbase with those when the subbase edge was flush with the concrete.

Reaction modulus was measured on the CTS at age 14 days with a 30-in. diameter plate. As it was impractical to depress the plate 0.05 in. on the CTS, the plate load was limited to 10 psi. Values of k (Table 1) ranged from 190 pci on a 3-in. layer to 580 pci on a 9-in. layer.

Cylinders and beams of CTS material were molded as suggested by Felt and Abrams (4). Compressive strength, modulus of rupture, and modulus of elasticity associated with each pavement at age 28 days are given in Table 2.

## Interlayer Treatments

The subbase was covered with one of three materials to develop the desired interlayer treatment. For no bond (N) a sheet of 4-mil polyethylene was placed on the subbase. For full bond (B) the subbase was brushed with a cement-sand grout consisting of 1 part concrete sand, 1 part cement, and water to form a thin paste. The third treatment (S) was a coat of SS-1 bituminous emulsion, a common asphalt cure treatment used on road bases.

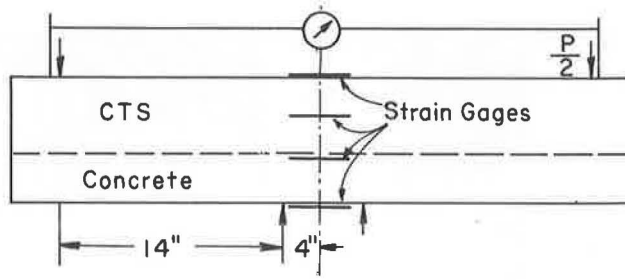


(a) INVERTED SIMPLY SUPPORTED BEAM

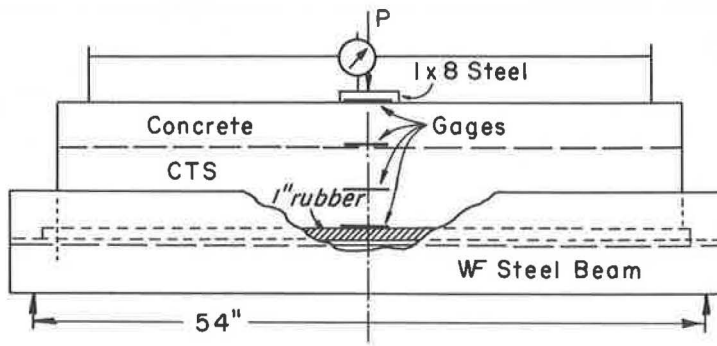


(b) CONTINUOUSLY SUPPORTED BEAM

Figure 4. Instrumentation and support of test beams.

## Concrete

The concrete mix consisted of sand, gravel aggregate of 1 in. maximum size, cement at 6 sk per cu yd, and water at a w/c ratio of 0.50. Air content was controlled between 4 and 5 percent, and slump maintained between 2.5 and 3.5 in. Cylinders and beams molded at placement were tested at age 28 days. Properties are given in Table 2.

## Pavements

The pavement slabs were 10 by 14 ft and were placed in pairs with a tied longitudinal joint as shown in Figure 1. At the ends of each pavement were short slabs connected to the test slab by butt joints. One of these joints contained smooth dowels on 12-in. centers and with diameters one-eighth the concrete thickness. The other joints had no dowels. The concrete was covered with wet burlap until dikes were built to contain surface water and protect the areas designated for instrumentation. After dike construction the slabs were flooded, thus achieving a water cure and insuring that the slab did not curl upward due to drying of the top surface.

## Stress Beams

Beams 12 in. wide and 48 in. long were manufactured in a heavy steel mold. A quantity of CTS material sufficient to give the required thickness when compressed to standard density was distributed in the mold and compressed by a 12- by 48-in. piston until desired thickness was attained. The specimen was left undisturbed and the following day the piston was removed, loose soil particles cleared away, the top

surface brushed with a cement-sand grout and the concrete placed. At age 24 to 30 hr the mold was inverted and removed. The beam was handled and stored in a fog room with the concrete on the bottom to provide support for the CTS.

## INSTRUMENTATION, FACILITIES AND OPERATIONS

### Pavements

A detailed description of the facilities and instrumentation is given elsewhere (3). Locations of gages, dials, pressure cells and loadings are shown in Figure 1. The housing, reaction frame and static load facilities for pavement studies are shown in Figure 2. Static loads were applied by a hydraulic jack and monitored by a strain-sensed load cell. Load increments were 2000 or 3000 lb depending on an estimate of slab capacity. Magnitude of load was limited by the development of about 100 millionths strain on the concrete surface.

On completion of load tests on ponded slabs, the water was drained and the slab surface dried until corners curled upward at least 0.015 in. Testing was resumed to study the effect of upward curl and consequent reduced subgrade support on response to load. Test positions for the curling study were the slab corners, extreme edge and interior.

At the conclusion of the curling study the pavement slabs were subjected to repetitive loading. A mechanical oscillator with two counter-rotating 800-lb eccentric cylinders developed centrifugal force that alternately augmented and relieved the dead weight of concrete ballast blocks. Dynamic thrust was controlled by varying eccentricity, speed of rotation and ballast. The device is shown in Figure 3. Thrust was applied through a pair of oval plates simulating dual tire prints. An instrumented plate spanned the oval plates and sensed the load. Slab deflection was measured with a recording deflectometer described by Nowlen (5). Maximum and minimum load, maximum deflection, and maximum strain measured at the gage location showing the greatest response were recorded at regular intervals.

### Beams

Beams representing isolated sections of the pavements were tested under two conditions. The first was a simple support as shown in Figure 4. The supports and loads were the inverse of normal procedure to minimize stress in the low modulus CTS due to the weight of the beam. Although a simply supported beam is not representative of pavements on subgrades, the tests provided information on the strength characteristics of the layers, and related compressive stress in the concrete with flexural stress in the CTS up to the point of rupture.

Instrumentation included SR-4 gages attached to the top and bottom surfaces and also to the vertical faces at several locations. Deflection of the beam center with respect to points on both ends at the load lines were measured with a single 0.0001-in. dial indicator.

A second method of support provided vertical and horizontal restraint at the CTS surface by means of a rubber pad placed on the web of a steel beam (Fig. 4). Load was applied through an 8- by 12- by 1-in. rectangular steel plate. Instrumentation was similar to that described for the simply supported beam.

This method of support produced relations between concrete surface and CTS surface tensile strains, and curvatures that were considered to be more representative of those in pavements than similar relations obtained with simple supports. It also resulted in failure patterns similar to those known to occur in slabs on the ground; i.e., a tension crack in the bottom widened and progressed upward with increasing load but the compression in the concrete delayed the appearance of the crack in the concrete surface.

Figure 5 shows a simply supported beam ready for a load test. Although the Amsler equipment shown is designed for repeated loading, it was used also to apply static loads to establish an ultimate strength value for subsequent fatigue studies. Automatic strain

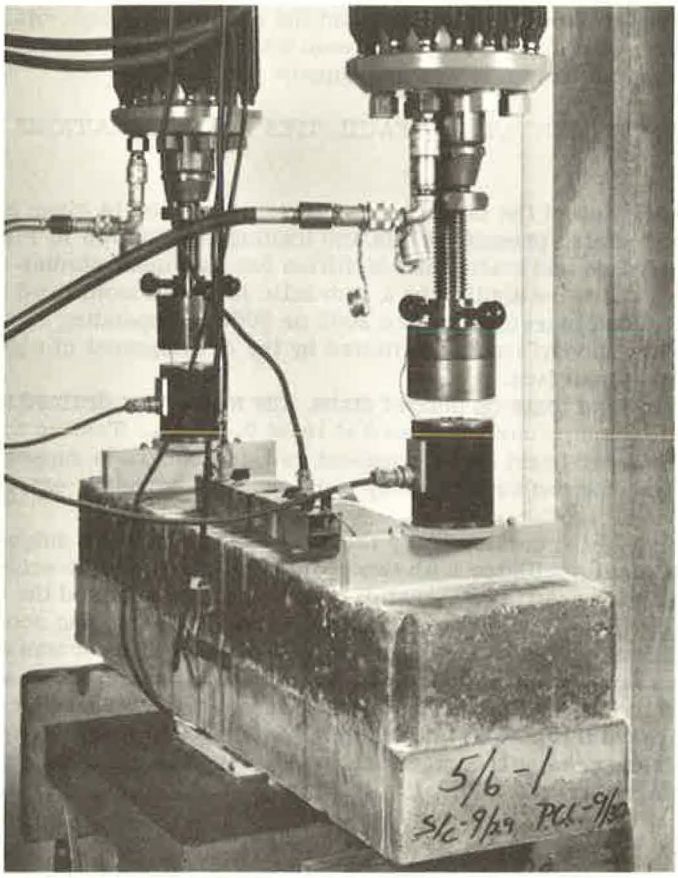


Figure 5. Beam in position for load-strain study.

recording equipment produced continuous traces as the load was applied, and cracking was detected at or near a gage when the strain response curve deviated sharply from its established slope.

## TEST RESULTS

### Subgrade and Subbase

Values of reaction modulus, k, for the cement-treated subbases are given in Table 1. Points representing these values and also those from previous untreated granular subbase studies are plotted in Figure 6 against subbase thickness to show the effect of increasing subbase thickness on the reaction modulus. The reaction modulus of a 3-in. cement-treated subbase was twice that of a 3-in. granular, and the modulus of a 9-in. CTS was more than three times that of the same thickness of granular material. Although it is known that small changes in k are not of consequence in thickness design, the large increases achieved by the use of cement-treated material over those normally attained on granular materials are significant, and subsequent data from load tests on slabs demonstrate the degree to which load-carrying ability is increased.

### Flat Slabs

Pavements were loaded in increments to obtain load-deflection, strain and pressure curves. Although 9-kip loads caused low responses on thicker designs, the curves from thinner designs began to deviate from linearity at this value. Therefore, 9 kips was the greatest load useful for direct comparison.

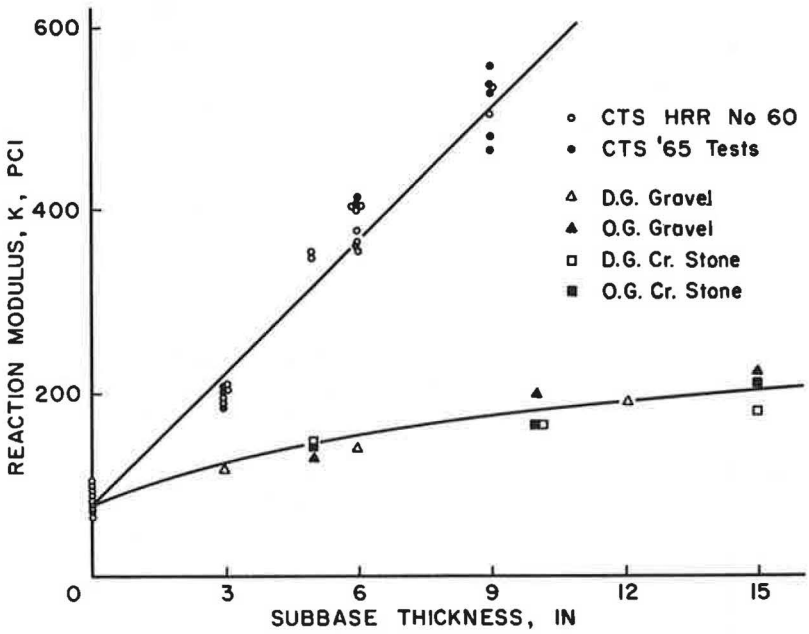


Figure 6. Effect of subbase on k.

TABLE 3

RESPONSE TO 9-KIP LOADS AT INTERIOR AND EDGE

| Pavement | Interior | | | Edge With Ledge | | | Edge Without Ledge | | |
|---|---|---|---|---|---|---|---|---|---|
| | Defl. ($10^{-3}$in.) | Strain ($10^{-6}$) | Press. (psi) | Defl. ($10^{-3}$in.) | Strain ($10^{-6}$) | Press. (psi) | Defl. ($10^{-3}$in.) | Strain ($10^{-6}$) | Press. (psi) |
| 3N3 | 23 | 101 | 6.1 | 46 | 150 | 8.5 | | | |
| 3S3[a] | 23 | 99 | 6.2 | 44 | 155 | 9.0 | — | — | — |
| 3B3[a] | 21 | 90 | 5.8 | 39 | 138 | 8.2 | | | |
| 3N6[a] | 17 | 83 | 5.0 | 31 | 131 | 7.1 | | | |
| 3S6 | 15 | 81 | 5.4 | 30 | 122 | 7.6 | 37 | 140 | 8.5 |
| 3B6[a] | 15 | 73 | 5.5 | 29 | 119 | 7.5 | | | |
| 3N9 | 13 | 69 | 5.5 | 22 | 107 | 7.2 | | | |
| 3S9 | 12 | 63 | 5.0 | 23 | 110 | 7.3 | 31 | 134 | 8.0 |
| 3B9 | 14 | 66 | 4.8 | 21 | 108 | 6.8 | | | |
| 5N3[a] | 13 | 58 | 4.2 | 26 | 99 | 5.5 | | | |
| 5S3 | 11 | 60 | 4.2 | 26 | 97 | 5.5 | 30 | 116 | 7.0 |
| 5B3[a] | 11 | 49 | 4.0 | 23 | 87 | 6.0 | | | |
| 5N6[a] | 8.5 | 45 | 4.0 | 19 | 69 | 4.9 | | | |
| 5S6 | 9.0 | 42 | 3.6 | 17 | 71 | 5.4 | 22 | 89 | 6.1 |
| 5B6 | 8.5 | 45 | 3.5 | 17 | 65 | 5.0 | | | |
| 5N9[a] | 7.5 | 40 | 3.5 | 17 | 62 | 4.6 | | | |
| 5S9 | 7.0 | 36 | 3.1 | 16 | 62 | 4.5 | 20 | 84 | 5.8 |
| 5B9 | 6.5 | 35 | 2.9 | 14 | 56 | 4.6 | | | |
| 7N3 | 6.5 | 35 | 3.4 | 15 | 65 | 5.0 | | | |
| 7S3 | 6.0 | 32 | 3.1 | 16 | 62 | 4.8 | 19 | 74 | 6.0 |
| 7B3[a] | 6.0 | 31 | 3.1 | 15 | 55 | 4.5 | | | |
| 7N6[a] | 5.0 | 29 | 3.1 | 14 | 45 | 4.0 | | | |
| 7S6 | 5.0 | 25 | 2.4 | 13 | 48 | 4.2 | 14 | 62 | 5.5 |
| 7B6 | 4.5 | 23 | 2.5 | 12 | 46 | 3.8 | | | |
| 7N9 | 4.5 | 22 | 2.2 | 11 | 38 | 3.5 | | | |
| 7S9 | 4.0 | 17 | 2.0 | 11 | 39 | 3.0 | 13 | 52 | 4.5 |
| 7B9 | 4.0 | 17 | 1.8 | 10 | 36 | 3.3 | | | |

[a]See Ref. (3).

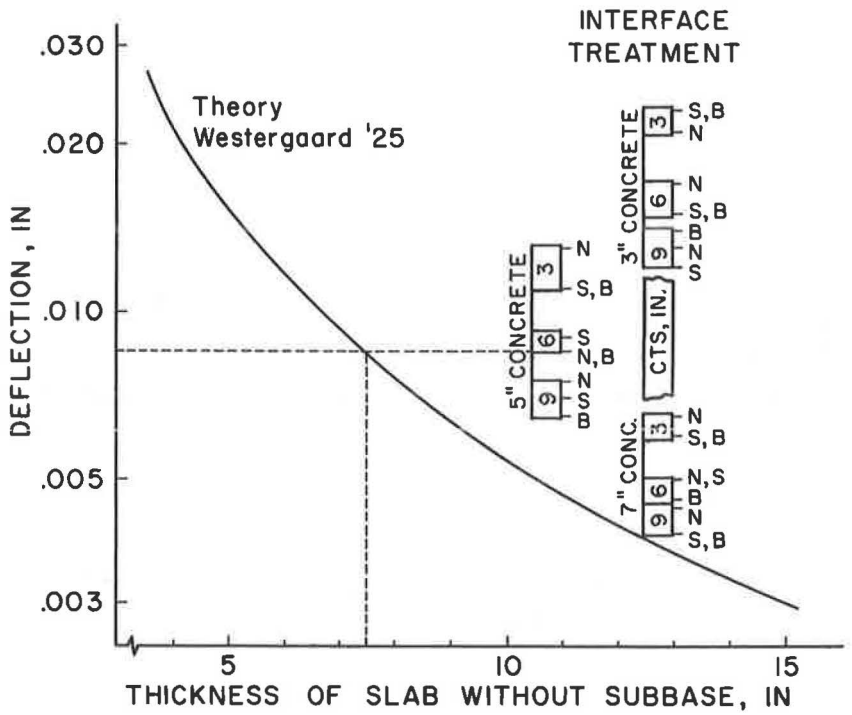


Figure 7. Comparison of interior deflections for 9-kip load.

Pavements are designed on flexural stress, and experimental comparisons are usually made from strains with the assumption that the neutral plane is at mid-depth. Varying degrees of composite action occurred with CTS layers and strain symmetry was lost. Also, as illustrated, CTS fracture did not always result in section failure. Thus concrete strain was unsuitable for direct comparison. Pressure and curvature were considered but reproducibility in both cases was unsatisfactory. A response somewhat deficient in sensitivity but quite reproducible was maximum deflection at load. As all pavements were built on approximately the same subgrade (average k = 81 pci), deflection was a simple measure of pavement stiffness. Furthermore, deflections are critical when pavements are built on pumping-susceptible subgrades. Therefore, deflection was considered a suitable response for pavement comparisons.

Interior Locations—The trend that thicker pavements yield smaller deflections is given in Table 3, but the data are more meaningful when interpreted in terms of thickness of plain concrete pavement. The curve in Figure 7 relates interior deflection and concrete slab thickness by means of the 1925 Westergaard (6) formula

$$d_i = \frac{P}{8kL^2} \tag{1}$$

where $d_i$ is deflection in inches, P = 9,000-lb load, k = 100 pci, and

$$L^2 = \left[\frac{E\,h^3}{12\,(1-\mu^2)\,k}\right]^{1/2} \tag{2}$$

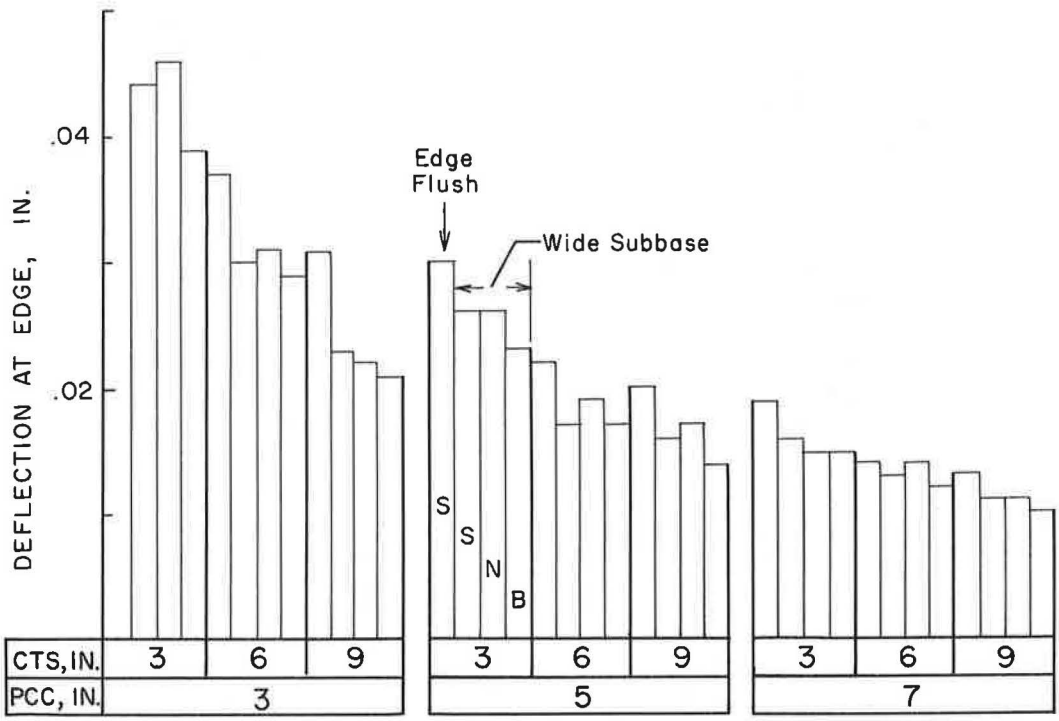


Figure 8. Edge deflections at 9-kip load.

To compute coordinates for the curve, Young's modulus, E, was selected at 5 million psi, k at 100 pci, and pavement thickness, h, was assigned values from 4 to 15 in.

In Figure 7, the test slabs are identified on the right with the measured test deflections at 9-kip load shown on the left. A horizontal line originating at any tested design intersects the curve at a point giving that thickness of slab without subbase that will produce the same deflection. For example, 5-in. concrete on 6-in. CTS with no bond deflects the same as $7\frac{1}{2}$ in. of plain concrete on a clay subgrade. By this method of evaluation, it is seen that the designs tested were equivalent to plain concrete pavements ranging in thickness from less than 4 in. to more than 12 in.

Table 3 and Figure 7 show that interface treatment did not alter pavement deflection response to interior loads significantly. For pavements with 3-in. concrete on CTS the deflections differed with treatment, but there was no consistent trend established to indicate that one type of treatment contributed more to load-carrying ability than another. For 5- and 7-in. concrete on CTS, pavements with grout bond deflected least and pavements without bond deflected most, with one exception. However, deflections were small and except for the 5-in. concrete on 3-in. CTS, deflection differences were at most 0.001 in. This difference was not sufficient to establish a trend, and it was concluded that interface treatment was not an important consideration from the standpoint of the ability of pavements to support interior loads.

Free Longitudinal Edge—As discussed previously, the cement-treated subbase extended 1 ft beyond the edge of the concrete. When pavements on these subbases were loaded at the edge of the concrete, the CTS ledge contributed to load-carrying ability by reducing responses below those for the flush construction. To ompare these treatments the pavements with bituminous interlayers were retested after the ledge was cut away. Data from edge tests under both of these conditions are given in Table 3. Relative magnitudes of responses to the 9-kip load are seen more readily in Figure 8.

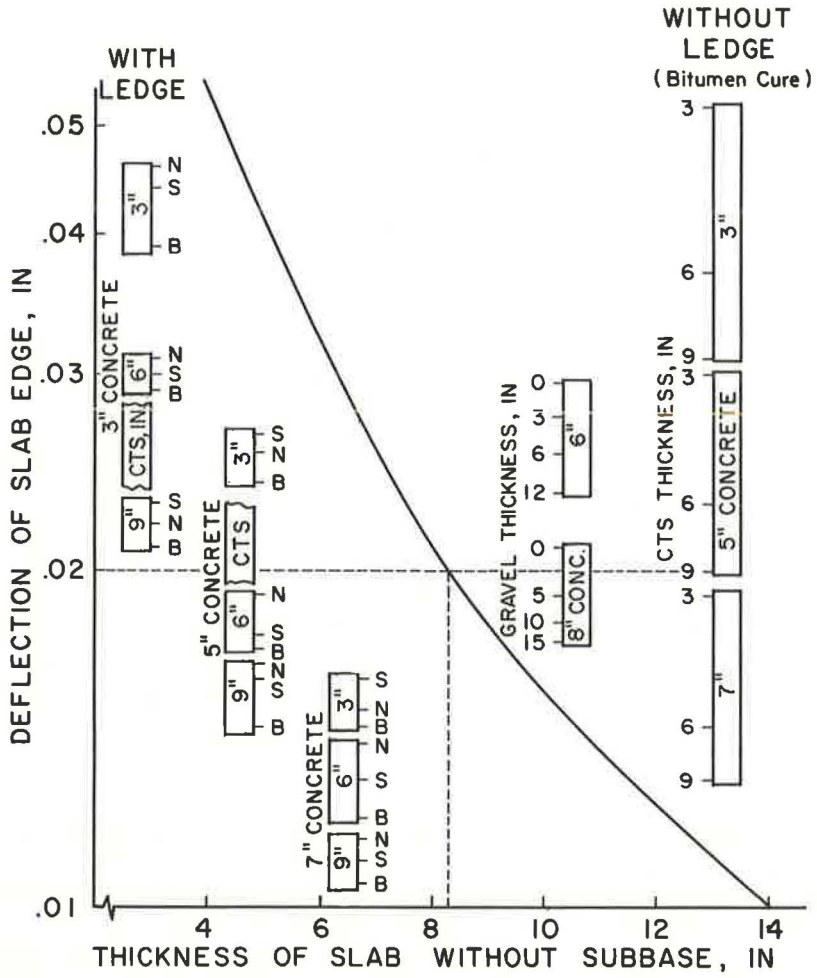


Figure 9. Equivalent designs, 9-kip edge loading.

Measured deflections are used to compare the tested designs with equivalent concrete slabs without subbase by use of a curve of edge deflections vs slab thickness computed from the Westergaard (7) expression

$$d_e = P\sqrt{\frac{2+1.20\mu}{Eh^3k}}\left[1-(0.76+0.40\mu)\frac{r}{L}\right] \qquad (3)$$

In this formula, r is the radius of the loading area and the remaining symbols are the same as defined for interior loading. The curve relating composite design, deflections, and plain concrete slabs without subbase is shown in Figure 9. Pavement designations on the left locate the designs at the deflections measured when the CTS extended beyond the slab edge. Those on the right are located at deflections measured on slabs with bituminous interlayers after the ledge of CTS was removed. Deflections of pavements of 6- and 8-in. concrete on gravel (8) subbase measured prior to the CTS study are included for direct comparison.

A study of Figure 9 confirms that deflection response to load at slab edges is affected by both edge construction and interlayer treatment. Edge deflections of the

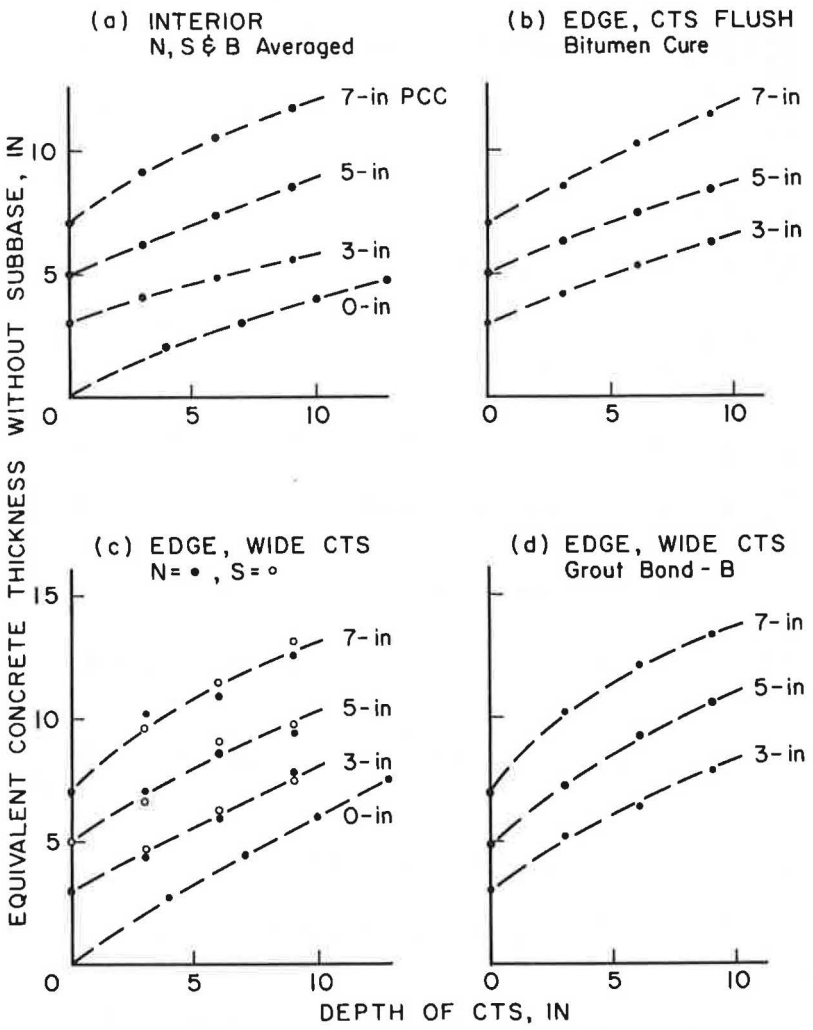


Figure 10. Relation between plain concrete and composite designs as determined from interior and edge loads.

pavement slabs with bitumen-cured CTS that had the ledge removed were consistently greater than the deflections of slabs when the ledge was intact. Also, the pavements with grout bond had lower deflections than other pavements. Although deflections of unbonded slabs were greater than those of slabs with bituminous cure in 6 cases out of 9, the partial bond effected by the bitumen was discounted because of its uncertainty.

Use of this chart is illustrated by comparing designs intercepted by the dashed line at a deflection of 0.02 in. For example, equivalence of design is noted for the 5N6 with a 1-ft ledge, the 8G3, and the 5S9 without a ledge. Further, each of these designs corresponds to a concrete pavement 8.2 in. thick on a subgrade with a k-value of 100.

The effects of interlayer treatment and extended width of subbase in terms of equivalent plain concrete depth can be seen also by comparing appropriate curves in Figure 10. These curves interpret the data from Figures 7 and 9 supplemented by results from a study on cement-treated bases by Nussbaum and Larsen (9).

When the subbase did not extend beyond the slab edge, composite slabs with a concrete layer of depth, d, and cement-treated layer of depth, t, can be related to concrete without subbase by

$$h = 0.4t + d \quad (4)$$

TABLE 4

RESPONSE TO 9-KIP LOADS AT UNDOWELED JOINT

| Pavement | Load at Corner | | | | Press. (psi) Load | Load at Mid-Joint | | | |
|---|---|---|---|---|---|---|---|---|---|
| | Deflection ($10^{-3}$ in.) | | Tensile Strain ($10^{-6}$) | | | Deflection ($10^{-3}$) | | Compressive Strain ($10^{-6}$) | |
| | Load | Opp. | Load | Opp. | | Load | Opp. | Load | Opp. |
| 3N3 | 49 | 42 | 41 | 39 | 9.6 | 28 | 25 | 98 | 76 |
| 3S3[a] | 46 | 42 | 40 | 35 | 9.0 | 28 | 27 | 101 | 83 |
| 3B3[a] | 41 | 41 | 35 | 32 | 8.5 | 24 | 24 | 95 | 71 |
| 3N6[a] | 34 | 32 | 29 | 20 | 9.0 | 17 | 15 | 65 | 60 |
| 3S6 | 38 | 35 | 32 | 26 | 8.5 | 18 | 16 | 75 | 70 |
| 3B6[a] | 28 | 28 | 26 | 16 | 8.1 | 16 | 14 | 60 | 46 |
| 3N9 | 26 | 23 | 22 | 16 | 8.0 | 12 | 11 | 49 | 40 |
| 3S9 | 25 | 22 | 24 | 20 | 8.8 | 13 | 11 | 46 | 37 |
| 3B9[a] | 20 | 19 | 17 | 15 | 8.0 | 12 | 12 | 38 | 30 |
| 5N3[a] | 39 | 37 | 30 | 27 | 8.0 | 27 | 25 | 81 | 70 |
| 5S3 | 34 | 32 | 32 | 25 | 7.5 | 23 | 21 | 67 | 57 |
| 5B3[a] | 33 | 32 | 27 | 21 | 7.0 | 20 | 19 | 70 | 60 |
| 5N6[a] | 19 | 16 | 18 | 14 | 7.2 | 11 | 11 | 35 | 28 |
| 5S6 | 23 | 21 | 16 | 14 | 7.5 | 15 | 13 | 49 | 32 |
| 5B6 | 21 | 19 | 20 | 17 | 7.0 | 11 | 12 | 44 | 28 |
| 5N9[a] | 18 | 17 | 17 | 16 | 6.6 | 11 | 10 | 30 | 30 |
| 5S9 | 17 | 16 | 19 | 15 | 6.0 | 11 | 10 | 38 | 28 |
| 5B9 | 16 | 16 | 21 | 16 | 6.2 | 10 | 9 | 35 | 26 |
| 7N3 | 21 | 19 | 28 | 19 | 6.5 | 15 | 14 | 50 | 44 |
| 7S3 | 20 | 19 | 24 | 20 | 6.2 | 14 | 12 | 46 | 36 |
| 7B3[a] | 22 | 21 | 20 | 13 | 6.0 | 12 | 12 | 41 | 32 |
| 7N6[a] | 18 | 18 | 17 | 15 | 5.2 | 10 | 10 | 26 | 21 |
| 7S6 | 17.5 | 17 | 19 | 14 | 5.0 | 11 | 8 | 33 | 24 |
| 7B6 | 17 | 16 | 20 | 18 | 4.3 | 10 | 8 | 32 | 20 |
| 7N9 | 16 | 14 | 18 | 18 | 4.6 | 9 | 7 | 31 | 26 |
| 7S9 | 15 | 14 | 16 | 15 | 4.0 | 9 | 9 | 29 | 24 |
| 7B9 | 14 | 14 | 14 | 14 | 4.0 | 8 | 8 | 28 | 32 |

[a]See Ref. (3).

TABLE 5

RESPONSE TO 9-KIP LOADS AT DOWELED JOINT

| Pavement | Load at Corner | | | | Press. (psi) Load | Load at Mid-Joint | | | |
|---|---|---|---|---|---|---|---|---|---|
| | Deflection ($10^{-3}$ in.) | | Tensile Strain ($10^{-6}$) | | | Deflection ($10^{-3}$) | | Compressive Strain ($10^{-6}$) | |
| | Load | Opp. | Load | Opp. | | Load | Opp. | Load | Opp. |
| 3N3 | 46 | 44 | 40 | 38 | 9.0 | 26 | 20 | 110 | 80 |
| 3S3[a] | 44 | 40 | 37 | 32 | 8.0 | 25 | 21 | 105 | 75 |
| 3B3[a] | 38 | 37 | 30 | 25 | 8.6 | 23 | 23 | 95 | 65 |
| 3N6[a] | 30 | 28 | 28 | 25 | 8.3 | 15 | 12 | 70 | 54 |
| 3S6 | 32 | 29 | 32 | 25 | 8.5 | 18 | 18 | 78 | 60 |
| 3B6[a] | 26 | 25 | 25 | 22 | 8.8 | 15 | 15 | 58 | 43 |
| 3N9 | 25 | 23 | 25 | 21 | 8.0 | 14 | 12 | 45 | 33 |
| 3S9 | 24 | 22 | 24 | 20 | 8.6 | 13 | 12 | 40 | 35 |
| 3B9[a] | 19 | 18 | 19 | 16 | 7.2 | 12 | 11 | 36 | 36 |
| 5N3[a] | 35 | 34 | 28 | 28 | 7.3 | 22 | 20 | 80 | 65 |
| 5S3 | 31 | 30 | 24 | 21 | 6.7 | 19 | 18 | 70 | 56 |
| 5B3[a] | 32 | 29 | 27 | 26 | 7.0 | 17 | 15 | 75 | 54 |
| 5N6[a] | 17.5 | 15 | 17 | 14 | 6.5 | 12 | 11 | 38 | 34 |
| 5S6 | 23 | 21 | 18 | 14 | 7.2 | 13 | 10 | 48 | 35 |
| 5B6 | 20 | 18 | 17 | 15 | 6.1 | 13 | 11 | 52 | 30 |
| 5N9[a] | 17 | 15 | 17 | 16 | 6.0 | 11 | 11 | 31 | 31 |
| 5S9 | 16.5 | 13 | 15 | 13 | 6.1 | 12 | 10 | 37 | 28 |
| 5B9 | 16 | 15 | 16 | 14 | 5.5 | 10 | 9 | 35 | 27 |
| 7N3 | 21 | 20 | 24 | 21 | 7.1 | 13 | 11 | 42 | 24 |
| 7S3 | 19 | 20 | 23 | 15 | 6.6 | 11 | 9 | 40 | 19 |
| 7B3[a] | 20 | 18 | 18 | 12 | 5.7 | 14 | 12 | 42 | 34 |
| 7N6[a] | 17 | 16 | 16 | 15 | 4.8 | 9 | 9 | 27 | 27 |
| 7S6 | 16 | 14 | 16 | 14 | 5.2 | 9 | 8 | 36 | 25 |
| 7B6 | 15.5 | 14 | 15 | 13 | 4.5 | 8 | 6 | 33 | 30 |
| 7N9 | 15 | 11 | 17 | 17 | 4.6 | 8 | 7 | 33 | 27 |
| 7S9 | 14 | 14 | 15 | 14 | 4.0 | 9 | 9 | 35 | 25 |
| 7B9 | 14.5 | 14 | 15 | 15 | 4.3 | 8 | 7 | 34 | 33 |

[a]See Ref. (3).

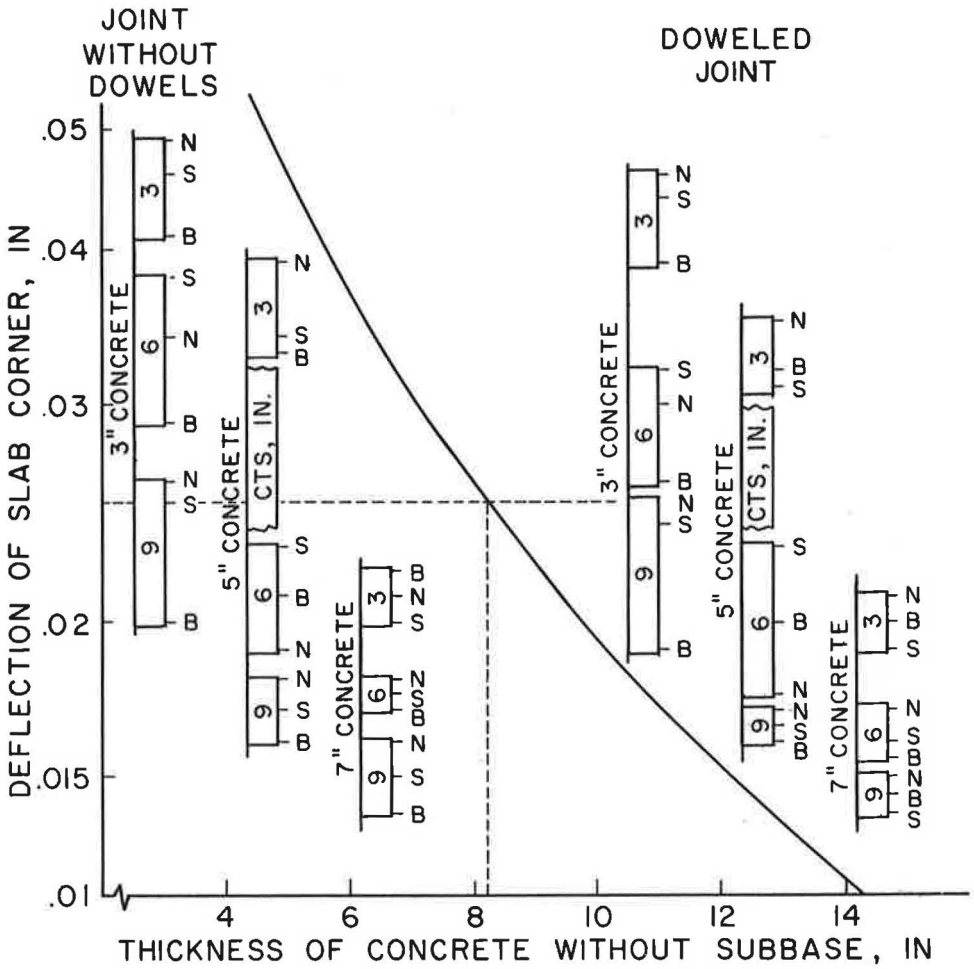


Figure 11. Comparison of tested joints with theory at full load transfer (corner load).

This expression is conservative for d = 7 in. Experimental values from interior tests on composite slabs with 3-in. concrete resulted in equivalent plain concrete thicknesses slightly below those computed by this empirical formula (Fig. 10a), but under edge loading there was better agreement (Fig. 10b). For composite design without grout bond and with no CTS beyond the concrete, about 2½ in. of CTS was required to support load as effectively as 1 in. of concrete.

Figure 10c relates plain concrete and composite pavements without bond when the controlling load was at the slab edge and the CTS extended 1 ft beyond the concrete. These curves are approximated by the equation

$$h = 0.6t + d \qquad (5)$$

The ledge construction improved the effectiveness of the CTS. When the CTS was wider than the concrete and the load was at the edge of the pavement less than 2 in. of CTS was required to support load as effectively as 1 in. of concrete.

Transverse Joints—Load tests were made at 4 positions along each transverse joint. Maximum deflections, strains and pressures caused by 9,000-lb loads at butt joints without dowels are given in Table 4, and those at doweled joints in Table 5. Deflections were largest for loads at the outside corner, and strains greatest when loads were at the load position at the joint edge farthest inward from the corner. Data for intermediate positions are not reported.

TABLE 6

SHAPE CHANGE DUE TO CURL

| Pavement | Change in Elevation (0.001 in.) | | | |
|---|---|---|---|---|
| | Undoweled Corner | Doweled Corner | Free Edge | Interior |
| 3N3 | 60 | 50 | 32 | -10 |
| 3S3[a] | 60 | 45 | 30 | -13 |
| 3B3[a] | 53 | 40 | 20 | -12 |
| 3N6[a] | 51 | 39 | 29 | -12 |
| 3S6 | 53 | 36 | 26 | -10 |
| 3B6[a] | 46 | 35 | 24 | -12 |
| 3N9 | 47 | 38 | 20 | - 9 |
| 3S9 | 34 | 31 | 20 | - 9 |
| 3B9[a] | 16 | 15 | 8 | - 7 |
| 5N3[a] | 42 | 31 | 15 | -10 |
| 5S3 | 40 | 26 | 15 | - 9 |
| 5B3[a] | 28 | 25 | 13 | - 8 |
| 5N6[a] | 40 | 28 | 6 | - 9 |
| 5S6 | 36 | 26 | 13 | - 8 |
| 5B6 | 25 | 25 | 10 | -10 |
| 5N9[a] | 34 | 31 | 12 | - 7 |
| 5S9 | 37 | 30 | 10 | - 9 |
| 5B9 | 20 | 20 | 8 | - 8 |
| 7N3 | 32 | 29 | 14 | -10 |
| 7S3 | 29 | 28 | 15 | - 9 |
| 7B3[a] | 30 | 18 | 4 | -10 |
| 7N6[a] | 27 | 26 | 9 | - 9 |
| 7S6 | 30 | 18 | 16 | - 9 |
| 7B6 | 18 | 16 | 11 | - 7 |
| 7N9 | 27 | 24 | 16 | - 9 |
| 7S9 | 25 | 20 | 15 | - 8 |
| 7B9 | 15 | 15 | 9 | - 8 |

[a]See Ref. (3).

In a manner similar to that for interior and edge loads, the corner load deflections are interpreted in Figure 11 in terms of concrete thickness required without subbase to maintain the same deflections as those obtained by test. The theoretical deflections were computed with the assumption that two abutting free corners, each loaded to one-half the test load, would deflect together in the same manner as corners at a joint with full load transfer. The Westergaard (6) formula for free corner deflection is

$$d_c = (1.10 - 1.24\frac{r}{L})\frac{P}{kL^2} \qquad (6)$$

Values of the variable were the same as for interior loading except that load P = 4500 lb.

Effectiveness of load transfer at the joints was computed by the Teller and Sutherland (10) expression

$$E_j = \left[\frac{2\,d_2}{d_1 + d_2}\right] 100 \qquad (7)$$

where $d_1$ is the deflection of the loaded slab and $d_2$ is the deflection of the adjacent slab due to this load. When loads were at corners of undoweled joints, $E_j$ ranged from 92 to 100 percent. When loads were at mid-joint, $E_j$ ranged from 84 to 100 percent. Similarly, corner loading at doweled joints produced $E_j$ values from 85 to 100 percent and

TABLE 7

RESPONSE OF CURLED PAVEMENTS TO 9-KIP LOAD AT INTERIOR AND EDGE

| Pavement | Interior | | Outside Free Edge[a] | |
|---|---|---|---|---|
| | Defl. ($-10^{-3}$ in.) | Strain ($10^{-6}$) | Defl. ($-10^{-3}$ in.) | Strain ($10^{-6}$) |
| 3N3 | 26 | 105 | 58 | 170 |
| 3S3[b] | 24 | 102 | 60 | 185 |
| 3B3[b] | 21 | 77 | 43 | 157 |
| 3N6 | 18 | 92 | 55 | 136 |
| 3S6 | 19 | 88 | 49 | 127 |
| 3B6[b] | 13 | 66 | 33 | 99 |
| 3N9 | 15 | 63 | 40 | 117 |
| 3S9 | 16 | 60 | 40 | 135 |
| 3B9[b] | 12 | 56 | 24 | 100 |
| 5N3[b] | 15 | 63 | 44 | 97 |
| 5S3 | 15 | 58 | 40 | 110 |
| 5B3[b] | 13 | 45 | 27 | 81 |
| 5N6[b] | 9 | 44 | 25 | 63 |
| 5S6 | 8 | 46 | 27 | 86 |
| 5B6 | 9 | 40 | 23 | 60 |
| 5N9[b] | 8 | 37 | 23 | 57 |
| 5S9 | 8 | 40 | 25 | 82 |
| 5B9 | 7 | 35 | 20 | 53 |
| 7N3 | 7 | 36 | 22 | 65 |
| 7S3 | 6 | 30 | 23 | 70 |
| 7B3[b] | 6 | 27 | 15 | 47 |
| 7N6[b] | 6 | 32 | 19 | 45 |
| 7S6 | 5 | 28 | 18 | 60 |
| 7B6 | 5 | 24 | 14 | 43 |
| 7N9 | 5 | 24 | 15 | 40 |
| 7S9 | 4 | 20 | 15 | 48 |
| 7B9 | 4 | 18 | 12 | 40 |

[a] Underlined values obtained after CTS ledge was removed.
[b] See Ref. (3).

mid-joint loading from 86 to 100 percent. These results indicate that in no case was effectiveness below 84 percent, i. e., at least 42 percent of the load was transferred across a joint.

In summary, pavements of concrete on CTS were equivalent in deflection resistance at joints to concrete pavements with thicknesses related as shown in Figure 11, and load transfer was good for both doweled and undoweled constructions.

## Curled Pavements

After completion of static tests on the ponded pavements, the water was drained and the concrete surface dried. Changes in elevations of corners, edges and slab centers were measured with slip-pin deflectometers. Testing was resumed when corners had raised at least 0. 015 in. Actual elevation changes at the beginning of curled slab tests are given in Table 6.

The elevation changes at corners and edges were greater for thin pavements than for the thick combinations. Increasing thickness of bonded CTS aided in curl restraint. There was also an effect due to increasing concrete thickness. Combinations without bond and with bituminous interlayer curled to about the same degree. Curl was less at corners of doweled butt joints than at undoweled butt joints. Restraint due to dowels was greater in pavements with thin concrete.

Interiors and Edges—Deflection and strain readings due to 9-kip loads at interiors and edges of curled slabs are given in Table 7. The values at interiors are essentially

TABLE 8

RESPONSE OF CURLED PAVEMENTS TO 9-KIP CORNER LOAD AT JOINTS

| Pavement[a] | Undoweled Joint | | | | Doweled Joint | | | |
|---|---|---|---|---|---|---|---|---|
| | Defl. ($10^{-3}$in.) | | Strain ($10^{-6}$) | | Defl. ($10^{-3}$in.) | | Strain ($10^{-6}$) | |
| | Load | Opp. | Load | Opp. | Load | Opp. | Load | Opp. |
| 3N3 | 75 | 66 | 55 | 40 | 70 | 60 | 60 | 56 |
| 3S3[b] | 70 | 65 | 54 | 34 | 69 | 63 | 57 | 54 |
| 3B3[b] | 61 | 49 | 45 | 36 | 45 | 39 | 49 | 35 |
| 3N6[b] | 58 | 43 | 48 | 39 | 39 | 42 | 48 | 38 |
| 3S6 | 62 | 48 | 54 | 42 | 48 | 42 | 53 | 38 |
| $\overline{3B6}$[b] | 33 | 26 | 30 | 14 | 27 | 26 | 36 | 22 |
| 3N9 | 42 | 40 | 44 | 39 | 42 | 37 | 42 | 37 |
| 3S9 | 46 | 42 | 48 | 40 | 45 | 36 | 42 | 30 |
| $\overline{3B9}$[b] | 25 | 23 | 30 | 23 | 24 | 19 | 35 | 13 |
| 5N3[b] | 59 | 44 | 46 | 33 | 53 | 50 | 42 | 30 |
| 5S3 | 59 | 48 | 49 | 34 | 48 | 46 | 44 | 35 |
| $\overline{5B3}$[b] | 43 | 33 | 33 | 16 | 44 | 38 | 38 | 33 |
| 5N6[b] | 25 | 21 | 20 | 18 | 28 | 22 | 28 | 10 |
| 5S6 | 42 | 33 | 31 | 30 | 39 | 35 | 38 | 32 |
| $\overline{5B6}$ | 33 | 25 | 23 | 20 | 30 | 27 | 30 | 24 |
| 5N9[b] | 30 | 26 | 32 | 28 | 34 | 30 | 27 | 24 |
| 5S9 | 31 | 26 | 35 | 29 | 34 | 28 | 36 | 31 |
| $\overline{5B9}$ | 22 | 20 | 27 | 20 | 22 | 19 | 26 | 20 |
| 7N3 | 25 | 25 | 28 | 23 | 25 | 22 | 27 | 25 |
| 7S3 | 31 | 29 | 34 | 25 | 32 | 24 | 30 | 21 |
| $\overline{7B3}$[b] | 29 | 26 | 22 | 12 | 25 | 21 | 24 | 11 |
| 7N6[b] | 28 | 26 | 29 | 25 | 24 | 21 | 21 | 20 |
| 7S6 | 30 | 26 | 31 | 24 | 24 | 22 | 27 | 24 |
| $\overline{7B6}$ | 20 | 19 | 21 | 18 | 20 | 19 | 20 | 18 |
| 7N9 | 22 | 20 | 25 | 23 | 19 | 18 | 20 | 16 |
| 7S9 | 24 | 22 | 29 | 24 | 24 | 20 | 21 | 17 |
| $\overline{7B9}$ | 16 | 16 | 21 | 20 | 18 | 18 | 17 | 16 |

[a] Underlined designs tested with CTS ledge removed.
[b] See Ref. (3).

TABLE 9

VALUES FOR SECTION ANALYSIS

| Design | C (in.) | $\frac{\epsilon_1}{\epsilon_2}$ | $\sigma_c$ (psi) | S (in.$^3$) | $M_f$ (in. lb) | $M_u$ (in. lb) |
|---|---|---|---|---|---|---|
| 3-in.conc. | 1.5 | 1.00 | — | (18) | — | 12, 200 |
| 3B3 | 3.9 | 0.54 | 240 | 101 | 11, 100 | 12, 200 |
| 3B6 | 6.0 | 0.50 | 218 | 216 | 23, 800 | 12, 200 |
| 3B9 | 7.93 | 0.51 | 224 | 386 | 42, 500 | 12, 200 |
| 5-in. conc. | 2.5 | 1.00 | — | (50) | — | 34, 000 |
| 5B3 | 4.98 | 0.61 | 270 | 206 | 22, 700 | 34, 000 |
| 5B6 | 7.23 | 0.52 | 230 | 331 | 36, 400 | 34, 000 |
| 5B9 | 9.33 | 0.50 | 218 | 522 | 57, 500 | 34, 000 |
| 7-in. conc. | 3.5 | 1.00 | — | (98) | — | 66, 500 |
| 7B3 | 6.02 | 0.66 | 290 | 368 | 40, 500 | 66, 500 |
| 7B6 | 8.35 | 0.56 | 250 | 490 | 54, 000 | 66, 500 |
| 7B9 | 10.55 | 0.52 | 230 | 695 | 76, 500 | 66, 500 |

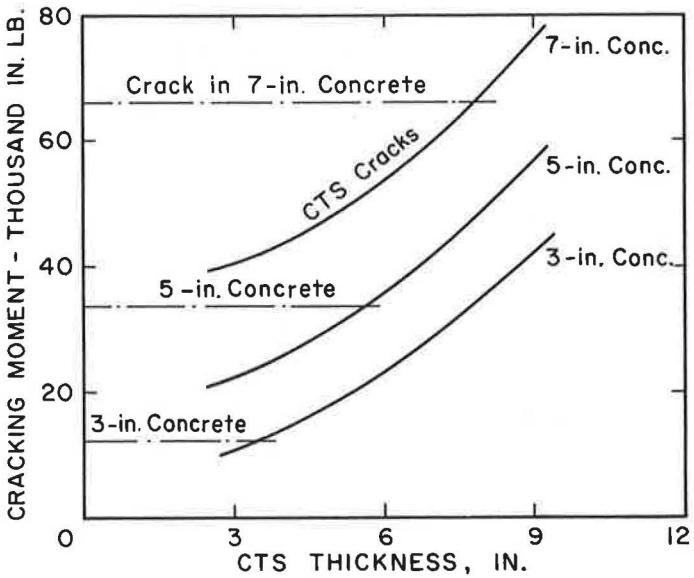


Figure 12. Moment to cause cracking in CTS and concrete.

the same as those for flat slabs. At edges there was a marked increase in deflections of pavements with unbonded and bituminous cured subbases, but only a moderate increase in deflections of bonded pavements. The data for edge tests on curled pavements with asphalt interlayer must be compared with the Table 3 data for pavements without ledge, except for the 3S3 combination.

Strains on the concrete surface due to loads on the outside free edge were larger for curled slabs than for flat pavements in some cases and smaller in others. Increases were noted for 5 of the 9 treatments with 3-in. concrete, but differences between values for curled and flat pavements were either less or insignificantly different for the remaining combinations.

Transverse Joints—Table 8 gives corner deflections and tensile strains inward along the joint for 9-kip loads at joint corners on curled pavements. All entries are greater than those for flat slabs, and values for the pavements with bituminous interlayer were the result of both curl and loss of the CTS ledge.

Corner deflections of curled unbonded pavements and asphalt cured designs were about 50 percent greater, and those of curled bonded designs about 25 percent greater than corresponding deflections of flat pavements. Tensile strains along the joint also increased but to a lesser extent than deflections. On thin pavements, deflections at doweled corners were slightly less than those at undoweled corners, but this trend did not hold for strains.

Effectiveness of load transfer for curled slabs was computed as described previously. At undoweled joints these values ranged from 85 to 100 percent compared with 92 to 100 percent for flat slabs. At doweled joints, effectiveness of curled slabs ranged from 85 to 100 percent. Although the ability of undoweled joints to transfer load was slightly better when slabs were flat than when curled, the effectiveness was as good as at doweled joints, and the ability to transfer load was generally very good for slabs in either flat or curled condition.

## Stress Ratios and Failure Criteria

In preparation for repetitive load studies on composite pavements, a study was made of stress distribution through typical fully bonded sections. This was necessary to permit computations of the load magnitude that would produce fatigue.

Computation of Cracking Moment—From Table 2, average values of elastic modulus and modulus of rupture of each material were found to be

$E_{conc} = 5.2 \times 10^6$ psi  $E_{cts} = 1.3 \times 10^6$ psi

$MR_{conc} = 680$ psi  $MR_{cts} = 110$ psi

Using these values, the moment required to cause cracking in the bottom of the CTS was computed for a 12-in. wide section. It was then assumed that cracking progressed upward through the CTS layer to the concrete, and the resulting tensile stress in the bottom of the concrete was noted. If this stress did not exceed the concrete modulus of rupture, moment to cause concrete failure was calculated. Critical values in this analysis are given in Table 9. Notation is as follows:

$c$ = distance from bottom of section to neutral plane;
$\epsilon_1$ = compressive strain in the top surface of concrete;
$\epsilon_2$ = tensile strain in bottom of CTS;
$\sigma_c$ = compressive stress in top surface concrete at CTS flexural crack in beam;
$S$ = section modulus transformed to CTS;
$M_f$ = moment at CTS cracking;
$M_u$ = moment to cause cracking in upper layer of concrete.

Cracking moment curves are shown in Figure 12. It is noted that:

1. Sections 3B3, 5B3, 7B3 and 7B6 should continue to support load after cracking in the CTS at moments below those causing flexural failure on the concrete; and
2. CTS thicknesses greater than $3\frac{1}{2}$ in. under 3-in. concrete, greater than $5\frac{1}{2}$ in. under 5-in. concrete, and greater than $7\frac{3}{4}$ in. under 7-in. concrete will increase the moment capacity of the section above that which can be sustained by concrete alone.

Beams for Stress Study—Beams described earlier in this report were tested to examine the validity of the preceding computations. The beams were loaded on simple supports for a direct comparison with the analysis. Similar beams were supported on rubber pads to note whether horizontal restraint developed.

Static load tests were made on 9-, 7-, and 5-in. concrete beams and also on 7B6, 5B6 and 3B9 composite beams. Three specimens of each type were tested on simple supports and three each on continuous supports. Mid-span deflections and upper and lower surface strains were measured. Data are shown in Figures 13a and b.

Theoretical calculations of deflections and strains were made for the simply supported beams with partial uniform load. The formulas reduced to

$$\text{Deflection, } y = \frac{948P}{EI}; \text{ Moment, } M = \frac{15P}{2}; \text{ Strain, } \epsilon = \frac{15Pc}{2EI} \qquad (8)$$

The data indicated that the moduli of the beam materials were lower than those of the pavements. Small batches and differences in length of curing time of the cement-treated material probably contributed to this discrepancy. Also, the CTS portions of the beams were compacted by static compression as against dynamic tamping for the pavement slabs.

Elastic moduli for concrete beams were computed from experimental deflections and found to vary from 4.0 to 4.4 million psi. To locate the theoretical deflection and strain lines in the figure, a modulus of 4.2 million psi was assumed.

Data from composite beam tests deviated considerably from linearity, and the theoretical lines in these charts were compromises using a modulus ratio n = 10. The usual transformed section analysis method was employed to obtain c and I for each composite beam.

There was sufficient scatter in the tests on concrete beams to obscure any effect that the continuous support might have had on reducing the ratio of tensile to compressive strains below those measured on simply supported beams. From these limited data it must be assumed that compressive strains on the top of concrete pavements at slab edges are approximately equal to the tensile strains on the lower surface up to the

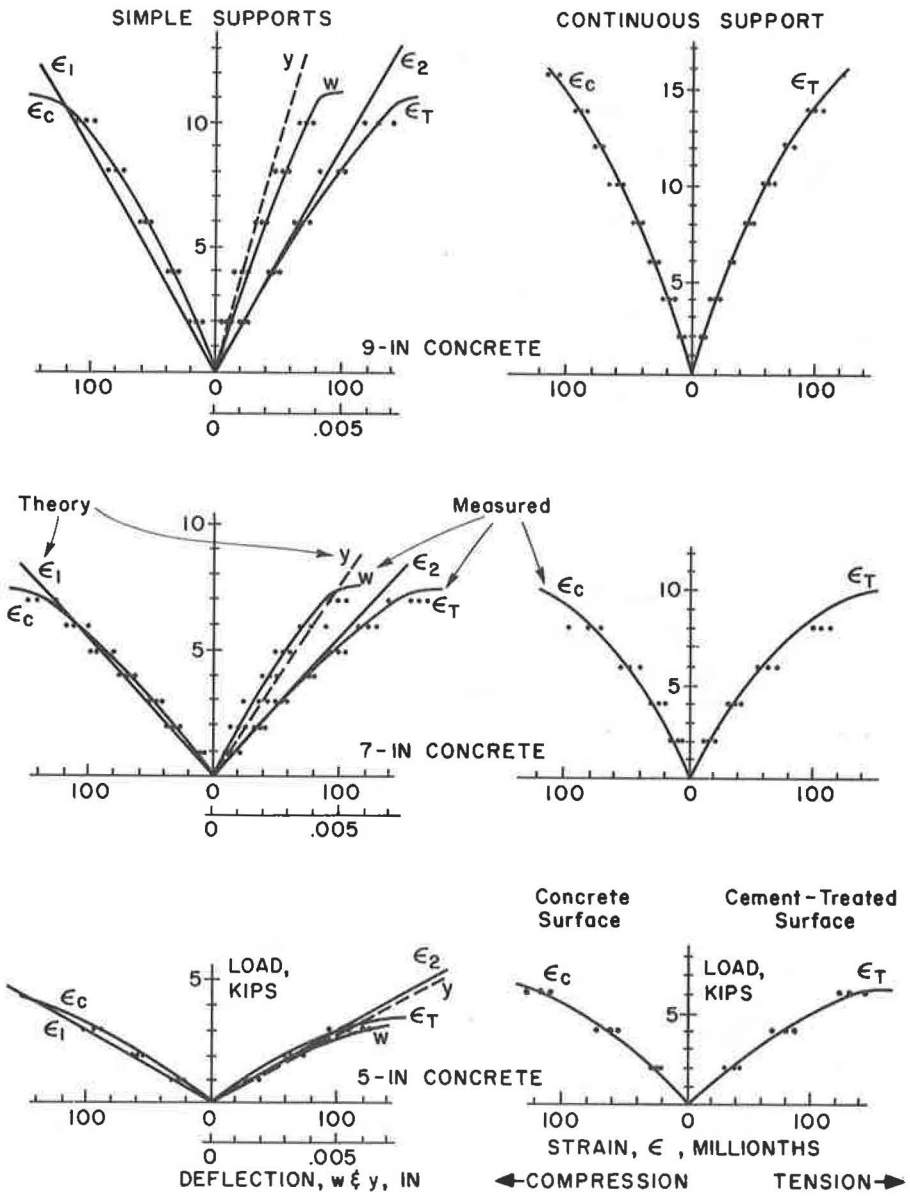


Figure 13a. Effect of support on surface strain in plain concrete beams.

state of fracture. The beam tests on continuous support showed, however, that fracture could occur in the CTS surface and not be evident at the concrete surface. In all cases no failure could be seen on the compressive face of the concrete even though the beam was overloaded and the fracture extended to within ¼ in. of the concrete surface.

From the tests on composite beams it was also concluded that tensile strains in the CTS could be approximated from measured compressive strains in the concrete. For the beams tested, CTS strain magnitudes were two to three times those of the concrete, the correct ratio depending on the beam composition.

A program of repetitive load studies on beams on continuous supports to obtain curves relating stress level and repetitions is now beginning. One of the difficulties encountered is the criterion for test termination because the specimens continue to

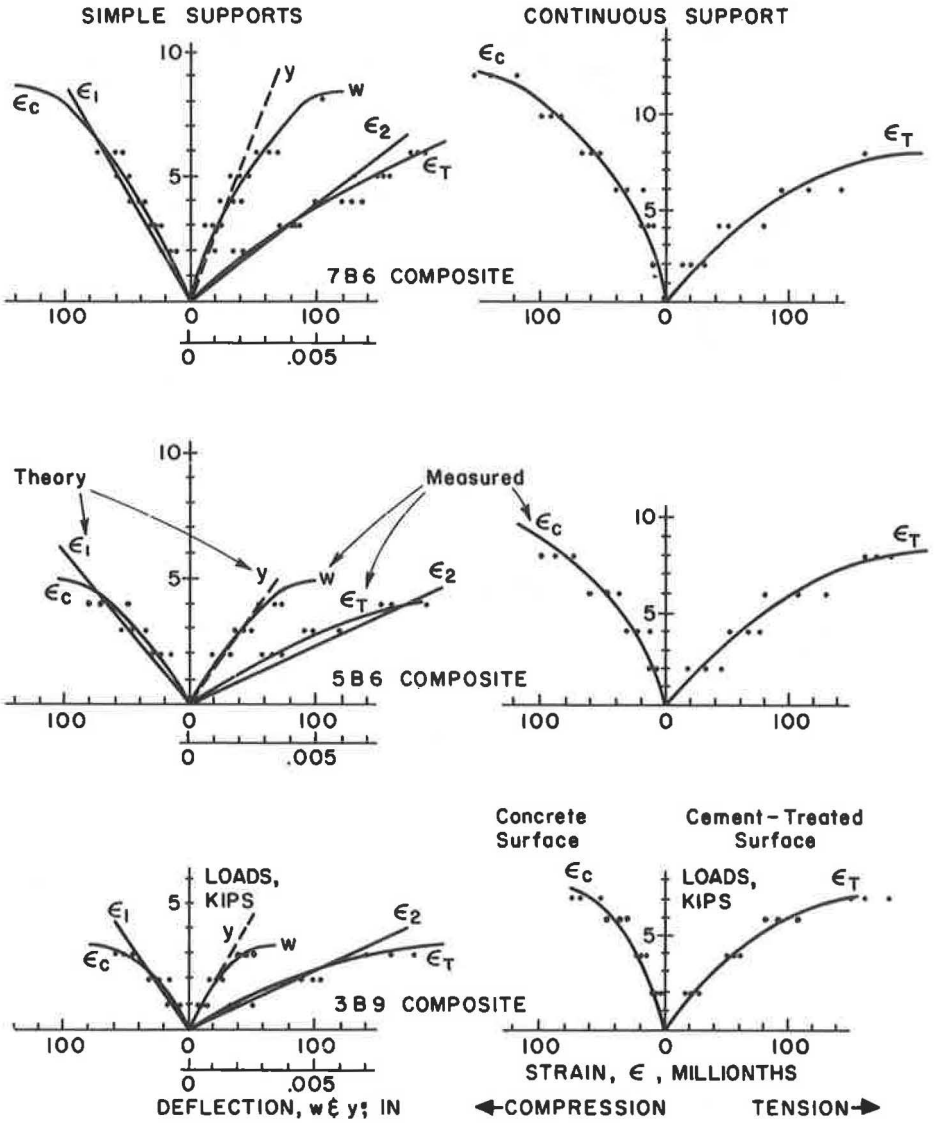


Figure 13b. Effect of support on surface strain in composite beams.

support load after almost complete fracture. This same condition exists in pavements where fractures serve as plastic hinges until such time as the foundation is weakened and total separation or faulting occurs.

## Repetitive Loads on Pavements

After completion of static load tests on curled slabs, repetitive loads were applied to a number of pavements to test their endurance. Positions selected for the test were free edge, doweled corner and undoweled corner. Loads were applied with a mechanical two-mass oscillator at rates from 180 to 240 rpm. The two 800-lb masses were capable of producing vertical thrusts up to 10, 000 lb. Rate of rotation, eccentricity and ballast were adjusted to obtain the desired load range. Results are summarized in Table 10.

TABLE 10

REPETITIVE LOAD RECORD

| Pavement | Position | Load (kips) | | Max. Defl. (in.) | Max. Conc. Strain ($10^{-6}$) | Cycles to First Crack | Cycles to End of Test |
|---|---|---|---|---|---|---|---|
| | | Max. | Min. | | | | |
| 3N6 | Edge | 9 | 1.5 | 0.085 | 140 | — | 1,500,000 |
| 3S6 | Edge | 11 | 2.0 | 0.095 | 135 | — | 1,750,000 |
| 3S6 | Und. cor. | 11 | 2.0 | 0.120 | 140 | 300,000 | 500,000 |
| 3S9 | Und. cor. | 14 | 2.6 | 0.130 | 115 | 200,000 | 2,000,000 |
| 3S9 | Dow. cor. | 14 | 2.6 | 0.090 | 110 | 250,000 | 2,100,000 |
| 5S6 | Und. cor. | 14 | 2.6 | 0.065 | 105 | 280,000 | 1,400,000 |
| 5B6 | Edge | 14 | 2.6 | 0.080 | 95 | — | 3,300,000 |
| 5N9 | Und. cor. | 15 | 3.1 | 0.070 | 100 | 500,000 | 2,500,000 |
| 5N9 | Dow. cor. | 15 | 3.1 | 0.065 | 35 | 500,000 | 2,000,000 |
| 5S9 | Und. cor. | 16 | 3.7 | 0.075 | 75 | — | 2,300,000 |
| 5S9 | Edge | 16 | 3.7 | 0.070 | 80 | — | 2,000,000 |
| 7S3 | Und. cor. | 16 | 3.7 | 0.075 | 72 | — | 1,500,000 |
| 7N3 | Dow. cor. | 16 | 3.7 | 0.070 | 80 | — | 1,400,000 |
| 7N3 | Und. cor. | 16 | 3.7 | 0.070 | 85 | — | 1,000,000 |
| 7B6 | Edge | 17 | 4.0 | 0.065 | 55 | — | 2,500,000 |

TABLE 11

STRESS DUE TO REPEATED LOADS AT PAVEMENT EDGE

| Pavement | $\epsilon_1$ ($10^{-6}$) | $\epsilon_2$ ($10^{-6}$) | $E_{cts}$ ($10^6$psi) | $\sigma_2$ (psi) | MR (psi) | $\frac{\sigma_2}{MR}$ (%) |
|---|---|---|---|---|---|---|
| 3N6 | 140 | 280 | 1.6 | 450 | 108 | >100 |
| 3S6 | 135 | 270 | 1.4 | 378 | 110 | >100 |
| 5B6 | 95 | 182 | 1.3 | 237 | 120 | >100 |
| 5S9 | 80 | 159 | 1.4 | 223 | 135 | >100 |
| 7B6 | 55 | 98 | 1.1 | 108 | 90 | >100 |

TABLE 12

STRESS DUE TO REPEATED LOADS AT JOINT CORNERS

| Pavement | Joint | Max. Strain ($10^{-6}$) | $E_{conc.}$ ($10^{-6}$) | Max. Stress (psi) | MR (psi) | $\frac{\sigma_{max}}{MR}$ (%) | $\sigma_g$ Goodman Max. Stress (psi) | $\frac{\sigma_{max}}{\sigma_g}$ (%) |
|---|---|---|---|---|---|---|---|---|
| 3S6 | No dowel | 140 | 5.9 | 826 | 710 | >100 | 546 | >100 |
| 3S9 | No dowel | 115 | 5.4 | 620 | 680 | 91 | 523 | >100 |
| 3S9 | Doweled | 110 | 5.4 | 593 | 680 | 87 | 490 | >100 |
| 5S6 | No dowel | 105 | 5.3 | 556 | 705 | 79 | 486 | >100 |
| 5N9 | No dowel | 100 | 5.8 | 580 | 650 | 89 | 480 | >100 |
| 5N9 | Doweled | 85 | 5.8 | 493 | 650 | 76 | 471 | >100 |
| 5S9 | No dowel | 75 | 5.2 | 390 | 690 | 57 | 450 | 88 |
| 7S3 | No dowel | 72 | 6.0 | 432 | 780 | 55 | 491 | 88 |
| 7N3 | No dowel | 85 | 5.6 | 475 | 715 | 66 | 458 | >100 |
| 7N3 | Doweled | 80 | 5.6 | 450 | 715 | 63 | 472 | 95 |

For loads at pavement edges, the CTS was in tension and the stress in the CTS material was calculated from recorded concrete strains and the strain ratios in Table 9. It was assumed that these ratios prevailed, although not all pavements were bonded. These calculated strains multiplied by elastic moduli from Table 2 determined stresses which were then compared with modulus of rupture values, also in Table 2, to find the ratio of actual stress to rupture stress. Table 11 gives these results for the five pavements subjected to edge loads. In all cases the modulus of rupture of the CTS was exceeded, but the pavements nevertheless endured 1.5 million or more cycles without indication of concrete failure.

When loads were at pavement corners the concrete was in tension. Four pavements were tested at undoweled corners only, and three pavements tested at both doweled and undoweled corners.

Table 12 is a compilation of strains, elastic moduli, stresses, and moduli of rupture necessary for the calculation of the ratio of maximum stresses to modulus of rupture. Because the maximum to MR ratio was low in several instances, and the minimum load on the slabs was appreciable, a Goodman diagram assuming infinite life at 50 percent MR was drawn to estimate the maximum stresses above which eventual fatigue would be expected (11). These stresses are listed in the last column, and it is seen that the actual maximum stresses, $\sigma_{max}$, exceeded the Goodman maximum on all but three pavements.

The test record (Table 10) showed that the concrete responded according to the Goodman predictions in all cases except 7N3 when loaded at the undoweled corner. Here fracture was predicted but had not actually occurred at the end of 1 million repetitions.

Although the concrete cracked under corner loads in six cases, these developed into faults on two pavements only. The thin 3S6 design faulted at 500,000 applications of the 11,000-lb load and the 5S6 design faulted at 900,000 applications of a 14,000-lb load. In each of these cases the joint was undoweled. In the four remaining tests no faulting developed, although the test was extended to at least two million cycles.

In three instances the doweled and undoweled joints could be compared, namely, 3S9, 5N9 and 7N3. There was no significant difference in endurance. The crack in the undoweled corner of 3S9 appeared about 50,000 cycles sooner than that in the doweled corner, but no progressive deterioration was observed in either case. Higher corner deflections in the undoweled joint may have contributed to earlier cracking. Pavement 5N9 gave parallel performance for both doweled and undoweled joints, although cracks occurred in the concrete at about 500,000 cycles. In 7N3 pavements no failure occurred in either case.

Test loads exceeded 9,000 lb on all structures except 3N6, and the only design removed from test before attaining 1 million load cycles was 3S6 with 11,000 lb on an undoweled corner. This evidence suggests that roads of composite pavements of concrete on cement-treated subbases will have good endurance under the repetitive loads imposed by traffic.

## SUMMARY AND CONCLUSIONS

Tests on pavements of concrete on cement-treated subbases reported to the Highway Research Board in 1964 were extended and bitumen interlayer treatments were included. Supplementary tests were made on beams to explore the ratio of concrete surface stress to cement-treated surface stress, and the effect of continuous beam support on this relation. A number of pavements were subjected to repetitive load tests at edges, doweled joint corners and undoweled joint corners.

Static-load studies on the composite pavements corroborated the results from earlier tests on designs with sand-cement grout bond and polyethylene film. Pavements with bitumen interlayer were not consistently better than unbonded pavements. On the average, the bitumen bond added very little to deflection resistance. Grout bond improved the section as much as might be realized by adding about $\frac{3}{4}$ in. of concrete.

Composite pavements of concrete on CTS were very effective in resistance to deflection. Additional resistance to edge load deflection was achieved by constructing the CTS 1 ft wider than the concrete.

Empirical charts were developed to relate composite pavements to equivalent plain concrete slabs without subbases, both supported by a basic foundation with k = 100 pci. The charts are suitable for pavements subjected to predominant loading (a) at interior locations; (b) along edges, either with the subbase flush with the concrete or extending 1 ft beyond the slab edge; and (c) at corners with good load transfer.

The cement-treated subbase contributed significantly to load transfer across joints, no joint being less than 84 percent effective. Dowels across the joint did not add significantly to load transfer under static loads.

Limited beam tests made to study stress distribution indicated that continuous support on rubber did not alter the ratio of upper to lower surface stresses appreciably from those observed for similar beams on simple supports. This observation permits calculation of CTS stresses from measured strains on the concrete surface when the elastic moduli are know.

Repetitive load tests on selected pavements proved that composite pavements have excellent endurance. Although the pavements were tested at loads considerably greater than those for which they were designed, there were no fatigue failures in the concrete under edge repetitions, and only limited cracking in pavements subjected to these repeated heavy loads at corners.

## REFERENCES


1. Reid, C. R. Concrete Pavement Subgrade Design, Construction, Control. HRB Proc., Vol. 19, 1939, pp. 541-551.
2. Hveem, F. N., and Zube, E. California Mix Design for Cement-Treated Bases. Highway Research Record 36, 1963, pp. 11-55.
3. Childs, L. D. Tests of Concrete Pavement Slabs on Cement-Treated Subbases. Highway Research Record 60, 1963, pp. 39-58; PCA Develop. Dept. Bull. D86.
4. Felt, E. J., and Abrams, M. S. Suggested Method of Making and Curing Soil-Cement Compression and Flexure Test Specimens in the Laboratory. ASTM Proc. for Testing Soils, 1958, p. 475.
5. Nowlen, W. J. Techniques and Equipment for Field Testing of Pavements. Jour. PCA R&D Labs, Vol. 6, No. 3, Sept. 1964; PCA Develop. Dept. Bull. D83.
6. Westergaard, H. M. Computation of Stresses in Concrete Roads. HRB Proc., Vol. 5, pt. 1, 1925, pp. 90-112.
7. Westergaard, H. M. New Formulas for Stresses in Concrete Pavements for Airfields. Proc. ASCE, Vol. 73, 1947.
8. Childs, L. D., and Kapernick, J. W. Tests of Concrete Pavements on Gravel Subbases. Proc. ASCE, Vol. 84 (HW 3), Oct. 1958; PCA Develop. Dept. Bull. D21.
9. Nussbaum, P. J., and Larsen, T. J. Load-Deflection Characteristics of Soil-Cement Pavements. Highway Research Record 86, 1965, pp. 1-14; PCA Develop. Dept. Bull. D96.
10. Teller, L. W., and Sutherland, E. C. A Study of the Structural Action of Several Types of Transverse and Longitudinal Joint Design. Public Roads, Vol. 17, No. 7, Sept. 1936.
11. Murdock, J. W. A Critical Review of Research on Fatigue of Plain Concrete. Univ. of Ill. Eng. Exp. Station, Bull. 475, Feb. 1965.
12. Kawala, E. L. Cement-Treated Subbase Practice in U. S. and Canada. Proc. ASCE, Vol. 92 (HW 2), Paper 4947, Oct. 1966.

# Estimating the Distribution of Axle Weights For Selected Parameters

KENNETH W. HEATHINGTON and PAUL R. TUTT, Texas Highway Department

An analysis of truck weight data taken in 1960 through 1963 by the Planning Survey Division of the Texas Highway Department was made. Loadometer stations were grouped according to different parameters, and three procedures for estimating an axle weight distribution for any given highway location in Texas were studied. The equivalent 18-kip single-axle applications were calculated at each location using each method of estimating an axle-weight distribution. Truck traffic characteristics of seven types of trucks are reported.

•WITH the conclusion of the AASHO Road Test in 1960 and with the concepts of pavement design originating from the test, new emphasis has been placed on the importance of accounting for the effect of repetitions of axle loads of different weights on highway pavements. The AASHO procedure for the design of highway pavements utilizes axle weight and the number of times axles of a given weight will use the pavement during its design life. In this design procedure, each axle weight is related on the basis of equivalent destructive effect to an 18-kip single-axle load (2).

For many years in Texas, pavements were designed structurally to account for the relationship of a design-wheel load to the stresses produced in the pavement. The design-wheel load was taken as the average of the ten heaviest wheel loads (ATHWL) on an average or representative day on the particular highway or farm-to-market road being designed. The ATHWL was a statistic that was found to be fairly stable over a period of time for any given section of road (3). However, since the introduction of the equivalent wheel load concept of the AASHO Road Test, much more information is needed about the magnitude and number of repetitions of all axle loads on highway pavements. To obtain the data needed for the structural design of pavements for all areas of Texas using the actual axle distribution for each area would require more loadometer stations than would be economically feasible. Thus, some method of relating the axle-weight distribution at one location to that at another for pavement design purposes is needed. To evaluate the feasibility of designing pavements for a selected location on the basis of related axle-weight information from other locations, the frequency with which axle weights of a given magnitude occur has been studied by grouping the data into the following categories: (a) loadometer stations having the same percent trucks, (b) a highway-system classification, and (c) statewide area.

Axle weights from 86, 805 trucks were used in this study. These vehicles were samples taken from the truck traffic on Texas highways from 1960 through 1963. The purpose of this study is to determine whether any of the three methods of grouping data provides an acceptable means for estimating an axle-weight distribution for a given location.

## LOADOMETER STATION OPERATION

### Regular Loadometer Stations

The Planning Survey Division of the Texas Highway Department operates 21 regular loadometer stations on a scheduled basis. Nineteen of these are located in rural areas

Paper sponsored by Committee on Flexible Pavement Design and presented at the 46th Annual Meeting.

and are operated periodically throughout each 12-month period. Two stations are located in urban areas and are operated periodically only during June, July, and August.

The 21 stations are located on three types of facilities. For the purpose of this study, a Type A facility meets, or at least approaches, Interstate design standards. It consists primarily of a four-lane divided highway and the truck traffic consists predominantly of through movements. Local truck movements constitute only a minor portion of the truck traffic. A Type B facility is a primary highway that has two or more lanes. Generally, it is undivided and is below interstate design standards. The truck-traffic stream contains more local traffic than for the Type A facility but still consists primarily of through truck movements. A Type C facility is one on which truck trips are predominantly local. Long-haul truck movements are minor. Of the 21 regular loadometer stations, 7 are on Type A facilities, 10 are on Type B facilities, and 4 are on Type C facilities.

A six-man crew operates the 21 regular loadometer stations on a periodic basis. The crew consists of a party chief and five helpers and moves about on a fixed schedule from one station to another. In addition to weighing the trucks, the six-man crew obtains the following information:

1. The origin and destination of each truck trip,
2. The direction of travel (inbound or outbound),
3. Whether the truck is loaded or empty,
4. The commodities carried,
5. The length of trip,
6. Whether the trip is intrastate or interstate,
7. The type of license of the truck,
8. The manufacturer's rated capacity,
9. The type of fuel being used,
10. The name and address of the truck owner,
11. The vehicle's classification as to type,
12. The type of body,
13. The axle spacing,
14. The wheelbase,
15. The height of the truck,
16. The width of the truck,
17. The total number of vehicles passing the loadometer station during the period or operation, and
18. The classification of each vehicle according to a standard coding system.

At each of the 19 regular loadometer stations located in rural areas, trucks are weighed during one 8-hr period each month. During this time, 4 hr of weighing operations are conducted for truck traffic traveling in one direction and 4 hr of operation are performed for truck traffic moving in the opposite direction. The three shifts of operation are from 6:00 a. m. to 2:00 p. m., 2:00 p. m. to 10:00 p. m., and 10:00 p. m. to 6:00 a. m. Each station is operated for a different 8-hr shift each month. Therefore, every 3 months, 24 hr of weighing operations are completed for each regular loadometer station. Over a period of one year, 96 hr of weighing operations are completed for each regular loadometer station. The two regular loadometer stations located in urban areas completed 24 hr of weighing operations in one year at each station.

The average daily truck traffic is the number of trucks which pass a given point on a highway on an average, or representative, day. Essentially, it is the total truck traffic for one year divided by 365. Table 1 gives the number of trucks that were weighed in a year's operation at each regular loadometer station in 1960, 1961, and 1962. The number of trucks weighed is expressed as a percent of the average daily truck traffic at that location. It is seen that the total number of trucks which were actually weighed at each station in one year varied considerably, but that the ratio of the number of trucks weighed to the average daily truck traffic was roughly 150 percent.

Seasonal variations in weights no doubt occur; however, this report does not deal with this variation. It is assumed that the seasonal fluctuations are not critical because of the aggregation of the data into large groups. A stratification of the data for interpretation would probably be desirable.

TABLE 1

RATIO OF NUMBER OF TRUCKS WEIGHED TO AVERAGE DAILY TRUCKS FOR REGULAR LOADOMETER STATIONS

| Station Number | ADT | Average Daily Trucks | Number of Trucks Weighed | Ratio (percent) |
|---|---|---|---|---|
| | | (a) 1960 | | |
| L-7 | 2500 | 355 | 550 | 154.9 |
| L-10-1 | 1640 | 307 | 528 | 172.0 |
| L-10-2 | 3490 | 771 | 949 | 123.1 |
| L-16 | 5160 | 686 | 1139 | 166.0 |
| L-20 | 6740 | 863 | 1317 | 152.6 |
| L-20-1 | 6300 | 1071 | 1671 | 156.0 |
| L-20-2 | 8270 | 1075 | 1620 | 150.7 |
| L-20-3 | 5680 | 903 | 1642 | 181.8 |
| L-30-1 | 5110 | 915 | 1301 | 142.2 |
| L-35-1 | 10670 | 1120 | 2499 | 223.1 |
| L-37-1 | 2970 | 743 | 906 | 121.9 |
| L-42 | 3320 | 382 | 485 | 127.0 |
| L-45-1 | 7540 | 1440 | 1651 | 114.7 |
| L-45-2 | 5870 | 1403 | 796 | 56.7 |
| L-72 | 4720 | 854 | 1230 | 144.0 |
| L-81 | 2360 | 510 | 756 | 148.2 |
| L-88 | 4390 | 1054 | 1704 | 161.7 |
| L-145 | 3800 | 787 | 1367 | 173.7 |
| L-147 | 1310 | 236 | 345 | 146.2 |
| L-149 | 1870 | 471 | 713 | 151.4 |
| 3-UP | 17823 | 1069 | 329 | 30.8 |
| 4-US | 9821 | 648 | 153 | 23.6 |
| | | (b) 1961 | | |
| L-7 | 2630 | 400 | 555 | 138.8 |
| L-10-1 | 1720 | 335 | 431 | 128.7 |
| L-10-2 | 3730 | 847 | 1063 | 125.5 |
| L-16 | 5340 | 651 | 1089 | 167.3 |
| L-20 | 7380 | 1041 | 1544 | 148.3 |
| L-20-1 | 6180 | 1112 | 1548 | 139.2 |
| L-20-2 | 8630 | 1217 | 2312 | 190.0 |
| L-20-3 | 6190 | 1028 | 1735 | 168.8 |
| L-30-1 | 4920 | 940 | 1553 | 165.2 |
| L-35-1 | 11310 | 1278 | 2401 | 187.9 |
| L-37-1 | 3060 | 701 | 1071 | 152.8 |
| L-42 | 3290 | 342 | 485 | 141.8 |
| L-45-2 | 5790 | 1401 | 3112 | 222.1 |
| L-72 | 4950 | 881 | 1408 | 159.8 |
| L-81 | 2700 | 618 | 1147 | 185.6 |
| L-88 | 4690 | 1107 | 1704 | 153.9 |
| L-145 | 4310 | 922 | 1681 | 182.3 |
| L-147 | 1250 | 221 | 317 | 143.4 |
| L-149 | 1750 | 448 | 692 | 154.5 |
| 3-UP | 18056 | 1138 | 325 | 28.6 |
| 4-US | 16420 | 706 | 150 | 21.2 |
| | | (c) 1962 | | |
| L-7 | 2860 | 383 | 623 | 162.7 |
| L-10-1 | 1570 | 294 | 451 | 153.4 |
| L-10-2 | 3300 | 736 | 1400 | 190.2 |
| L-16 | 5490 | 752 | 1082 | 143.9 |
| L-20 | 3160 | 240 | 425 | 177.1 |
| L-20-1 | 6960 | 1260 | 1911 | 151.7 |
| L-20-2 | 8820 | 1173 | 2067 | 176.2 |
| L-20-3 | 6390 | 1080 | 1889 | 174.9 |
| L-30-1 | 4740 | 1090 | 1783 | 163.6 |
| L-35-1 | 11940 | 1276 | 2074 | 162.5 |
| L-37-1 | 2760 | 591 | 1029 | 174.1 |
| L-42 | 3010 | 313 | 381 | 121.7 |
| L-45-2 | 5830 | 1656 | 2781 | 167.9 |
| L-72 | 4650 | 879 | 1492 | 169.7 |
| L-81 | 2630 | 597 | 1149 | 192.5 |
| L-88 | 4780 | 1166 | 1592 | 136.5 |
| L-145 | 4390 | 887 | 1232 | 138.9 |
| L-147 | 1280 | 259 | 435 | 167.9 |
| L-149 | 1870 | 454 | 695 | 153.1 |
| 3-UP | 17104 | 1214 | 358 | 29.5 |
| 4-US | 25283 | 1062 | 306 | 28.8 |

TABLE 2

RATIO OF NUMBER OF TRUCKS WEIGHED TO AVERAGE DAILY TRUCKS FOR SPECIAL LOADOMETER STATIONS, 1963

| Station Number | ADT | Average Daily Trucks | Number of Trucks Weighed | Ratio (percent) |
|---|---|---|---|---|
| MS-47 | 1290 | 194 | 29 | 14.9 |
| MS-54 | 880 | 143 | 87 | 60.8 |
| MS-103 | 1580 | 199 | 200 | 100.5 |
| 121-A | 2810 | 747 | 493 | 66.0 |
| M-173 | 1390 | 243 | 172 | 70.8 |
| M-175 | 640 | 118 | 154 | 130.5 |
| M-176 | 710 | 99 | 94 | 94.9 |
| 178 | 700 | 143 | 109 | 76.2 |
| M-278 | 400 | 69 | 74 | 107.2 |
| M-500 | 560 | 125 | 106 | 84.8 |
| M-526 | 1300 | 88 | 96 | 109.1 |
| M-620 | 1070 | 131 | 27 | 20.6 |
| M-675 | 1290 | 163 | 134 | 82.2 |
| 724 | 330 | 38 | 40 | 105.3 |
| M-778 | 1320 | 187 | 97 | 51.9 |
| M-882 | 320 | 29 | 67 | 231.0 |
| 901 | 1050 | 190 | 78 | 41.1 |
| 903 | 820 | 156 | 115 | 73.7 |
| 904 | 650 | 120 | 108 | 90.0 |
| 905 | 1360 | 220 | 85 | 38.6 |
| 906 | 1110 | 123 | 76 | 61.8 |
| 907 | 690 | 139 | 88 | 63.3 |
| 908-A | 1680 | 141 | 82 | 58.2 |
| 909 | 1230 | 128 | 95 | 74.2 |
| 911 | 1420 | 186 | 80 | 43.0 |
| 912 | 1560 | 183 | 130 | 71.0 |
| 913 | 1290 | 166 | 67 | 40.4 |
| 914 | 1350 | 234 | 104 | 44.4 |
| 915 | 960 | 61 | 57 | 93.4 |
| 917 | 1550 | 171 | 72 | 42.1 |
| 919 | 1940 | 167 | 72 | 43.1 |
| 921 | 900 | 206 | 100 | 48.5 |
| 922 | 1490 | 235 | 126 | 53.6 |
| 923 | 1280 | 274 | 84 | 30.7 |
| 926 | 1380 | 161 | 127 | 78.9 |
| 927 | 470 | 52 | 55 | 105.8 |
| 929 | 1160 | 137 | 95 | 69.3 |
| 930 | 860 | 101 | 60 | 59.4 |
| 931 | 1060 | 73 | 94 | 128.8 |
| 935 | 1080 | 137 | 78 | 56.9 |
| 936 | 1710 | 180 | 127 | 70.6 |
| 937 | 1660 | 151 | 100 | 66.2 |
| 939 | 1810 | 363 | 263 | 72.5 |
| 940 | 1280 | 110 | 41 | 37.3 |
| 941 | 1720 | 110 | 52 | 47.3 |
| 942 | 1530 | 243 | 106 | 43.6 |
| 943 | 1160 | 153 | 99 | 64.7 |
| 944 | 370 | 50 | 27 | 54.0 |
| 945 | 850 | 126 | 90 | 71.4 |
| 946 | 490 | 55 | 40 | 72.7 |
| 949 | 1550 | 281 | 138 | 49.1 |
| 950 | 540 | 62 | 57 | 91.9 |
| 951 | 960 | 132 | 103 | 78.0 |
| 952 | 1130 | 182 | 174 | 95.6 |
| 953 | 1200 | 168 | 146 | 86.9 |
| 954 | 940 | 222 | 105 | 47.3 |
| 955 | 370 | 85 | 52 | 61.2 |
| 956 | 1150 | 158 | 166 | 105.1 |
| 957 | 710 | 57 | 74 | 129.8 |
| 959 | 1440 | 158 | 117 | 74.1 |
| 960 | 1810 | 136 | 98 | 72.1 |
| 961 | 1160 | 84 | 52 | 61.9 |
| 1000 | 560 | 68 | 38 | 55.9 |
| 1001 | 1240 | 234 | 61 | 26.1 |
| 1002 | 1080 | 217 | 95 | 43.8 |
| 1003 | 500 | 117 | 56 | 47.9 |
| 1004 | 1340 | 168 | 118 | 70.2 |

TABLE 2 (Continued)

RATIO OF NUMBER OF TRUCKS WEIGHED TO AVERAGE DAILY TRUCKS FOR SPECIAL LOADOMETER STATIONS, 1963

| Station Number | ADT | Average Daily Trucks | Number of Trucks Weighed | Ratio (percent) |
|---|---|---|---|---|
| 1005 | 1050 | 151 | 103 | 68.2 |
| 1006 | 760 | 165 | 146 | 88.5 |
| 1007 | 1220 | 211 | 164 | 77.7 |
| 1008 | 550 | 73 | 66 | 90.4 |
| 1009 | 1800 | 284 | 93 | 32.7 |
| 1010 | 810 | 101 | 84 | 83.2 |
| 1011 | 380 | 40 | 33 | 82.5 |
| 1012 | 1320 | 162 | 120 | 74.1 |
| 1013 | 1620 | 245 | 159 | 64.9 |
| 1014 | 920 | 146 | 27 | 18.5 |
| 1015 | 1490 | 226 | 113 | 50.0 |
| 1016 | 280 | 30 | 40 | 133.3 |
| 1017 | 1190 | 194 | 91 | 46.9 |
| 1018 | 820 | 127 | 66 | 52.0 |
| 1019 | 1630 | 209 | 67 | 32.1 |
| 1020 | 1680 | 264 | 148 | 56.1 |
| 1021 | 1510 | 180 | 84 | 46.7 |
| 1022 | 1480 | 201 | 113 | 56.2 |
| 1023 | 1350 | 90 | 84 | 93.3 |
| 1024 | 410 | 33 | 17 | 51.5 |
| 1025 | 230 | 17 | 34 | 200.0 |
| 1026 | 580 | 68 | 73 | 107.4 |
| 1027 | 1630 | 165 | 65 | 39.4 |
| 1028 | 1910 | 346 | 204 | 59.0 |
| 1029 | 750 | 89 | 95 | 106.7 |
| 1030 | 950 | 100 | 150 | 150.0 |
| 1031 | 1240 | 175 | 115 | 65.7 |
| 1032 | 1140 | 251 | 100 | 39.8 |
| 1033 | 1650 | 241 | 63 | 26.1 |
| 1034 | 1110 | 139 | 95 | 68.3 |
| 1035 | 1360 | 207 | 133 | 64.3 |
| 1036 | 1410 | 300 | 102 | 34.0 |
| 1037 | 1060 | 130 | 100 | 76.9 |
| 1038 | 850 | 89 | 60 | 67.4 |
| 1039 | 1420 | 280 | 101 | 36.1 |
| 1040 | 1140 | 127 | 52 | 40.9 |
| 1041 | 1140 | 180 | 80 | 44.4 |
| 1042 | 530 | 47 | 57 | 121.3 |
| 1044 | 420 | 90 | 76 | 84.4 |
| 1045 | 380 | 103 | 75 | 72.8 |
| 1046 | 2320 | 292 | 122 | 41.8 |
| 1047 | 1460 | 232 | 148 | 63.8 |
| 1048 | 970 | 149 | 117 | 78.5 |
| 1049 | 310 | 38 | 67 | 176.3 |
| 1050 | 1380 | 102 | 79 | 77.5 |
| 1051 | 790 | 91 | 75 | 82.4 |
| 1052 | 1430 | 176 | 86 | 48.9 |
| 1053 | 780 | 137 | 52 | 38.0 |
| 1054 | 1160 | 94 | 144 | 153.2 |
| 1055 | 260 | 14 | 14 | 100.0 |
| 1056 | 1400 | 244 | 245 | 100.4 |
| M-1497 | 660 | 63 | 52 | 82.5 |
| M-1498 | 1180 | 133 | 125 | 94.0 |

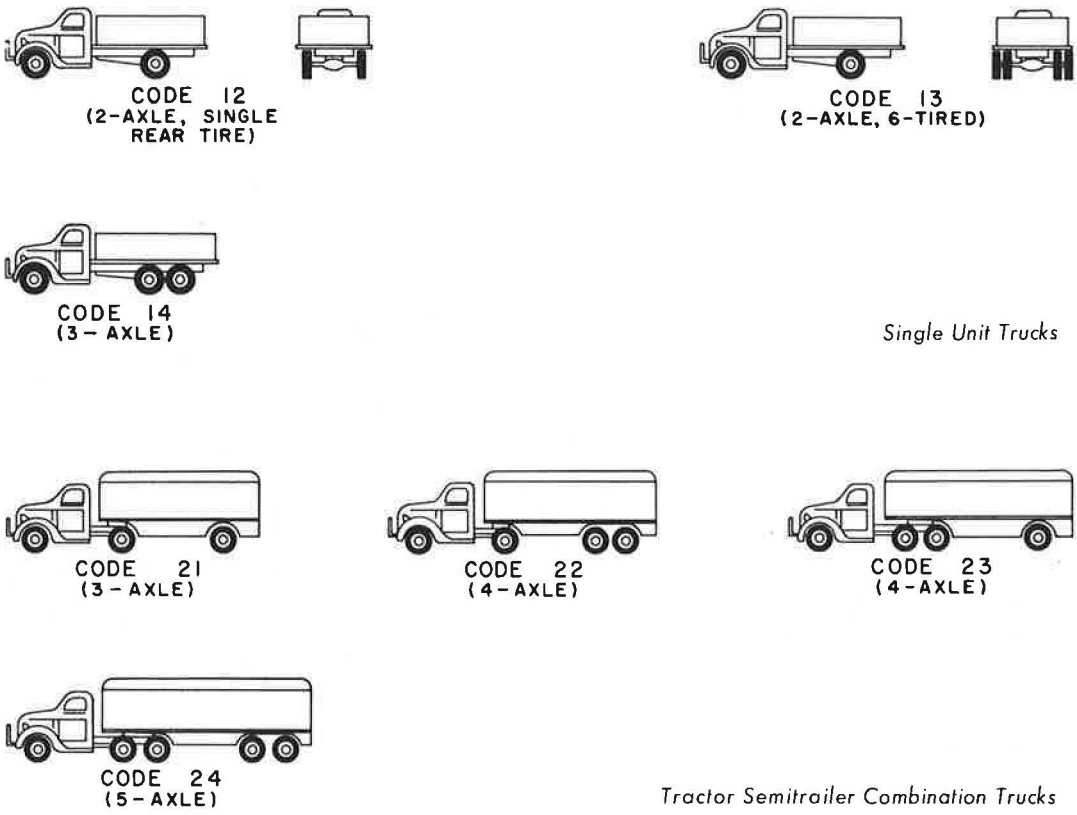


Figure 1. Types of vehicles weighed at loadometer stations.

## Special Loadometer Stations Operated in 1963

Because additional weight data were needed, a group of special loadometer stations on selected sites were operated in June, July, and August of 1963. These special stations were operated in addition to the regular stations but were not located at the same places as the regular stations. They were operated by a two-man crew who obtained only weight data and did not secure the additional information normally required of the six-man crew. The stations were operated on the same schedule of shifts as the regular stations. Each station operated for an 8-hr period and the shift of operation was rotated each month. Twenty-four hours of weighing operations were completed for each special loadometer station in the summer of 1963. Table 2 gives the percent of the average daily truck traffic that was weighed at each of the special loadometer stations. Notice that a wide range of values exists for the ratio of the number of trucks weighed to the average daily truck traffic.

## Types of Trucks Weighed

Seven types of trucks (Fig. 1) may be operated on Texas highways without obtaining special permission from the Texas Highway Department (4). Three types are single-unit trucks and four are tractor semitrailer combination trucks. Of the single-unit trucks, the 2-axle, 6-tired (Code 13) vehicle was the predominant type. The most frequently observed tractor semitrailer combination trucks were the 4-axle (Code 22) and the 5-axle (Code 24).

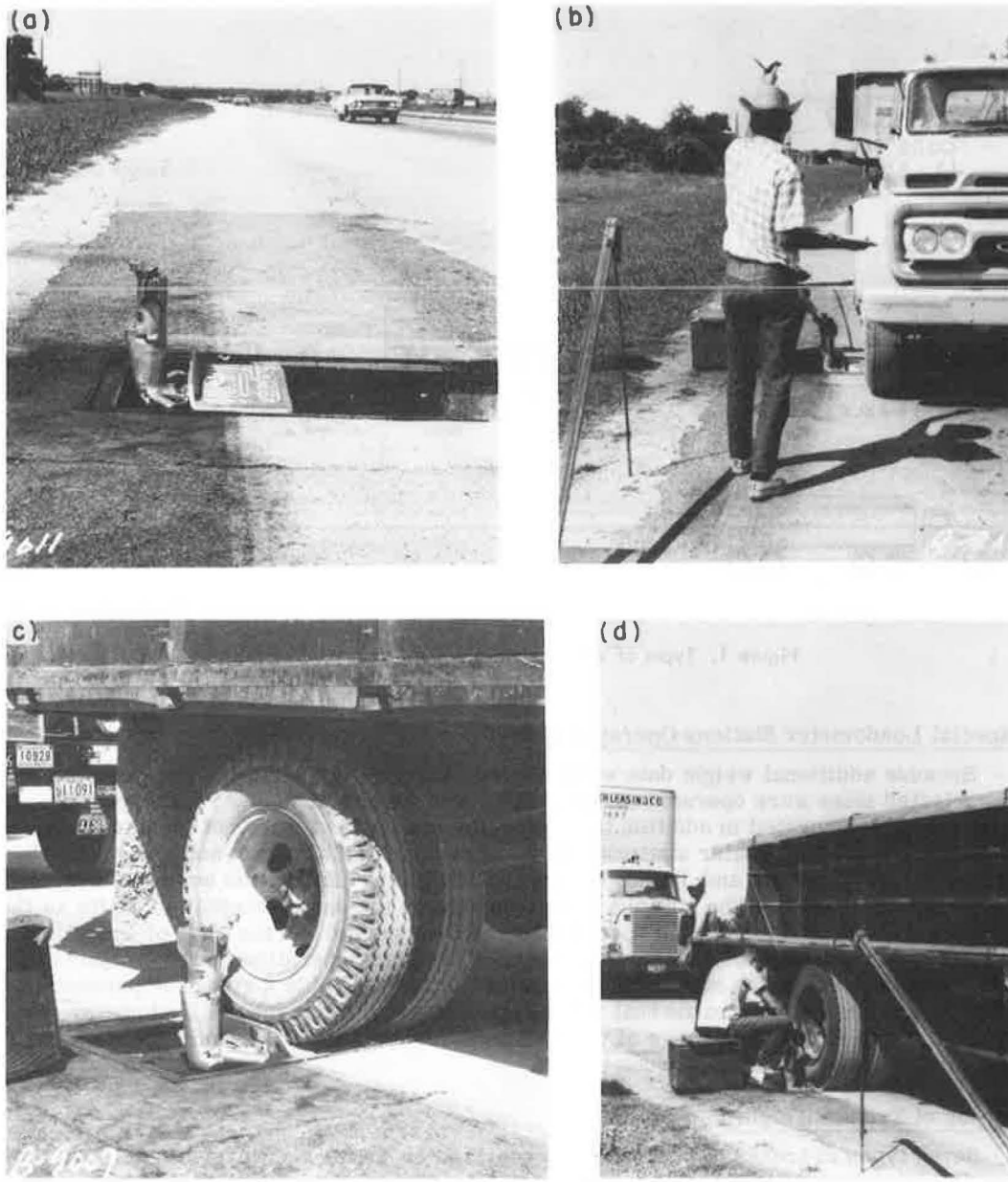


Figure 2. Loadometer station in operation: (a) loadometer flush with ground; (b) truck being guided onto loadometer; (c) wheel resting on loadometer; (d) loadometer being balanced and static weight read.

### Method of Weighing Axles and Recording Data

A Black and Decker "Hi-way" loadometer is used to measure the static weight of vehicles at each loadometer station. Figure 2 shows a loadometer station in operation. The loadometer is placed flush with the ground in a pit. One wheel of each axle is brought to rest on the loadometer and the scale operator balances the scale and records the wheel weight. The truck then moves forward and stops with each successive wheel on the scale until all wheels on one side of the truck have been weighed. To obtain the axle weight each wheel load is multiplied by two. Only the static load is measured. The data are recorded at each loadometer station by hand and later transferred to data processing cards. An attempt is made to weigh all trucks that pass the weighing station during its operation.

## DETERMINATION OF TRUCK TRAFFIC CHARACTERISTICS

### Axle Factor Determination

Traffic volumes are usually expressed in terms of the number of vehicles per unit of time, but in order to use the AASHO procedure for determining the number of applications of an equivalent 18-kip axle load, the number of axle loads passing over a given road section during some given time interval must be known. The number of axles that a truck may have under Texas law varies from 2 to 5 (Fig. 1). Because all trucks do not have the same number of axles (or axle loads), an adjusting factor must be used to convert the number of trucks to the number of axle loads that will be produced by a given volume of truck traffic. This adjusting factor is called an axle factor.

In the past, it has been suggested that an axle factor of two be used for an approximation. If the traffic volume is high and the percent of trucks is low, this is a reasonable approximation; however, for traffic on low-volume roads with a high percentage of trucks an axle factor of two is too low.

An analysis of the vehicle classification data obtained as a part of the loadometer surveys described previously has been made in order to determine whether or not a single axle factor might possibly be used to calculate reasonably precise estimates of the number of axle loads which will result from various volumes of truck traffic. A linear correlation (method of least squares) of the number of truck axles with the number of trucks was made for a statewide area and for Type A, Type B, and Type C facilities. A tandem axle is considered to be one axle, i.e., carrying one axle load, in order to conform to the AASHO design procedure. Figure 3 shows the relationship between the number of axles and the number of trucks for the statewide area. Each loadometer station in the state is represented in this plot. The total number of trucks sampled at each station for each year was plotted against the total number of axles on these trucks. There are 184 points plotted in Figure 3. The range of values for the number of trucks weighed at the various stations is broad, but a linear relationship holds regardless of the number of trucks included in the sample. The coefficient of determination is 0.999 with a standard error of the estimate of 65 axles. The slope of the regression line in Figure 3 is 2.75; therefore, for a large number of trucks in which the y-intercept is not considered to be significant, the total number of axle loads which will be produced by a given number of trucks is approximately 2.75 times the number of trucks. Or each truck, on the average, produces 2.75 axle loads. Thus, the axle factor would be 2.75 axle loads per truck.

Figures 4 through 6 show the relationship of the number of axles to the number of trucks for Type A, Type B, and Type C facilities, respectively. Again, the linear correlation is very good for all three types of facilities. Table 3 gives the coefficients of determination and correlation and the standard error of estimate for the categories used in correlating the number of axles with the number of trucks. For all methods of grouping the data, the slope of the regression line ranges from 2.75 to 2.78. The Type A facility exhibits the largest standard error of estimate of 142 axles; however, this value is small when considering thousands of axles.

Since there is only a small variation in the slope of the regression lines obtained by four different methods of grouping data, it seems that any one of the methods can be

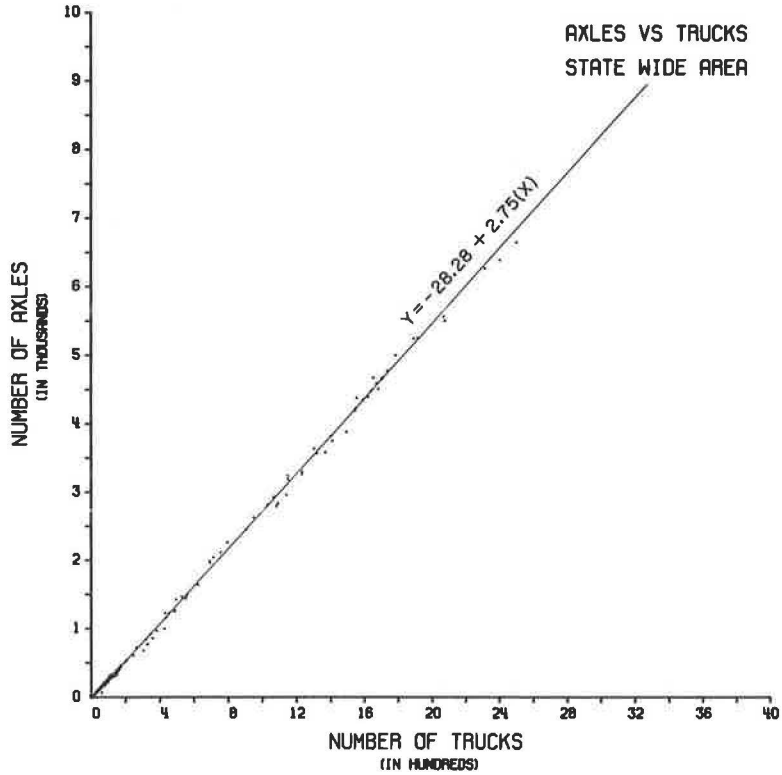


Figure 3. Correlation of the number of axles with the number of trucks for a statewide area.

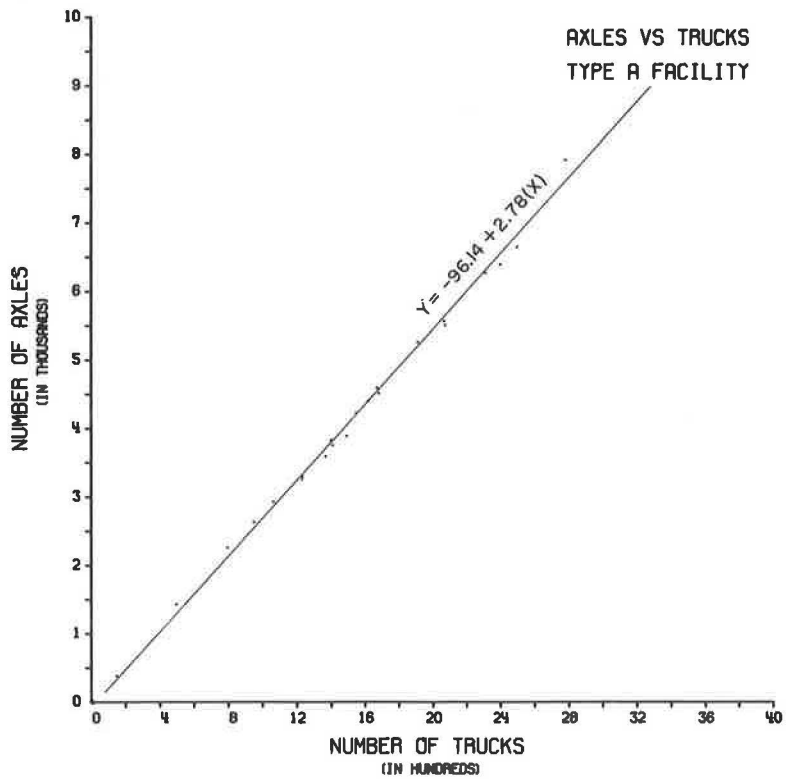


Figure 4. Correlation of the number of axles with the number of trucks for a Type A facility.

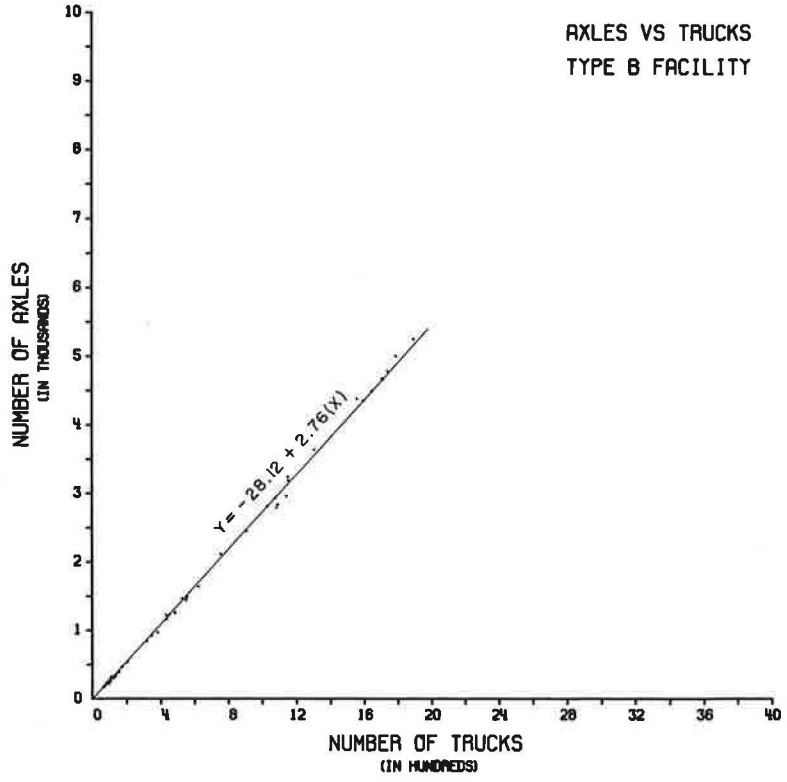


Figure 5. Correlation of the number of axles with the number of trucks for a Type B facility.

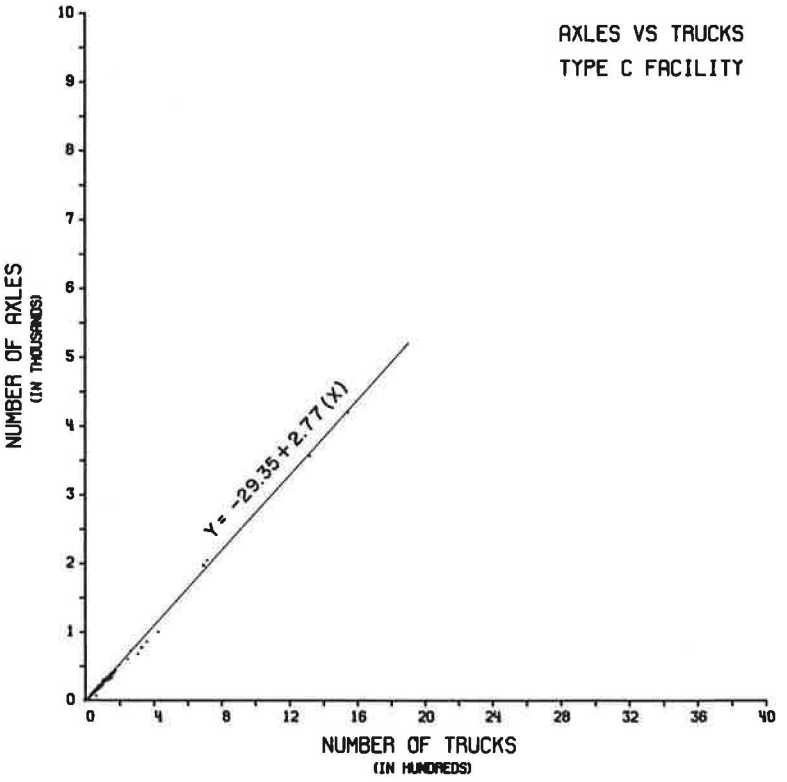


Figure 6. Correlation of the number of axles with the number of trucks for a Type C facility.

TABLE 3

SUMMARY OF CORRELATION OF NUMBER OF AXLES WITH NUMBER OF TRUCKS

| Method of Grouping Data | A | B | Coefficient of Correlation | Coefficient of Determination | Standard Error of Estimate |
|---|---|---|---|---|---|
| Statewide area | -28.28 | 2.75 | 0.999 | 0.999 | 65.30 |
| Type A facility | -96.14 | 2.78 | 0.997 | 0.995 | 141.76 |
| Type B facility | -28.12 | 2.76 | 0.999 | 0.999 | 53.45 |
| Type C facility | -29.35 | 2.77 | 0.999 | 0.997 | 38.79 |

Note: Y = A + B(X), where Y = number of axles (axle loads), X = number of trucks, B = slope of linear regression line, and A = y-intercept of linear regression line.

used to arrive at an acceptable axle factor. The statewide area method of grouping data is probably the most logical approach in determining the best axle factor for general use. For practical purposes, the axle factor is 2.75 axle loads per truck. By way of comparison, if an axle factor of 2 is used, there will be an error of about 30 percent in the estimated number of truck axles. For low-volume roads with a large percent of trucks, this is a significant error in the number of axles.

## Correlation of Type Vehicle With Percent Trucks for Statewide Area

The percent of the total trucks of a given type at each loadometer station was plotted against the percent trucks for that location. Thus, if the percent of trucks is known for a given location, then an estimate can be made of the percent of the truck traffic that will be of a given type of truck. The plots showed a linear correlation of each truck type with the percent trucks for a statewide area. There was considerable scatter of data about the linear regression line in each plot. A linear relationship does not represent these data precisely, although visual observation of the data does not indicate that a curvilinear fit of the data would be more appropriate. Table 4 shows the coefficients of determination and correlation and the standard error of estimate for the statewide area. It is seen from Table 4 that the correlations in general are poor and that the standard errors of estimate are high.

On a statewide basis, the Code 12 vehicle is very insignificant in the makeup of truck traffic. A Code 12 vehicle is a 2-axle, single-unit truck that can travel at high speeds and is primarily used for short hauls. With an increase in percent trucks, the percent of Code 13 vehicles decreased. The 2-axle, 6-tired vehicle is used primarily for short hauls and is capable of maintaining acceptable speeds on any highway. Studies have shown that as the total traffic volume becomes large the percent of trucks becomes small (5, 6). Only those trucks that are capable of maintaining speeds similar to, or nearly equal to, passenger cars will operate where the traffic volume is high. The percentage of Code 14 vehicles decreased slightly as the percent trucks increased. The

TABLE 4

SUMMARY OF CORRELATION OF TYPE VEHICLE WITH PERCENT TRUCKS

| Type Vehicle | A | B | Coefficient of Correlation | Coefficient of Determination | Standard Error of Estimate |
|---|---|---|---|---|---|
| 12 | 1.75 | -0.08 | 0.263 | 0.069 | 1.44 |
| 13 | 71.34 | -2.16 | 0.680 | 0.462 | 12.28 |
| 14 | 5.87 | -0.15 | 0.228 | 0.052 | 3.19 |
| 21 | 8.83 | 0.10 | 0.070 | 0.005 | 5.23 |
| 22 | 8.39 | 1.20 | 0.595 | 0.354 | 8.55 |
| 23 | 0.03 | 0.01 | 0.020 | 0.000 | 0.56 |
| 24 | 3.81 | 1.07 | 0.510 | 0.260 | 9.48 |

Note: Y = A + B(X), where Y = percent of the total truck traffic that is a given type of truck, X = percent trucks, B = slope of linear regression line, and A = y-intercept of linear regression line.

percent of single-unit trucks, in general, decreased as the percent trucks increased. This is due to the operating characteristics of the single-unit trucks. They are normally used for local short-haul trips, and they can maintain adequate speeds on a facility with high traffic volumes.

The percent of Code 21 vehicles remained relatively constant, increasing only slightly as the percent trucks increased. This type vehicle lends itself to longer hauls than the single-unit trucks and, in general, cannot maintain as high a speed as the single-unit trucks. There is a general increase in the percent of Code 22 type vehicles with an increase in percent trucks. This suggests that the 4-axle truck is primarily used for long hauls and that it will decrease in the percentage of trucks as the traffic volume becomes large. The number of Code 23 vehicles on Texas highways is insignificant. This type vehicle apparently does not lend itself to the transportation of commodities in any significant quantity in Texas. The 5-axle combination vehicle (Code 24) increased in the percentage of trucks as the percent trucks increased. The Code 24 vehicle is used primarily for long hauls and cannot maintain adequate speeds on high-volume roads.

The 5-axle (Code 24) and the 4-axle (Code 22) were the predominant vehicles of the tractor, semitrailer combinations. These trucks are primarily designed for long hauls. In general, they are not capable of maintaining high speeds on high-volume facilities. Thus, when the traffic volume increased, these vehicles, expressed as a percentage of the trucks, decreased.

For a statewide area, the single-unit trucks represented a small percentage of the trucks when the percent of trucks was large, whereas the tractor, semitrailer combination vehicles represented a small percentage of the trucks when the percent of trucks was small, as on high-volume roads.

### Correlation of Type Vehicle With Percent Trucks for Highway Systems

A correlation of the type of vehicle with the percent of trucks for a Type A, Type B, and Type C facility was made. For all three types, the relationship that existed for the statewide area also existed for each type of facility. In general, the single-unit trucks decreased as a percentage of the trucks when the percent of trucks increased. The tractor, semitrailer combination trucks decreased as a percentage of the trucks when the percent of trucks decreased. If the traffic volume on a facility is high, the percent of trucks can be expected to be low; however, the converse is not true (7).

## DETERMINATION OF THE DISTRIBUTION OF AXLE WEIGHTS

The loadometer stations were divided into three groups for analysis of the axle weight distributions. These groups are (a) grouping by percent trucks, (b) grouping by highway system, and (c) grouping by statewide area.

Within each group a determination was made of the number of axle weights that fell in each of 55 different weight classes. These classes cover the range from 2 to 56 kips and each includes weights in a 1-kip range. Even though the maximum legal axle weight for single axles in Texas is 18 kips and for tandem axles 32 kips, this study is concerned with the actual weight of vehicles operating on the highway system rather than with only those vehicles operating within the legal weight limits.

A tabulation of the actual axle weight distribution for Station 121-A in Hudspeth County is shown in Table 5. A tabulation such as this was made for each year of operation (1960-1962) of the regular loadometer stations and for each special loadometer station operated in 1963. It may be seen from Table 5 that for each increment of axle weight the following items were calculated:

1. The number of single axles,
2. The percent of the total number of axles that are single axles,
3. The cumulative percent of the total axles that are single axles,
4. The number of tandem axles,
5. The percent of the total number of axles that are tandem axles, and
6. The cumulative percent of the total axles that are tandem axles.

TABLE 5

SAMPLE CALCULATION OF AXLE WEIGHT DISTRIBUTION FOR LOADOMETER STATION 121-A

| Groups | Single Axles | Percent of Total | Cumulative Percent | Tandem Axles | Percent of Total | Cumulative Percent |
|---|---|---|---|---|---|---|
| 2 kip | 0 | 0 | 0 | 0 | 0 | 54.02 |
| 3 kip | 2 | 0.14 | 0.14 | 0 | 0 | 54.02 |
| 4 kip | 8 | 0.56 | 0.70 | 0 | 0 | 54.02 |
| 5 kip | 30 | 2.10 | 2.80 | 0 | 0 | 54.02 |
| 6 kip | 46 | 3.21 | 6.01 | 0 | 0 | 54.02 |
| 7 kip | 53 | 3.70 | 9.71 | 2 | 0.14 | 54.16 |
| 8 kip | 56 | 3.91 | 13.63 | 3 | 0.21 | 54.37 |
| 9 kip | 109 | 7.62 | 21.24 | 8 | 0.56 | 54.93 |
| 10 kip | 120 | 8.39 | 29.63 | 13 | 0.91 | 55.84 |
| 11 kip | 105 | 7.34 | 36.97 | 15 | 1.05 | 56.88 |
| 12 kip | 71 | 4.96 | 41.93 | 20 | 1.40 | 58.28 |
| 13 kip | 28 | 1.96 | 43.89 | 29 | 2.03 | 60.31 |
| 14 kip | 15 | 1.05 | 44.93 | 19 | 1.33 | 61.64 |
| 15 kip | 23 | 1.61 | 46.54 | 21 | 1.47 | 63.10 |
| 16 kip | 19 | 1.33 | 47.87 | 14 | 0.98 | 64.08 |
| 17 kip | 27 | 1.89 | 49.76 | 15 | 1.05 | 65.13 |
| 18 kip | 21 | 1.47 | 51.22 | 20 | 1.40 | 66.53 |
| 19 kip | 16 | 1.12 | 52.34 | 12 | 0.84 | 67.37 |
| 20 kip | 15 | 1.05 | 53.39 | 8 | 0.56 | 67.92 |
| 21 kip | 7 | 0.49 | 53.88 | 7 | 0.49 | 68.41 |
| 22 kip | 2 | 0.14 | 54.02 | 8 | 0.56 | 68.97 |
| 23 kip | 0 | 0 | 54.02 | 13 | 0.91 | 69.88 |
| 24 kip | 0 | 0 | 54.02 | 17 | 1.19 | 71.07 |
| 25 kip | 0 | 0 | 54.02 | 19 | 1.33 | 72.40 |
| 26 kip | 0 | 0 | 54.02 | 19 | 1.33 | 73.72 |
| 27 kip | 0 | 0 | 54.02 | 14 | 0.98 | 74.70 |
| 28 kip | 0 | 0 | 54.02 | 20 | 1.40 | 76.10 |
| 29 kip | 0 | 0 | 54.02 | 46 | 3.21 | 79.32 |
| 30 kip | 0 | 0 | 54.02 | 22 | 1.54 | 80.85 |
| 31 kip | 0 | 0 | 54.02 | 38 | 2.66 | 83.51 |
| 32 kip | 0 | 0 | 54.02 | 42 | 2.94 | 86.44 |
| 33 kip | 0 | 0 | 54.02 | 39 | 2.73 | 89.17 |
| 34 kip | 0 | 0 | 54.02 | 36 | 2.52 | 91.68 |
| 35 kip | 0 | 0 | 54.02 | 39 | 2.73 | 94.41 |
| 36 kip | 0 | 0 | 54.02 | 25 | 1.75 | 96.16 |
| 37 kip | 0 | 0 | 54.02 | 19 | 1.33 | 97.48 |
| 38 kip | 0 | 0 | 54.02 | 14 | 0.98 | 98.46 |
| 39 kip | 0 | 0 | 54.02 | 8 | 0.56 | 99.02 |
| 40 kip | 0 | 0 | 54.02 | 8 | 0.56 | 99.58 |
| 41 kip | 0 | 0 | 54.02 | 4 | 0.28 | 99.86 |
| 42 kip | 0 | 0 | 54.02 | 1 | 0.07 | 99.93 |
| 43 kip | 0 | 0 | 54.02 | 1 | 0.07 | 100.00 |
| 44 kip | 0 | 0 | 54.02 | 0 | 0 | 100.00 |
| 45 kip | 0 | 0 | 54.02 | 0 | 0 | 100.00 |
| 46 kip | 0 | 0 | 54.02 | 0 | 0 | 100.00 |
| 47 kip | 0 | 0 | 54.02 | 0 | 0 | 100.00 |
| 48 kip | 0 | 0 | 54.02 | 0 | 0 | 100.00 |
| 49 kip | 0 | 0 | 54.02 | 0 | 0 | 100.00 |
| 50 kip | 0 | 0 | 54.02 | 0 | 0 | 100.00 |
| 51 kip | 0 | 0 | 54.02 | 0 | 0 | 100.00 |
| 52 kip | 0 | 0 | 54.02 | 0 | 0 | 100.00 |
| 53 kip | 0 | 0 | 54.02 | 0 | 0 | 100.00 |
| 54 kip | 0 | 0 | 54.02 | 0 | 0 | 100.00 |
| 55 kip | 0 | 0 | 54.02 | 0 | 0 | 100.00 |
| 56 kip | 0 | 0 | 54.02 | 0 | 0 | 100.00 |
| Total axles | 1431 | | | | | |

TABLE 6

CALCULATION OF NUMBER OF TRUCKS OF EACH CLASS AND PERCENT OF TOTAL TRUCKS THAT EACH CLASS REPRESENTS FOR LOADOMETER STATION 121-A

| Type of Vehicle | Number of Vehicles | Percent of Total Trucks |
|---|---|---|
| Single unit trucks | | |
| 2-Axle, single rear tire (Code 12) | 0 | 0 |
| 2-Axle, 6-tired (Code 13) | 41 | 8.32 |
| 3-Axle (Code 14) | 7 | 1.42 |
| Tractor Semitrailer Combinations | | |
| 3-Axle (Code 21) | 66 | 13.39 |
| 4-Axle (Code 22) | 107 | 21.70 |
| 4-Axle (Code 23) | 0 | 0 |
| 5-Axle (Code 24) | 272 | 55.17 |
| Total trucks = 493 | | |

Note: ADT = 2810, percent trucks = 26.6.

Since an axle weight distribution is composed of two parts—a frequency distribution for single axles, and a frequency distribution for tandem axles—items 2 and 5 constitute an axle-weight distribution. The frequency distribution for single axles can be called a single-axle weight distribution and the frequency distribution for tandem axles can be called a tandem-axle weight distribution.

Table 6 shows the number of vehicles of each type that was weighed at Station 121-A in Hudspeth County. Calculations of this kind were made for each loadometer station.

## Grouping by Percent Trucks

At the loadometer stations included in this study, truck traffic accounted for between 4 and 28 percent of the total traffic volume. All stations with a given percent trucks were grouped together and the actual axle-weight distribution for each station within each group was calculated. For each grouping according to percent trucks, the actual frequency distribution for axle weights for single axles and for tandem axles was plotted.

Figure 7 represents the frequency distributions of the single-axle weights for all stations having 15 percent trucks. Figure 8 shows the frequency distributions of the tandem-axle weights for all stations having 15 percent trucks. Eight individual frequency distributions are superimposed in each of these figures.

Plots of each percent truck group (4 to 28 percent) were made but these are not shown in this study. For each percent truck group, the arithmetic mean of the percentage of the truck axles which fell into the various 1-kip axle-weight classes was calculated. The standard deviation and coefficient of variation were also calculated. An example of these values for single and tandem axles for a 15 percent trucks group is given in Table 7. For the lower and higher ranges of groups by percent trucks, the number of loadometer stations in each percent trucks group became small.

## Grouping by Highway System

A parameter of highway systems was selected for study. Table 8 gives the type of facility into which each loadometer station was grouped. For each type of facility, the arithmetic mean of the percentage of the truck axles which fell into the various 1-kip axle-weight classes, the standard deviation, and the coefficient of variation were calculated. These values are listed in Table 9. Figures 9 and 10 show frequency distributions of the axles by weight for single and tandem axles for each loadometer station on a Type A facility. Figures 11 and 12 show the frequency distribution of the arithmetic means for single and tandem axles for the Type A facility. They show that the arithmetic mean relationship, of course, represents the pattern shown in Figures 9 and 10 for the raw data.

Figures 13 and 14 show the superimposed frequency distributions of the 1-kip increments of axle weights for single and tandem axles for the Type B facility. Figures

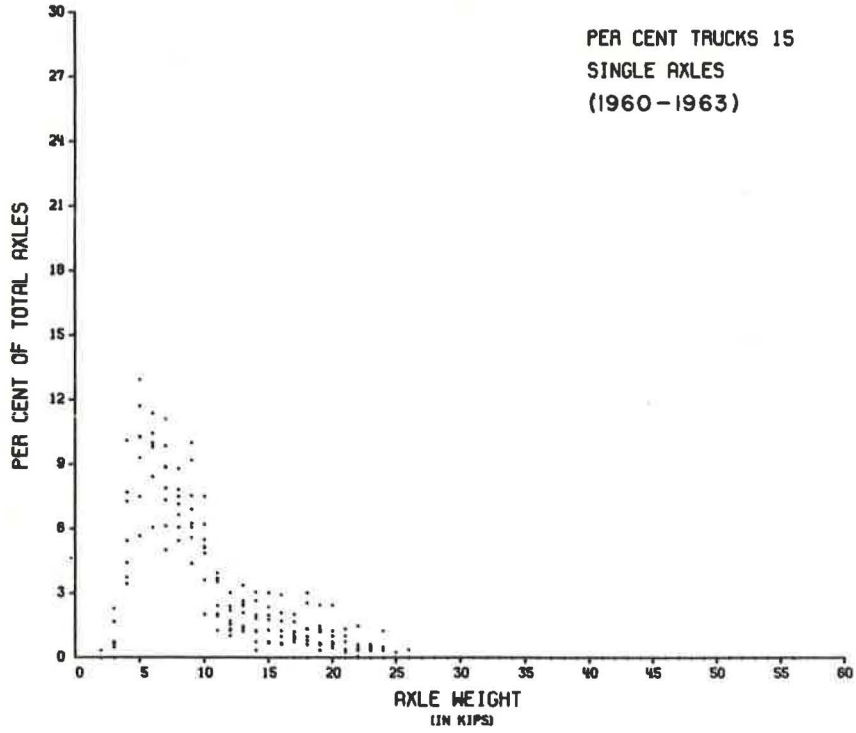


Figure 7. Single-axle weight distributions for 15 percent trucks.

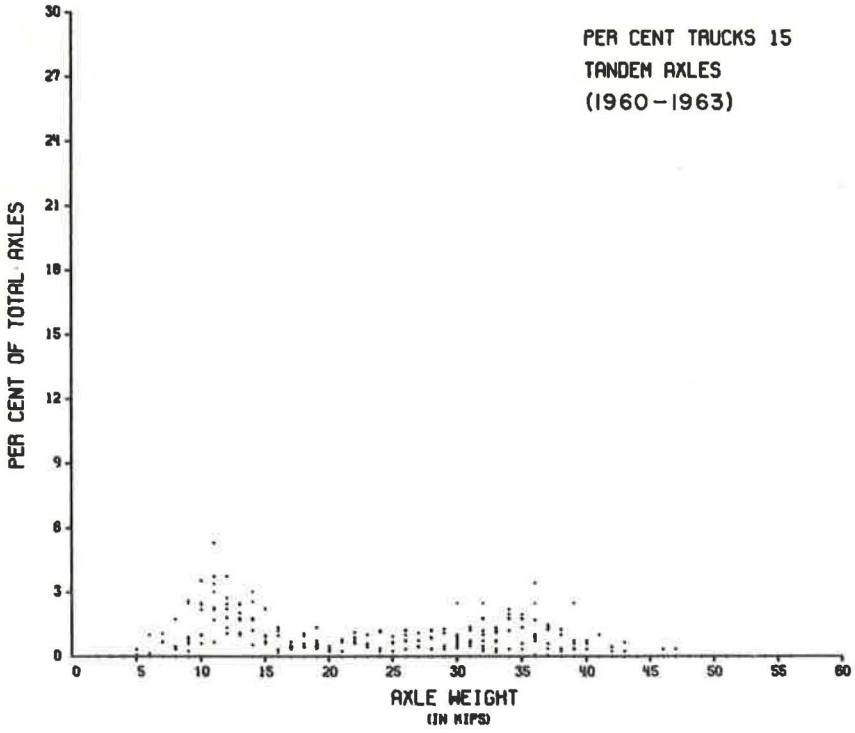


Figure 8. Tandem-axle weight distributions for 15 percent trucks.

TABLE 7

SUMMARY OF ARITHMETIC MEANS OF PERCENT OF TOTAL TRUCK AXLES WHICH FELL INTO VARIOUS 1-KIP AXLE WEIGHT CLASSES FOR A 15 PERCENT TRUCKS GROUPING

| Axle Weight (kips) | Single Axles | | | Tandem Axles | | |
|---|---|---|---|---|---|---|
| | Mean | Standard Deviation | Coefficient of Variation | Mean | Standard Deviation | Coefficient of Variation |
| 2 | 0.04 | 0.1124 | 264.5751 | 0 | 0 | 0 |
| 3 | 0.81 | 0.7437 | 91.8198 | 0 | 0 | 0 |
| 4 | 5.95 | 2.1194 | 35.6419 | 0 | 0 | 0 |
| 5 | 11.28 | 4.7680 | 42.2785 | 0.05 | 0.1115 | 217.5932 |
| 6 | 9.47 | 1.4961 | 15.8047 | 0.14 | 0.3306 | 232.0238 |
| 7 | 8.13 | 1.8527 | 22.7951 | 0.22 | 0.3940 | 179.0701 |
| 8 | 7.92 | 2.4759 | 31.2817 | 0.32 | 0.5670 | 179.2772 |
| 9 | 6.98 | 1.7450 | 24.9906 | 0.95 | 0.9782 | 103.1060 |
| 10 | 4.99 | 1.5299 | 30.6362 | 1.79 | 0.9595 | 53.7161 |
| 11 | 2.81 | 0.9515 | 33.8305 | 2.80 | 1.3200 | 47.2054 |
| 12 | 1.81 | 0.6349 | 35.1032 | 2.15 | 0.7890 | 36.6572 |
| 13 | 2.14 | 0.6954 | 32.5530 | 1.70 | 0.5590 | 32.7843 |
| 14 | 1.63 | 0.8683 | 53.3123 | 1.35 | 1.0548 | 77.9167 |
| 15 | 1.48 | 0.9310 | 63.0112 | 0.68 | 0.6981 | 101.9157 |
| 16 | 1.28 | 0.8732 | 68.2164 | 0.68 | 0.5627 | 82.8965 |
| 17 | 1.07 | 0.5700 | 53.4624 | 0.25 | 0.2635 | 104.8595 |
| 18 | 1.34 | 0.9405 | 70.3859 | 0.39 | 0.4323 | 110.8585 |
| 19 | 1.17 | 0.6165 | 52.8014 | 0.51 | 0.4079 | 80.3711 |
| 20 | 0.90 | 0.6852 | 76.4478 | 0.17 | 0.1836 | 104.9003 |
| 21 | 0.47 | 0.4825 | 102.9344 | 0.22 | 0.3167 | 145.6236 |
| 22 | 0.41 | 0.4533 | 109.5636 | 0.50 | 0.4185 | 82.8731 |
| 23 | 0.24 | 0.2448 | 104.1902 | 0.26 | 0.3632 | 141.0510 |
| 24 | 0.26 | 0.4149 | 159.5922 | 0.37 | 0.4822 | 129.8978 |
| 25 | 0.03 | 0.0827 | 264.5751 | 0.31 | 0.3556 | 114.7204 |
| 26 | 0.05 | 0.1224 | 264.5751 | 0.70 | 0.4199 | 59.7685 |
| 27 | 0.16 | 0.4134 | 264.5751 | 0.35 | 0.3925 | 113.3453 |
| 28 | 0 | 0 | 0 | 0.61 | 0.4723 | 76.7981 |
| 29 | 0 | 0 | 0 | 0.40 | 0.4894 | 121.9685 |
| 30 | 0 | 0 | 0 | 0.96 | 0.6219 | 65.1175 |
| 31 | 0 | 0 | 0 | 0.63 | 0.4642 | 73.2537 |
| 32 | 0 | 0 | 0 | 1.04 | 0.7224 | 69.3814 |
| 33 | 0 | 0 | 0 | 0.70 | 0.4594 | 65.6327 |
| 34 | 0 | 0 | 0 | 0.94 | 0.8959 | 95.6895 |
| 35 | 0 | 0 | 0 | 1.38 | 1.5447 | 111.8320 |
| 36 | 0 | 0 | 0 | 1.29 | 1.1186 | 86.5464 |
| 37 | 0 | 0 | 0 | 0.64 | 0.5931 | 92.3082 |
| 38 | 0 | 0 | 0 | 0.36 | 0.4688 | 129.7753 |
| 39 | 0 | 0 | 0 | 0.57 | 0.7765 | 136.2193 |
| 40 | 0 | 0 | 0 | 0.25 | 0.2819 | 111.0977 |
| 41 | 0 | 0 | 0 | 0.13 | 0.3373 | 264.5751 |
| 42 | 0 | 0 | 0 | 0.09 | 0.1568 | 181.7498 |
| 43 | 0 | 0 | 0 | 0.11 | 0.2252 | 195.7970 |
| 44 | 0 | 0 | 0 | 0 | 0 | 0 |
| 45 | 0 | 0 | 0 | 0 | 0 | 0 |
| 46 | 0 | 0 | 0 | 0.04 | 0.1124 | 264.5751 |
| 47 | 0 | 0 | 0 | 0.04 | 0.1124 | 264.5751 |
| 48 | 0 | 0 | 0 | 0 | 0 | 0 |
| 49 | 0 | 0 | 0 | 0 | 0 | 0 |
| 50 | 0 | 0 | 0 | 0 | 0 | 0 |
| 51 | 0 | 0 | 0 | 0 | 0 | 0 |
| 52 | 0 | 0 | 0 | 0 | 0 | 0 |
| 53 | 0 | 0 | 0 | 0.16 | 0.4134 | 264.5751 |
| 54 | 0 | 0 | 0 | 0 | 0 | 0 |
| 55 | 0 | 0 | 0 | 0 | 0 | 0 |
| 56 | 0 | 0 | 0 | 0 | 0 | 0 |

TABLE 8

CLASSIFICATION OF LOADOMETER STATIONS INTO HIGHWAY SYSTEMS

| Type A Facility | Type B Facility | | Type C Facility | | | | |
|---|---|---|---|---|---|---|---|
| L-10-2 | M-173 | 1020 | L-20 | 909 | 944 | 1011 | 1038 |
| L-20-1 | M-175 | 1027 | L-45-1 | 911 | 945 | 1012 | 1039 |
| L-20-2 | 178 | 1028 | L-149 | 915 | 946 | 1013 | 1040 |
| L-35-1 | M-675 | 1031 | 3-UP | 917 | 949 | 1014 | 1041 |
| L-45-2 | 901 | 1033 | 4-US | 919 | 950 | 1015 | 1042 |
| L-72 | 905 | 1036 | MS-47 | 921 | 951 | 1016 | 1044 |
| L-145 | 907 | 1052 | MS-54 | 922 | 952 | 1017 | 1045 |
| 121-A | 912 | L-7 | MS-103 | 923 | 953 | 1018 | 1046 |
| 1047 | 913 | L-10-1 | M-176 | 926 | 954 | 1021 | 1047 |
| | 914 | L-16 | M-278 | 927 | 955 | 1022 | 1048 |
| | 936 | L-20-3 | M-500 | 929 | 956 | 1023 | 1049 |
| | 959 | L-30-1 | M-526 | 930 | 957 | 1024 | 1050 |
| | 960 | L-37-1 | M-620 | 931 | 961 | 1025 | 1051 |
| | 1002 | L-42 | 724 | 935 | 1000 | 1026 | 1053 |
| | 1004 | L-81 | M-778 | 937 | 1001 | 1029 | 1054 |
| | 1005 | L-88 | M-882 | 939 | 1003 | 1030 | 1055 |
| | 1009 | L-147 | 903 | 940 | 1006 | 1032 | 1056 |
| | 1019 | | 904 | 941 | 1007 | 1034 | M-1497 |
| | | | 906 | 942 | 1008 | 1035 | M-1498 |
| | | | 908-A | 943 | 1010 | 1037 | |

15 and 16 show the frequency distribution of the arithmetic means for single and tandem axles for a Type B facility. The superimposed frequency distributions of the axle weights for a Type C facility are shown in Figures 17 and 18 for single and tandem axles. Figures 19 and 20 show the frequency distribution of the arithmetic means for single and tandem axles for a Type C facility.

### Grouping by a Statewide Area

The third method of grouping loadometer stations for analysis was on the basis of the statewide area. All of the stations were grouped together without regard to percent trucks or to the type of facility on which they were operated. Table 10 gives the arithmetic mean of the percentage of the truck axles which fell into the various 1-kip weight classes, the standard deviation, and the coefficient of variation for single and tandem axles. Figures 21 and 22 show the frequency distribution of the arithmetic means for single and tandem axles for a statewide area.

## EVALUATION OF THE THREE METHODS OF ESTIMATING AN AXLE WEIGHT DISTRIBUTION

### Characteristics of Locations Selected for Evaluation

Three loadometer stations were selected to evaluate the suitability of the three methods which were used for grouping data to estimate the axle-weight distribution for a given location. A determination of the number of equivalent 18-kip single-axle load applications was made for each selected station by using:

1. The actual axle-weight distribution calculated from the data for each selected station;
2. The axle-weight distribution calculated from a grouping of data by percent trucks;
3. The axle-weight distribution calculated from a grouping of data by a highway system; and
4. The axle-weight distribution calculated from a grouping of data by a statewide area.

The stations selected were L-35-1, L-30-1, and 3-UP. Figure 23 shows the physical characteristics of each of these locations. For each location selected, the ADT, the percent trucks, and the estimated increase in traffic (growth factor) were obtained.

TABLE 9

SUMMARY OF ARITHMETIC MEANS OF PERCENT OF TOTAL TRUCK AXLES WHICH FELL INTO VARIOUS 1-KIP AXLE WEIGHT CLASSES

| Axle Weight (kips) | Single Axles | | | Tandem Axles | | |
|---|---|---|---|---|---|---|
| | Mean | Standard Deviation | Coefficient of Variation | Mean | Standard Deviation | Coefficient of Variation |
| (a) Type A Facility Grouping | | | | | | |
| 2 | 0.06 | 0.0879 | 149.7359 | 0.00 | 0.0020 | 469.0416 |
| 3 | 1.00 | 0.4067 | 40.7452 | 0.00 | 0.0020 | 469.0416 |
| 4 | 5.47 | 1.9500 | 35.6541 | 0.01 | 0.0127 | 195.0499 |
| 5 | 8.07 | 1.7776 | 22.0407 | 0.04 | 0.0606 | 153.1933 |
| 6 | 8.42 | 1.3096 | 15.5595 | 0.23 | 0.2828 | 124.5865 |
| 7 | 8.18 | 1.2249 | 14.9780 | 0.76 | 0.5829 | 76.6926 |
| 8 | 7.97 | 1.2527 | 15.7090 | 1.60 | 0.9487 | 59.1680 |
| 9 | 7.03 | 0.6801 | 9.6707 | 2.14 | 0.8361 | 39.0208 |
| 10 | 4.90 | 0.9812 | 20.0370 | 1.95 | 0.6126 | 31.3991 |
| 11 | 3.07 | 1.0380 | 33.8194 | 1.60 | 0.5271 | 32.8570 |
| 12 | 2.24 | 0.6593 | 29.4538 | 1.27 | 0.4238 | 33.4158 |
| 13 | 1.78 | 0.2853 | 16.0215 | 1.08 | 0.5015 | 46.4894 |
| 14 | 1.73 | 0.3876 | 22.4522 | 0.93 | 0.4655 | 50.1052 |
| 15 | 1.76 | 0.3811 | 21.6904 | 0.79 | 0.5154 | 65.4255 |
| 16 | 1.94 | 0.4187 | 21.6042 | 0.72 | 0.3019 | 41.8012 |
| 17 | 1.77 | 0.4258 | 24.0332 | 0.67 | 0.2962 | 44.0133 |
| 18 | 1.26 | 0.3184 | 25.3420 | 0.68 | 0.2103 | 30.8029 |
| 19 | 0.85 | 0.3056 | 35.9913 | 0.70 | 0.2045 | 29.1489 |
| 20 | 0.46 | 0.2366 | 51.6300 | 0.78 | 0.2510 | 32.3819 |
| 21 | 0.19 | 0.1374 | 70.8350 | 0.83 | 0.2305 | 27.6305 |
| 22 | 0.12 | 0.1007 | 85.4576 | 0.97 | 0.3075 | 31.8580 |
| 23 | 0.07 | 0.0926 | 129.0496 | 1.09 | 0.3532 | 32.3650 |
| 24 | 0.04 | 0.0585 | 164.1411 | 1.28 | 0.4452 | 34.6669 |
| 25 | 0.01 | 0.0143 | 205.2057 | 1.50 | 0.4522 | 30.2001 |
| 26 | 0.01 | 0.0121 | 198.2062 | 1.59 | 0.5526 | 34.7243 |
| 27 | 0.00 | 0.0085 | 324.0370 | 1.53 | 0.5409 | 35.4419 |
| 28 | 0.00 | 0.0041 | 469.0416 | 1.38 | 0.5012 | 36.3219 |
| 29 | 0.00 | 0.0056 | 324.0370 | 1.25 | 0.5695 | 45.3893 |
| 30 | 0.00 | 0.0122 | 469.0416 | 0.95 | 0.3210 | 33.7234 |
| 31 | 0 | 0 | 0 | 0.81 | 0.4794 | 59.3769 |
| 32 | 0 | 0 | 0 | 0.58 | 0.5657 | 97.6863 |
| 33 | 0 | 0 | 0 | 0.48 | 0.5588 | 116.4157 |
| 34 | 0 | 0 | 0 | 0.37 | 0.5090 | 137.0774 |
| 35 | 0 | 0 | 0 | 0.29 | 0.5487 | 191.1976 |
| 36 | 0 | 0 | 0 | 0.19 | 0.3580 | 187.5375 |
| 37 | 0 | 0 | 0 | 0.16 | 0.3134 | 190.7149 |
| 38 | 0 | 0 | 0 | 0.10 | 0.2116 | 211.5985 |
| 39 | 0 | 0 | 0 | 0.07 | 0.1304 | 187.4500 |
| 40 | 0 | 0 | 0 | 0.08 | 0.1551 | 204.9574 |
| 41 | 0 | 0 | 0 | 0.05 | 0.1360 | 269.7463 |
| 42 | 0 | 0 | 0 | 0.05 | 0.1514 | 290.2346 |
| 43 | 0 | 0 | 0 | 0.02 | 0.0497 | 219.8877 |
| 44 | 0 | 0 | 0 | 0.01 | 0.0307 | 271.4742 |
| 45 | 0 | 0 | 0 | 0.01 | 0.0117 | 225.1543 |
| 46 | 0 | 0 | 0 | 0.01 | 0.0395 | 349.3019 |
| 47 | 0 | 0 | 0 | 0.01 | 0.0174 | 307.8846 |
| 48 | 0 | 0 | 0 | 0.00 | 0.0114 | 261.1513 |
| 49 | 0 | 0 | 0 | 0.01 | 0.0240 | 324.6505 |
| 50 | 0 | 0 | 0 | 0.00 | 0.0082 | 469.0416 |
| 51 | 0 | 0 | 0 | 0.00 | 0.0184 | 469.0416 |
| 52 | 0 | 0 | 0 | 0 | 0 | 0 |
| 53 | 0 | 0 | 0 | 0 | 0 | 0 |
| 54 | 0 | 0 | 0 | 0.00 | 0.0061 | 469.0416 |
| 55 | 0 | 0 | 0 | 0 | 0 | 0 |
| 56 | 0 | 0 | 0 | 0.00 | 0.0072 | 331.0589 |
| (b) Type B Facility Grouping | | | | | | |
| 2 | 0.14 | 0.3040 | 218.5744 | 0 | 0 | 0 |
| 3 | 1.46 | 1.3957 | 95.3794 | 0.00 | 0.0027 | 734.8469 |
| 4 | 5.46 | 2.5385 | 46.4830 | 0.00 | 0.0165 | 336.1200 |
| 5 | 8.32 | 2.8871 | 34.6953 | 0.02 | 0.0411 | 209.1773 |
| 6 | 9.02 | 2.6199 | 29.0369 | 0.20 | 0.2670 | 132.1847 |
| 7 | 8.35 | 1.6951 | 20.2974 | 0.76 | 0.8820 | 116.1588 |
| 8 | 7.54 | 1.9293 | 25.5831 | 1.37 | 1.3147 | 95.7327 |
| 9 | 6.99 | 1.4302 | 20.4648 | 1.78 | 1.1784 | 66.2928 |
| 10 | 4.89 | 1.6386 | 33.5098 | 2.04 | 0.9673 | 47.5291 |

TABLE 9 (Continued)

SUMMARY OF ARITHMETIC MEANS OF PERCENT OF TOTAL TRUCK AXLES WHICH FELL INTO VARIOUS 1-KIP AXLE WEIGHT CLASSES

| Axle Weight (kips) | Single Axles | | | Tandem Axles | | |
|---|---|---|---|---|---|---|
| | Mean | Standard Deviation | Coefficient of Variation | Mean | Standard Deviation | Coefficient of Variation |
| (b) Type B Facility Grouping (Continued) | | | | | | |
| 11 | 3.23 | 1.2480 | 38.6399 | 1.61 | 0.7030 | 43.6873 |
| 12 | 2.15 | 0.7616 | 35.4781 | 1.43 | 0.8521 | 59.6078 |
| 13 | 1.61 | 0.5668 | 35.2063 | 1.18 | 0.7376 | 62.2460 |
| 14 | 1.59 | 0.7470 | 47.1239 | 0.99 | 0.7116 | 72.0813 |
| 15 | 1.62 | 0.7606 | 47.0214 | 0.89 | 0.6805 | 76.5038 |
| 16 | 1.57 | 0.6463 | 41.1497 | 0.79 | 0.5240 | 66.1780 |
| 17 | 1.48 | 0.5401 | 36.4168 | 0.64 | 0.4580 | 71.2822 |
| 18 | 1.23 | 0.5980 | 48.4778 | 0.55 | 0.3543 | 64.9517 |
| 19 | 0.94 | 0.6827 | 72.7160 | 0.66 | 0.5209 | 79.1027 |
| 20 | 0.63 | 0.4797 | 76.1008 | 0.56 | 0.4250 | 75.6390 |
| 21 | 0.59 | 0.1926 | 202.4458 | 0.68 | 0.5005 | 73.5040 |
| 22 | 0.30 | 0.5175 | 173.5664 | 0.82 | 0.5060 | 61.8207 |
| 23 | 0.18 | 0.2888 | 163.7521 | 0.89 | 0.6398 | 72.0230 |
| 24 | 0.09 | 0.1679 | 196.0413 | 1.07 | 0.8060 | 75.5593 |
| 25 | 0.03 | 0.0862 | 289.1646 | 1.10 | 0.6689 | 60.8673 |
| 26 | 0.00 | 0.0155 | 473.5602 | 1.23 | 0.7868 | 64.1612 |
| 27 | 0.01 | 0.0643 | 512.5888 | 1.18 | 0.7915 | 67.1169 |
| 28 | 0.00 | 0.0131 | 552.8838 | 1.04 | 0.6067 | 58.3468 |
| 29 | 0.01 | 0.0454 | 734.8469 | 1.07 | 0.6687 | 62.7070 |
| 30 | 0 | 0 | 0 | 0.82 | 0.6571 | 80.0253 |
| 31 | 0 | 0 | 0 | 0.75 | 0.6483 | 86.6094 |
| 32 | 0 | 0 | 0 | 0.67 | 0.7019 | 104.9616 |
| 33 | 0 | 0 | 0 | 0.57 | 0.6121 | 107.2176 |
| 34 | 0 | 0 | 0 | 0.64 | 0.7209 | 112.7012 |
| 35 | 0 | 0 | 0 | 0.55 | 0.6420 | 117.4312 |
| 36 | 0 | 0 | 0 | 0.55 | 0.7460 | 136.5768 |
| 37 | 0 | 0 | 0 | 0.41 | 0.5760 | 137.7725 |
| 38 | 0 | 0 | 0 | 0.42 | 0.6045 | 142.3991 |
| 39 | 0 | 0 | 0 | 0.25 | 0.3792 | 151.8894 |
| 40 | 0 | 0 | 0 | 0.11 | 0.1936 | 180.4587 |
| 41 | 0 | 0 | 0 | 0.09 | 0.2203 | 258.3817 |
| 42 | 0 | 0 | 0 | 0.04 | 0.1355 | 321.1210 |
| 43 | 0 | 0 | 0 | 0.07 | 0.1873 | 277.7097 |
| 44 | 0 | 0 | 0 | 0.05 | 0.1731 | 329.4336 |
| 45 | 0 | 0 | 0 | 0.03 | 0.0922 | 354.4537 |
| 46 | 0 | 0 | 0 | 0.02 | 0.0688 | 402.3949 |
| 47 | 0 | 0 | 0 | 0.00 | 0.0261 | 598.8125 |
| 48 | 0 | 0 | 0 | 0 | 0 | 0 |
| 49 | 0 | 0 | 0 | 0.00 | 0.0059 | 543.6502 |
| 50 | 0 | 0 | 0 | 0 | 0 | 0 |
| 51 | 0 | 0 | 0 | 0 | 0 | 0 |
| 52 | 0 | 0 | 0 | 0 | 0 | 0 |
| 53 | 0 | 0 | 0 | 0 | 0 | 0 |
| 54 | 0 | 0 | 0 | 0 | 0 | 0 |
| 55 | 0 | 0 | 0 | 0.00 | 0.0040 | 734.8469 |
| 56 | 0 | 0 | 0 | 0 | 0 | 0 |
| (c) Type C Facility Grouping | | | | | | |
| 2 | 0.11 | 0.4324 | 387.1237 | 0 | 0 | 0 |
| 3 | 1.41 | 1.7718 | 125.7416 | 0 | 0 | 0 |
| 4 | 7.03 | 3.8772 | 55.1859 | 0.01 | 0.0479 | 725.8942 |
| 5 | 11.49 | 4.8081 | 41.8399 | 0.05 | 0.1954 | 424.5253 |
| 6 | 10.23 | 3.2894 | 32.1651 | 0.08 | 0.3523 | 417.7156 |
| 7 | 8.97 | 2.4672 | 27.5090 | 0.23 | 0.6368 | 278.1434 |
| 8 | 7.50 | 2.3493 | 31.3195 | 0.40 | 0.6498 | 163.4023 |
| 9 | 6.55 | 2.1577 | 32.9371 | 0.84 | 0.7794 | 92.7488 |
| 10 | 5.10 | 1.6706 | 32.7603 | 1.48 | 1.2430 | 83.9131 |
| 11 | 3.47 | 1.5585 | 44.9098 | 1.82 | 1.1595 | 63.6201 |
| 12 | 2.35 | 1.2029 | 51.1204 | 1.58 | 1.0625 | 67.2897 |
| 13 | 1.77 | 1.0004 | 56.6168 | 1.35 | 0.9807 | 72.5444 |
| 14 | 1.51 | 0.9599 | 63.5129 | 1.21 | 0.9259 | 76.6862 |
| 15 | 1.36 | 0.8358 | 61.4418 | 0.88 | 0.8514 | 96.3314 |
| 16 | 1.37 | 0.9901 | 72.2690 | 0.68 | 0.6326 | 93.1732 |
| 17 | 1.24 | 0.8981 | 72.2423 | 0.58 | 0.6293 | 108.9303 |
| 18 | 1.18 | 0.9739 | 82.1835 | 0.54 | 0.5558 | 102.6274 |
| 19 | 1.02 | 0.8193 | 80.0380 | 0.42 | 0.4641 | 109.2685 |
| 20 | 1.04 | 0.9170 | 88.5224 | 0.44 | 0.5517 | 124.8200 |
| 21 | 0.61 | 0.5685 | 92.8508 | 0.40 | 0.4957 | 124.7457 |
| 22 | 0.37 | 0.6239 | 170.4791 | 0.41 | 0.4853 | 117.2152 |

TABLE 9 (Continued)

SUMMARY OF ARITHMETIC MEANS OF PERCENT OF TOTAL TRUCK AXLES WHICH FELL INTO VARIOUS 1-KIP AXLE WEIGHT CLASSES

| Axle Weight (kips) | Single Axles | | | Tandem Axles | | |
|---|---|---|---|---|---|---|
| | Mean | Standard Deviation | Coefficient of Variation | Mean | Standard Deviation | Coefficient of Variation |
| | (c) Type C Facility Grouping (Continued) | | | | | |
| 23 | 0.24 | 0.4774 | 196.9247 | 0.39 | 0.5324 | 136.0909 |
| 24 | 0.13 | 0.3138 | 235.5930 | 0.39 | 0.5387 | 139.0265 |
| 25 | 0.04 | 0.1569 | 420.9545 | 0.38 | 0.4905 | 129.1315 |
| 26 | 0.03 | 0.1131 | 363.4186 | 0.48 | 0.5416 | 113.5264 |
| 27 | 0.03 | 0.1409 | 537.2820 | 0.53 | 0.5994 | 114.0049 |
| 28 | 0.02 | 0.1112 | 574.9672 | 0.53 | 0.6673 | 125.3572 |
| 29 | 0.01 | 0.0525 | 611.8787 | 0.57 | 0.6570 | 114.4366 |
| 30 | 0.00 | 0.0445 | 1024.6951 | 0.63 | 0.6671 | 105.8934 |
| 31 | 0.00 | 0.0261 | 1024.6951 | 0.73 | 0.7767 | 105.8615 |
| 32 | 0.00 | 0.0512 | 1024.6951 | 0.66 | 0.7062 | 106.4917 |
| 33 | 0 | 0 | 0 | 0.76 | 0.6971 | 91.3986 |
| 34 | 0 | 0 | 0 | 0.83 | 0.8617 | 103.7756 |
| 35 | 0 | 0 | 0 | 0.79 | 0.7762 | 98.3986 |
| 36 | 0 | 0 | 0 | 0.77 | 0.8115 | 104.7885 |
| 37 | 0 | 0 | 0 | 0.59 | 0.6737 | 114.5885 |
| 38 | 0 | 0 | 0 | 0.34 | 0.4204 | 121.9088 |
| 39 | 0 | 0 | 0 | 0.33 | 0.5070 | 153.1847 |
| 40 | 0 | 0 | 0 | 0.19 | 0.3822 | 198.1242 |
| 41 | 0 | 0 | 0 | 0.13 | 0.2644 | 208.8771 |
| 42 | 0 | 0 | 0 | 0.10 | 0.1981 | 206.4395 |
| 43 | 0 | 0 | 0 | 0.08 | 0.1649 | 212.9503 |
| 44 | 0 | 0 | 0 | 0.04 | 0.1342 | 329.2627 |
| 45 | 0 | 0 | 0 | 0.04 | 0.1184 | 291.2990 |
| 46 | 0 | 0 | 0 | 0.03 | 0.1030 | 395.7172 |
| 47 | 0 | 0 | 0 | 0.01 | 0.0590 | 449.8589 |
| 48 | 0 | 0 | 0 | 0.01 | 0.0433 | 819.8199 |
| 49 | 0 | 0 | 0 | 0.02 | 0.0954 | 515.8948 |
| 50 | 0 | 0 | 0 | 0.01 | 0.0481 | 728.5714 |
| 51 | 0 | 0 | 0 | 0.00 | 0.0126 | 1024.6951 |
| 52 | 0 | 0 | 0 | 0 | 0 | 0 |
| 53 | 0 | 0 | 0 | 0.01 | 0.1208 | 1024.6951 |
| 54 | 0 | 0 | 0 | 0.01 | 0.0895 | 672.7013 |
| 55 | 0 | 0 | 0 | 0.00 | 0.0126 | 1024.6951 |
| 56 | 0.01 | 0.0551 | 1024.6951 | 0.01 | 0.0783 | 715.5172 |

Station L-35-1, located in Bell County on I-35, was chosen to be a typical loadometer station operating on a Type A facility. The ADT at this station was 11,940 in 1963. The percent trucks was 10.7 percent and the expected increase in traffic was 4.6 percent per year. Station L-30-1, located in Hunt County on US 67, was chosen as a typical loadometer station operating on a Type B facility. The ADT for 1963 was 4,740 and the percent trucks was 23.0 percent. The expected growth in traffic was 7.0 percent per year.

The last station selected was 3-UP, located in the city limits of San Antonio, in Bexar County. This station was considered to be a typical one located on a Type C facility. Station 3-UP had an ADT of 17,104 and a percent trucks of 7.1 percent for 1963. The estimated increase in traffic was 0.9 percent per year.

## Calculation of Equivalent 18-Kip Load Applications

The serviceability of a given pavement is its ability to provide adequate support and a satisfactory ride at any specific time. The serviceability of a given pavement will decrease with applications of axle loads. Certain relationships were developed from the AASHO Road Test that related the destructiveness of an application of an 18-kip single-axle load to the serviceability of a flexible pavement. Also, methods were developed to relate the relative destructive effect of one application of any given axle load

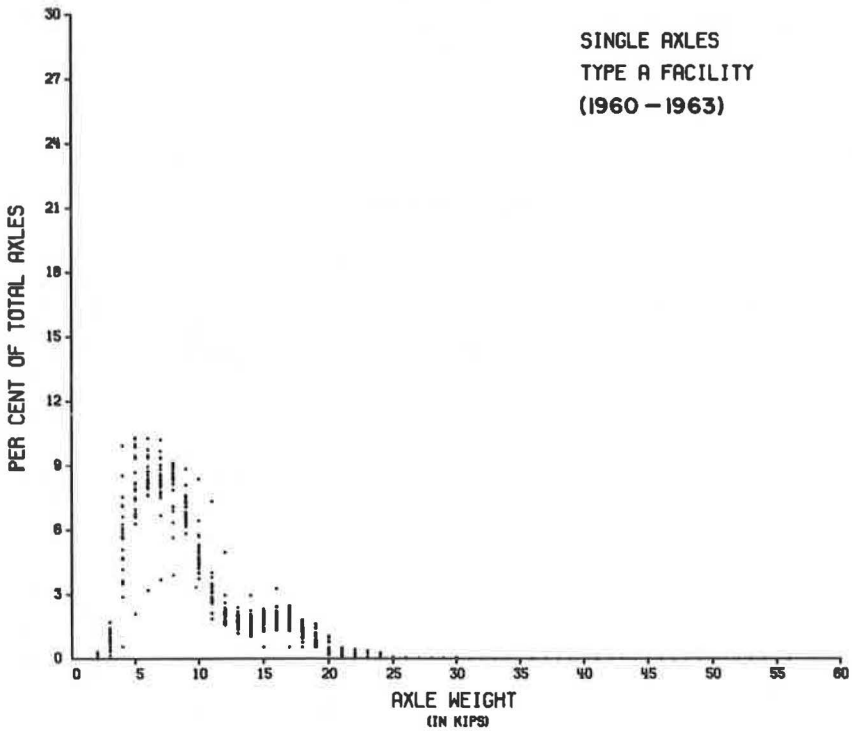


Figure 9. Single-axle weight distributions for Type A facility.

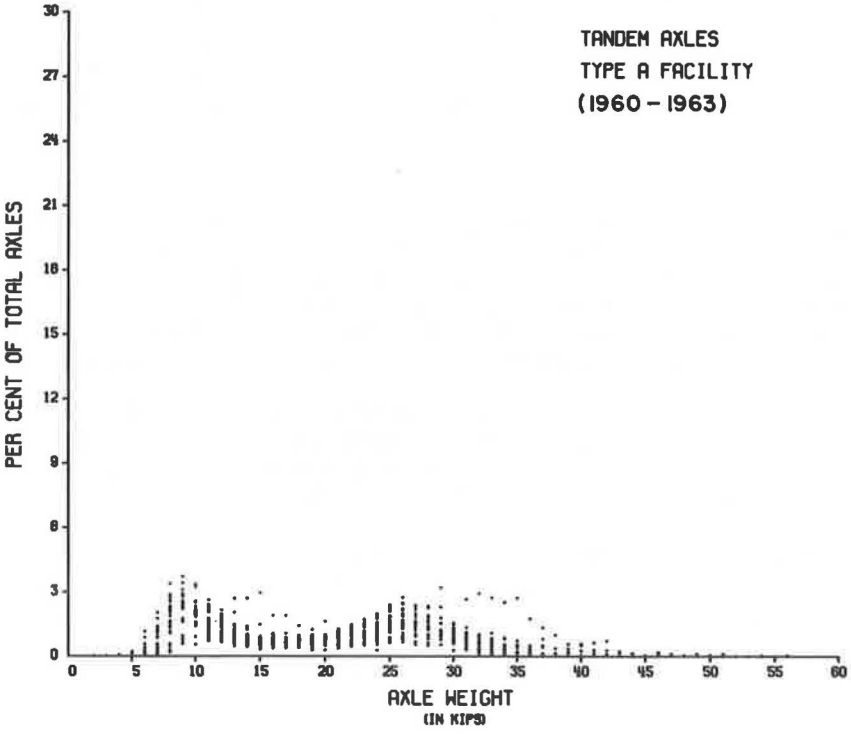


Figure 10. Tandem-axle weight distributions for Type A facility.

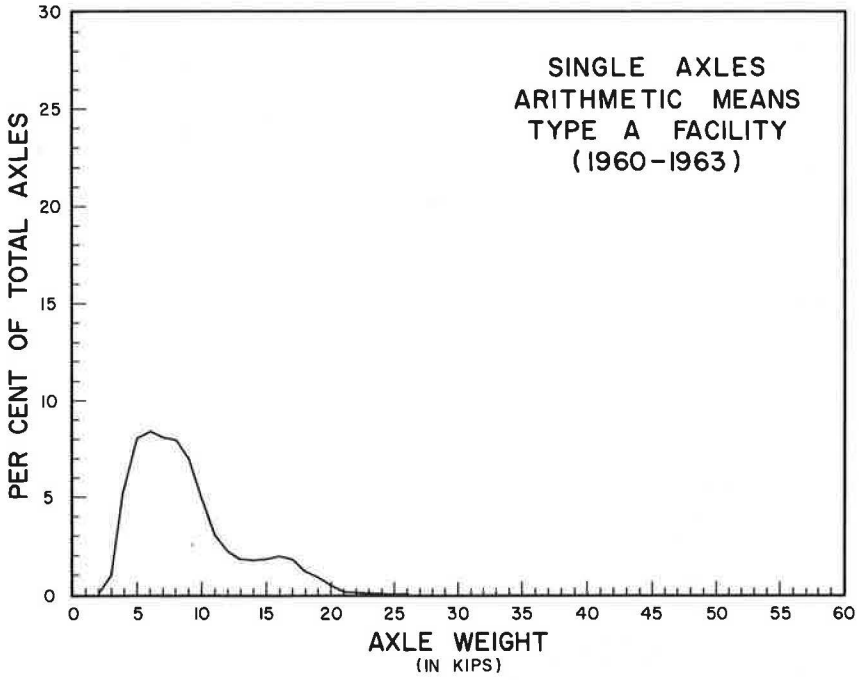


Figure 11. Single-axle weight distribution of arithmetic means for Type A facility.

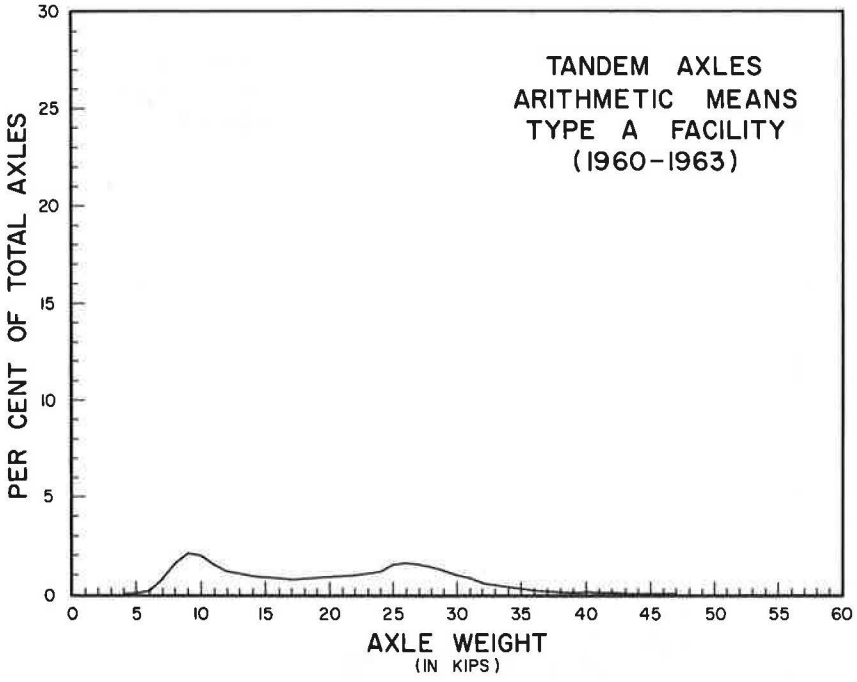


Figure 12. Tandem-axle weight distribution of arithmetic means for Type A facility.

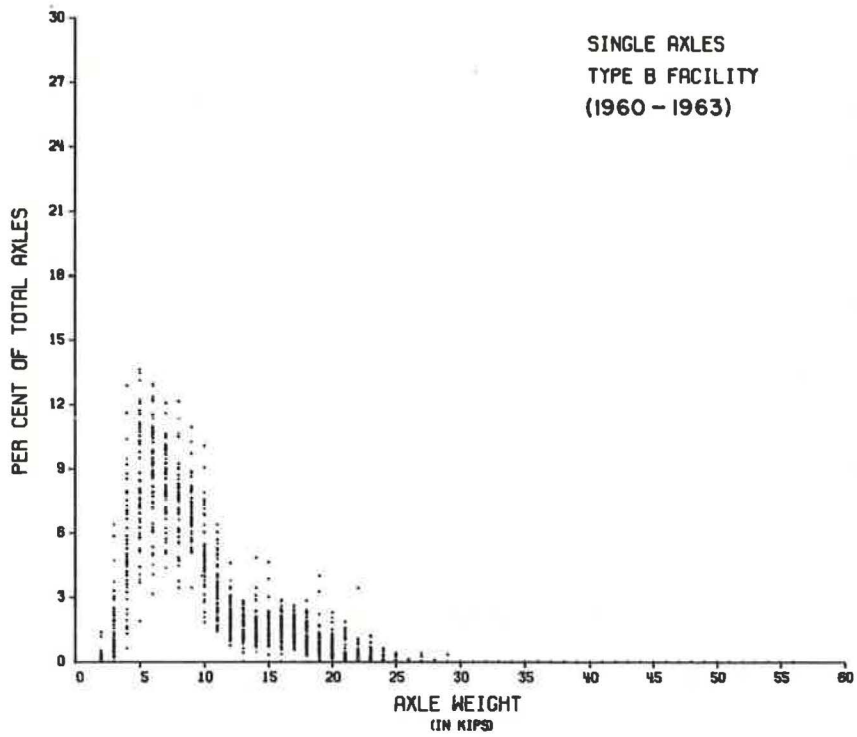


Figure 13. Single-axle weight distributions for Type B facility.

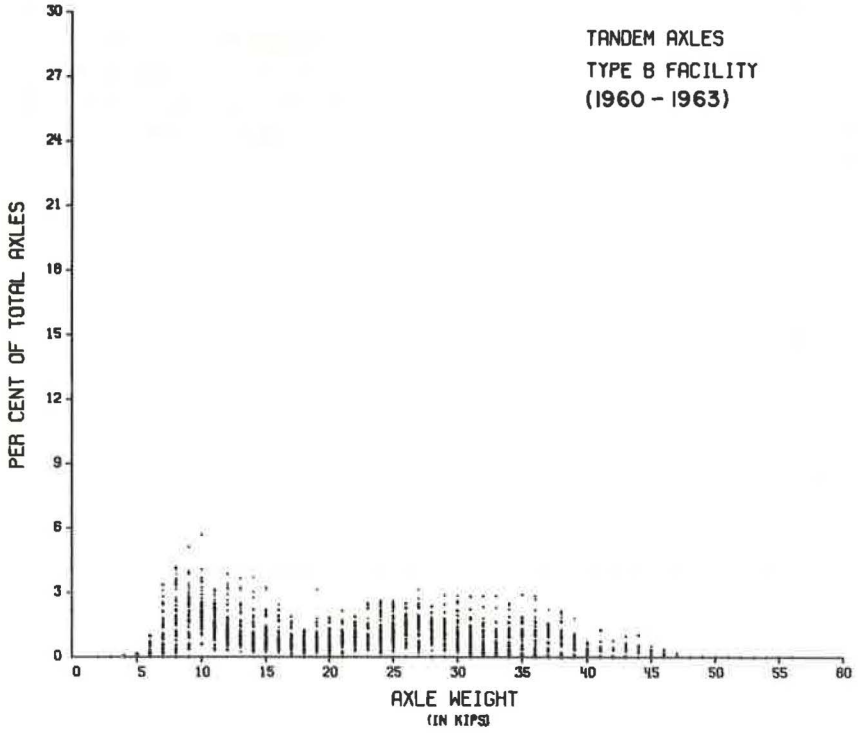


Figure 14. Tandem-axle weight distributions for Type B facility.

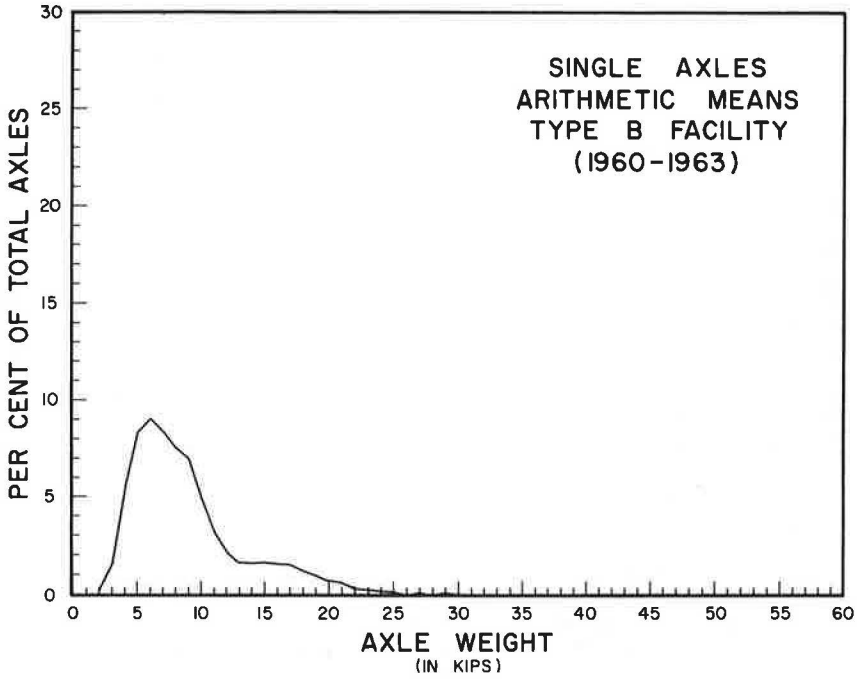


Figure 15. Single-axle weight distribution of arithmetic means for Type B facility.

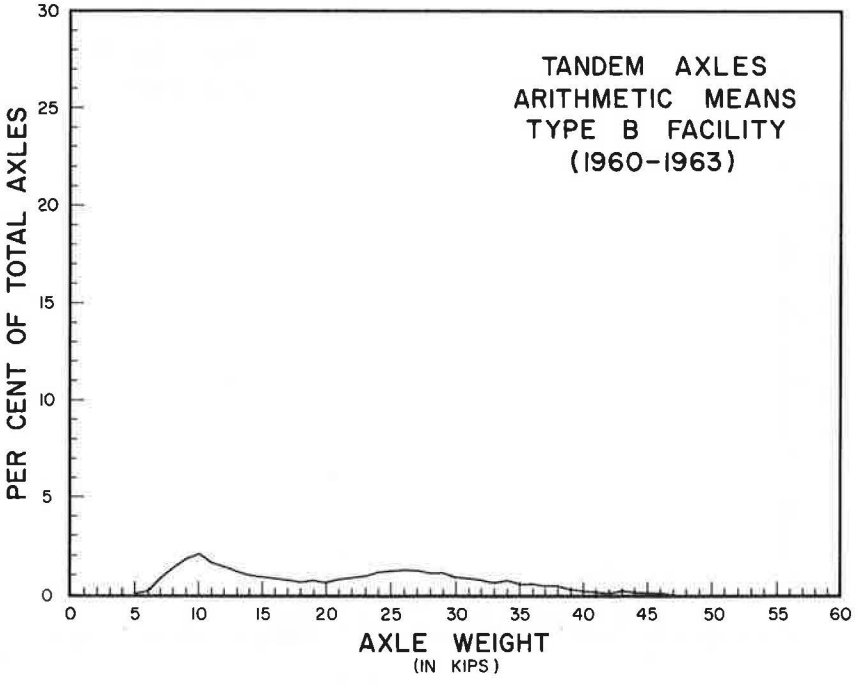


Figure 16. Tandem-axle weight distribution of arithmetic means for Type B facility.

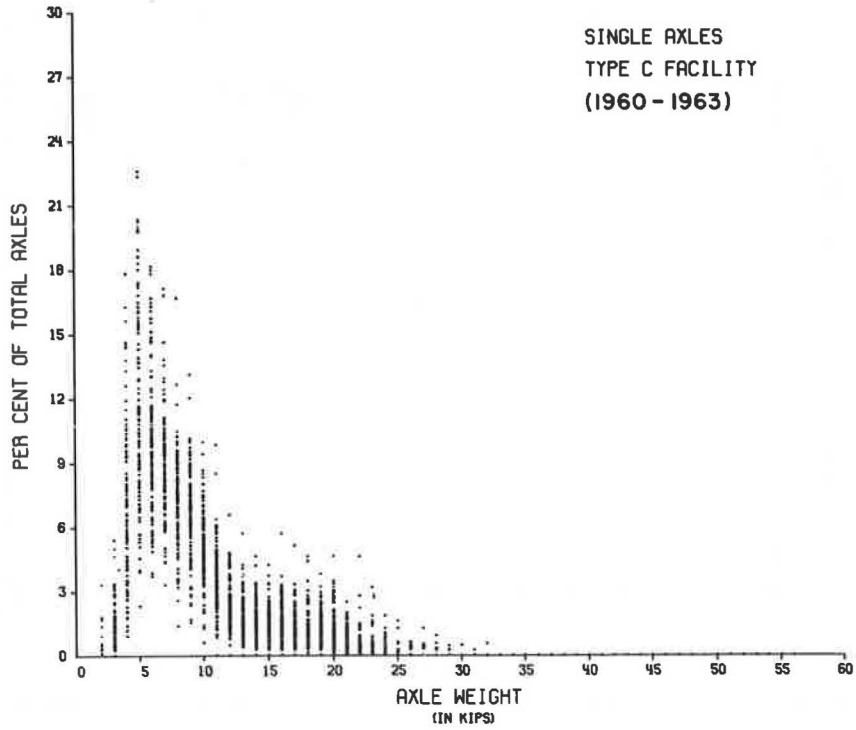


Figure 17. Single-axle weight distributions for Type C facility.

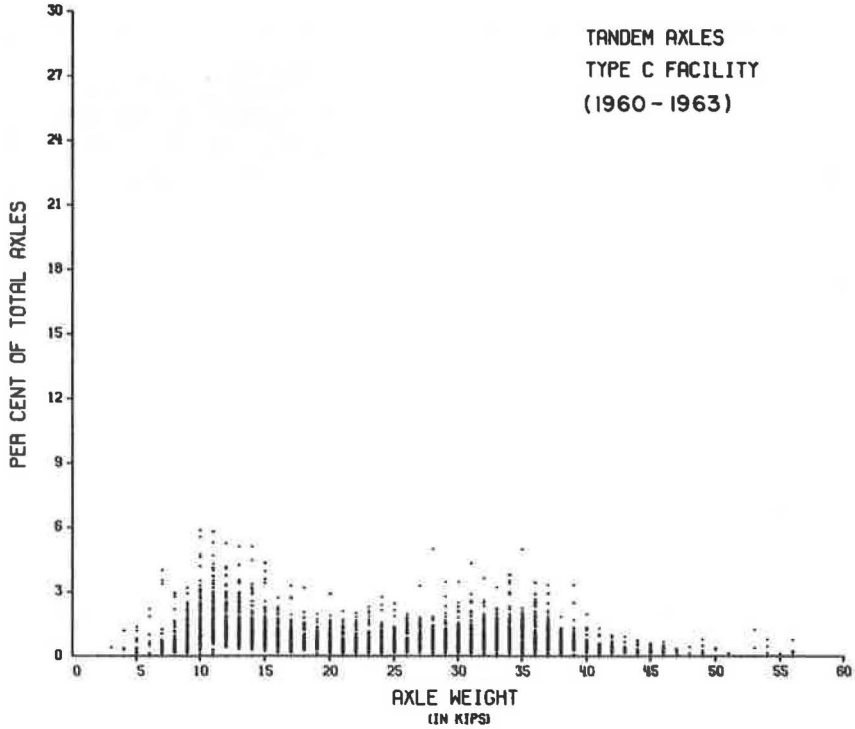


Figure 18. Tandem-axle weight distributions for Type C facility.

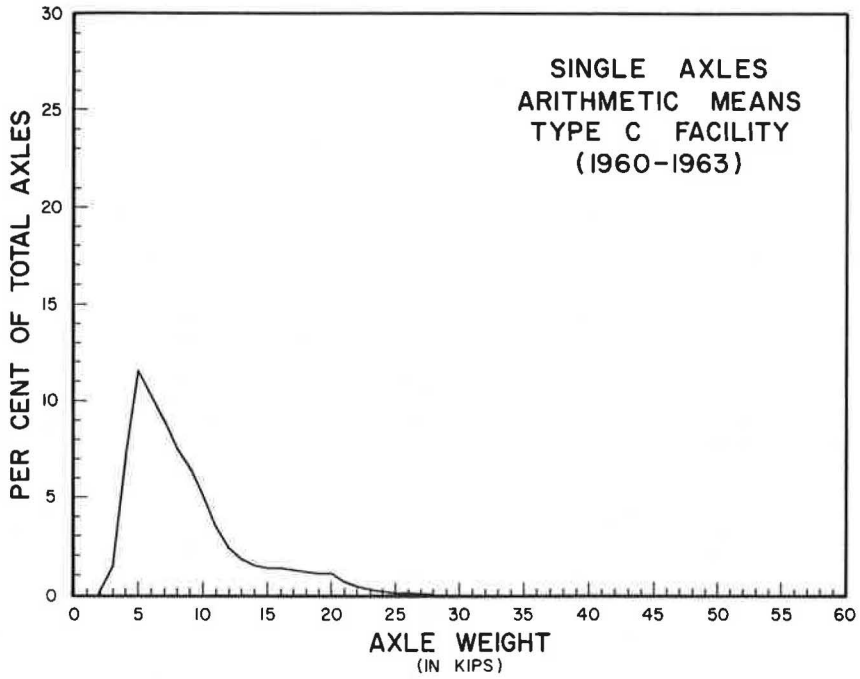


Figure 19. Single-axle weight distribution of arithmetic means for Type C facility.

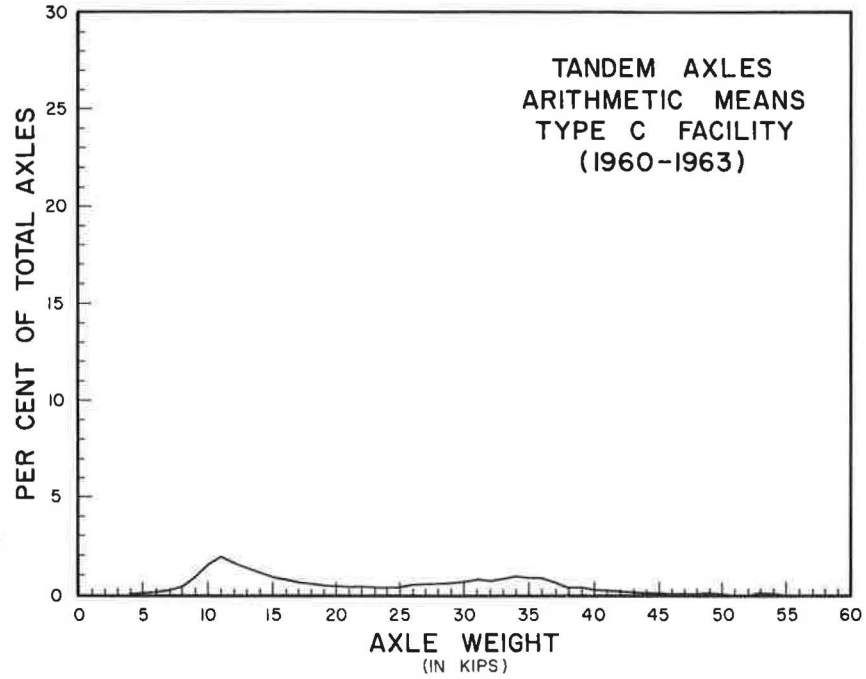


Figure 20. Tandem-axle weight distribution of arithmetic means for Type C facility.

TABLE 10

SUMMARY OF ARITHMETIC MEANS OF PERCENT OF TOTAL TRUCK AXLES WHICH FELL INTO VARIOUS 1-KIP AXLE WEIGHT CLASSES FOR STATEWIDE AREA GROUPING

| Axle Weight (kips) | Single Axles | | | Tandem Axles | | |
|---|---|---|---|---|---|---|
| | Mean | Standard Deviation | Coefficient of Variation | Mean | Standard Deviation | Coefficient of Variation |
| 2 | 0.11 | 0.3700 | 326.6577 | 0.00 | 0.0007 | 1352.7749 |
| 3 | 1.37 | 1.5593 | 113.4670 | 0.00 | 0.0294 | 1259.8364 |
| 4 | 6.37 | 3.4154 | 53.6503 | 0.01 | 0.0956 | 757.8248 |
| 5 | 10.16 | 4.3500 | 42.7998 | 0.04 | 0.1620 | 388.6102 |
| 6 | 9.65 | 3.0051 | 31.1463 | 0.14 | 0.3266 | 237.8212 |
| 7 | 8.70 | 2.1581 | 24.8101 | 0.45 | 0.7605 | 168.2542 |
| 8 | 7.57 | 2.1300 | 28.1492 | 0.84 | 1.0695 | 127.8408 |
| 9 | 6.73 | 1.8588 | 27.6138 | 1.28 | 1.0630 | 83.0083 |
| 10 | 4.99 | 1.6036 | 32.1670 | 1.71 | 1.1348 | 66.4575 |
| 11 | 3.33 | 1.4238 | 42.7432 | 1.73 | 0.9860 | 57.0481 |
| 12 | 2.28 | 1.0352 | 45.4824 | 1.49 | 0.9494 | 63.5122 |
| 13 | 1.72 | 0.8348 | 48.6344 | 1.27 | 0.8708 | 68.7154 |
| 14 | 1.56 | 0.8487 | 54.3720 | 1.10 | 0.8301 | 75.2325 |
| 15 | 1.48 | 0.7871 | 53.0466 | 0.87 | 0.7681 | 87.8751 |
| 16 | 1.49 | 0.8631 | 57.8365 | 0.72 | 0.5714 | 79.5746 |
| 17 | 1.38 | 0.7805 | 56.4531 | 0.61 | 0.5491 | 89.8338 |
| 18 | 1.21 | 0.8202 | 67.7536 | 0.56 | 0.4739 | 84.8516 |
| 19 | 0.98 | 0.7518 | 76.3633 | 0.53 | 0.4747 | 89.6365 |
| 20 | 0.84 | 0.7829 | 92.9643 | 0.52 | 0.5006 | 96.7233 |
| 21 | 0.55 | 0.7943 | 143.8569 | 0.54 | 0.5001 | 92.7932 |
| 22 | 0.31 | 0.5561 | 178.6615 | 0.60 | 0.5262 | 87.6703 |
| 23 | 0.20 | 0.3994 | 199.8832 | 0.63 | 0.6167 | 97.9203 |
| 24 | 0.11 | 0.2632 | 236.8417 | 0.70 | 0.7261 | 103.6181 |
| 25 | 0.04 | 0.1727 | 432.2447 | 0.73 | 0.6948 | 94.6047 |
| 26 | 0.02 | 0.0918 | 420.0652 | 0.84 | 0.7637 | 90.8845 |
| 27 | 0.02 | 0.1164 | 544.8188 | 0.84 | 0.7646 | 90.9612 |
| 28 | 0.01 | 0.0851 | 712.1635 | 0.79 | 0.7065 | 89.6046 |
| 29 | 0.01 | 0.0471 | 671.3765 | 0.80 | 0.7060 | 88.1313 |
| 30 | 0.00 | 0.0341 | 1205.9762 | 0.73 | 0.6430 | 88.2898 |
| 31 | 0.00 | 0.0199 | 1352.7749 | 0.74 | 0.7078 | 95.3806 |
| 32 | 0.00 | 0.0390 | 1352.7749 | 0.66 | 0.6906 | 105.0992 |
| 33 | 0 | 0 | 0 | 0.67 | 0.6655 | 98.9519 |
| 34 | 0 | 0 | 0 | 0.71 | 0.8001 | 111.9881 |
| 35 | 0 | 0 | 0 | 0.65 | 0.7350 | 113.4004 |
| 36 | 0 | 0 | 0 | 0.63 | 0.7747 | 122.6367 |
| 37 | 0 | 0 | 0 | 0.49 | 0.6310 | 128.8021 |
| 38 | 0 | 0 | 0 | 0.34 | 0.4739 | 140.6962 |
| 39 | 0 | 0 | 0 | 0.27 | 0.4478 | 163.2411 |
| 40 | 0 | 0 | 0 | 0.15 | 0.3172 | 210.3035 |
| 41 | 0 | 0 | 0 | 0.10 | 0.2400 | 233.3286 |
| 42 | 0 | 0 | 0 | 0.07 | 0.1767 | 243.5816 |
| 43 | 0 | 0 | 0 | 0.07 | 0.1625 | 247.0653 |
| 44 | 0 | 0 | 0 | 0.04 | 0.1400 | 344.8286 |
| 45 | 0 | 0 | 0 | 0.03 | 0.1073 | 315.3105 |
| 46 | 0 | 0 | 0 | 0.02 | 0.0923 | 389.6891 |
| 47 | 0 | 0 | 0 | 0.01 | 0.0476 | 497.4366 |
| 48 | 0 | 0 | 0 | 0.00 | 0.0332 | 925.6224 |
| 49 | 0 | 0 | 0 | 0.01 | 0.0734 | 616.6702 |
| 50 | 0 | 0 | 0 | 0.00 | 0.0368 | 914.0051 |
| 51 | 0 | 0 | 0 | 0.00 | 0.0116 | 969.7491 |
| 52 | 0 | 0 | 0 | 0 | 0 | 0 |
| 53 | 0 | 0 | 0 | 0.01 | 0.0963 | 1074.3140 |
| 54 | 0 | 0 | 0 | 0.01 | 0.0683 | 872.1072 |
| 55 | 0 | 0 | 0 | 0.00 | 0.0098 | 1126.6654 |
| 56 | 0.00 | 0.0419 | 1352.7749 | 0.01 | 0.0597 | 907.9388 |

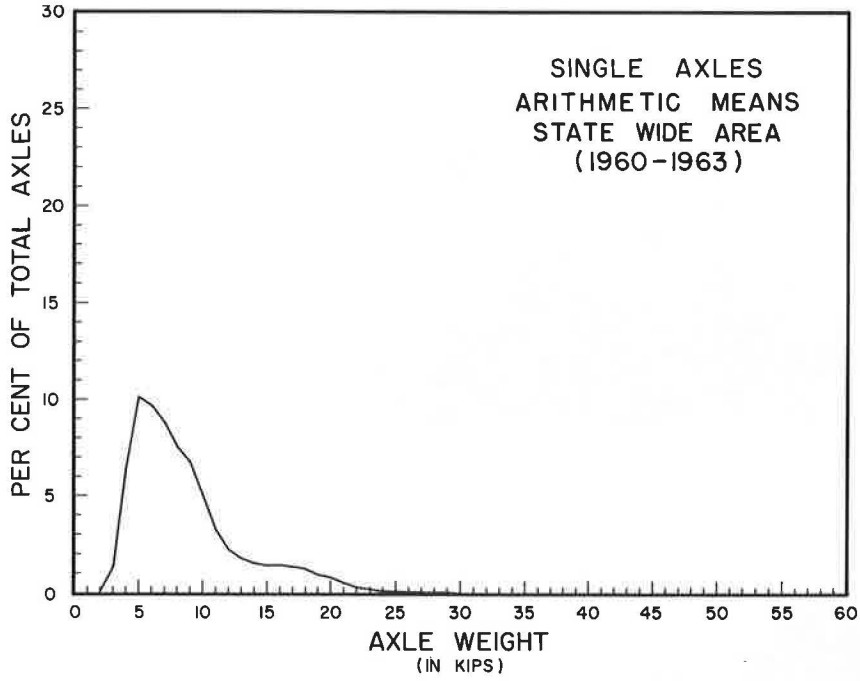


Figure 21. Single-axle weight distribution of arithmetic means for statewide area.

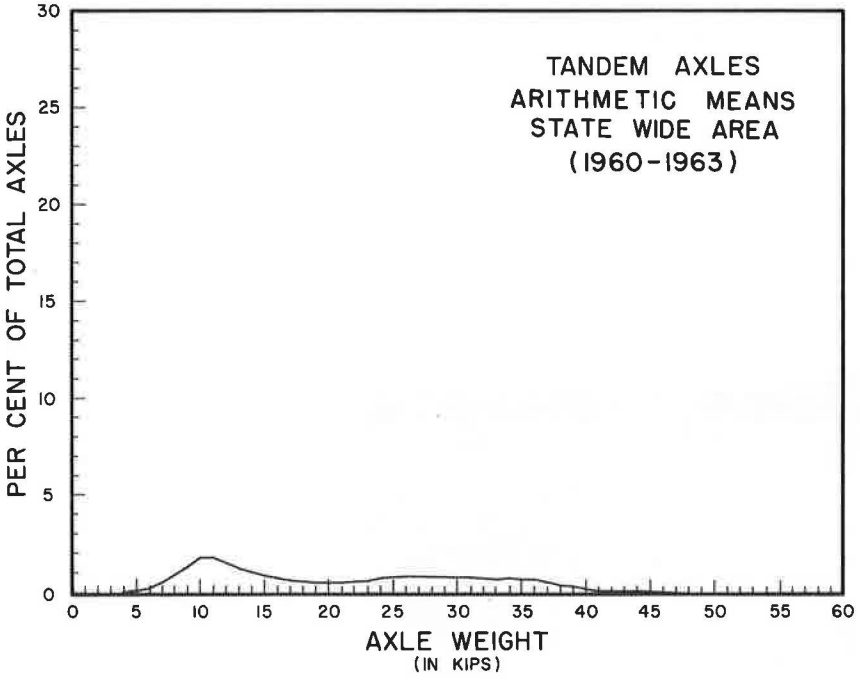


Figure 22. Tandem-axle weight distribution of arithmetic means for statewide area.

*L-35-1 on I-35 in Bell County*
*–Type A facility*

*3-UP in San Antonio in Bexar County*
*–Type C facility*

*L-30-1 on US 67 in Hunt County*
*–Type B facility*

Figure 23. Locations selected for evaluation of three methods of grouping data.

to that of one application of an 18-kip single-axle load. The factor that is multiplied by the applications of a given axle load to convert these to an equivalent number of applications of an 18-kip single-axle load is called an equivalence factor (EF). The AASHO Road Test equations used to calculate equivalence factors are:

For single axles

$$\log EF = 4.79 \log (L_x + 1) - 4.79 \log (18 + 1) + \frac{G_t}{B_{18}} - \frac{G_t}{B_x} \quad (1)$$

For tandem axles

$$\log EF = 4.79 \log (L_x + 2) - 4.79 \log (18 + 1) - 4.33 \log 2 + \frac{G_t}{B_{18}} - \frac{G_t}{B_x} \quad (2)$$

where

$$G_t = \log \left[ \frac{4.2 - P_t}{4.2 - 1.5} \right]$$

$$B_x = 0.40 + \frac{0.081 (L_x + L_2)^{3.23}}{(SN + 1)^{5.19} (L_2)^{3.23}}$$

$$B_{18} = 9.40 + \frac{1094}{(SN + 1)^{5.19}}$$

and

$G_t$ = a function (the logarithm) of the ratio of loss in serviceability at time t to the total potential loss at the time when the serviceability index will be 1.5;
$P_t$ = serviceability index at end of time t;
$L_x$ = load on one single axle or on one tandem axle in kips;
$L_2$ = axle code = 1 for single axles, 2 for tandem axles;
SN = structural number (a measure of pavement strength); and
EF = the equivalence factor.

An SN of 3.0 and a $P_t$ of 2.5 were used in calculating the number of equivalent 18-kip single-axle applications.

The solution of the right side of Eqs. 1 and 2 yields the logarithm of the EF. Tables showing EF for a variety of conditions are given in HRB Spec. Rept. 73 (8). The equivalence factor for an 18-kip single axle is, of course, 1.00; for lighter single-axle loads the factor is less than 1.00, and for heavier single-axle loads the factor is greater than 1.00.

To estimate the number of applications of an 18-kip single axle which will cause the same damage to a pavement as a given number of applications of some selected axle load, the number of applications of the selected axle load is multiplied by the appropriate equivalence factor. The cumulative effect of various numbers of applications of different loads can be expressed in terms of the equivalent number of applications of an 18-kip single-axle load. By this means various loading patterns can all be compared for design or performance.

The number of applications of an equivalent 18-kip single-axle load was calculated for each selected location using the actual distribution of axle weights that existed in 1963 and the equivalence factors given by the AASHO Road Test equations. Equivalent 18-kip single-axle load applications were then calculated for each selected location using the axle-weight distribution of: (a) percent trucks group within which the selected station lies, (b) type of facility on which the selected station lies, and (c) statewide area.

The number of equivalent 18-kip single-axle load applications was calculated to be 7,402,760 for Station L-35-1 using the actual axle-weight distribution for 1963. The number of equivalent 18-kip single-axle load applications is 10,209,820 for Station L-35-1 when using the axle-weight distribution obtained from a statewide area grouping.

Thus, a variation of 37.9 percent in equivalent 18-kip single-axle load applications resulted when using the statewide area axle-weight distribution for this particular loadometer location.

The number of equivalent 18-kip single-axle load applications was calculated for Station L-35-1 using the axle-weight distribution obtained from a Type A facility grouping. The equivalent 18-kip single-axle load applications are 8,783,847. This represented a variation from the actual number of equivalent 18-kip single-axle load applications of 18.7 percent. The equivalent 18-kip single-axle load applications were calculated for Station L-35-1 using the axle-weight distribution from an 11 percent truck grouping. The equivalent 18-kip single-axle load applications are 11,141,503. The variation from the actual equivalent 18-kip single-axle load applications is 50.5 percent.

It is seen that for the three methods of grouping data, the difference in the number of actual and estimated equivalent 18-kip single-axle load applications calculated for Station L-35-1 varies from 18.7 to 50.5 percent. The Type A facility axle-weight distribution produced the smallest variation in equivalent 18-kip single-axle load applications. For a Type A facility, the truck movement is primarily of a long-haul nature and does not experience the fluctuations in axle weights due to local movements.

Using the actual axle-weight distribution for Station L-30-1, the equivalent 18-kip single-axle load applications are 8,251,685. The statewide area axle-weight distribution was used to calculate equivalent 18-kip single-axle load applications of 11,220,708. This represents a variation of 36.0 percent from the actual equivalent 18-kip single-axle load applications. The Type B facility axle-weight distribution was used to calculate equivalent 18-kip single-axle load applications of 11,134,830. The variation from the actual equivalent 18-kip single-axle load applications of the facility grouping is 34.9 percent. The axle-weight distribution of a 25 percent trucks grouping was used to calculate equivalent 18-kip single-axle load applications of 12,089,317. This produces a variation from the actual equivalent 18-kip single-axle load applications of 46.5 percent. It is seen that for Station L-30-1 the estimated equivalent 18-kip single-axle load applications calculated using the axle-weight distribution of each of the three methods of grouping data produce a variation from the actual equivalent 18-kip single-axle load applications of 34.9 to 46.5 percent.

Using the actual axle-weight distribution of Station 3-UP in San Antonio, the equivalent 18-kip single-axle load applications were calculated to be 5,050,296. The equivalent 18-kip single-axle load applications using the statewide area, Type C facility, and 7 percent trucks grouping of axle-weight distributions were 6,686,146 and 7,349,439 and 4,683,927 respectively. The variation from the actual equivalent 18-kip single-axle load application ranges from -7.3 percent for the percent trucks axle-weight distribution to 45.5 percent for the type facility axle-weight distribution.

A summary of the calculation of the number of equivalent 18-kip single-axle load applications for the three selected loadometer stations is given in Table 11. It is seen from Table 11 that the variation in the equivalent 18-kip single-axle load applications calculated ranges from -7.3 percent to 50.5 percent. The number of equivalent 18-kip single-axle load applications resulting from a statewide area axle-weight distribution differs by a fairly consistent percentage from the number of equivalent 18-kip single-axle load applications resulting from an actual axle-weight distribution.

## Structural Design of Pavement

One test of the reliability of an axle-weight distribution is to determine the variation in pavement design thickness that will result from a variation in the total number of equivalent 18-kip single-axle load applications that are calculated from various axle-weight distributions. Therefore, after the equivalent 18-kip single-axle load applications were calculated, a flexible pavement was designed using the AASHO Design Chart for Flexible Pavements shown in Figure 24. This method gives the structural number for a given number of equivalent 18-kip single-axle load applications and soil support values. The Texas triaxial class of soil has been added to the AASHO Design Chart to correspond with the soil support value. A triaxial class of 5.0 for the subgrade was used for all designs. Each structural number was converted to a total depth of cover

TABLE 11

RESULTS OF THREE METHODS OF GROUPING DATA TO ESTIMATE AXLE-WEIGHT DISTRIBUTION

| Station | Actual Data | Statewide Area Method | Percent Difference | Type Facility Method | Percent Difference | Percent Truck Method | Percent Difference |
|---|---|---|---|---|---|---|---|
| | | | (a) Number of Equivalent 18-Kip Single-Axle Load Applications | | | | |
| L-35-1 | 7, 402, 760 | 10, 209, 820 | 37. 9 | 8, 783, 847 | 18. 7 | 11, 141, 503 | 50. 5 |
| L-30-1 | 8, 251, 685 | 11, 220, 708 | 36. 0 | 11, 134, 830 | 34. 9 | 12, 089, 317 | 46. 5 |
| 3-UP | 5, 050, 296 | 6, 686, 146 | 32. 4 | 7, 349, 439 | 45. 5 | 4, 683, 927 | -7. 3 |
| | | | (b) Total Depth of Cover Required in Inches[a] | | | | |
| L-35-1 | 27. 7 | 29. 1 | 5. 1 | 28. 4 | 2. 5 | 29. 5 | 6. 5 |
| L-30-1 | 28. 2 | 29. 5 | 4. 6 | 29. 5 | 4. 6 | 30. 0 | 6. 4 |
| 3-UP | 26. 0 | 27. 3 | 5. 0 | 27. 7 | 6. 5 | 25. 8 | -0. 8 |

[a]Based on AASHO Design Chart for Flexible Pavements shown in Figure 24.

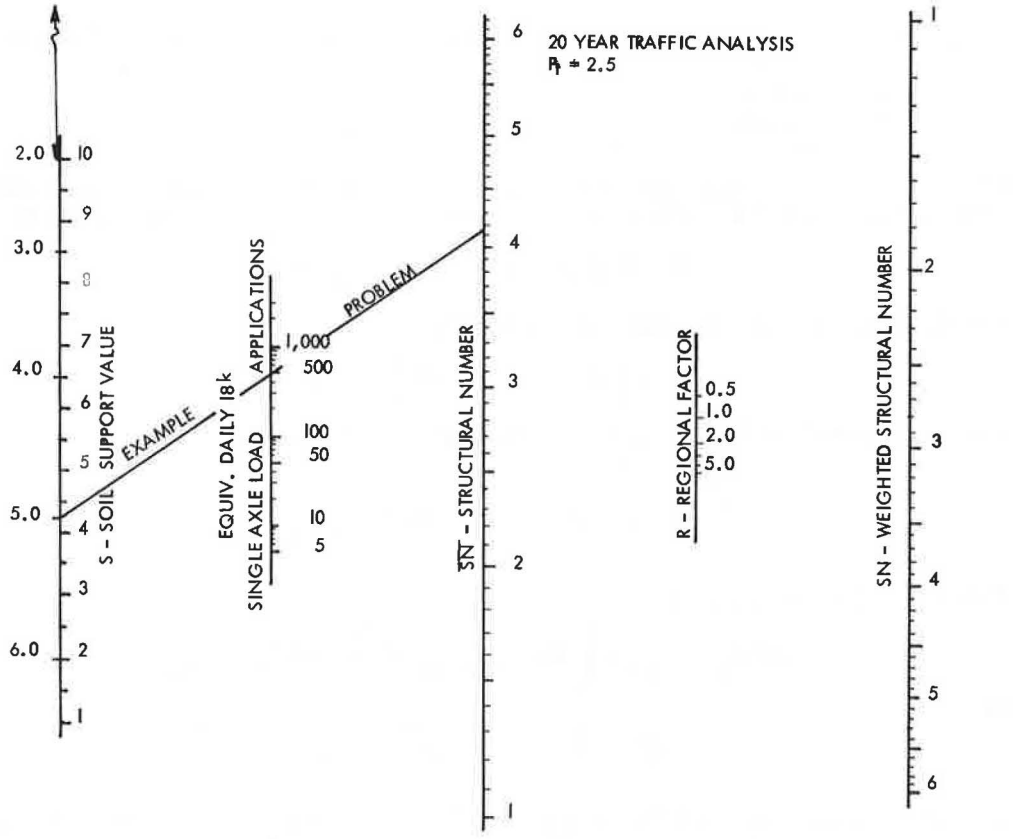


Figure 24. AASHO Design Chart—flexible base.

required for a coefficient of strength of 0.15. Table 11 lists the various depths of cover that are required for each design. The total variation in total depth of cover is less than 2 in. when a total depth of cover of approximately 30 in. is required. Thus, it would appear that regardless of the three methods of determining an axle-weight distribution to be used in calculating the number of equivalent 18-kip single-axle load applications, variation in pavement thickness will be small. The same order of variation in pavement thickness will result from using a subgrade of any triaxial class.

Example Problem

Station L-35-1: ADT = 11,940, percent trucks = 10.7 percent, percent growth per year = 4.6 percent, and design period = 20 years.

Assumptions:

1. The percent trucks (10.7%) will remain constant over the design period of 20 years.
2. The growth factor (4.6%) will remain constant over the design period of 20 years.
3. The axle-weight distribution will remain constant over the design period of 20 years.
4. The AASHO Road Test equations for equivalent factors are applicable.
5. All car axles weigh 2 kips each.

Let:

Y = number of truck axles (axle loads),
X = average daily trucks,
P = the percent of the total axles that fall into each axle-weight group of a given axle-weight distribution,
C = total car axles,
T = percent trucks, and
G = growth factor.

For a statewide grouping, the equation used for calculating the number of truck axles is Y = 28.28 + 2.75 (X). Therefore, the total truck axles for one year is given by

$$Y = \left[28.28 + 2.75\,(ADT)\,(T)\right]\,(365)$$

and the total car axles for one year is given by

$$C = \left[\,ADT - (ADT)\,(T)\right]\,(2)\,(365)$$

The total equivalent 18-kip single-axle applications for one year would be

$$\sum_{i=2}^{i=56} \left[(P_i)\,(EF_i)\,(Y)\right] + (C)\,(EF_{2\text{-kip single}})$$

Calculate ADT for next year:

$$ADT_{2nd\ year} = \left[\,ADT_{1st\ year}\,(G)\right] + ADT_{1st\ year}$$

or

$$ADT_n = \left[\,ADT_{n-1}\,(G)\right] + ADT_{n-1}$$

Recalculate total equivalent 18-kip single-axle applications for the second year and continue procedure over the design period. Thus, the total equivalent 18-kip single-axle applications for the design period would be

$$\sum_{n=1}^{n=20} \sum_{i=2}^{i=56} \left\{ (P_i)\ (EF_i) \left[ 28.28 + 2.75\ (ADT_n)\ (T) \right] (365) \right\}$$

$$+ \left[ ADT_n - ADT_n\ (T) \right]\ (2)\ (365)\ (EF_{2\text{-kip single}})$$

For Station L-35-1, the number of equivalent 18-kip single-axle load applications was calculated to be 7, 402, 760. Entering Figure 24 with the number of equivalent 18-kip single-axle load applications of 507 (equivalent daily 18-kip single-axle load applications in one direction) and using a triaxial class of 5. 0, a structural number of 4. 16 is obtained. The SN of 4. 16 is equivalent to a total depth of cover of 27. 7 in. for a soil with a coefficient of strength of 0. 15.

## CONCLUSIONS

For the data analyzed, the total number of axles (axle loads) produced by a given number of trucks was approximately 2. 75 multiplied by the number of trucks. A tandem-axle set is considered to be one axle. The linear regression equation is

$$Y = 28.28 + 2.75\ (X)$$

where

Y = number of axles (axle loads), and
X = number of trucks.

This equation was determined by correlating the number of axles with the number of trucks for a statewide area.

The predominant single-unit truck observed was the 2-axle, 6-tired (Code 13) vehicle. As the percent of trucks increased from 3 to 30 percent, the percentage of the total trucks made up of 2-axle, 6-tired vehicles decreased from 65 to 7 percent.

In the tractor, semitrailer combination class, the 4-axle (Code 22) and the 5-axle (Code 24) were the predominant vehicles. As the percent of trucks increased from 3 to 30 percent, the percent that the 4-axle (Code 22) vehicle represented of the total trucks increased from 12 to 44 percent and the percent that the 5-axle (Code 24) represented of the total trucks increased from 7 to 36 percent.

Based on the survey of data from loadometer stations operated in 1960 through 1963, loadometer stations operating on a Type A facility should be grouped in order to estimate the axle-weight distribution for the purpose of calculating the number of equivalent 18-kip single-axle load applications at a given location. The statewide area method of grouping loadometer stations may be used to estimate the axle-weight distribution for all types of highways other than those that meet or approach Interstate design standards and carry predominantly through truck traffic.

## RECOMMENDATIONS

For all types of facilities, the statewide area equation for calculating the number of truck axles should be used. In estimating an axle-weight distribution to be used in calculating the number of equivalent 18-kip single-axle applications for a given location, good engineering judgment should be used. If the location under consideration for pavement design purposes is located in the vicinity of a regular loadometer station and the truck traffic characteristics are very similar to those of the regular loadometer station, then the axle-weight distribution of the regular loadometer station should be used to calculate the number of equivalent 18-kip single-axle load applications. If the location under consideration is not in the vicinity of a regular loadometer station or the truck

traffic characteristics are different, then the Type A facility axle-weight distribution should be used if the location is on a Type A facility. If the location is on any other type of facility, then the statewide area axle-weight distribution should be used to calculate the number of equivalent 18-kip single-load applications.

## ACKNOWLEDGMENTS

The authors wish to express their sincere appreciation to Clyde E. Lee, Associate Professor, Civil Engineering Department of the University of Texas for the technical suggestions made during this investigation. Special thanks are given to Charles R. Davis, Assistant Traffic Manager of the Planning Survey Division of the Texas Highway Department for his help in securing the data and for his comments during the study.

## REFERENCES

1. Mills, Frederick C. Statistical Methods, Third Edition. Henry Holt and Co., New York, 1955.
2. The AASHO Road Test: Report 5—Pavement Research. HRB Spec. Rept. 61E, 1962.
3. Texas Highway Department Plan Preparation, Book II. Texas Highway Dept., Austin, 1952.
4. Texas Motor Vehicle Laws. Texas Highway Dept., Austin, 1963-1964.
5. Derdeyn, Conrad J. A New Method of Traffic Evaluation for Use in Pavement Design. Texas Highway Dept., File D-8, Austin, 1964.
6. Traffic Volume Counting Manual. U. S. Bureau of Public Roads, 1965.
7. Unpublished studies in truck traffic characteristics performed by the Texas Highway Department, File D-8, Austin, 1964.
8. The AASHO Road Test: St. Louis Conference Proceedings. HRB Spec. Rept. 73, 1962.

# A Resilience Design Procedure for Flexible Pavements

ERNEST ZUBE and RAYMOND FORSYTH
Respectively, Assistant Materials and Research Engineer, and Senior Materials and Research Engineer, California Division of Highways

For several years the California Division of Highways has been engaged in a research project with the objectives of measuring and allowing for the resilient behavior of soils within flexible pavement systems. The ultimate objective of the study has been the incorporation of the resilience factor into pavement design for the purpose of eliminating or minimizing early "fatigue" failure of asphalt-concrete surfacing due to excessive transient deflection.

Design criteria in the form of maximum tolerable deflection were available from previous field studies. A laboratory testing device, the resiliometer, was developed to measure the resilience properties of various roadway materials. This report describes the apparatus itself, its development and the results of qualitative tests on the main types of soils encountered in roadway construction.

The incorporation of the resilience factor into pavement design required the establishment of the relationship between field deflection and laboratory resilience tests. The correlation program involved the sampling and testing of 20 different roadways. Field sampling and laboratory procedures are presented along with sample computations which illustrate the method of analysis of laboratory resilience data.

The report presents the results of a field trial of the resilience design procedure in which preliminary samples from a number of roadways were tested using resilience design criteria. Predicted deflections resulting from these preliminary resilience analyses are compared with those measured in the field following the completion of construction. The results indicate that the resilience design procedure is generally consistent and effective in isolating potential resilience problems.

•FATIGUE cracking of bituminous pavements has been recognized as a major problem with respect to flexible pavement performance. This is, of course, primarily because preliminary design procedures incorporating the factor of transient deflection have not been developed. During the past 20 years, however, several agencies have developed tolerable deflection criteria for in-place pavements. Middlebrooks (1) in 1943 stated, "Experience to date indicates that the critical deflection will vary from approximately 0.05 in. to 0.15 in. depending upon the type of subgrade, the type of base material, wheel load, and probably other factors."

The necessity of permanently installing electronic gage units for deflection measurement was eliminated during the operation of the WASHO Road Test (1953) with the development of the Benkelman beam. This device greatly simplified and speeded up the

Paper sponsored by Committee on Flexible Pavement Design and presented at the 46th Annual Meeting.

TABLE 1

TENTATIVE MAXIMUM PAVEMENT DEFLECTIONS

| Thickness, In. | Type of Pavement | Max. Deflection for Design Purposes, In. (tentative) |
|---|---|---|
| 8 | Portland cement concrete | 0.012 |
| 6 | Cement-treated base (surface with bituminous pavement) | 0.012 |
| 4 | Asphalt concrete (plant mixed) on untreated aggregate base | 0.017 |
| 3 | Asphalt concrete (plant mixed) on untreated aggregate base | 0.020 |
| 2 | Asphalt concrete (plant mixed) on untreated aggregate base | 0.025 |
| 1 | Asphalt concrete (road mixed) on untreated aggregate base | 0.036 |
| ½ | Asphalt concrete surface treatment | 0.050 |

measurement of transient pavement deflection. Utilizing this apparatus, approximately 60,000 individual readings were made on the WASHO test road. Analysis of these data revealed that this particular test pavement could withstand transient deflections of 0.045 in. in warm weather and 0.030 in. in cold weather (2) for a period of two years. It was emphasized in the report, however, that these values may not be applicable to older pavements or to those containing different types of asphalt or aggregate.

The results of a comprehensive statewide deflection study made by the California Division of Highways beginning in 1951 were made available in 1955 (3). The test data for this investigation were derived from readings of nearly 400 permanently installed General Electric travel gage units on 43 different projects.

Analysis of these data resulted in the safe limits (Table 1) for maximum deflection under a 15,000-lb single-axle load for several types of pavement and base construction necessary to preclude cracking after several millions of load repetitions.

These values were determined from tests on roadways with approximately 10 million equivalent 5000-lb wheel loads (EWL) and have been used as a guide criteria by the Division of Highways since 1955 for planning the reconstruction of existing roadways. Although no additional evidence has been found that would seriously invalidate these criteria, further adjustment may be warranted from experience gained from present-day construction.

In order to reevaluate these criteria in view of possible improvements in the fatigue resistance properties of current asphalt mixes and to make appropriate adjustments for variations in traffic volume, an investigation (4) is currently being made by the California Division of Highways in cooperation with the U.S. Bureau of Public Roads. The investigation will further determine the effect of varying amounts of traffic on tolerable deflection levels of various types of roadway structural sections.

As an interim method of adjustment for varying traffic volumes, a family of curves has been developed by the Materials and Research Department based on AC surfacing fatigue tests made by the department several years ago. The results of this work indicate that while fatigue life of individual AC specimens varied widely, presumably due to variation of mix design, age and number of previous traffic loadings, the slopes of their load repetition vs deflection lines were relatively uniform when plotted as logarithmic functions. By utilizing an average AC surfacing fatigue line slope and by pivoting lines through known deflection criteria at the traffic volume from which Table 1 was developed, Figure 1 was developed for the purpose of making "rule of thumb" adjustment in tolerable deflection for varying traffic volumes. Although these curves are based solely on laboratory surfacing fatigue data, they appear quite reasonable within the ranges of 6.0 to 10.0 TI. The traffic index (TI) is an exponential function of total 5000-lb EWL anticipated on the highway between the time construction is completed and the end of the design period, usually 20 years (see Test Method No. Calif. 301-B).

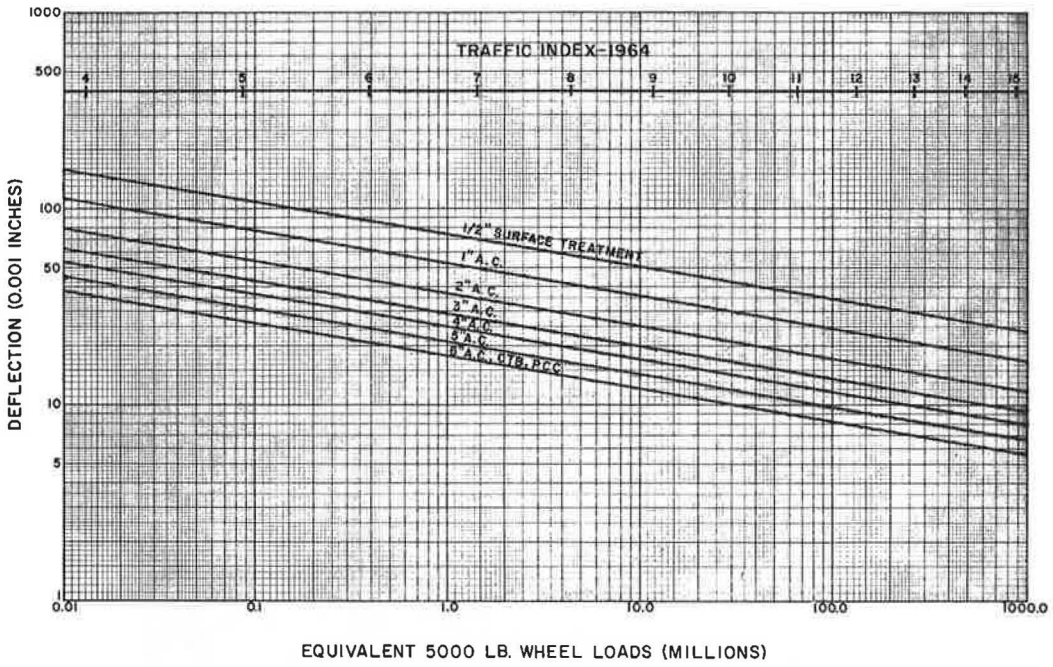


Figure 1. Variation in tolerable deflection based on AC fatigue tests.

The curves have, therefore, been utilized since 1964 in planning the reconstruction of lightly traveled roads based on deflection measurement.

Preliminary review of deflection data from the AASHO test road in Illinois indicates that the tested pavements tolerated deflections somewhat greater than those given in Table 1. However, differences in asphalt quality, design and control of the mixes, and duration of the test may have greatly influenced these values.

The results of a pavement deflection study of three years' duration in North Carolina were reported in 1960 by L. D. Hicks (5). In the course of this study, periodic deflection measurements were made over 4 projects with a Benkelman beam and a dump truck loaded to provide 7500 lb on each rear dual wheel assembly (15,000-lb axle load). This is the same arrangement as that employed by California.

Undoubtedly, the results of these and future deflection investigations, over a variety of pavement structural sections throughout the United States, will enable highway engineers to assign safe levels of deflection to pavements for a given traffic situation with reasonable certainty that the pavements will not be overly fatigued during their design life. These deflection levels will, of necessity, take into account local materials, weather, mixture design, and construction practices.

## DEVELOPMENT OF THE RESILIENCE TEST

Pavement deflections in the past have been measured in situ. Therefore, the designer has had no basis from which to predict the probable deflection of a proposed structural section or to adjust the section so as to reduce an anticipated high deflection to within permissible limits. Over the past 20 years, the Materials and Research Department of the California Division of Highways has developed a testing device and procedure for the purpose of incorporating the deflection factor into pavement design by providing a definite measure of the compression and rebound of a soil specimen under dynamic loading. Since, for a given load and specimen size, this measurement is directly related to the recoverable strain energy of a deformed body when the load causing strain is removed, the instrument has been designated the resiliometer. The

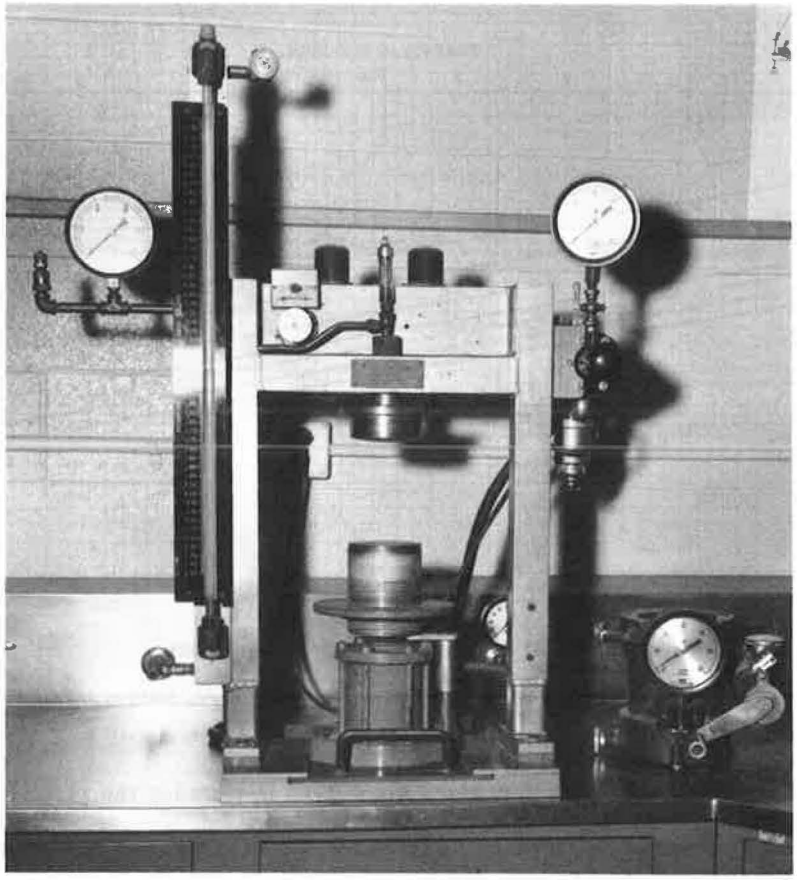

Figure 2. Resiliometer.

test will supplement existing tests because it measures a separate and distinct soil property (resilience) not measured by commonly used test methods.

The resiliometer (Fig. 2) is an apparatus which measures the volumetric displacement resulting from repetitions of a cyclic dynamic load applied to soil specimens ranging from $2\frac{1}{2}$ to 4 in. in height and 4 in. in diameter. The load is applied to the top of the specimen through a rubber diaphragm associated with a pressure system containing ethylene glycol solution, the fluid being acted on by air pressures of from 0 to 60 psi. Volumetric displacement is measured by a manometer tube. Lateral pressures are applied and measured by the stabilometer. The apparatus, test method, and procedure are further described in another report (6).

During the period from 1954 to 1959, several modifications in equipment and technique were instituted which improved the instrument's sensitivity and test reproducibility. This period was also devoted to studies of the effect on resilience of specimen height, density, gradation, moisture content, and number of load repetitions. Qualitative resilience appraisals were made on roadway materials from locations throughout California. In addition, samples from Idaho and Washington, as well as from the WASHO and AASHO test roads, were tested.

The data assembled from these tests seem to warrant certain general observations concerning the resilient behavior of soils:

1. Resilience (internal compression and rebound) increases rapidly with increasing compaction moisture content and, to a lesser extent, with increasing void ratio. Resilience also increases with increasing post-compaction moisture content.

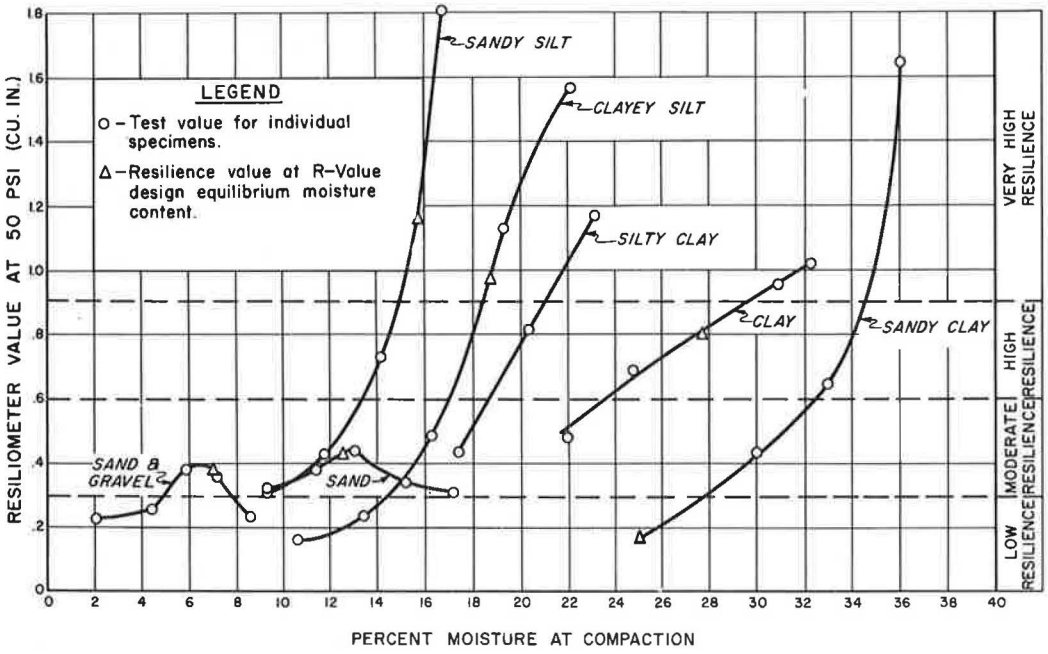


Figure 3. Typical resilience-moisture curves.

2. Although individual clay specimens have been found to be extremely resilient at elevated moisture contents, the greatest sensitivity to moisture, i.e., the largest variations in resilience for a given increase in moisture content, are consistently found in the soils classed as silts or silty types.

3. Sands and gravels are generally low in resilience. The resilience vs compaction moisture content plots shown in Figure 3 illustrate fairly typical behavior of several distinct types of soil. The general descriptive ratings on the right side of the chart are based on an evaluation of results from hundreds of individual tests.

4. As a general rule, the greatest soil "sensitivity" begins slightly on the wet side of optimum moisture content as determined by Test Method No. Calif. 301-F (7).

The accumulation of these data and the assignment of general resilience classifications proved beneficial for the qualitative appraisal of roadway materials for special projects and distress investigations. However, in order to introduce the resilience factor into the California flexible pavement structural design procedure on a rational basis, it was apparent that a relationship was required between laboratory resilience measurements and field performance as measured by pavement deflections.

## RESILIENCE-DEFLECTION CORRELATION STUDY

In order to establish a relationship between pavement deflection and resilience values determined in the laboratory, a correlation study was initiated in the spring of 1959 at the Franklin Airport, southeast of Sacramento. This program consisted of measuring pavement deflections and taking undisturbed samples for resilience testing in the laboratory. Subsequent samplings were made at the California State Fair Grounds and in the Division of Highways Service and Supply Yard in Sacramento. The results of these early correlation samplings were beneficial primarily for development of a procedure for deflection measurements, sampling, and testing, specifically for the resilience-deflection correlation study. In addition, several basic changes in the method of analysis of data were made. The samplings which will be discussed in this report are from roadways

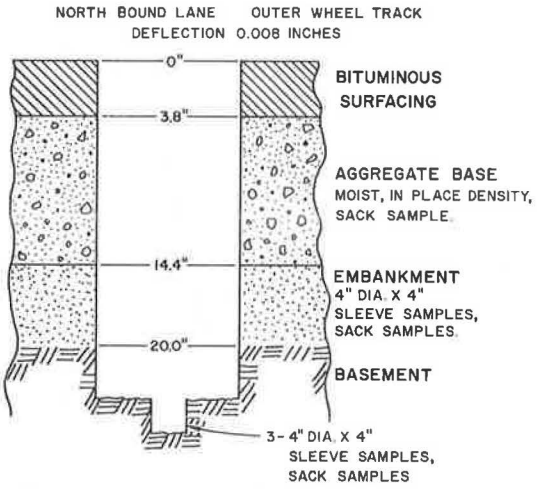


Figure 4. Structural section sampling diagram, Road 04-Mrn-Son-1.

throughout California and from I-15 in in Idaho. At present, the resilience-deflection correlation consists of 44 individual samplings from 20 different roadways.

## Field Procedure

During the correlation study (1959-1963), a Benkelman beam was used to measure deflections produced by a dump truck with a rear-axle load of 15,000 lb. The load was supported by two dual wheel assemblies with 10:00 x 20 tires inflated to 70 psi. The test interval varied from 15 to 20 ft in each wheel track of a selected lane throughout a test area of 500 lineal ft. The temperature of the pavement surface was recorded at the time deflection measurement was made.

Locations from which samples were obtained were selected from within an area of relatively uniform deflection. Thus, samples representative of the general state of the roadway were obtained, thereby minimizing the effects of localized conditions. Areas with cracked surfacings were considered unsuitable for sampling since they yield abnormally high deflections due to the rocking action of individual blocks.

Sampling operations included taking moisture samples and a 40 to 50-lb disturbed sample from each different material to a depth of 30 in. from the surface. These samples were obtained from a 2 by 3-ft hole excavated to a depth of 30 to 36 in. In addition to thickness measurements, at least three undisturbed 4-in. high by 4-in. diameter samples were obtained from the basement or embankment soil and, in some cases, the subbase. Those materials from which undisturbed samples could not be taken, due to lack of cohesion, were tested for in-place density utilizing the sand-volume method (Test Method No. Calif. 216-F). A typical sampling diagram used for the sample taken on one of the roads is shown in Figure 4.

## Laboratory Testing Parameters

In order to minimize the adverse effects of different loading variables, an attempt was made to reproduce in the laboratory the expected field conditions. The variables considered included lateral confining pressure, surcharge, vertical stress, distribution, effective depth of deformation, and rate of load application.

Lateral Confining Pressure—For correlation purposes, it was considered desirable to test specimens using a lateral confining pressure in the stabilometer comparable to that exerted on an in-place element of soil resulting from dynamic loading representative of the traffic using the highway. The in-place passive-active pressure state in soils covered with different pavements, however, cannot be duplicated with any known laboratory device. Therefore, a uniform lateral confining pressure of 3 psi was used for all tests. This value was selected as a result of a series of resilience tests in which several confining pressures were used with a variety of soils. The results indicated that, for the range of vertical pressures utilized, the least permanent lateral distortion occurred in the test specimens at 3 psi.

Vertical Surcharge—During the early developmental stages of the test procedure, varying vertical surcharge pressures representing different thicknesses of overburden were used. The varying surcharge pressure, however, was found to have no significant effect on the test data. It was, therefore, decided to adopt the more practical approach

of utilizing equal vertical and lateral confining pressures. The vertical pressure is composed of two parts, a constant surcharge component of 2.4 psi and an average component of 0.6 psi due to the weight of the manometer fluid. Thus, the test specimen has a uniform confining pressure of approximately 3 psi.

The vertical surcharge pressure is maintained by a spring-loaded "pop-off" valve on the air exhaust line which expels air at the end of each loading cycle until the pressure is reduced to 2.4 psi. This residual pressure is then maintained until the beginning of the next cycle.

Vertical Stress Distribution—Probably the most important single variable in the correlation of field deflection and laboratory resilience is the application of a vertical dynamic pressure with the resiliometer which corresponds to that absorbed by the soil as the result of a transient wheel loading. The more important variables which must be considered include stiffness and stratification of overlying material, wheel loading and spacing, and rate of load application.

A review of the literature on the subject of depth-vertical pressure relationships in soils must inevitably begin with the work of Boussinesq (8), who introduced in 1885 what is now a well-known mathematical expression for calculating the vertical pressure distribution pattern in a homogeneous, elastic, level and semi-infinite medium.

A great deal of productive research in recent years has been devoted to modifying the theory so that it may closely parallel experience with actual soil conditions. In 1936, a modification of the Boussinesq equation was proposed by A. E. Cummings (9). This involved the application of a concentration factor (n) as a parameter which could be adjusted to fit materials other than isotropic elastic solids. The concentration factor concept was empirical by nature and thus required verification by field data. The accelerated traffic test at Stockton Airfield (10) in 1948 was partially devoted to the comparison of recorded vertical pressures with theoretical values. These values were obtained using concentration factors ranging from 2 to 8 with varying wheel loads, temperatures, and structural sections. Examination of the resulting plots indicates that, for the range of variables included in the test, the concentration factor (n) fell generally between 2 and 4 (n = 3 for the theoretical equation). There appears to be a tendency toward larger concentration factors with heavier structural sections. The magnitude of the wheel loading, however, had no noticeable effect on the parameter.

In 1938, Westergaard (11) introduced a further modification of the Boussinesq equation, with the inclusion of Poisson's ratio. This change was based on the nonisotropic conditions found in sedimentary soils. These equations express relationships that are undoubtedly closer to conditions in sedimentary soils and are generally believed to be preferable for settlement predictions.

A comparatively recent and comprehensive physical pressure-depth investigation was conducted by the Civil Aeronautics Administration Technical Development and Evaluation Center under the direction of Raymond C. Herner (12). Herner utilized a "mechanical subgrade" with which it was possible to measure, on a plane, the vertical pressures induced by a variety of static aircraft and truck wheel loadings through asphaltic concrete surfacing and flexible bases of differing thickness and quality. Herner's study provided a great deal of useful physical data. The tests indicated wide variation in maximum vertical pressure with varying pavement and base thickness and quality, wheel load, and subgrade reaction. Although the tests were primarily concerned with aircraft-tire loadings, a number of readings were made utilizing 8.25 × 20 and 10:00 × 20 dual truck-tire loadings over a weak subgrade (modulus of subgrade reaction = 82). These data for the 7 and 8-kip loadings and 70-psi inflation pressure are shown in Figure 5 along with the theoretical Boussinesq curve utilizing the loading and configuration (twin circular discs at a uniform pressure of 70 psi with 5½ in. between inside edges) most representative of tire print of California's Benkelman beam truck. Since the beam truck wheel load is 7.5 kips and utilizes 10:00 × 20 tires, the data from the load transmission test is approximately applicable. It is interesting to note that these points are in comparatively good agreement with the theoretical curve.

In 1943, Burmister (13) introduced a rigorous mathematical development of the elastic theory for the general case of a two-layer system for the determination of

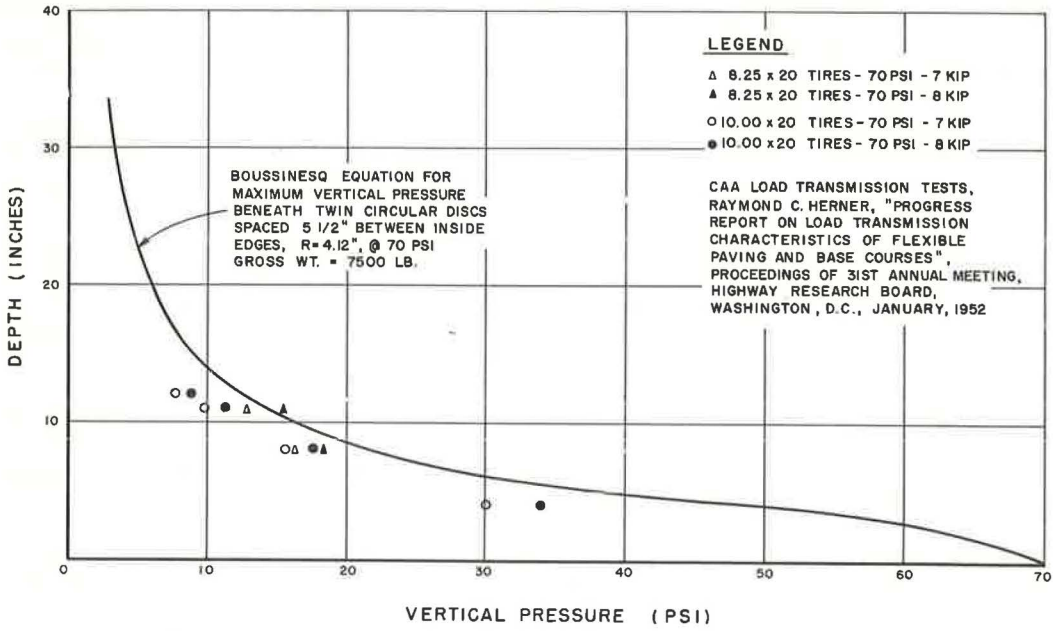


Figure 5. Vertical pressure vs depth.

stresses in layered soil deposits. Burmister enlarged his original analysis in 1945 to include a three-layer system (14).

In 1951, W. E. A. Acum and L. Fox (15) published a series of tables for the three-layer system in which stresses were numerically presented for a series of specific conditions. These computations were based on the following assumptions:

1. All materials involved behave elastically.
2. Perfect continuity (or friction) exists at each interface.
3. Poisson's ratio equals 0.5 for all elements of the structural section.

Whether these assumptions are valid for highway design will have to be determined by further physical measurements.

The evolution of influence diagrams or equations for application of the elastic theory for the more complex structural sections is continuing through efforts of Burmister and others. At the present time, however, the material available for convenient application of the elastic theory to the present day multilayered sections is still inadequate. The results of the accelerated traffic test at Stockton and the work of the CAA with the mechanical subgrade agree well enough with the theoretical Boussinesq equation for flexible pavement systems so that its use for assumed variation of pressure with depth was adopted with reasonable confidence.

Further justification for the use of the Boussinesq pressure distribution curve for flexible sections was provided by Vesic and Domaschuk (16), who, in a recent study of the deflection data from the AASHO Road Test, found the Boussinesq theory to fit the AASHO data more adequately than the layered-solid theory.

Effective Depth of Deformation—The electronic gage units referred to previously were installed throughout California from 1951 to 1955 and provided not only the data on total pavement deflection but also some idea of the amounts contributed by individual layers of strata. Examination of these data indicated that compression and rebound is developed in measurable amounts to depths of 21 ft. However, computations for flexible sections revealed that, on the average, approximately 86 percent of the deflection in the upper 8 ft of material occurred in the upper 2 ft and that 82 percent of that in the top 18 ft depth was in the top 3 ft. A typical example of this phenomenon is shown in Figure 6.

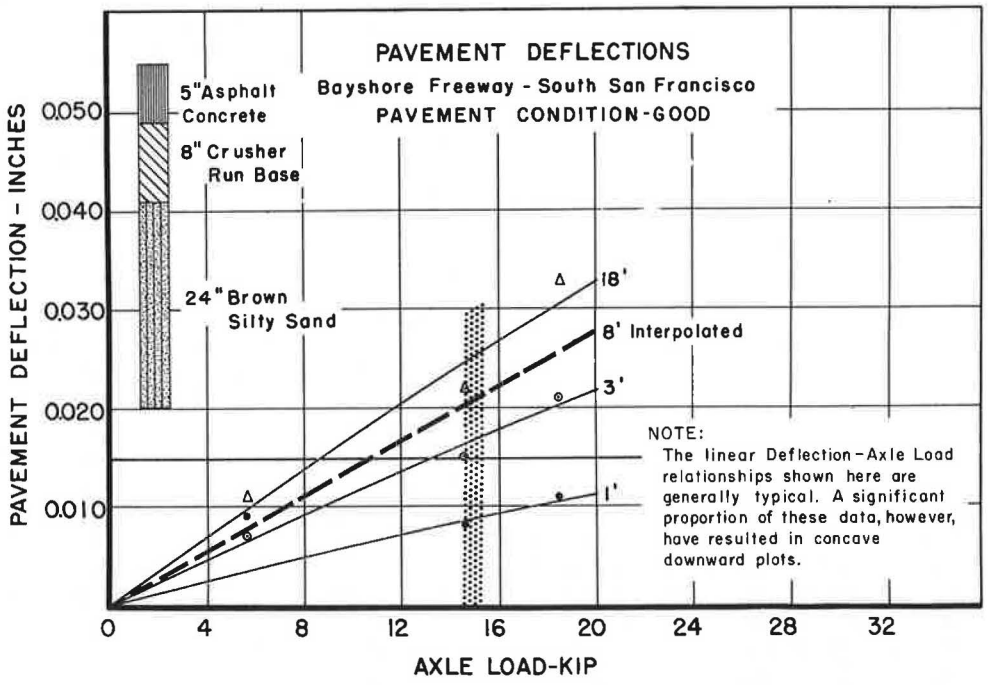


Figure 6. Typical pavement deflections.

It was apparent that either sampling or taking into account the effects of depths below 2 to 3 ft would be unrealistic. In addition, pressures occurring at depths below 2 ft are so low that experimental errors begin to mask out the significance of the resulting resilience data (Fig. 5). Accordingly, the limiting depth for sampling and consideration in computations was set at 30 in.

For purposes of computation, the test resilience value for any stratum is obtained by determining the average pressure at the depth the material exists. This can be conveniently done by using the depth-vertical pressure curve shown in Figure 5. Since this curve is not linear, calculations are made in 4-in. increments of depth. The pressure so determined is adjusted by adding 10 psi and the test resilience value is determined at the adjusted pressure reading. The addition of the 10 psi is a deviation from the theoretical curve and is utilized because it distorts the depth-pressure curve in favor of those materials appearing at lower depths and, therefore, tends to compensate for the 30-in. depth limitation.

Rate of Load Application—The rate of load application has been held to a constant 8 cycles per minute, the minimum period found necessary for full rebound of the specimen. The 7.5-sec cycle is divided so that pressure is applied to the specimen for 0.75 sec, the minimum period of time needed to secure an accurate reading of the manometer tube. A typical Benkelman beam deflection vs time plot is shown in Figure 7 superimposed on a Brush Analyzer record chart of the resiliometer test in which the dynamic load is plotted against time. The deflection trace indicates the rate of load application at a given point at the approximate operating speed of the Benkelman beam truck.

The number of load repetitions applied at each increment of pressure is dependent on the nature and state of the material being tested. The volumetric displacement is recorded only when the rebound reading is within 0.02 cu in. of the initial reading, so that the data reflect, almost entirely, resilient deformation of the specimen.

Thus, with sands and silts, readings can be taken almost immediately while clays require a large number of repetitions at each increment of pressure in order to reduce

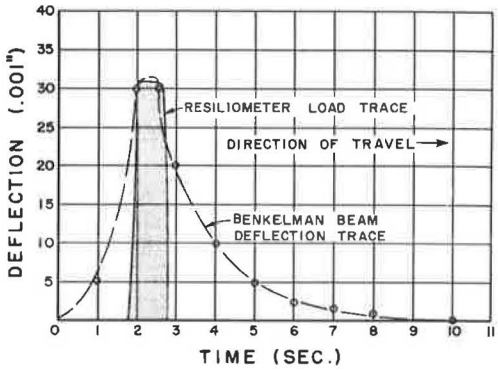


Figure 7. Deflection-resiliometer loading trace.

the plastic deformation to an acceptable minimum. Although plastic deformation is cumulative throughout the test, resilient deformation remains virtually constant for each applied pressure after the initial period of preliminary consolidation. This behavior is illustrated graphically by the compression and rebound history of an undistrubed clay specimen (Fig. 8).

## Analysis of Resiliometer Data

Method of Analysis—The method of analyzing resilience test data now differs from that reported previously (6, 17). At present, the characteristic slope of the individual plotted points for each specimen is projected through the "no load" pressure (confining pressure) on the pressure-resilience plot rather than using the curve of best fit through the actual plotted points as was the previous practice. This revised procedure was adopted because samples prepared in an identical manner frequently produce widely dispersed pressure-resilience curves even though each curve has approximately the same slope (Fig. 9). The scatter in absolute resilience values is possibly due to individual specimen end effects and variations in specimen densification. These differences tend to offset the curves in varying amounts laterally. The use of a curve having the characteristic slope of all the individual samples projected through the ordinate confining pressure value appears to have eliminated this problem and has produced a better correlation between resilience summation and field deflection.

Typical Computation—The mechanics of sampling, testing, and analysis of data for the resilience-deflection correlation study can best be illustrated by a typical example, in this case, from Project 04-Mrn-Son-1 near Bodega Bay, California. A series of four deflection measurements taken on November 29, 1960, on the northbound outer wheel track from Station 0+00 to Station 8+00 were found to range from 0.004 in. to 0.016 in. Station 6+00, with a deflection of 0.008 in. was selected for sampling. The structural section and sampling pattern are shown in Figure 4. Disturbed samples and

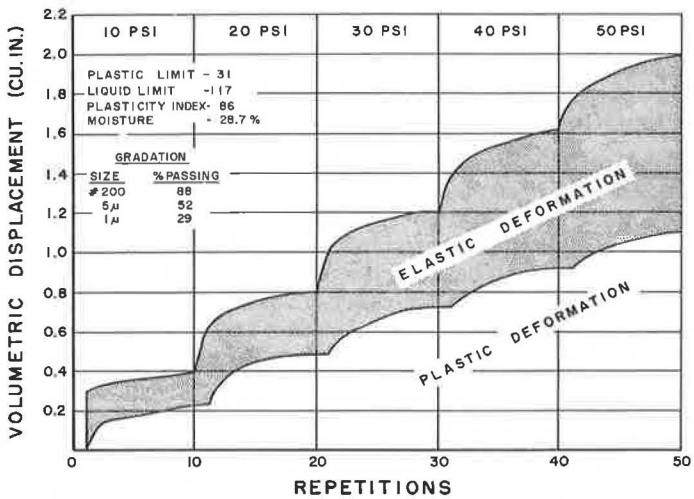


Figure 8. Compression and rebound history of undisturbed clay specimen.

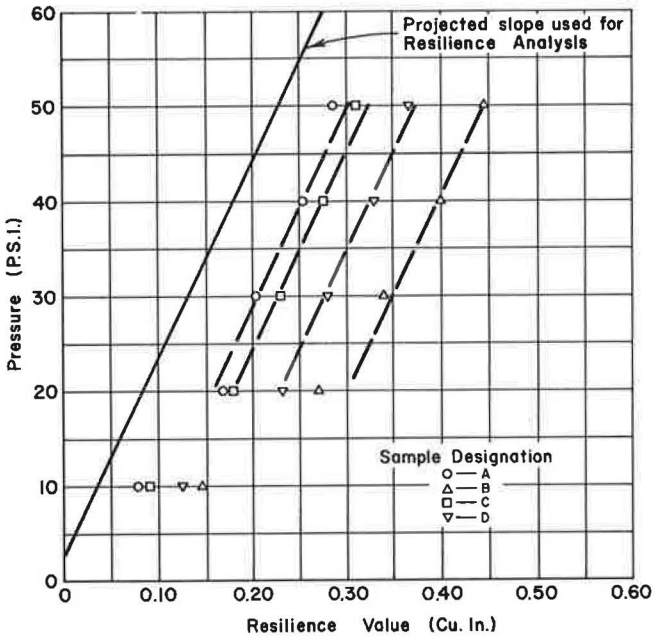


Figure 9. Resilience test results illustrating slope method of analysis, Road 10-Cal-12, 49 (aggregate base).

moisture samples of all elements of the structural section were taken. In-place density measurement of the base was made using Test Method No. Calif. 215-F (sand volume). Three 4-in. diameter by 4-in. high undisturbed samples were obtained from the embankment and basement soil at depths ranging from 14.4 to 32 in.

Samples of base and embankment were compacted in the laboratory at field moisture and density and tested in the resiliometer under pressures ranging from 10 to 50 psi in 10-psi increments.

Undisturbed samples which were taken by driving a brass sleeve into the embankment and basement soil were trimmed to proper length and tested in a like manner. The results are shown in Figures 10 to 12. The pressure-resilience relationship is obtained by drawing the slope of the plotted points through the confining pressure value on the ordinate scale. In establishing the representative resilience slope of basement or borrow samples, greater weight is given to data taken at lower pressures (10 to 30 psi); similarly, the resilience slope of base and subbase materials is largely determined from the resilience readings at high pressures (30 to 50 psi).

From Figure 5 it may be seen that the first 4-in. increment of depth (3.8 to 7.8 in.) has an average pressure of 37.0 psi. Adding 10 psi, the resilience at 47.0 psi is observed to be 0.099 cu in. from Figure 10. The average pressure for the second 4-in. increment of the base (7.8 to 11.8 in.) is 17.4 + 10 = 27.4 psi (Fig. 5). The resilience for the remainder of the base (11.8 to 14.4 in.) at 11.2 + 10 = 21.2 psi is 0.044 cu in.

However, since the resilience data applied only to tests on specimens 4 in. in height, a correction is made on the last increment by multiplying the resilience value by a ratio of the actual thickness of the increment to 4 in., in this case 0.044 (2.6/4.0) = 0.029 cu in. The total contribution to resilience by the layer of the base material is, therefore, 0.099 + 0.057 + 0.029 = 0.185 cu in. The vertical pressure for the first 4-in. increment of the embankment (14.4 to 18.4 in.) was found to average 8.1 psi + 10 psi = 18.1 psi. From the resilience pressure plot, for a pressure of 18.1 psi, the resilience was found to be 0.120 cu in. The resilience for the increment of embankment from 18.4 to 20.0 in. corrected for height was found to be 0.044 cu in., thus making the total embankment resilience equal to 0.164 cu in.

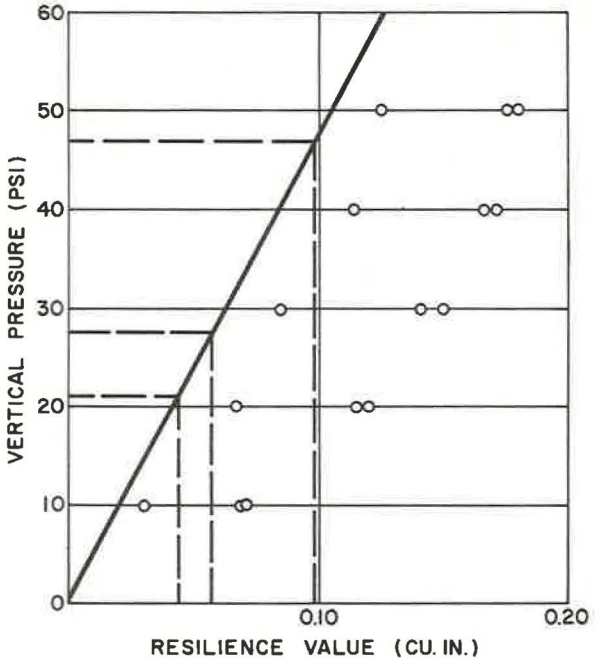


| DEPTH (IN) | AV PRESSURE (PSI) | RESILIENCE VALUE (CU. IN.) |
|---|---|---|
| 3.8 - 7.8 | 37 + 10 | .099 |
| 7.8 - 11.8 | 17.4 + 10 | .057 |
| 11.8 - 14.4 | 11.2 + 10 | $.044 \times \frac{2.6}{4} = .029$ |
| | | TOTAL .185 |

Figure 10. Pressure-resilience plot of aggregate base, Road 04-Mrn-Son-1.

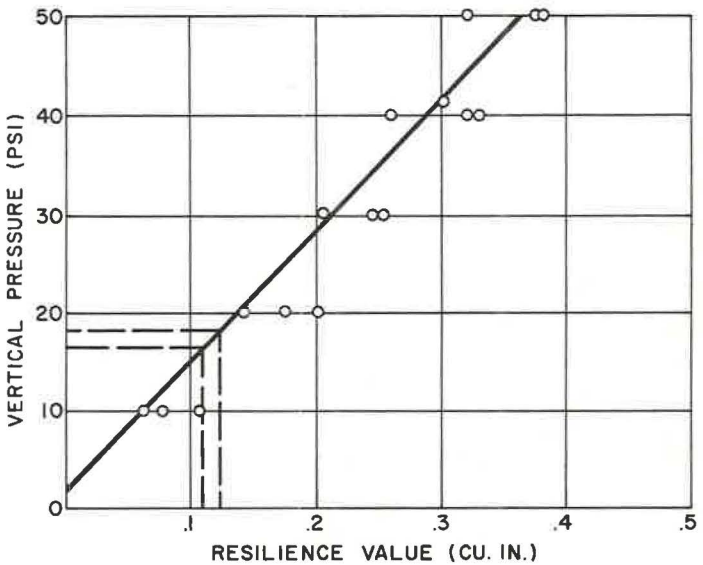


| DEPTH (IN.) | AV PRESSURE (PSI) | RESILIENCE VALUE (CU. IN.) |
|---|---|---|
| 14.4 - 18.4 | 8.1 + 10 | 0.120 |
| 18.4 - 20.0 | 6.5 + 10 | $110 \times \frac{1.6}{4} = 0.044$ |
| | | TOTAL 0.164 |

Figure 11. Pressure-resilience plot of embankment, Road 04-Mrn-Son-1.

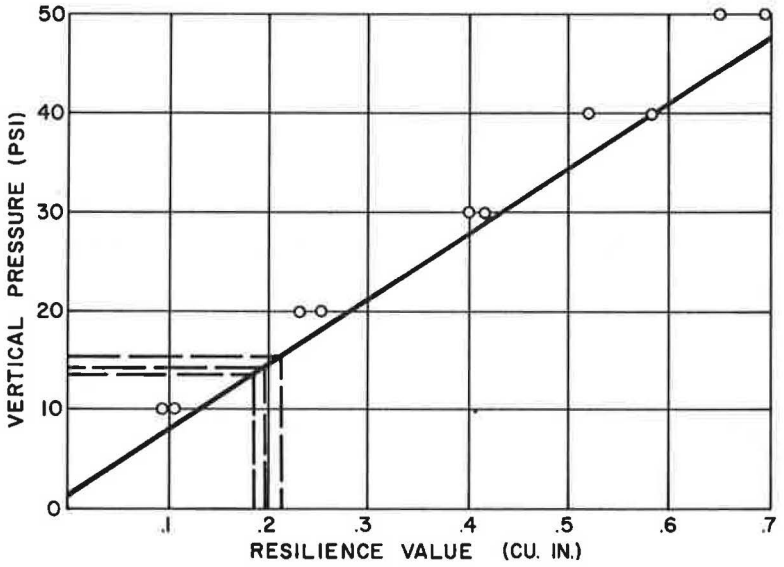


| DEPTH (IN) | AV PRESSURE (PSI) | RESILIENCE VALUE (CU. IN.) |
|---|---|---|
| 20.0-24.0 | 5.4+10 | 0.215 |
| 24.0-28.0 | 4.3+10 | 0.200 |
| 28.0-30 | 3.6+10 | 0.190 X $\frac{2.0}{4}$ = 0.095 |
| | | TOTAL 0.510 |

RECAPITULATION

| MATERIAL | TOTAL RESILIENCE VALUE |
|---|---|
| AGGREGATE BASE | 0.185 |
| EMBANKMENT | 0.164 |
| BASEMENT SOIL | 0.510 |
| GRAND TOTAL | 0.859 |

Figure 12. Pressure-resilience plot of basement soil, Road 04-Mrn-Son-1.

This procedure was repeated for the basement or embankment soil (Fig. 12) to a depth of 30 in. The total resilience for a depth of 30 in. totaled 0.859 cu in. This was plotted against the field deflection at that point (0.008 in.) in Figure 13.

It may be noted from the foregoing example that no resilience value was computed for the AC surface. This is based on the assumption that the resilience of AC is negligible compared to that of the underlying soils.

Discussion of Correlation Plot—The results of 44 samplings from 20 projects are shown in Figure 13 with a regression line of correlation. Although there is considerable scatter, a fairly well-defined pattern emerges. These data produced a coefficient of correlation of 0.85 with a 95 percent confidence bank of 0.74 to 0.92. It is interesting to note that samples from the same project usually check each other, i.e., the lower deflections result in the lower summations of resilience. The average deflections

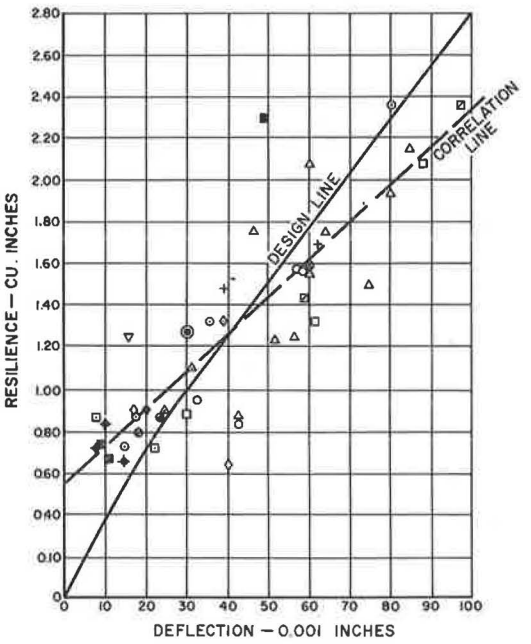


| LEGEND | |
|---|---|
| ROAD LOCATION | |
| ⊡ 04-Mrn,Son-1 | ⊠ City of Woodland |
| ○ 03-But-32 | ■ City of Woodland |
| △ 03-Sac-99 | ▽ 02-Teh-FAS-1078 |
| □ City of Hawthorne | ◉ 03-Col-45 |
| ⊙ 05-SBt-156 | ▲ 03-Sut-99 |
| ⧋ 10-Mer-FAS-914 | + 03-Yol-16 |
| ◈ 06-Sac-16 | ◆ 04-Son-FAS-780 |
| ◇ 04-SCr-FAS-1270 | ⊕ 04-Son-FAS-787 |
| ● Striplin Road (County) | ⊛ 05-SBt-156 |
| ✦ INTERSTATE 15-IDAHO | ⊠ 06-Tul-FAS-1143 |

COEFFICIENT OF CORRELATION = 0.85
STD. ERROR OF ESTIMATE = 0.269 CU. IN.

Figure 13. Resilience summary vs field deflection, 44 individual samples from 20 road locations.

and resilience summations of individual projects are shown in Figure 14. Averaging results from the same projects increased the coefficient of correlation to 0.95 with a 95 percent confidence band of 0.82 to 0.98. Considering the variables which are not controlled in the study, the trend toward correlation is gratifying. The following factors are believed to be responsible for the scatter in results:

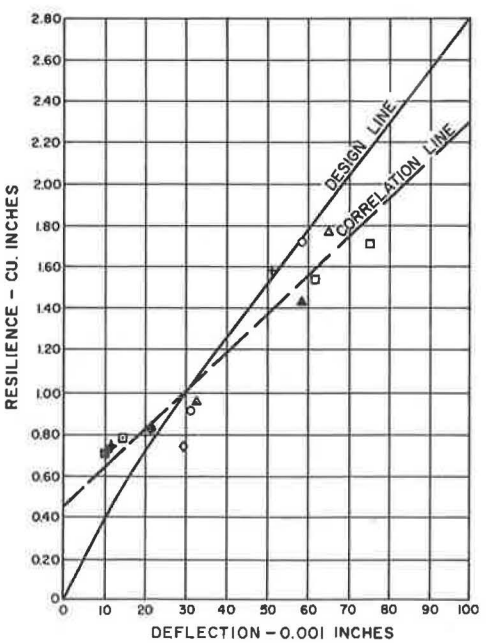


| LEGEND |
|---|
| ROAD LOCATION |
| ⊡ 04-Mrn-Son-1 |
| ○ 03-But-32 |
| △ 03-Sac-99 |
| □ City of Hawthorne |
| ⊙ 05-SBt-156 |
| ⧋ 10-Mer-FAS-914 |
| ◇ 04-SCr-FAS-1270 |
| ✦ INTERSTATE 15-IDAHO |
| ⊠ City of Woodland |
| ▲ 03-Sut-99 |
| + 03-Yol-16 |
| ● 05-SBt-156 |
| ⊠ 06-Tul-FAS-1143 |

COEFFICIENT OF CORRELATION = 0.95
STD. ERROR OF ESTIMATE = 0.127 CU. IN.

Figure 14. Resilience summary vs field deflection, averages of samples from 13 road locations.

1. Variations in density and moisture content in the materials as they exist in the field;
2. Deviation from the assumed depth-pressure distribution due primarily to varying states of hardness of the asphalt surfacing and, to a lesser extent, its temperature; and
3. The inability to reproduce in the testing apparatus the in-place lateral active-passive pressure state of the surrounding soil.

## APPLICATION OF LABORATORY RESILIENCE-FIELD DEFLECTION CORRELATION TO PRELIMINARY PAVEMENT DESIGN

The primary purpose of the correlation experiment described was to determine whether a relationship existed between the laboratory resilience measurements and pavement deflection as measured on the roadway. In order to prove the existence of such a relationship, every effort was made to reproduce, under laboratory conditions, those which existed in place when the deflection measurement was made. Thus, wherever possible, soil specimens were subjected to resilience tests in an undisturbed state. For coarse-grain materials, individual specimens were fabricated and tested at field moisture content and density. Having produced what is believed to be a satisfactory relationship between laboratory resilience and field deflection, the final phase of the investigation was begun, i.e., the application of the correlation to a preliminary design situation. Here, of course, it was necessary to assign design moisture and density criteria in the fabrication of specimens from preliminary samples and to take into consideration possible thixotropic effects which will have existed in the original undisturbed samples. In subsequent sections, the evolution of resilience design criteria for preparation of preliminary specimens will be described.

### Resilience Design Moisture Content

Of primary concern in the adoption of the resilience-field deflection correlation to preliminary design was the selection of design moisture content. Because it has long been observed that moisture content is the prime variable with respect to resilience

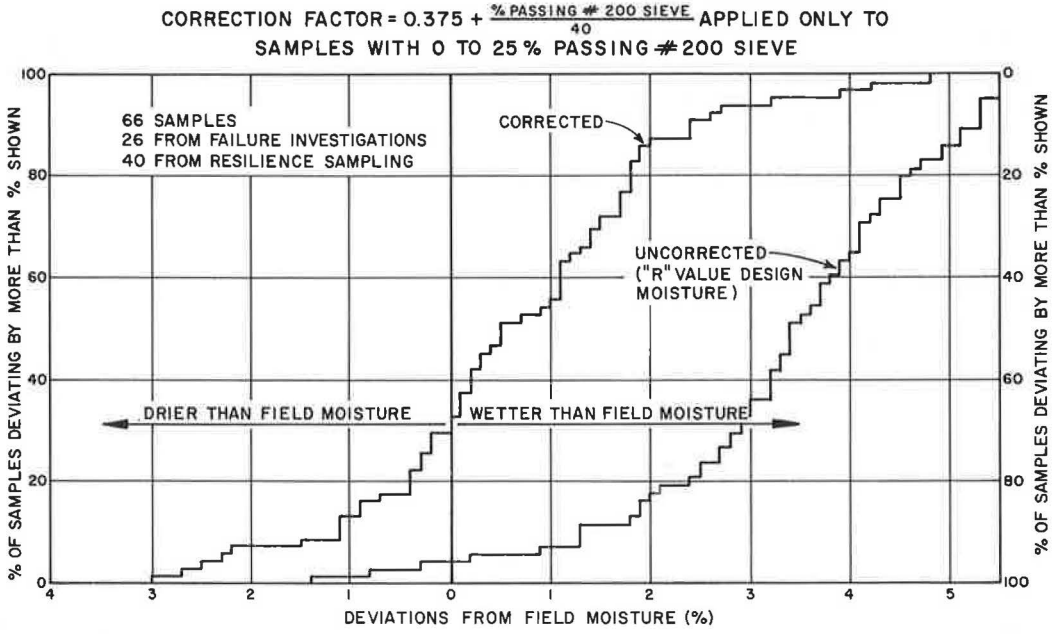


Figure 15. Ogive curve showing deviation of "R" value design moisture from field moisture.

even in coarse-grained materials, it was decided to compare in-place field moisture data from various distress investigations and resilience samplings with the current 300-psi exudation pressure R-value design moisture criteria. Exudation pressure is the moisture condition at which a soil specimen will be saturated under a static load of 300 psi. This represents the worst condition the roadway is expected to attain in its design life (12).

The results of this investigation for coarse materials (0 to 25% passing the No. 200 sieve) are shown in Figure 15. As shown by the ogive curve, approximately 95 percent of the samples were wetter at R-value design moisture criteria than at field moisture content.

A similar plot for fine-grained materials (25% plus passing the No. 200 sieve) revealed that only 70 percent of the samples by the R-value moisture criteria were wetter than field moisture (Fig. 16). Although excess moisture has relatively little effect on the results of stability tests on coarse-grained materials, deviations between field and laboratory moisture content can induce large increases in resilience. It was, therefore, decided to adjust the R-value criteria (300-psi exudation pressure) for coarse-grained material by a factor sufficient to bring it into line with that for fine-grained materials. The following corrective equation is simply a straight-line function which accomplishes this adjustment:

$$C_f = 0.375 + \frac{x}{40}$$

where

$C_f$ = a correction factor to be multiplied by the 300-psi exudation pressure moisture content for soils with 0 to 25 percent passing the No. 200 sieve; and

$x$ = percent passing the No. 200 sieve.

As shown by Figure 15, the corrected values for the coarse-grained soils result in an ogive curve which is quite similar to the uncorrected curve for fine-grained soils (Fig. 16), which, in effect, brings the corrected coarse-grained design moisture con-

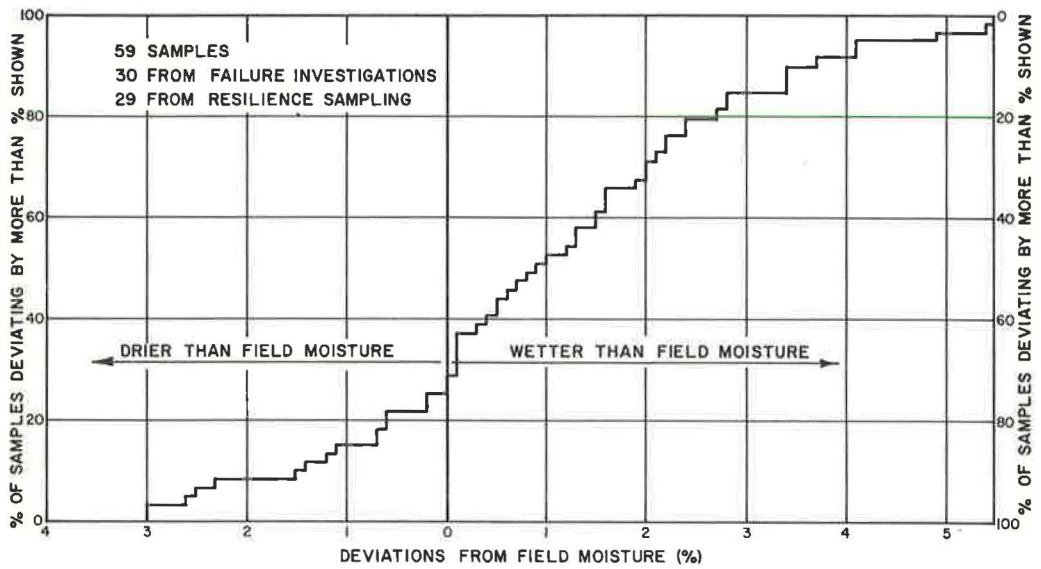


Figure 16. Ogive curve showing deviation of "R" value design moisture from field moisture, for materials having greater than 25 percent passing No. 200 sieve.

tents to a state of accuracy commensurate with that being used at present in R-value design procedure for fine-grained materials. A correction of this nature has not been necessary for the R-value design procedure since the R-value of coarse-grained soils is not generally sensitive to moisture variation within the range under consideration. This correction, therefore, is applied for all resilience design testing.

## Effects of Thixotropy

Preliminary data on the effect of thixotropy with respect to clay soils were presented in 1962 by Hveem et al (17). It was found that freshly remolded AASHO embankment soils resulted in resilience values up to three times as great as those for the undisturbed samples of this material at the same moisture and density. It was decided therefore, to investigate various "sensitive" California clays in order to compare remolded with in-place resilience characteristics and possibly to determine a suitable curing period for remolded clay soils to allow for a thixotropic regain of strength which would be comparable to that eventually attained in the finished roadway. This problem was not as serious as originally envisioned since only 3 of the 16 soils tested established a remolding loss and thixotropic regain of strength to a significant degree. The test data for the most sensitive material (Road 03-Sut-99) will be discussed further.

Approximately 200 lb of clay basement soil and five undisturbed samples from Project 03-Sut-99 (El Centro Road) were obtained. The undisturbed samples were tested for resilience upon receipt by the laboratory. Subsequently, a number of specimens were compacted in sets of four each at the average moisture and density of the undisturbed samples. The first set of specimens was tested immediately after compaction and succeeding sets were tested after moist-curing 1 day, 6 days, 14 days, 57 days and 76 days. Moisture loss during the curing was prevented by placing these specimens, while still in the mold, in metal cans, sealing them in plastic bags, and curing in a 100 percent humidity cabinet.

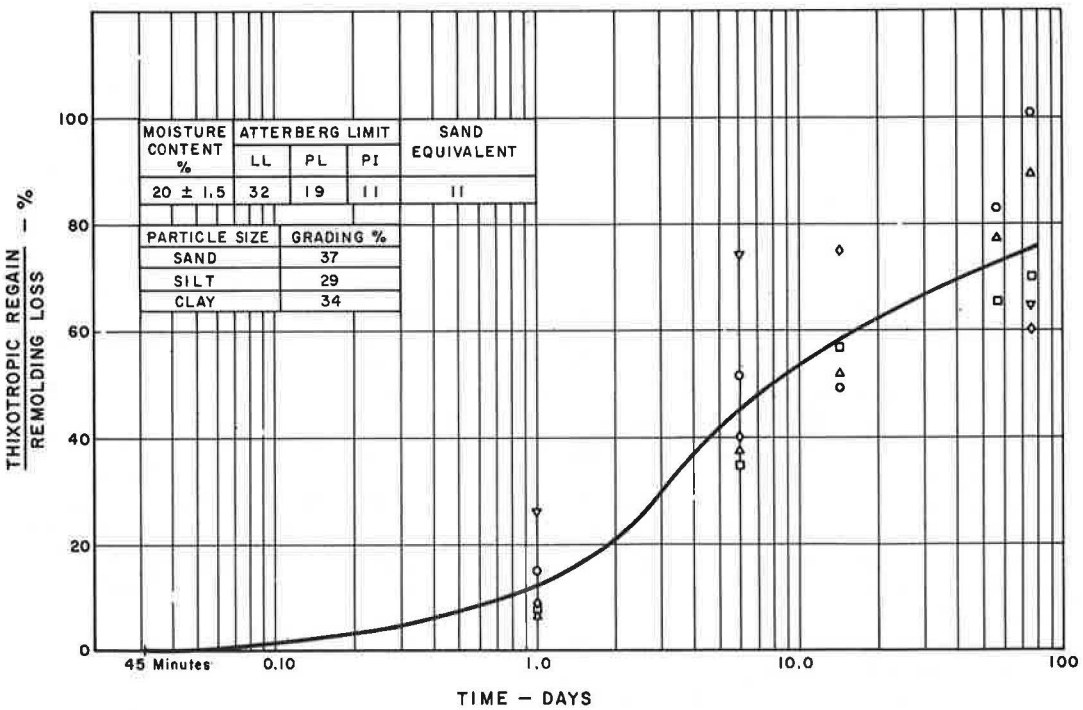


Figure 17. Thixotropic regain of a sandy silty clay from Project 03-Sut-232-A.

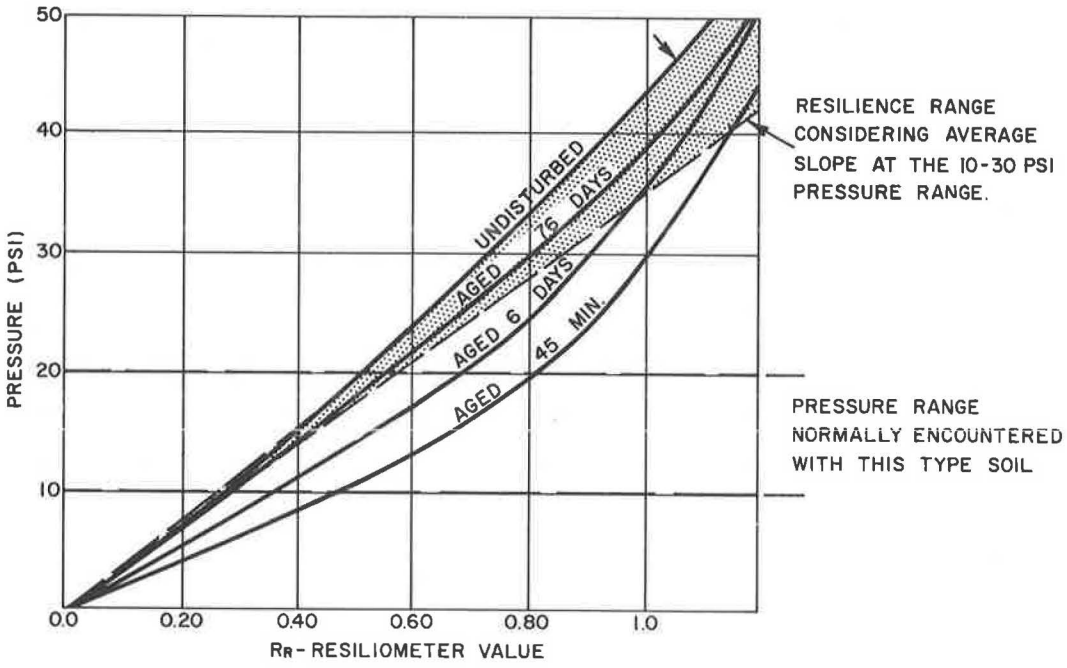


Figure 18. Change in resilience due to thixotropy of a sandy silty clay from Project 03-Sut-99.

Plots of thixotropic strength regain vs curing time are shown in Figures 17 and 18. The thixotropic strength regain was calculated as a ratio of the decrease in resiliometer value at a given curing time to the increase in resiliometer value immediately after compaction.

Curing 7 days resulted in recovery of half the strength lost by disturbing the material (Fig. 17). After 7 more days of curing, approximately 10 percent additional strength was regained. In the next 7 days, only 4 percent additional strength was regained.

For this material, a point of diminishing return is reached after approximately 15 days of curing. Based on the results of this study, a 2-week curing period was initially established as standard procedure for preliminary resilience samples containing a significant clay percentage.

With the adoption of the present procedure for the analysis of resilience data, i.e., the utilization of the slopes of plotted values rather than absolute resilience measurements, a 2-week curing period did not appear to be justified by the relatively slight increase in test accuracy. As shown in Figure 18, the shaded zone represents the range in resilience, considering average slopes at the 10- to 30-psi pressure range. Between the 10- and 20-psi pressure increments which represent the usual range under consideration for basement soil, the shaded band indicates a deviation range from the undisturbed resilience curve of only approximately one-fourth of that shown by the various solid curves representing individual plotted values. In this particular case, we note a deviation of 0.02 to 0.07 cu in. in resilience which would represent a small portion of the resilience summation for an entire structural section. It should also be emphasized that the material represented by Figure 18 is an extreme case and is, therefore, not representative of most clayey soils.

Although the potential problem of thixotropy has not been entirely discounted, the use of an extended curing period for fine-grain soils has been, for the present, discontinued. Unless further study reveals the need for a longer curing period, or a modification in the method of analysis of tests of clayey soils, a one-day cure between the time of compaction and the time of testing will be used.

## Application to Design

The relationship obtained from the correlation study between field deflection and laboratory resilience determination for various pavement systems provides a basis for the design of flexible pavement structural sections. An example of the resilience analysis applied to a design situation is included herein utilizing the resilience-deflection design curve (Fig. 13). The design curve provides a factor of safety to the resulting design and, therefore, is used instead of the resilience-deflection correlation line.

The basis of this analysis is the determination of a resilience summation for the proposed structural section to a depth of 30 in. with which it is possible to predict a deflection from the design curve. When a predicted deflection exceeds the tentative criteria given in Table 1 and shown in Figure 1, adjustment of the structural section is required to reduce the summation of resilience and thus bring the predicted field deflection within tolerable limits. Examination of resilience data will indicate which element of the structural section is critical or may be adjusted most economically. Alternative solutions for excessive resilience would include:

1. Reduction of surfacing thickness, thereby increasing the allowable deflection;
2. Utilizing a composite, i.e., semirigid, structural section (for example, AC surfacing over a cement-treated base) to reduce deflection by increasing stiffness; or
3. Increasing the thickness of subbase, base or surface layers.

## Design Example No. 1

The design application just described is illustrated by the following example. A roadway pavement design is proposed with a structural section consisting of 3 in. of AC surfacing, 8 in. of aggregate base and 10 in. of aggregate subbase for a county road with a traffic index of 8.0. Resilience test results on preliminary samples compacted at resiliometer design moisture content are shown in Figure 19. The test values used in the illustration are considered generally representative for these materials.

The calculation of the summation of individual layer resilience is also shown in Figure 19. The average vertical pressure in the upper 4 in. of the base layer (3 to 7 in.) is found from the Boussinesq equation (Fig. 5) to be 41.9 psi plus 10 = 51.9 psi. The resilience from this curve at 51.9 psi equals 0.210 cu in. Similarly, for the next 4-in. increment of the base layer a resilience of 0.115 cu in. is obtained. The resilience contribution for the base layer will, therefore, equal 0.325 cu in.

Similar computations for subbase and basement soil (to a depth of 30 in.) result in the resilience increments shown in the tabular material in Figure 19 for a total of 0.970 cu in. for the proposed section. From the design line in Figure 13, the predicted equivalent transient deflection of this section equals 0.029 in. Tentative criteria indicate that the 3-in. AC pavement will not tolerate deflections in excess of 0.023 in. for a TI of 8.0 (Table 1 and Fig. 1). Therefore, a design adjustment is required.

For a second trial (Fig. 20), the thickness of surfacing was increased to 4 in. which decreased the allowable deflection to 0.020 in. In addition, the thickness of the least resilient material, aggregate base, was increased from 8 to 10 in. and the aggregate subbase was increased from 10 to 12 in.

As shown by Figure 20, this manipulation reduced the resilience summation to 0.740 cu in. with a new predicted deflection of 0.020 in., just equal to the tolerable limit. The redesign, therefore, meets the criteria for both stability and resilience. An alternate solution would involve the utilization of a cement-treated base (CTB) with a 3-in. AC surfacing.

Studies on the deflection damping characteristics of various roadway materials indicate that reductions of from 0.002 in. to 0.0035 in. of deflection per inch of thickness are possible with a CTB over and above that resulting from an equivalent layer of gravel base. Thus, utilizing the original design with a 6-in. CTB instead of the gravel base, the predicted deflection of this roadway could reasonably be expected to be reduced from 0.029 in. to 0.014 in. or less than the tolerable limit for a CTB section at a TI of 8.0.

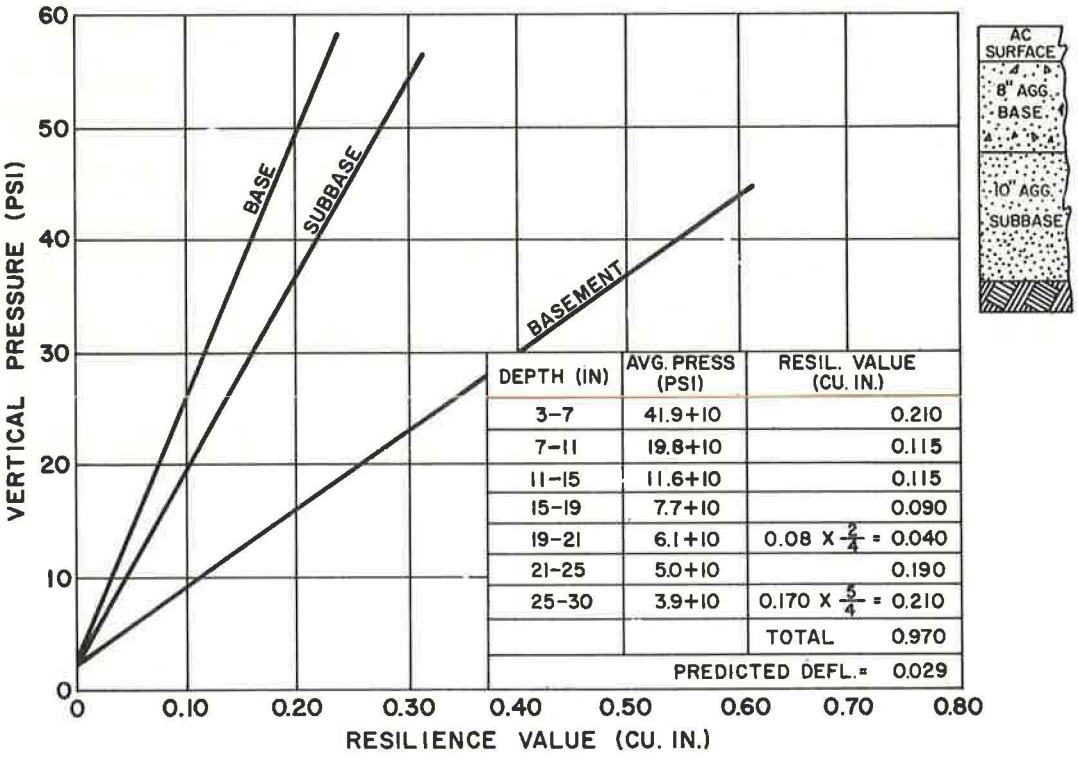


Figure 19. Design trial No. 1.

The decision as to whether the 4-in. AC surfacing and gravel base or 3-in. AC surfacing with cement-treated base should be used would depend on construction and economic considerations.

## Design Example No. 2

As a second example of the application of the resilience design method, a proposed structural section consisting of 2 in. of AC surfacing and 6 in. of aggregate base for a municipal street with a TI of 6.5 will be checked for compliance with the deflection criteria of Table 1 and Figure 1.

The first step, as in design example No. 1, is to compute the resilience summation for a depth of 30 in. The base and basement soil are treated separately and divided into 4-in. increments (or portions thereof) in order to determine from Figure 5 the vertical pressures at various depths below the surface. These average pressures are shown with the constant 10 psi added to each in Table 2. For purposes of this example, it will be assumed that Figures 10 and 12 represent the results of laboratory resilience tests on the aggregate base and basement soil, respectively. From Figure 10, therefore, the resilience of the upper 4 in. of base is found to be 0.120 cu in. The resilience of the remaining increments of base are found to be 0.076 and 0.061 cu in. after the necessary height correction.

Similarly, the resilience for each increment of basement soil is determined from Figure 12. The total resilience to a depth of 30 in. is found to be 1.15 cu in. (Table 2).

A deflection for the proposed structural section can now be predicted from the design line of Figure 13. The predicted deflection for a resilience of 1.085 cu in. is approximately 0.034 in. This predicted deflection must now be checked against the maxi-

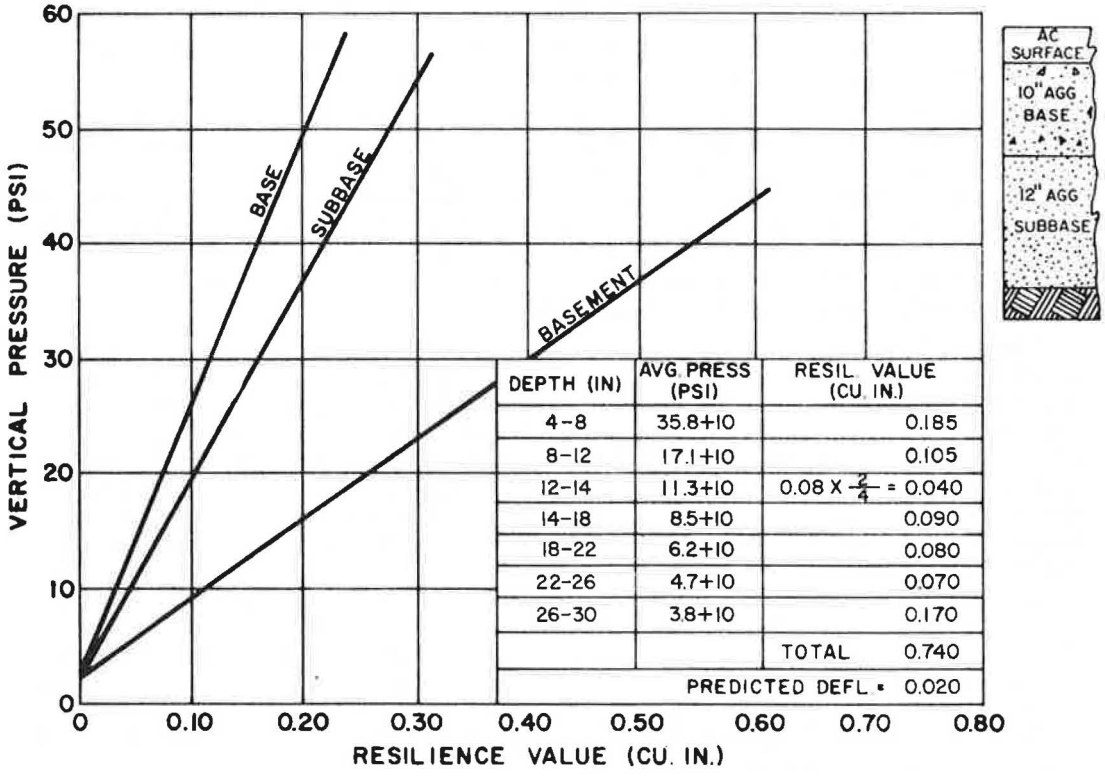


Figure 20. Design trial No. 2.

mum allowable deflection for a 2-in. AC surfacing for a roadway with a TI of 6.5. From Figure 1, the maximum allowable deflection for the stated conditions is found to be approximately 0.038 in. Since the predicted deflection is less than the maximum allowable deflection, the proposed structural section meets the resilience criteria.

TABLE 2

INCREMENTAL RESILIENCE VALUES FOR DESIGN EXAMPLE NO. 2

| Depth (in.) | Material | Average Pressure (psi) | Resilience (cu. in.) |
|---|---|---|---|
| 2.0- 6.0 | Base | 47.0 + 10 | 0.120 |
| 6.0-10.0 | Base | 23.5 + 10 | 0.070 |
| 10.0-14.4 | Base | 12.8 + 10 | 0.050 × 4.4/4 = 0.055 |
| 14.4-18.4 | Basement | 8.2 + 10 | 0.250 |
| 18.4-22.4 | Basement | 6.0 + 10 | 0.215 |
| 22.4-26.4 | Basement | 4.7 + 10 | 0.200 |
| 26.4-30.0 | Basement | 3.8 + 10 | 0.200 × 3.6/4 = 0.175 |
| | | | Total = 1.085 |

## FIELD TRIAL OF THE RESILIENCE DESIGN METHOD

The development of the resilience design procedure was accomplished in four distinct phases. Three of these have been described. They are:

1. Qualitative resilience tests on a variety of soil types for the purpose of evolving a reproducible and practical testing device and procedure for the determination of the general resilience characteristics of various soil types;
2. The establishment of a satisfactory correlation between measured field deflection and laboratory resilience tests on samples of roadway structural sections which were either in an undisturbed state or tested at field moisture and density; and
3. The establishment of suitable test criteria for the extension of the resilience design procedure to preliminary design situations.

The fourth and final phase involved field trial of the resilience design procedure under conditions which would prevail in a preliminary design situation. For this phase, soil samples were tested utilizing the newly established design criteria rather than in the undisturbed state or at field moisture or density. To determine the confidence with which field deflection could be predicted, 40 test locations from 21 different projects were analyzed. In several instances, excess material from the correlation phase of the study was retested utilizing the design criteria. For the most part, however, embankment or basement soils were recovered from construction projects along with pit samples of aggregate base and subbase.

Deflection measurements were then made during the first spring season after the completion of construction for the purpose of comparing predicted vs actual deflection. These results are presented in Figure 21, which is a plot of median predicted vs median measured deflection. The plot reveals the design with few exceptions to be conservative since only approximately one-fourth of the predicted deflections are larger than those actually measured. The data in Figure 21 produce a coefficient of correlation of 0.86 with a 95 percent confidence band of 0.73 to 0.92.

In Figure 22, the average predicted deflection from two or more sampling locations on the same project is plotted against the average measured deflection for that particular

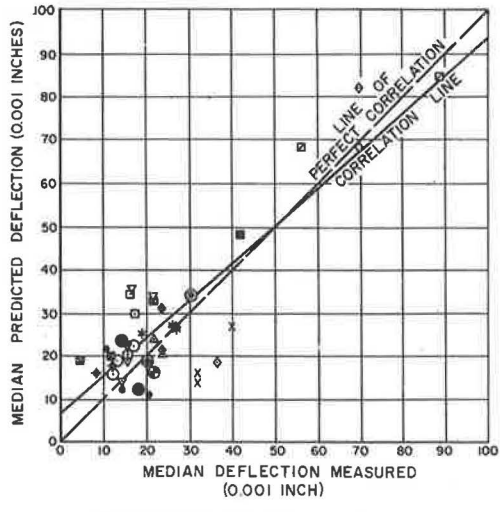


| LEGEND | |
|---|---|
| ROAD LOCATION | |
| • 03-But-33 | ■ 06-Tul-FAS-1143 |
| ⊙ 03-Sac-FAS-1223 | ◐ 04-Son-787 |
| △ 04-Nap-FAS-607 | □ City of Woodland |
| ⊡ 04-SCl-FAS-1015 | ■ City of Woodland |
| x 05-Mon-FAS-652,593 | ⊕ 05-SBT-156 |
| ▽ 05-SB-246 | ♦ 04-Son-FAS-780 |
| ◇ 10-Cal-12, 49 | ▽ 02-Teh-FAS-1078 |
| ✱ 10-Mpa-49 | ■ 04-Mrn-Son-1 |
| ⊕ 10-Mpa-132 | ◉ 03-Col-45 |
| ● 10-Sta-FAS-913,904 | ◈ 03-Yol-16 |
| | ✦ INTERSTATE 15-IDAHO |

Figure 21. Predicted deflection vs median measured deflection, 40 individual samples from 21 road locations.

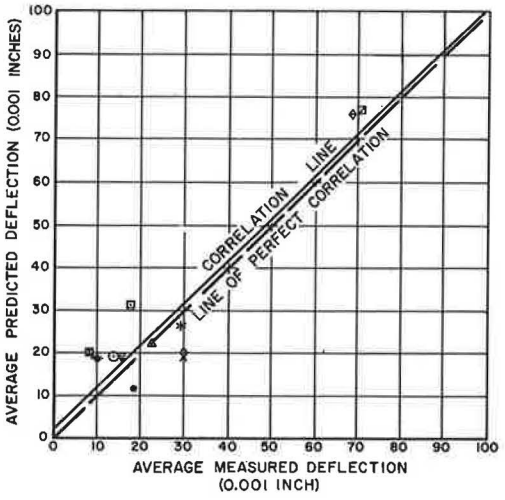


Figure 22. Average predicted deflection from several similar sample locations vs average measured deflection (see Figure 21 for legend).

project. Consideration of averages rather than individual sampling locations improved the coefficient of correlation to 0.93 with a 95 percent confidence band range from 0.75 to 0.98.

Here, the results of 9 of 12 projects indicate that the resilience procedure would have resulted in the selection of a design in which measured deflections were either less or very close to the predicted values. For the remaining three projects, the resilience design could have resulted in measured field deflections slightly in excess of those predicted and designed for. The measured range of deflection on all three of these projects, however, is probably too low for these deviations to have a significant effect on ultimate pavement performance.

The field-trial phase of the development of resilience design procedure will be continued for a period of from one to three years in order to further verify this procedure and to make necessary modification of the method of analysis, test equipment and procedure.

## SUMMARY AND CONCLUSIONS

Since 1946 the Materials and Research Department of the California Division of Highways has been engaged in the development of a testing device which applies a dynamic repetitive load to soil specimens. During the early years of this project, primary attention was given to the development of the apparatus itself and the modifications necessary to improve test reproducibility. Subsequently, the resiliometer was utilized for qualitative resilience evaluations of many different soil types.

Beginning in 1960, a correlation program was initiated to relate the resilience properties of individual elements of the various roadway structural sections to pavement deflection measurement. This phase of the investigation was carried out utilizing soil specimens in an undisturbed state or compacted at field moisture and density. Subsequently, design criteria were established for the purpose of using resilience test data in a preliminary pavement design situation in order to predict the deflection of a proposed structural section. The results of these phases of investigation permit the following general conclusions:

1. The relationship between the resilient characteristics of the structural section components and pavement deflections appears to be a realistic and effective basis for a flexible pavement design method.
2. Pavement deflections can be predicted from laboratory resilience values with sufficient accuracy for design purposes. This accuracy is substantiated by the correlation plots of predicted and measured deflections.
3. Our present resilience design method tends to produce conservative structural sections since the majority of predicted deflections are somewhat larger than the measured deflections (Fig. 22).
4. The effectiveness of the resilience design method in relieving fatigue cracking in asphaltic concrete pavements should prove to be as reliable as the deflection criteria on which it is based. Refinements in criteria and design method may be expected when more information regarding effects of different traffic conditions and variables in materials, construction practices and environment is obtained.

ACKNOWLEDGMENTS

The results of the Resilience Research Program and the preparation of the report were accomplished under the general direction of John L. Beaton, Materials and Research Engineer of the California Division of Highways. The authors wish to acknowledge the contribution of many individuals who have participated directly in obtaining, tabulating and analyzing the resilience test data utilized for this report. We are particularly grateful to Harold Munday and Rogel Prysock of this department.

REFERENCES

1. Middlebrooks, T. A. Discussion on the Theory of Stress and Displacements in Layered Systems and Applications to the Design of Airport Runways. HRB Proc., Vol. 23, p. 148, 1943.
2. The WASHO Road Test, Part 2: Data, Analyses and Findings. HRB Spec. Rept. 22, p. 105, 1955.
3. Hveem, F. N. Pavement Deflections and Fatigue Failures. HRB Bull. 114, pp. 43-87, 1955.
4. Highway Research In Progress, Developmental Issue. HRB Highway Research Information Service, p. 96, Sept. 1965.
5. Hicks, L. D. Flexible Pavement Deflection Study in North Carolina. HRB Proc., Vol. 39, pp. 403-415, 1960.
6. A Final Progress Report on the Development of a Test to Measure the Resilience of Soils. Calif. Div. of Highways Rept., Nov. 1964.
7. California Division of Highways Materials Manual, Testing and Control Proc., Vol. 1.
8. Boussinesq, J. Application des potentials á l'etude de l'equilibre et du mouvement des solids elastiques. Gauthier-Villars, Paris, 1885.
9. Cummings, A. E. Distribution of Stresses Under a Foundation. Trans. ASCE, Vol. 101, p. 1072, 1936.
10. Accelerated Traffic Test at Stockton Airfield, Stockton, California. O. J. Porter and Co., Consulting Engineers, 1948.
11. Westergaard, H. M. A Problem of Elasticity Suggested by a Problem in Soil Mechanics: Soft Material Reinforced by Numerous Strong Horizontal Sheets. Contributions to the Mechanics of Solids, Stephen Timoshenko, 60th Anniversary Volume, Macmillan, 1938.
12. Herner, R. C. Progress Report on Load Transmission Characteristics of Flexible Paving and Base Courses. HRB Proc., Vol. 31, pp. 101-120, 1952.
13. Burmister, D. M. The Theory of Stresses and Displacements in Layered Systems and Applications to the Design of Airport Runways. HRB Proc., Vol. 23, pp. 126-144, 1943.
14. Burmister, D. M. The General Theory of Stresses and Displacements in Layered Systems. Jour. Appl. Phys., Vol. 16, Nos. 2, 3 and 5, 1945.
15. Acum, W. E. A., and Fox, L. Computation of Load Stresses in a Three-Layer Elastic System. Geotechnique, Vol. 2, No. 4, pp. 293-300, Dec. 1951.
16. Vesic, A. S., and Domaschuk, L. Theoretical Analysis of Structural Behavior of Road Test Flexible Pavements. NCHRP Rept. 10, 1964.
17. Hveem, F. N., Zube, E., Bridges, R., and Forsyth, R. The Effect of Resilience-Deflection Relationship on the Structural Design of Asphaltic Pavements. Proc. Internat. Conf. on Structural Design of Asphalt Pavements, Ann Arbor, Michigan, 1962.

## *Discussion*

W. H. CAMPEN, Omaha Testing Laboratories, Inc.—Mr. Zube and his co-workers have done a tremendous amount of work in developing a method for thickness design based on rebound or elastic deformation. They have apparently succeeded in determining

in the laboratory the rebound value of the components of a layered system and then in correlating total rebound with actual field rebound on the same system. Finally, a procedure was established for determining thicknesses of base, subbase and select material required on a given basement soil in order to adequately carry a 15,000-lb axle load. In my opinion, the method is very complicated and it may be that the answer could be obtained more directly by constructing a small test section and testing it with the Benkelman beam.

Based on my own research and that of my associates in the evaluation of flexible pavement test sections for airport runways, I can say that the use of elastic deformation as a criterion for the determination of thickness is sound. In 1944, we presented a paper entitled "Analyses of Field Load Bearing Tests Using Plates" (HRB Proc., Vol. 24, p. 87, 1944). The data in the paper reveal three principal reasons for the use of the elastic deformation criterion. They are as follows:

1. With a given plate and given load, the rebound or elastic deformation decreases as the thickness of superimposed layers increases.
2. With a given thickness and a given plate, the elastic deformation increases as the load increases and the load-deflection relationship is a straight line.
3. With a given thickness and a given plate, the elastic deformation remains constant with the repetition of load.

Before asking a few questions, I wish to point out that, in addition to restricting elastic deformation, the layered system as a whole must not show any appreciable permanent consolidation or lateral displacement. I am sure Mr. Zube will agree with me on this.

In addition to the foregoing comments, I wish to ask a few questions.

1. Under general conclusions concerning the behavior of soils, it is stated that resilience increases rapidly with increase in moisture content above optimum moisture. This statement gives the impression that the rebound is due to moisture itself, whereas it is fairly well known that rebound is due to the decompression of trapped air or other gases. I am wondering therefore if the increase in moisture content is the cause of lateral flow of the soil against the air sack surrounding the sample under test. If this is so, the rebound would be a measure of the backflow of the soil-water mixture rather than the increase in volume of the trapped gases in the soil.
2. I am of the opinion that well-graded, highly densified bases and subbases do not possess any rebound quality when loaded normally. For that reason, I ask the following: Would a soil-aggregate mixture having a maximum density of 140 pci, an optimum moisture of 5 percent, an air content of 4.7 percent and CBR of about 100 show any significant resilience in your test?
3. You say that bituminous mixtures have no resilience. How can this be since they may contain 5 percent or more air?
4. You have established a correlation between rebound results obtained in a 4-in. diameter mold and a 15,000-lb axle load. How would you determine thickness for a smaller or a larger wheel load?

ERNEST ZUBE AND RAYMOND FORSYTH, Closure—Before going on to Mr. Campen's specific questions, it would be appropriate to comment on his statement to the effect that in addition to restricting the elastic deformation, the layered system as a whole must not show any appreciable permanent consolidation or lateral displacement.

We agree with this statement wholeheartedly. The resilience design procedure was originated, in fact, to measure the propensity of and eliminate excessive transient deflection and thus possible early fatigue cracking of asphalt concrete pavement designs which satisfied the R-value design criteria. It has been our experience that the R-value test effectively eliminates plastic deformation within a flexible structural section.

It would seem reasonable, however, that a pavement design procedure which satisfied certain elastic criteria would automatically preclude failure due to plastic deformation. Put another way, if a maximum pavement deflection were built into the design, is it likely that the system would suffer any appreciable permanent distortion? In the authors' opinion, this possibility is remote. Therefore, future consideration should be given to the possible elimination of conventional static tests once effective procedures have been established which satisfactorily control the elastic properties of the pavement section.

The following are answers to the four specific questions posed by Mr. Campen:

1. The nature of the mechanics of resilient deformation of soils is beyond the intended scope of this project, although we would agree that this deformation is probably associated with compression of trapped air within the system. It seems likely that increased moisture content tends to lubricate individual soil particles, thus reducing the amount of energy required to effect a given volumetric compression. During the resilience test, the soil specimen is enclosed in a stabilometer with which it is possible to obtain a measurement of the horizontal pressure induced within the soil specimen by the vertical dynamic load. This, of course, is possible through the compression of a known volume of air within the stabilometer system. It is, therefore, possible to convert the lateral pressure measurement to lateral volumetric displacement. This is subtracted from the total measurement obtained by reading the resiliometer manometer tube. Therefore, the resilience value for a given soil reflects net internal compression and rebound only.

2. There can be little doubt that a well-graded densified base and subbase would not manifest a high degree of resilience when loaded normally. Even for these materials, however, there is a very definitely measurable and significant amount of resilience. From a quantitative standpoint, the resilience in a base or subbase material would be substantially lower than that in a basement or embankment material. However, when considering the fact that the pressures applied to a base or even a subbase may be five to ten times greater than that applied to the basement or embankment soil, the resilience contributions of these materials may be equal in importance or even exceed that of the basement and embankment material.

3. Our tests indicate that bituminous mixes have a measurable, though relatively small, amount of resilience. This and the relative uniformity of newly constructed AC surfacing resilience measurements are such that the inclusion of AC resilience testing as part of the test procedure does not appear to be justified at this time.

4. Critical deflection levels for various types of pavement structural sections have been determined for California highways utilizing a 15,000-lb test axle load (3). Thus the performance of several pavement types had been related reasonably well to deflection measurements at this test load, even though these pavements are subject to a wide variety of wheel loadings throughout their service life. This being the case, it does not appear to be necessary to correlate resilience laboratory test data with deflection measurements obtained at other than the standard 15,000-lb single-axle loading. Such a conversion would not be difficult, however, since lineal deflection has been found to be almost directly proportional to test axle load. Thus, deflection measurements obtained with a different axle loading can be conveniently corrected to the 15,000-lb standard. Another approach would involve simply utilizing a revised pressure distribution curve appropriate to test loading and wheel configuration of interest in the analysis of resilience test data.

# Laboratory Tests With a Heavy-Duty Rolling Load Machine

R. R. HAYNES and D. T. WORRELL
Respectively, Instructor, and Professor of Theoretical and Applied Mechanics, West Virginia University, Morgantown

•THIS paper describes a high-capacity rolling load testing machine and the results of tests performed with it over the last three years at West Virginia University. The testing machine is being used for the evaluation of base-course materials in a simulated highway.

Considerable economy in road and highway construction could be realized in West Virginia if some construction method were devised that would utilize the state's abundant and well-distributed supply of sandstone. The best evaluation would come from highways constructed of such materials—an evaluation expensive in both time and money. A properly designed rolling load testing machine, along with a carefully planned testing program, might reduce the cost in both aspects. Opinion as to the usefulness of rolling load machines or test tracks over the past several years has been divided. One machine has been abandoned while another very large machine has been constructed recently at Washington State University (1 to 12). Circular tracks are in use at the University of Illinois and at the American Oil Company in Whiting, Indiana.

## MACHINE DESCRIPTION

The basic design considerations were: (a) a large, constant load was to be applied by a single truck tire; (b) field thickness for surface and base layers was to be maintained; (c) sufficient soil to duplicate elastic and plastic effects found in the field was to be employed; and (d) a specimen of sufficient size to reduce the lateral confining stresses to a level believed to exist in an actual highway was to be used.

The machine (Fig. 1) was designed for a 20,000-lb load on a single wheel. The heaviest load applied to date has been 14,000 lb on an 11.00 × 20, 12-ply truck tire at 100-psi inflation pressure, which was found to be more than sufficient for most materials tested. The minimum load that can be applied to a specimen is 2750 lb—the dead weight of the fluid-filled tire, wheel, and other load application components. Readout of the wheel load is by means of electrical resistance strain gages and can be monitored at intervals or continuously as conditions dictate. Load variation as the wheel assumes different positions is within 5 percent of the average load. The loading devices, heavy coil springs and tension rods are shown in Figure 2.

Rate of loading is constant at 40 load repetitions per minute, 2400 per hour and approximately 50,000 per day. The distance of the tire's reciprocating travel is 24 in., center to center, which results in a rolled-over surface approximately 42 in. in length at a wheel load of 11,500 lb. The 20-rpm, 12-in. crank arm is shown in Figure 2. The entire cell travels laterally at a slow rate, driven by a small motor, reducing gear, sprockets, and lead screws. The tire contact width is 8 in. and lateral cell motion, while adjustable, is usually set so that the rolled-over width is 12 to 24 in.

The dynamic and residual deformations of the various interfaces between layers are monitored throughout the test by means of linear variable differential transformers mounted inside telescoping pipe structures and placed in the center of the specimen.

Paper sponsored by Committee on Flexible Pavement Design.

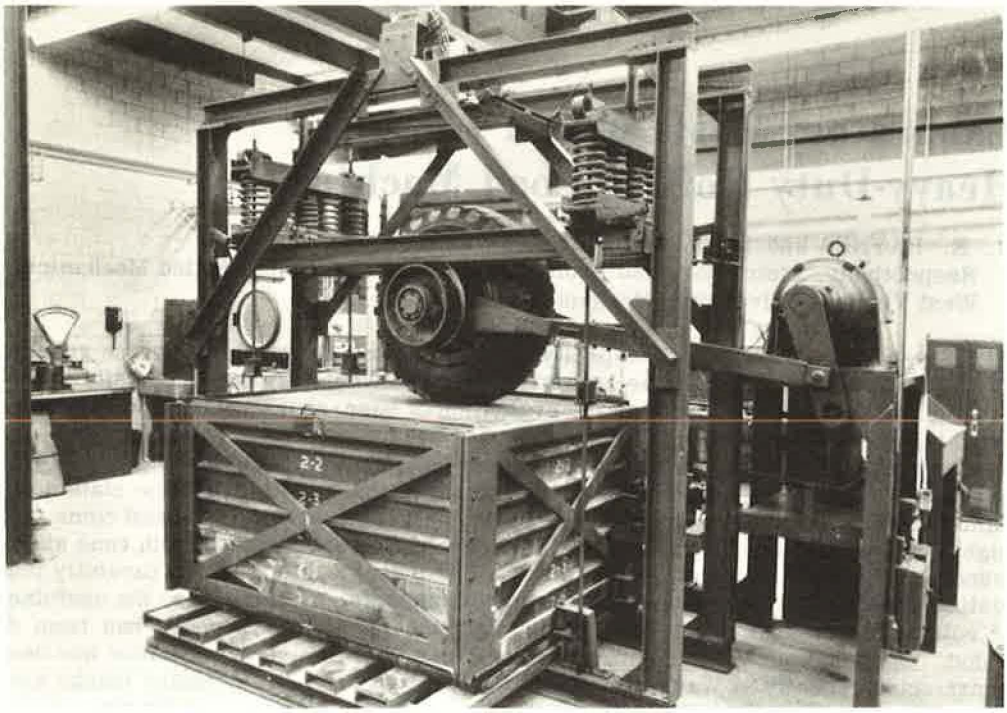

Figure 1. Rolling load testing machine, front view.

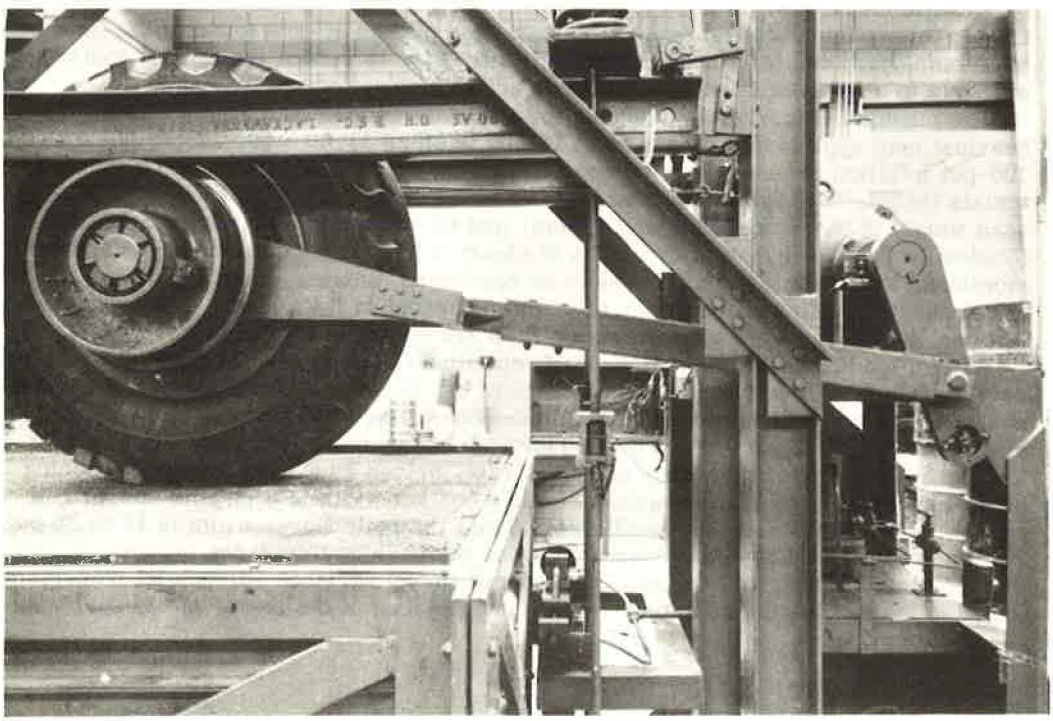

Figure 2. Close view of tire, load tension rods, heavy coil springs (top center) and crank arm.

Readout of these devices is a vacuum-tube voltmeter which is shown in the control cabinet in Figure 3. This figure also shows the heavy drive motor-gear reducer unit and the hydraulic pump used in adjusting the load.

A feature of the machine, which has not yet been employed, is an extension of the load axle to which a braking action component can be added. The primary drive unit was overdesigned to provide sufficient power for large braking energy.

The roadway specimen employed is approximately 5½ ft long, 4½ ft wide and 3 ft deep. The confining effect of container sides has always been of serious concern. It has been found, however, that the lateral pressure of the cell walls was below that calculated from curves by Foster and Ahlvin (13). This calculation is based on a uniform material (soil), whereas the paving components are much stiffer than soil. The vertical deflection due to a wheel load is estimated to be 86 percent of the value it would be if the specimen were infinitely deep instead of 3 ft. Because of these comparisons, it is felt that the initial design requirements of minimum confinement and field-condition soil action have been satisfied.

## CONSTRUCTION AND TESTING METHODS

A typical specimen consists of 3 in. of asphaltic-concrete surface, 11 in. of crushed-sandstone base and 22 in. of A-6(8) soil subbase. This material, along with the container of segmented layers and heavy bracing frame, weighs approximately 12,000 lb.

Materials placed in a test specimen are compacted to a specified density with either a vibratory or impact device, or both. Soil is placed at optimum moisture and compacted to 100 percent of the AASHO T99 density. Sandstone (or limestone) is placed at or near its optimum moisture and compacted to 100 percent of its AASHO T99-Method D density. Gradations of the base material have varied from crusher run to specific gradations. All placement and testing were performed at room temperature, 65 to 85 F.

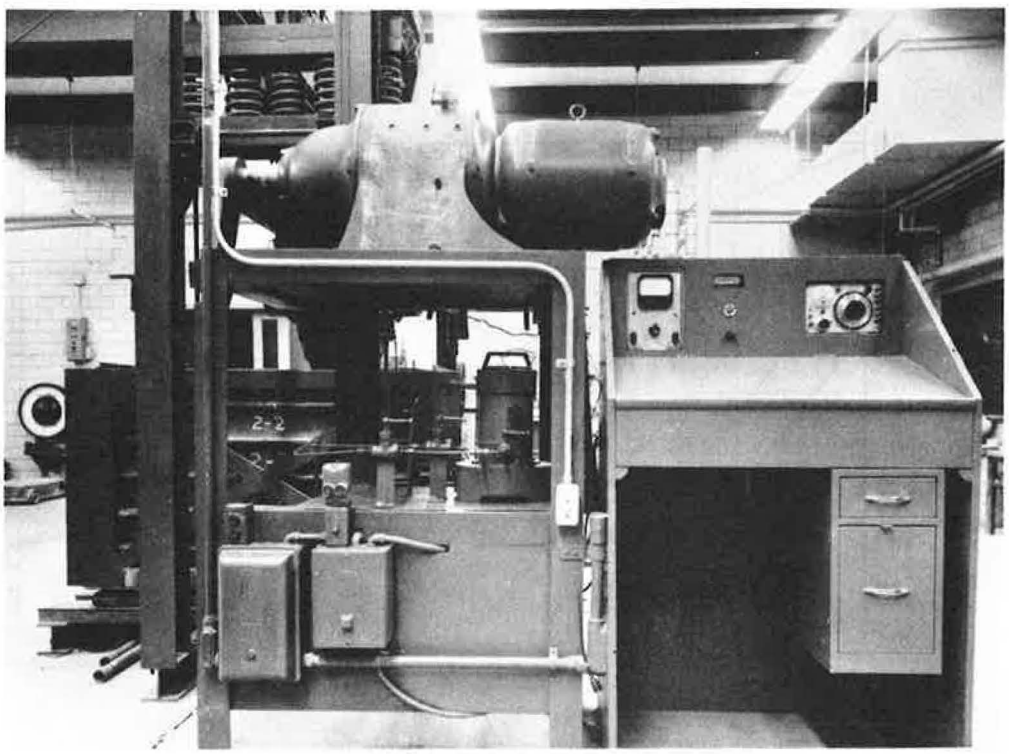

Figure 3. End view of machine showing drive unit and control cabinet.

Failure of a specimen has been arbitrarily defined as the number of load repetitions at which a residual surface deformation of 1 in. is present. If the residual asphalt-base interface deformation is more than 0.6 of the surface deformation, the failure is said to occur in the base course or soil. It is believed that the failures in asphalt in specimens tested to date have been chiefly of the shearing type. Failures in base-course materials appear to have been a combination of shearing and densification such as would be found in an actual roadway (14).

The best indication of specimen performance has been through curves generated by plotting of surface and interface residual deformation with the logarithm of the number of load repetitions. In general, straight lines have resulted. The dynamic deflection which occurs during each cycle is also an indication of specimen performance, but the magnitude of such a deflection and thus the electrical output signal is very small and rapidly changing and is, therefore, read with much less accuracy.

## TEST RESULTS

Testing completed to date using this machine consists of three phases. Phase I testing was directed primarily at determining the minimum thickness of a poor sandstone base that would effectively distribute the load to a poor clay soil typical of that which underlies most West Virginia highways. The base material in this phase was a silica-argillaceous sandstone having a Los Angeles percent wear of approximately 64, B grading. The material was crusher run and always within State Road Commission specifications. The crushed sandstone was soaked for 24 hours, then spread for surface drying until a moisture content of 7 percent resulted. It was then weighed and compacted in 2-in. lifts. The asphalt surface on Phase I specimens consisted of 2-in. leveling and 1-in. wearing course Type 1. Wheel load was 11, 500 lb at 100-psi inflation pressure with a 24-in. wide path.

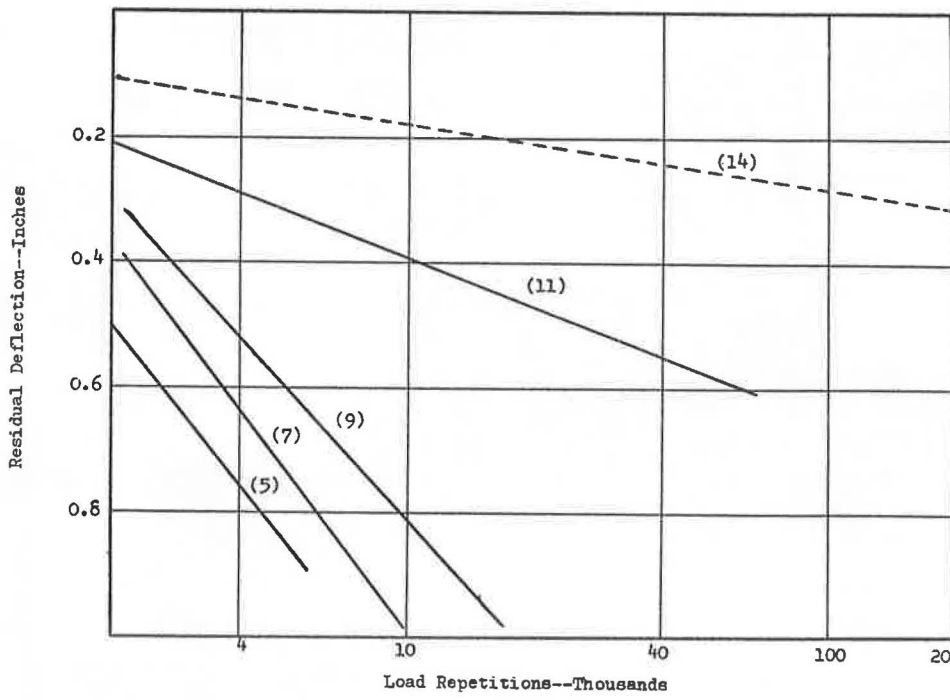


Figure 4. Average residual deflections of the asphalt-base interface of roadway specimens as 11,500-lb rolling load was repeatedly applied. Numbers in parentheses are base course thicknesses in inches.

Testing results are shown in Figure 4. These curves depict the relative deflection of the asphalt-base interface for the various base thicknesses tested as increasing replications of load are applied. The asphalt-base interface measurement was chosen because asphalt failures occurred in some tests. Although surface deflection was the criterion of failure, an asphalt surface curve in the case of asphalt failure would be misleading.

In the 14- and 11-in. thick specimens, there was no soil motion evident, indicating that these thicknesses were well in excess of the desired thickness. The 5- and 7-in. specimens show considerably lower running times and did exhibit enough soil deformation to indicate that these thicknesses were not sufficient for suitable load distribution.

The 9-in. base samples performed somewhat better than those of the lesser thickness but considerably fewer repetitions were required than in the 11- and 14-in. samples. Some soil deflection was evident in the 9 in., but to a small degree. It was felt that this thickness could then be considered the minimum thickness for the base material and gradation used in order to create a suitable load distribution to the soil.

The scatter evident in Figure 5 was of some concern at the completion of Phase I. After more experience was gained in Phase II, this scatter was attributed to variations in gradation, even though all gradations were within state specifications. As a result of these observations, gradation was very closely controlled in later phases.

The Phase II series of tests was an examination of different types of base-course material. Three types of sandstone, calcareous, silicious, and argillaceous, were used and separate tests were performed on material having a Los Angeles wear of approximately 67, 77, and 87 percent (B grading) for each of the types. The following were held constant throughout this phase: 3 in. of asphaltic surface; 9 in. of base thickness; 7100-lb load at 80-psi tire inflation; and a 24-in. wide load pattern. The results of Phase II testing are described by Figures 6 through 12. In these figures, the deflection curves are concerned with asphalt-base interface deflection as was the case in the Phase I figures.

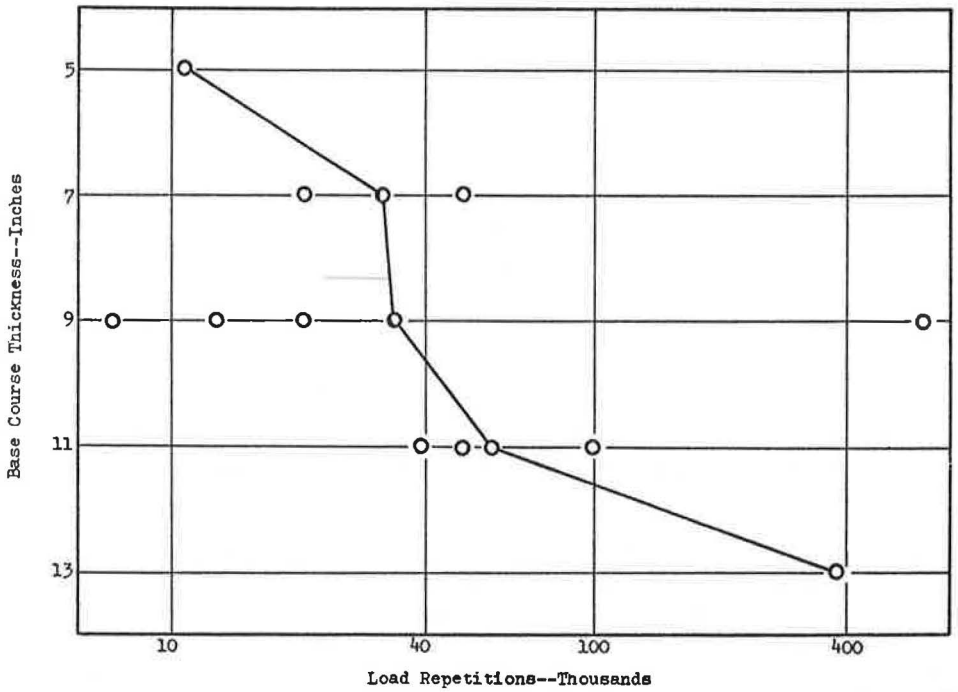


Figure 5. Number of repetitions of 11,500-lb rolling load before failure of specimens having various thicknesses of sandstone base course.

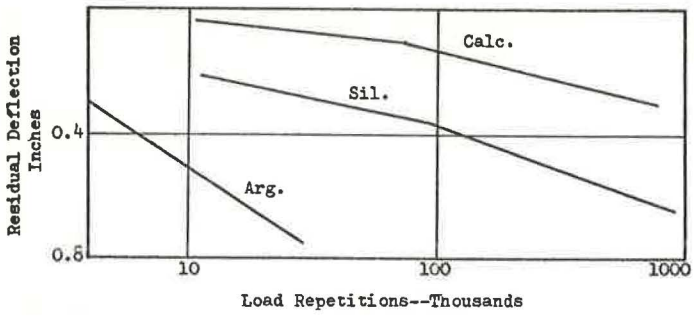


Figure 6. Comparative sandstone-asphalt interface residual deflections for the different type sandstones, all having a Los Angeles wear of approximately 69 percent.

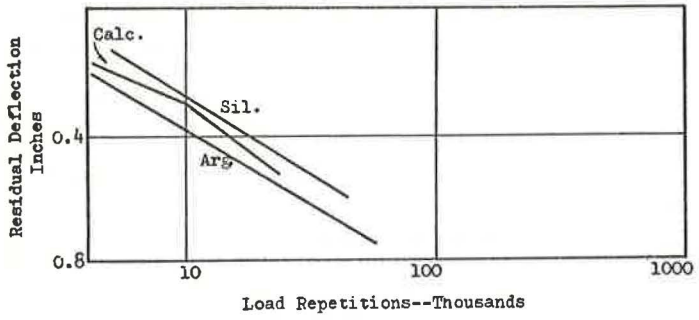


Figure 7. Comparative sandstone-asphalt interface residual deflections for the different type sandstones, all having a Los Angeles wear of approximately 79 percent.

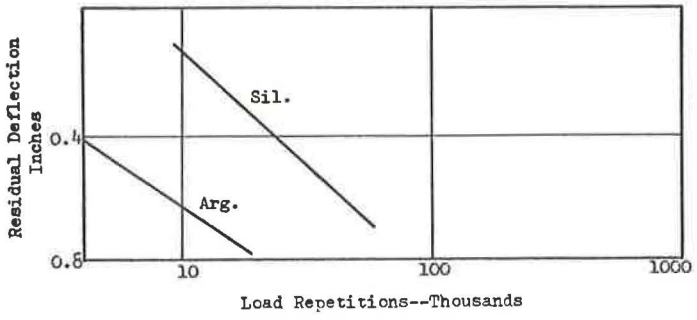


Figure 8. Comparative sandstone-asphalt interface residual deflections for the different type sandstones, all having a Los Angeles wear of approximately 89 percent.

Figures 6, 7, and 8 are comparative curves for the different types of sandstone having the same Los Angeles wear value. In the harder material (Fig. 6), a calcareous material of 69 percent Los Angeles performed much better than the other two types, with silicious being second and argillaceous being the poorest. In the high wear range of 89 percent Los Angeles (Fig. 8), the silicious was far superior to argillaceous. Calcareous material is absent from the last figure due to the inability to locate such a material, and it is likely that no such material exists naturally.

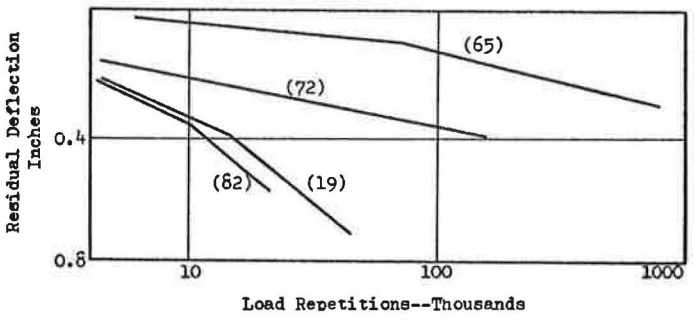


Figure 9. Comparative sandstone-asphalt interface residual deflections for calcareous sandstone base. Numbers in parentheses indicate percent L. A. wear.

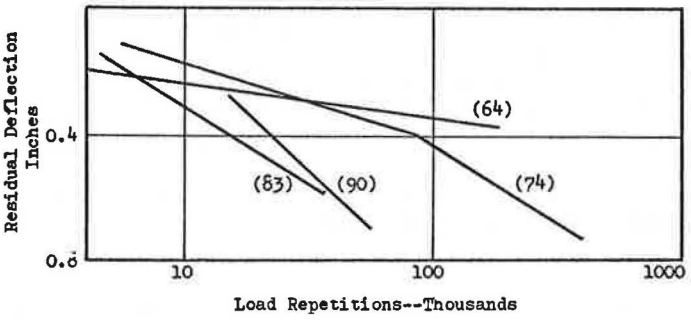


Figure 10. Comparative sandstone-asphalt interface residual deflections for silicious sandstone base. Numbers in parentheses indicate percent L. A. wear.

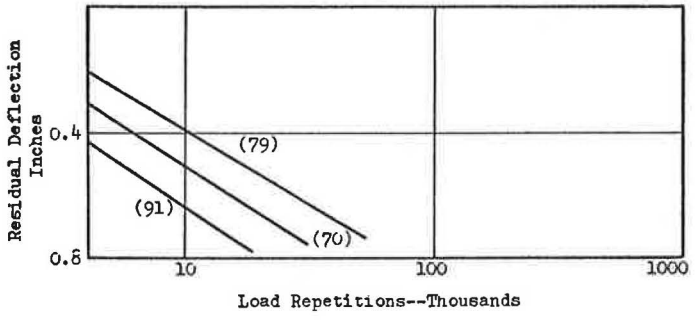


Figure 11. Comparative sandstone-asphalt interface residual deflections for argillaceous sandstone base. Numbers in parentheses indicate percent L. A. wear.

Figures 9, 10, and 11 compare the action of each type of sandstone with the Los Angeles wear as the variable. The calcareous curve (Fig. 9) includes a limestone sample, shown by the 19 percent L. A. wear. The performance of the limestone shown in this curve is typical of most of the limestone tests performed with this machine. The limestone, even though much harder, does not perform as well as its hardness would seem to indicate, yet it undergoes no great amount of degradation. The poor performance is attributed to densification due to keying in as opposed to degradation.

Figures 9 and 10 indicate a definite relationship between the L.A. wear and material performance. The 90 percent silicious is offset but possesses a much steeper slope than does the 83 percent and would thus fail earlier. The argillaceous material performed much more poorly than did the other two types, and displayed a scatter in the performance-L.A. wear relationship.

In practically all testing in Phase II, the specimen failures were in the base. This was the desired result and justified the load reduction for the phase. The generally poor performance of the argillaceous base, regardless of its L.A. wear, was a prime factor in scheduling the third phase of testing.

Phase III dealt with a poor argillaceous sandstone—L.A. wear approximately 85 percent (B grading)—which was stabilized with various admixtures. The stabilizing materials and their percentages by weight used were: SS-1 emulsion, 6.5 percent; portland cement, 4 percent; and 85-100 penetration asphalt, 5 percent. These amounts are approximately the median of State Road Commission specification limits. The SS-1 emulsion cured 5 days, uncovered and at room temperature; testing began within 7 days of application. The portland cement specimens cured 14 days with seal and were tested within 21 days of base application. The 85-100 penetration asphalt specimens cured in a minimum of 24 hours and were tested within 5 days. These treated base courses were tested at thicknesses of 4 and 6 in., with the total base thickness being held constant at 11 in. The remainder of the base was the same sandstone, untreated, at optimum moisture and 100 percent of T99 density. All base material in this phase was sized and mixed according to a straight-line gradation using sieve sizes to the 0.45 power scale.

This phase was begun using an 11,500-lb wheel load at 100-psi tire inflation pressure, 3 in. of asphaltic-concrete surface and a 24-in. wide load pattern. Due to much

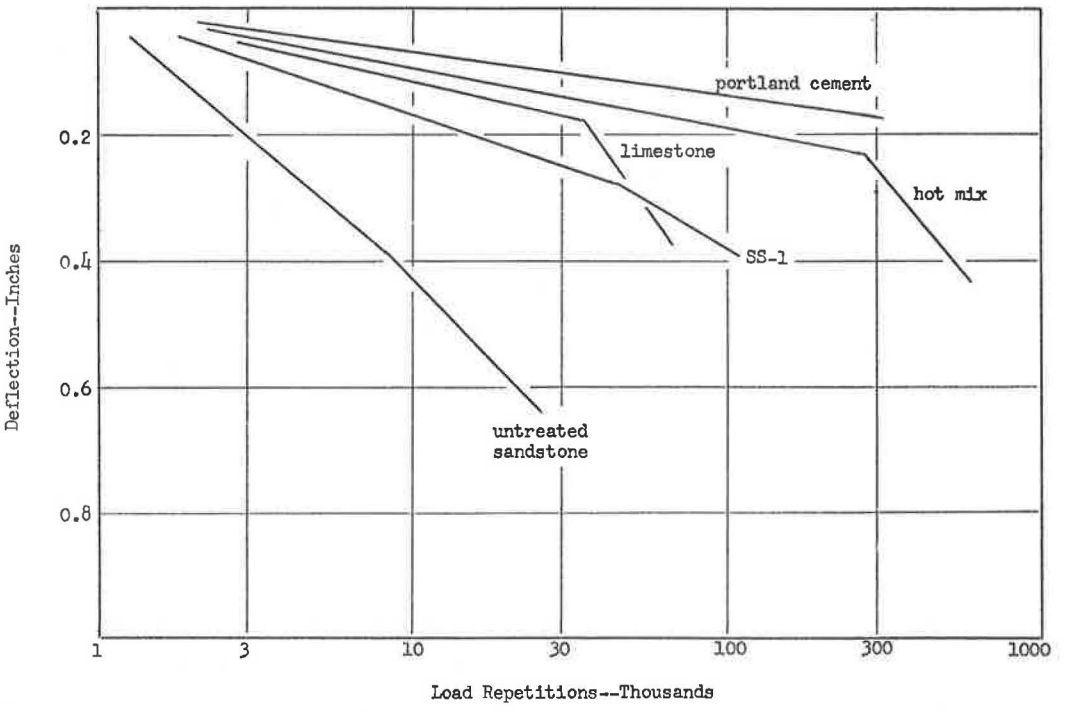


Figure 12. Residual deflections of asphalt surface-base interface of roadway specimens as 11,500-lb rolling load was repeatedly applied. Except for the untreated sandstone, all specimens had 1 in. asphalt surfacing, 4 in. treated sandstone or untreated limestone base, 7 in. untreated sandstone, and 22 in. A-6 soil. Sandstone L. A. wear was 85 percent.

asphalt rutting and some very lengthy test runs (one million load repetitions for a 0.75-in. surface deflection) the asphalt surface thickness was decreased to 1 in. of wear course Type 1. The lateral cell travel was reduced to a 12-in. wide load pattern, making the test much more severe. The tests performed under the latter conditions cover all scheduled base configurations and are the only tests discussed in this phase.

Figure 12 shows the comparative performance of the 4-in. treated, 7-in. untreated bases. Also included is an all-untreated sandstone base 14 in. thick instead of 11 in. treated and untreated. The improved ability of the treated material to resist load is clearly indicated.

Performance of the portland cement and hot mix treated specimens was consistently good. No shrinkage cracks were noted in the cement-treated specimens as they were dismantled. The deflection curves start after a "rolling in" period of 1000 repetitions of load. Considerably greater deflection occurred in the SS-1 treated and in the untreated sandstone specimens than in the cement and hot mix treated specimens during this early period.

Figure 13 shows the curves for the specimens with 6-in. treated base and 5-in. untreated base. The 14-in. untreated base is repeated for comparison. Again, the hot mix specimen performed very well. The SS-1 treated specimens gave poorer performance in the 6-in. than in the 4-in. thickness. This was attributed to a slower curing rate in the thicker layer. The poorer performance of the limestone specimens cannot be accounted for.

No portland cement treated specimen in the 6-in. thickness was constructed in view of the minimal deflection of the 4-in. specimens.

Throughout this phase, the scatter in results was considerably less than occurred in Phase I and II testing. It is believed that this scatter reduction can be traced in part

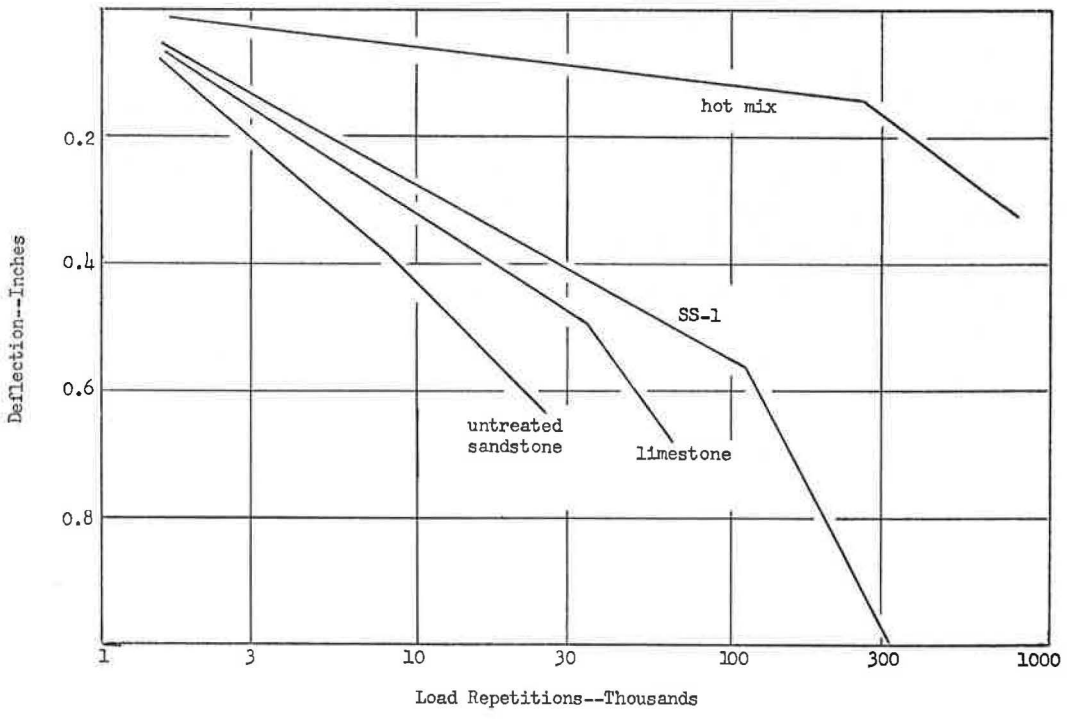


Figure 13. Residual deflections of asphalt surface-base interface of roadway specimens as 11,500-lb rolling load was repeatedly applied. Except for the untreated sandstone, all specimens had 1 in. asphalt surfacing, 6 in. treated sandstone or untreated limestone base, 5 in. untreated sandstone, and 22 in. A-6 soil. Sandstone L. A. wear was 85 percent.

to the closer control of gradation of the base courses. Even though this control created immense screening and material handling problems (a specimen required approximately 3000 lb of stone), the results justify the increase in effort.

A fourth phase of testing is presently under way. The primary variable in this phase is gradation of poor argillaceous sandstone and of limestone, in untreated base courses.

## ACKNOWLEDGMENTS

This research is being conducted by West Virginia University in cooperation with the State Road Commission of West Virginia and the U.S. Bureau of Public Roads.

## REFERENCES

1. Broome, D. C., and Please, A. The Use of Mechanical Tests in the Design of Bituminous Road Surfacing Mixtures. Jour. Appl. Chem., Vol. 8, p. 121, 1958.
2. Csanyi, L. H., and Fung, H. Traffic Simulator for Checking Mix Behavior. Highway Research Record 51, pp. 57-67, 1964.
3. Ekse, Martin. On the Right Track. Asphalt Institute Quarterly, Vol. 13, No. 4, pp. 7-9, Oct. 1961.
4. Fast Track at University of Illinois Tests Highway Building Materials. Builder, Vol. 38, No. 3, p. 16, March 1966.
5. Goldbeck, A. T., Gray, J. E., and Ludlow, L. L., Jr. ASTM Proc., Vol. 34, Pt. 2, 1934.
6. Housel, W. S. Discussion of Laboratory Test for Pavement Materials. ASTM Proc., Vol. 34, Pt. 2, p. 631, 1934.
7. Lin, P. C. Determination of Gravel Equivalent. Trend in Engineering, Vol. 13, No. 4, p. 25, Oct. 1961.
8. Mack, Charles. Study of Bituminous Mixtures on Road Testing Machines. Soc. Chem. Ind. Jour., Trans. Vol. 60, pp. 111-120, 1941.
9. Mathews, D. H., and Colwill, D. M. The Immersion Wheel Tracking Test. Jour. Appl. Chem., Vol. 12, No. 11, pp. 510-520, 1962.
10. Speer, T. L. Progress Report on Laboratory Traffic Tests of Miniature Bituminous Highways. Proc. AAPT, Vol. 29, pp. 316-361, 1960.
11. St. Clair, G. P., Editor. A Laboratory Traffic Test for Low Cost Road Types. Public Roads, Vol. 14, No. 11, p. 219, Jan. 1934.
12. Willis, E. A., and Carpenter, C. A. Studies of Water-Retentive Chemicals as Admixtures with Nonplastic Road Building Materials. Public Roads, Vol. 20, No. 9, Nov. 1939.
13. Foster, C. R., and Ahlvin, R. E. Stresses and Deflections Induced by a Uniform Circular Load. HRB Proc., Vol. 33, pp. 467-474, 1954.
14. Yoder, E. J. Principles of Pavement Design. John Wiley and Sons, N. Y., p. 21, 1959.

# Skid Testing With an Automobile

ROLANDS L. RIZENBERGS and HUGH A. WARD
Respectively, Research Engineer and Assistant Research Engineer, Division of Research, Kentucky Department of Highways

This study evaluates the theoretical and practical aspects of using an automobile as a testing device for measuring pavement slipperiness. Every parameter and significant event of a skidding automobile was measured and recorded. Twenty-five skid-resistance values were compared and correlated. As a result, the measurement of time in the velocity increment between 30 mph and 20 mph was selected as an interim standard test. A number of experiments were also conducted to aid in the interpretation of test results and to establish control tolerances for the standard test.

•THE frictional or tractional stability between automobile tires and pavement surfaces has long been an important factor in highway design. Improved pavement surfaces and various types of de-slicking treatments have resulted from studies of skidding mechanisms and skid testing. Unfortunately, test methods employed in the past have not been wholly reliable and realistic. Considerable effort has been devoted to developing better skid-resistance testing methods and standardization of testing devices. The trailer method—which yields a constant velocity measurement of friction—has received attention because it is seemingly reliable and safe. However, a standard trailer-type testing device is not yet commercially available.

The Kentucky Department of Highways has been engaged in laboratory skid-resistance studies since 1956 (9), and in field testing since 1958 (10, 11, 12). During these studies, numerous methods of measurement have been employed in the laboratory as well as on the road. Several methods have been abandoned because they yielded unreliable results. Other methods have been continued temporarily until a more reliable test is found. Consequently, meaningful, accurate, long-term histories of pavement surfaces have not been accumulated. Hence, a standard method of testing has been—and is—needed. Certainly, any test method should correlate well with the coefficients of friction derived from real skidding excursions of an automobile; skidding decelerations are fundamentally more complex than steady-state friction (constant-velocity friction). It is the fundamental aspects of skidding decelerations with which this report is concerned. The purpose of the study was to develop a standard skid-test method using an automobile.

In the summer of 1964, a test automobile was instrumented to record the various parameters associated with a vehicle in skid. Five pavements having different compositions and skid resistances were selected as test sites to represent a typical array of road surfaces found in Kentucky. The sites were tested in series at three different times. Every possible skid-resistance value and coefficient of friction, 25 in all, was then determined from the resultant recordings and on-the-spot measurements. The test results were compared, and regression equations were determined in order to correlate the results. A number of experiments were also conducted to aid in the interpretation of test results and to establish control tolerances for a standard test. In conjunction with the skid test automobile, the British Portable Tester was used to further evaluate the instrument on 45 pavement surfaces of varying types and ages.

Paper sponsored by Committee on Surface Properties—Vehicle Interaction and presented at the 46th Annual Meeting.

## THEORETICAL CONSIDERATIONS

### Classical Laws

The study of friction phenomena dates back to 1500, when Leonardo Da Vinci noted that friction between two solid bodies is proportional to the load and independent of the apparent contact area. Additional study was done by Amontons in 1700 and by Coulomb and Morin in 1781. Their findings form the classical laws of dry friction which may be stated as follows:

1. Friction is independent of the apparent contact area and the load;
2. The static coefficient of friction is greater than the kinetic coefficient of friction; and
3. The kinetic coefficient of friction is independent of velocity.

Most materials do not obey these classical laws, especially viscoelastic materials. Kummer and Meyer (1) have shown that the coefficient of friction of rubber is dependent on normal pressure (load and contact area), velocity and temperature. Their studies also indicated that the highest coefficient of friction does not occur at rest but at a sliding velocity of 0. 1 to 5 ips.

### Mechanisms of Friction

Classical laws explain nothing about the mechanism of friction. In general, friction is regarded phenomenalistically, i.e., it can be observed and measured but not explained. Coulomb's law, $F = fN$, is phenomenalogical in that sense; f is considered to be a phenomenalogical coefficient. However, other physical laws provide additional insight and understanding. In the case of the deceleration of an inertial body, for instance, the doctrine of conservation of energies may be invoked:

$$\text{Kinetic energy (loss)} = \text{Mechanical energy (loss)} + \text{Heat}$$

Heat arises from inter- and intra-molecular straining (or internal friction); it is irreversible and is known as a hysteretic loss.

Static friction is conceived as the interlocking (or mating) of surface asperities. Sliding friction involves the inherent shear resistance of the materials and is a function of discrete interfacial pressures and bearing areas. Interfacial welding, or adhesion, has been suggested as a mechanism. Antifriction mechanisms, such as fluid lubrication of the interface, are infinitely complex.

Tire friction (traction) is thus not altogether definable in terms of discrete mechanistic parameters; however, some general observations may be cited:

1. Coarse wear, or abrasion, is thought to be a combination of ploughing, tearing, and shearing (filing and rasping); this action would account for the deposition of skid marks if the rubber were powdery and nonadherent to the pavement.
2. Adhesion of skid-deposited rubber would strongly indicate melting at the surface of contact. Rubber tends to become tacky from the hysteretic heating accompanying severe abrasion. Melting and tackiness may result from surface heating and drying—even when the surfaces are wet.
3. "Scratching off" burns tire rubber—due to hysteresis heating—and has been observed on ice and under water.
4. Normal wear on tires may involve vaporization of rubber because rubber debris does not accumulate on roads in direct proportion to tire wear.
5. Wet friction is usually less than dry friction due to lubrication and hydrostatic pressures. Captive water in surface cavities interferes with the mating of the surfaces.

### Coefficient of Friction Equations

All coefficients of friction in this study were calculated from three different equations that incorporate various measured physical parameters. These equations were derived on the assumption that Coulomb's Law ($F = fN$)—the friction force "F" is constant and proportional to the normal force "N"—is applicable. The proportionality

is expressed by the coefficient of friction, f. This law, however, applies only to dry surfaces, low speeds and low contact pressures (6). Viscoelastic materials, such as rubber, do not fully adhere to the classical concept of friction. Many other tire, vehicle and road characteristics influence f. In fact, Moyer lists over 30 variables (4).

In the application of these equations, the tire and vehicle characteristics, as well as all other influencing variables, are assumed to be constant—except when intentionally varied—and the road surface friction is expressed by f. The resultant f denotes a relative skid-resistance value, but will be referred to in this report as a coefficient of friction. This skid-resistance value may be subject to large "incremental" errors arising from the assumption that a linear relationship exists between velocity and time or velocity and distance while the automobile is skidding. Actually such a relationship does not exist, and f (calculated) is higher than the actual f at the midpoint of the velocity increment; i.e., the average f calculated for the increment $V_1 - V_2$ will be greater than f for $V_2 + \frac{V_1 - V_2}{2}$, where $V_1$ and $V_2$ are velocities in mph.

Skidding Distance—The work-energy principle of physics states (13): "The work of the resultant force on a body is equal to the change in kinetic energy of the body." For a skidding vehicle, the resultant force is the friction force, $F_e$, and

$$F_e S = \tfrac{1}{2} m v_1^2 - \tfrac{1}{2} m v_2^2 \tag{1}$$

When S is the distance in feet, the vehicle skids while decelerating from a velocity of $v_1$ to a velocity of $v_2$ ft/sec, and m is the mass of the vehicle.

Coulomb's law of friction defines the friction force as a function of the normal force:

$$F_e = fN \tag{2}$$

For a skidding vehicle, the normal force is equal to the weight of the vehicle, W, substituting in Eq. 2:

$$F_e = fW \tag{3}$$

Combining Eqs. 1 and 3 equates frictional energy to the change in kinetic energy; then, substituting w/g for m, where g is the acceleration due to gravity:

$$fws = \tfrac{1}{2} \frac{W}{g} v_1^2 - \tfrac{1}{2} \frac{W}{g} v_2^2$$

which simplifies to

$$f = \frac{v_1^2 - v_2^2}{2gS} \tag{4}$$

Multiplying by $1.47^2$ to allow substitution of V in mph and substituting 32.2 $ft/sec^2$ for g, Eq. 4 becomes

$$f = \frac{V_1^2 - V_2^2}{30S} \tag{5}$$

Skidding Time—The skidding distance, S, can be expressed as the product of the average velocity and the time in skid, or

$$S = \tfrac{1}{2}(v_1 + v_2)(t_2 - t_1) \tag{6}$$

where $t_1$ is the time at the start of measurement, in sec, and $t_2$ is the time at the end of measurement, in sec. The initial and terminal velocities for $t_i$ and $t_2$ are $v_1$ and $v_2$, in ft/sec.

Substituting the above value for S, Eq. 4 can be written as

$$f = \frac{(v_1 + v_2)(v_1 - v_2)}{\frac{1}{2}(2g)(v_1 + v_2)(t_2 - t_1)} \tag{7}$$

or

$$f = \frac{v_1 - v_2}{g(t_2 - t_1)} \tag{8}$$

Multiplying by 1.47 to allow substitution of V in mph and substituting 32.2 ft/sec$^2$ for g, Eq. 8 becomes

$$f = \frac{0.0456\,(V_1 - V_2)}{t_2 - t_1} \tag{9}$$

Deceleration—The equation for a force due to acceleration (or deceleration), a, is

$$F = ma = \frac{w}{g}a \tag{10}$$

Combined with Eq. 3,

$$fW = \frac{w}{g}a$$

or

$$f = \frac{a}{g} \tag{11}$$

To determine the average coefficient over a time interval, it is necessary to integrate f with respect to time. Then the effective coefficient of friction, $f_e$, is

$$f_e = \frac{\int_{t_1}^{t_2} (a/g)_t \, dt}{\int_{t_1}^{t_2} dt} \tag{12}$$

## CORRELATION STUDY

Many testers are used today to obtain a friction measurement between tire and pavement. The mode of operation of the testers varies, but the various modes can generally be divided into three groups: (a) steady-state sliding, (b) non-steady-state sliding, and (c) steady-state slip (8). The steady-state sliding group includes all testers which measure the sliding coefficient at a constant velocity, such as the towed trailer testers. The non-steady-state sliding group, also referred to as energy devices, operates on the principle of converting kinetic or potential energy into frictional energy during the test. These devices usually measure a mean coefficient over a velocity range. A skidding, decelerating automobile would be included in this category since it is converting the kinetic energy of the automobile into frictional energy. The British Portable Tester, another example of this group, converts potential energy into kinetic energy, then into frictional energy. The steady-state slip group includes testers which operate at a constant rate of slip with respect to the pavement surface (most of these testers are found in Europe).

The coefficients obtained by friction-testing devices are largely dependent on the mode of operation and may not be directly comparable since rubber friction is dependent on speed and accompanying temperature changes. The coefficient of friction is therefore not an absolute number and may best be regarded as a performance value. This does not mean that a specific coefficient of friction does not exist between a given tire and pavement surface for specific test conditions. On a given pavement,

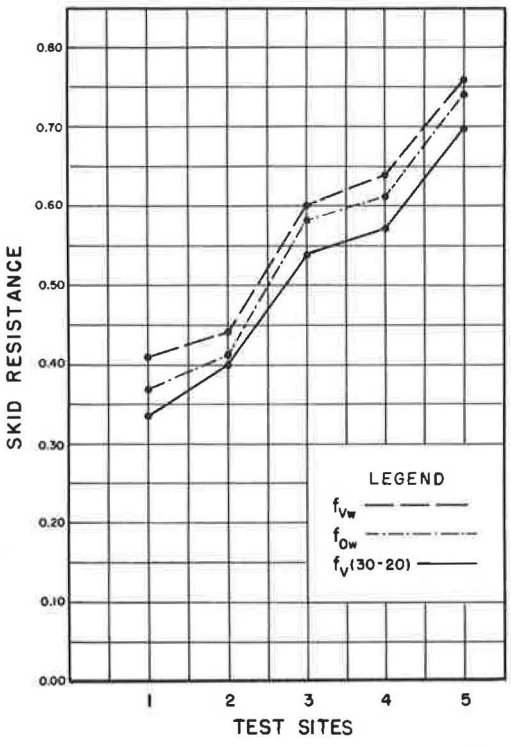


Figure 1. Several skid-resistance values vs test sites.

under identical test conditions, the coefficient should be reproducible, either by the particular tester involved or by a similar tester.

Coefficients obtained by means of a skidding automobile may be determined by using one of three combinations of measurements—velocity and distance, velocity and time, or deceleration. Using any one of these, several coefficients can be determined: (a) mean f, (b) f for a velocity increment, and (c) f at a specific velocity in the case of a deceleration measurement. To examine the various coefficients and the practical aspects of measuring them, a correlation study was conducted in the summer of 1964. This study had the following purposes:

1. Compare theoretically similar coefficients obtained from measurements of different parameters,
2. Determine repeatability of tests,
3. Correlate dissimilar coefficients, and
4. Select a standard test.

## Test Sites

The five pavements selected for use in the correlation study provided a wide range of skid-resistance values (Fig. 1). Other criteria used in the selection of the test sites were accessibility, gradient, surface uniformity and safety to testing personnel. Pertinent information concerning the test pavements is given in Table 1.

Each site was tested at 40 mph in three rounds during a two-month period. Site 1a, however, was tested at 35 mph, because of the inherent danger of skidding on a slippery surface having a large cross-slope. Wherever coefficients at a higher test velocity were required, Site 1b was substituted for 1a. Five tests per site were conducted in Round I and ten in Rounds II and III. Unfortunately, Site 3 was resurfaced before testing in Round III could be carried out; therefore, the test results for Site 3 are based on measurements in Rounds I and II only.

TABLE 1

TEST PAVEMENTS

| Test Site | Route No. | Location | Type of Pavement | $f_{v(30-20)}$ |
|---|---|---|---|---|
| 1a | Ky 89 | Winchester-Irvin | Chip-Seal | 0.33 |
| 1b | I 64 | Winchester-Mt. Sterling | Bituminous | 0.47 |
| 2 | US 60 | Frankfort-Shelbyville | Bituminous | 0.40 |
| 3 | US 25 | Georgetown-Corinth | Bituminous | 0.54 |
| 4 | I 64 | NE C.L. of Lexington | Concrete | 0.57 |
| 5 | US 62 | Lawrenceburg-Bloomfield | Ky. Rock Asp. | 0.70 |

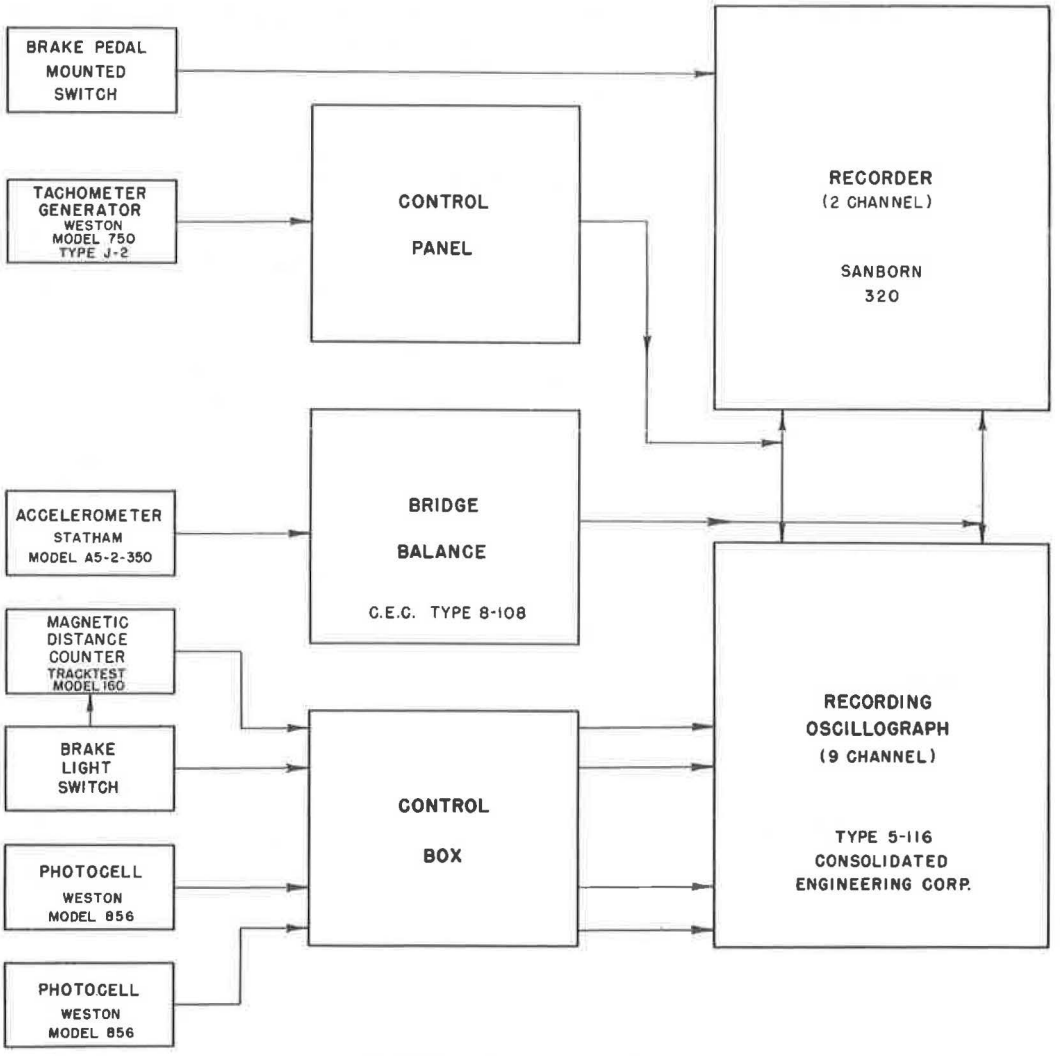


Figure 2. Skid-resistance measuring system.

## Instrumentation

The test vehicle, a 1962 Ford sedan, was instrumented to record time, distance, velocity and deceleration. Also recorded were brake application, brake light energization, and wheel rotation. A block diagram of the instrumentation is shown in Figure 2, and accommodation of the equipment in the automobile is shown in Figure 3. The manner in which each of the parameters and events were detected and recorded follows.

Time—A Sanborn recorder, operated at a chart speed of 100 mm/sec, permitted measurement of very small increments of time. Since chart speed is inversely proportional to the frequency of the ac power supply, it was necessary to monitor the frequency of the inverter and to correct the measurement of time appropriately. A vibratory-reed type frequency meter was used for this purpose.

Distance—A magnetic counter, cam-operated microswitch on the fifth wheel summated the skidding distance. The total count represented the distance measured from the instant power was provided for brake lights to the point where the vehicle came to rest—each full count being equivalent to 1. 32 ft. The position of rotation of the cam

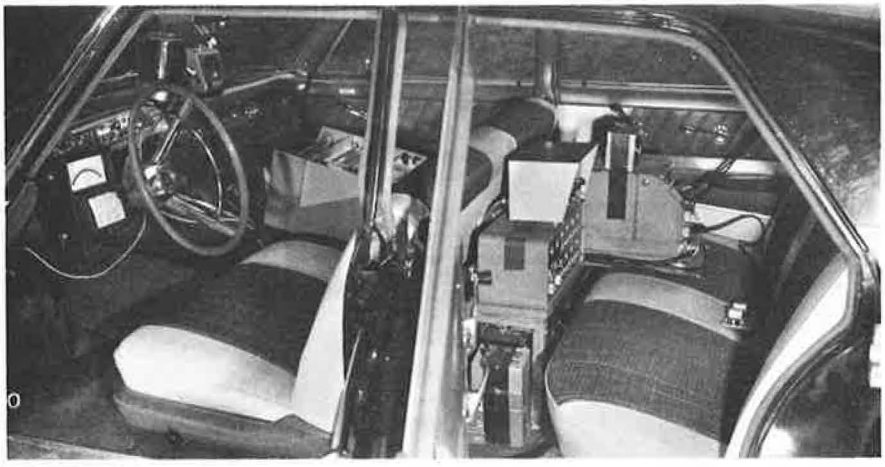

Figure 3. Equipment in the test vehicle. Front: Weston 901 Speedmeter, magnetic counter and Sanborn recorder; Back: C. E. recording oscillograph and balance, control panel, frequency meter, dc power supply and accelerometer.

was unknown for any given test; thus, a maximum error of one count could result. The operation of the microswitch was recorded on a 9-channel Consolidated Engineering recording oscillograph. The resultant rectangular wave, representing one count per cycle, could be counted on the oscillograph chart.

The "observed" stopping distance, from the approximate point of wheel lock to where the vehicle stopped, was measured with a metallic tape. Figure 4 shows the measurement of observed stopping distance in progress.

Velocity—A tachometer generator, mounted on the axle of the fifth wheel, was used in conjunction with a Weston Model 910 Speedmeter to indicate test velocity. The output of the tachometer generator was recorded by both the Sanborn and the C. E. recorders.

Deceleration—A Statham ±2G resistive type horizontally sensitive accelerometer was used to detect deceleration. A C. E. Wheatstone bridge balance was used to balance and to calibrate the accelerometer. The bridge voltage was recorded by both the Sanborn and the C. E. recorders.

Figure 4. Measurement of observed stopping distance.

Figure 5. Push-button switch mounted in brake pedal.

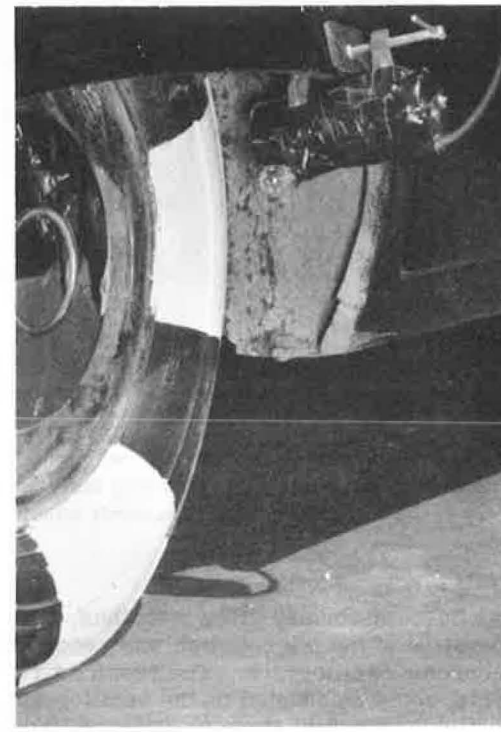

Figure 6. Photocell aimed at the test tire.

Brake Application—A push-button switch, mounted in the brake pedal (Fig. 5), activated an event marker in the Sanborn recorder to indicate the instant of brake application.

Brake Lights—Voltage on the pressure-activated brake-light switch in the brake master cylinder was recorded by the C. E. recorder.

Wheel Rotation—The rear wheel rotation was monitored to determine when the tires were fully skidding. Weston photocells, mounted in black waterproof tubes 6 in. in length, were clamped on the fender of the vehicle (Fig. 6) and aimed at the tires.

## Procedures

Skid Test—All skid measurements were made using ASTM E 17 Standard Tires inflated to 24 psi. The front suspension of the vehicle was partially neutralized at the test site by placing 5-in. wood blocks, padded with $^{3}/_{4}$ in. of rubber at both ends, near the coil springs.

The fifth-wheel speedometer was accurately calibrated on a two-mile section of Interstate highway. The magnetic distance counter was also found to be reliable for speed calibration purposes. The velocity calibration of the Sanborn and C. E. recorders was then based on the accurately calibrated Weston Speedmeter.

Two operators were required in the vehicle during the test. The driver's responsibilities were to monitor test speed and to operate the Sanborn recorder. The other operator, seated in the back seat, calibrated and checked all the equipment, operated the C. E. recorder and monitored the power supply frequency; he also held a platform-mounted accelerometer, slightly angled to compensate for vehicle tilt, during the period of testing.

After traffic control had been established, a water truck equipped with spray bar and water pump wetted the pavement in the test lane. Two or three applications of water were required before testing, and one re-wetting was required for every two or three

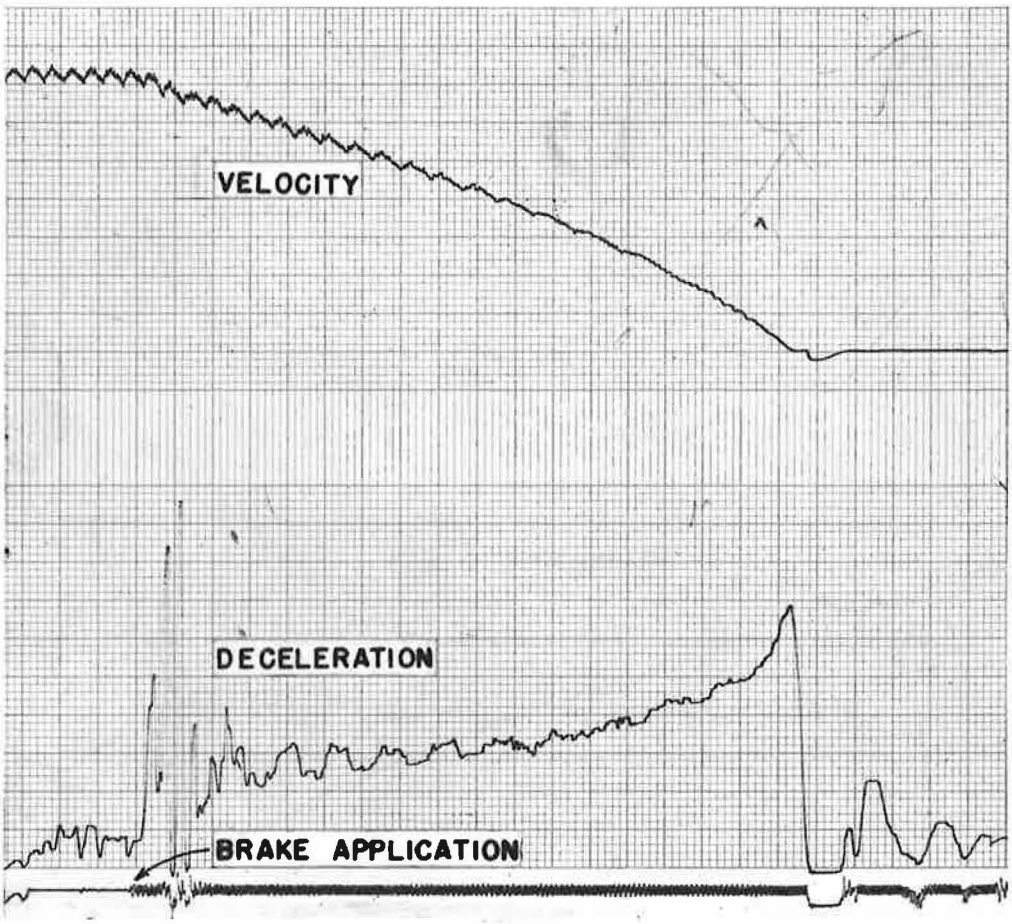


Figure 7. Sanborn recording taken on Site 1 at reduced chart speed.

repeat tests. The beginning of each successive test was advanced approximately 10 ft to minimize skid overlaps. The wetted pavement could be described as well-saturated—i.e., surface cavities filled with water until runoff resulted.

Sufficient starting distance preceded the test section to permit the vehicle to attain the desired speed. The vehicle was accelerated to above the test speed, the recorders turned on and the transmission placed in neutral. The last two maneuvers, executed a few seconds before brake application, insured a steady ac power supply throughout the test and permitted the recorders to attain the desired chart speed. At the appropriate velocity, the vehicle brakes were applied quickly and firmly to facilitate rapid wheel lock. During the skid the vehicle was guided so as to remain in the wheel tracks.

Immediately after the completion of a skid the recorders were turned off; power supply frequency, magnetic counter and observed stopping distances, velocity at brake application, etc., were recorded.

Coefficient Determination—The Sanborn and the C. E. recorder charts (Figs. 7 and 8) were carefully analyzed to obtain the various recorded parameters. Both charts display velocity and deceleration, but only the Sanborn chart was used to obtain the readings of recorded velocity. The deceleration curves were used to transpose a particular instant during the skid from one chart onto the other. The Sanborn chart was used to measure time, velocity and deceleration, and to determine brake-pedal application. The C. E. chart provided a record of distance skidded, the instant the brake light was energized, and the time of wheel lock.

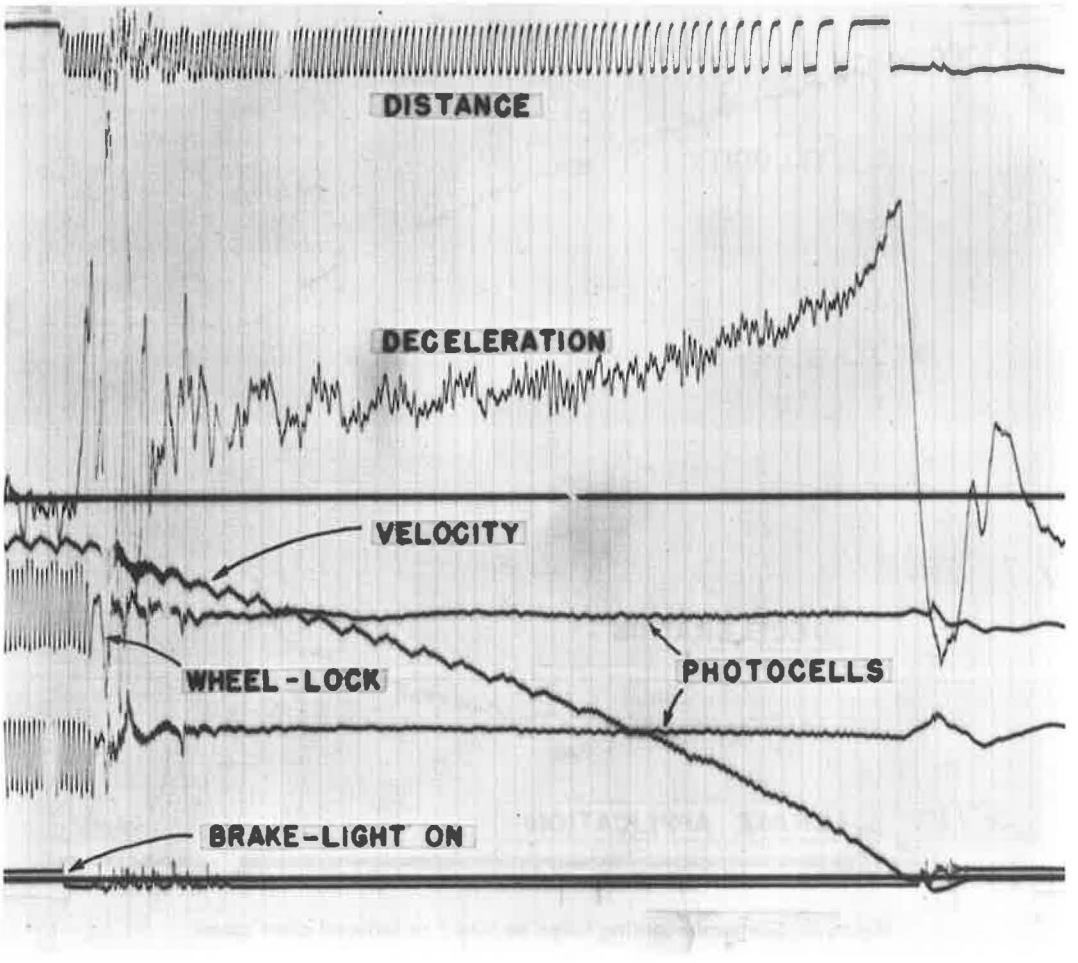


Figure 8. C.E. recording taken on Site 1 at reduced chart speed.

The following procedure was used in arriving at the individual coefficients using the data derived from chart analysis and on-the-site measurements.

$f_{O_0}$ = Coefficient, computed from Eq. 5, obtained from measurement of observed stopping distance and meter-indicated velocity at the instant of brake application.

$f_{O_W}$ = Coefficient (Eq. 5) obtained from the measurement of observed stopping distance and the actual (Sanborn chart) velocity at wheel lock.

$f_{M_0}$ = Coefficient (Eq. 5) obtained from measurement of magnetic counter-indicated stopping distance and meter-indicated velocity at the instant of brake application.

$f_{M_1}$ = Coefficient (Eq. 5) obtained from measurement of magnetic counter-indicated stopping distance and actual velocity at the instant brake light was energized.

$f_{M_W}$ = Coefficient (Eq. 5) obtained from measurement of skid distance by counting impulses of the input to magnetic counter on the C. E. chart, in the velocity increment between wheel lock and 0 mph.

$f_{M(30-0)}$ = Coefficient (Eq. 5) obtained from measurement of skid distance by counting impulses of the input to magnetic counter in the velocity increment between 30 mph and 0 mph.

$f_{M(20-0)}$ = Coefficient (Eq. 5) obtained from measurement of skid distance by counting impulses of the input to magnetic counter in the velocity increment between 20 mph and 0 mph.

$f_{M(10-0)}$ = Coefficient (Eq. 5) obtained from measurement of skid distance by counting impulses of the input to magnetic counter in the velocity increment between 10 mph and 0 mph.

$f_{M(V_w-30)}$ = Coefficient (Eq. 5) obtained from measurement of skid distance by counting impulses of the input to magnetic counter in the velocity increment between wheel lock and 30 mph.

$f_{M(30-20)}$ = Coefficient (Eq. 5) obtained from measurement of skid distance by counting impulses of the input to magnetic counter in the velocity increment between 30 mph and 20 mph.

$f_{M(20-10)}$ = Coefficient (Eq. 5) obtained from measurement of skid distance by counting impulses of the input to magnetic counter in the velocity increment between 20 mph and 10 mph.

$f_{M(V_w-10)}$ = Coefficient (Eq. 5) obtained from measurement of skid distance by counting impulses of the input to magnetic counter in the velocity increment between wheel lock and 10 mph.

$f_{V_l}$ = Coefficient (Eq. 9) obtained from measurement of elapsed time in the velocity increment between brake light energization and 0 mph.

$f_{V_w}$ = Coefficient (Eq. 9) obtained from measurement of elapsed time in the velocity increment between wheel lock and 0 mph.

$f_{V(30-0)}$ = Coefficient (Eq. 9) obtained from measurement of elapsed time in the velocity increment between 30 mph and 0 mph.

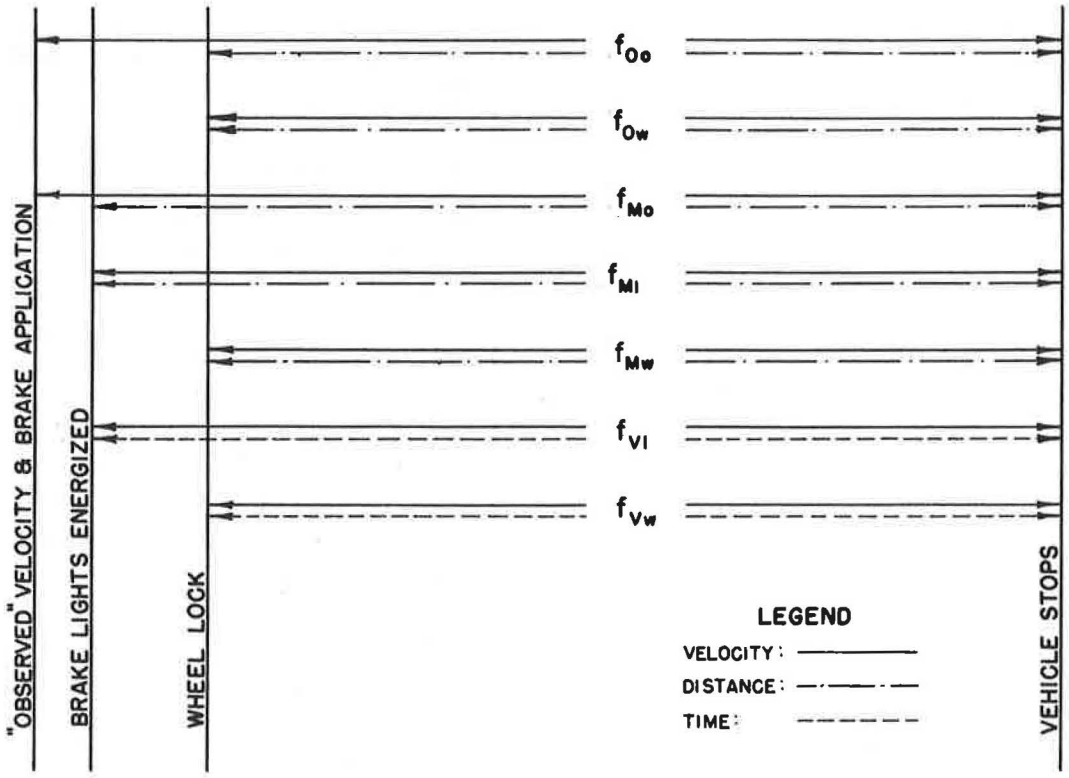


Figure 9. Measurements made for determination of several skid-resistance values.

$f_{V(20-0)}$ = Coefficient (Eq. 9) obtained from measurement of elapsed time in the velocity increment between 20 mph and 0 mph.

$f_{V(10-0)}$ = Coefficient (Eq. 9) obtained from measurement of elapsed time in the velocity increment between 10 mph and 0 mph.

$f_{V(V_W-30)}$ = Coefficient (Eq. 9) obtained from measurement of elapsed time in the velocity increment between wheel lock and 30 mph.

$f_{V(30-20)}$ = Coefficient (Eq. 9) obtained from measurement of elapsed time in the velocity increment between 30 mph and 20 mph.

$f_{V(20-10)}$ = Coefficient (Eq. 9) obtained from measurement of elapsed time in the velocity increment between 20 mph and 10 mph.

$f_{V(V_W-10)}$ = Coefficient (Eq. 9) obtained from measurement of elapsed time in the velocity increment between wheel lock and 10 mph.

$f_{D_W}$ = Average coefficient obtained from measurement of area under the deceleration curve on the Sanborn recording between wheel lock and 0 mph divided by the corresponding chart length (Eq. 12).

$f_{D(15)}$ = Coefficient obtained from measurement of deceleration at 15 mph by interpolating the deceleration trace between 12 and 18 mph (Eq. 11).

$f_{D(25)}$ = Coefficient obtained from measurement of deceleration at 25 mph by interpolating the deceleration trace between 22 and 28 mph (Eq. 11).

$f_{D(35)}$ = Coefficient obtained from measurement of deceleration at 35 mph by interpolating the deceleration trace between 32 and 38 mph (Eq. 11).

Figure 9 may be helpful in visualizing what measurements were used in the computation of some of the skid-resistance values.

TABLE 2

CORRELATION STUDY TEST DATA

| Velocity (mph) | Site 1a | Site 1b | Site 2 | Site 3 | Site 4 | Site 5 |
|---|---|---|---|---|---|---|
| $V_o$ | 34.9 | | 40.0 | 40.1 | 40.0 | 40.1 |
| $V_b$ | 35.4 | | 40.4 | 40.5 | 40.1 | 40.4 |
| $V_l$ | 35.3 | | 40.3 | 40.5 | 39.9 | 40.1 |
| $V_w$ | 34.3 | | 39.4 | 39.6 | 38.5 | 38.9 |
| Coefficients | Velocity and Distance | | | | | |
| $f_{O_o}$ | 0.38 | 0.49 | 0.43 | 0.60 | 0.65 | 0.79 |
| $f_{O_W}$ | 0.37 | 0.46 | 0.41 | 0.58 | 0.61 | 0.74 |
| $f_{M_o}$ | 0.34 | 0.43 | 0.39 | 0.52 | 0.56 | 0.68 |
| $f_{M_l}$ | 0.35 | 0.43 | 0.40 | 0.52 | 0.55 | 0.68 |
| $f_{M_W}$ | 0.36 | 0.46 | 0.41 | 0.55 | 0.58 | 0.72 |
| $f_{M(30-0)}$ | 0.37 | 0.52 | 0.44 | 0.60 | 0.61 | 0.74 |
| $f_{M(20-0)}$ | 0.45 | 0.60 | 0.50 | 0.66 | 0.68 | 0.79 |
| $f_{M(10-0)}$ | 0.59 | 0.69 | 0.61 | 0.76 | 0.77 | 0.83 |
| $f_{M(V_W-30)}$ | 0.35 | 0.39 | 0.37 | 0.50 | 0.54 | 0.71 |
| $f_{M(30-20)}$ | 0.33 | 0.46 | 0.40 | 0.53 | 0.57 | 0.69 |
| $f_{M(20-10)}$ | 0.41 | 0.58 | 0.47 | 0.62 | 0.66 | 0.79 |
| $f_{M(V_W-10)}$ | 0.35 | 0.45 | 0.41 | 0.54 | 0.57 | 0.72 |
| | Velocity and Time | | | | | |
| $f_{V_l}$ | 0.40 | 0.49 | 0.44 | 0.48 | 0.62 | 0.73 |
| $f_{V_W}$ | 0.41 | 0.52 | 0.44 | 0.60 | 0.64 | 0.76 |
| $f_{V(30-0)}$ | 0.42 | 0.57 | 0.47 | 0.64 | 0.67 | 0.78 |
| $f_{V(20-0)}$ | 0.50 | 0.66 | 0.54 | 0.72 | 0.73 | 0.83 |
| $f_{V(10-0)}$ | 0.63 | 0.75 | 0.62 | 0.81 | 0.81 | 0.87 |
| $f_{V(V_W-30)}$ | 0.34 | 0.41 | 0.36 | 0.50 | 0.55 | 0.71 |
| $f_{V(30-20)}$ | 0.33 | 0.47 | 0.40 | 0.54 | 0.57 | 0.70 |
| $f_{V(20-10)}$ | 0.41 | 0.59 | 0.48 | 0.64 | 0.67 | 0.80 |
| $f_{V(V_W-10)}$ | 0.36 | 0.47 | 0.41 | 0.55 | 0.59 | 0.73 |
| | Deceleration | | | | | |
| $f_{D_W}$ | 0.36 | 0.41 | 0.38 | 0.56 | 0.60 | 0.66 |
| $f_{D(15)}$ | 0.38 | 0.46 | 0.41 | 0.60 | 0.61 | 0.68 |
| $f_{D(25)}$ | 0.28 | 0.36 | 0.34 | 0.45 | 0.51 | 0.61 |
| $f_{D(35)}$ | | 0.30 | 0.31 | 0.42 | 0.49 | 0.54 |

## TEST RESULTS AND DISCUSSION

The various skid-resistance values determined in the correlation study are given in Table 2, according to the parameters used in their computation. The most obvious observation about the three groups of skid-resistance data—other than the fact that skid resistance varies with velocity—is that the corresponding coefficients were generally quite different. The coefficients determined from the velocity and time measurements were larger than the coefficients computed from the velocity and distance measurements for the same interval of skid. This is not surprising because the equations used do not properly describe the relationship between the measured parameters. The only exceptions were the coefficients determined over small increments of velocity above 10 mph using the velocity, distance and time measurements. The closeness of these coefficients must be attributed to the nearly linear skid characteristics of the pavements at those velocities and to the accuracy of the velocity, distance and time measurements.

The error due to the nonlinearity of the coefficient-velocity relationship in the velocity increment measurements was determined for 100 skid

TABLE 3

PERCENT DIFFERENCE BETWEEN COEFFICIENTS

| Coefficients | Site 1 | Site 2 | Site 3 | Site 4 | Site 5 | Avg. | Primary Sources of Difference |
|---|---|---|---|---|---|---|---|
| $f_{O_o} - f_{O_w}$ | 2.7 | 4.8 | 3.4 | 6.3 | 6.5 | 4.7 | Unlike velocities |
| $f_{O_o} - f_{M_o}$ | 11.1 | 9.8 | 14.3 | 14.9 | 15.0 | 13.0 | Unlike distances |
| $f_{O_o} - f_{M_w}$ | 5.4 | 4.8 | 8.7 | 11.4 | 9.3 | 7.9 | Unlike velocities and error in distance |
| $f_{O_w} - f_{M_w}$ | 2.7 | 0.0 | 5.3 | 5.0 | 2.7 | 3.1 | Error in distance |
| $f_{M_1} - f_{M_o}$ | 2.9 | 2.5 | 0.0 | -1.8 | 0.0 | 0.7 | Unlike velocities |
| $f_{M_w} - f_{M_1}$ | 2.8 | 2.5 | 5.6 | 5.3 | 5.7 | 4.5 | Unlike velocities and distance |
| $f_{V_w} - f_{O_w}$ | 10.3 | 7.1 | 3.4 | 4.8 | 2.7 | 5.7 | Incremental error |
| $f_{V_w} - f_{O_o}$ | 7.6 | 2.3 | 0.0 | -1.5 | -3.9 | 0.9 | Unlike velocities and incremental error |
| $f_{V_w} - f_{M_w}$ | 13.0 | 7.1 | 8.7 | 9.8 | 5.4 | 8.8 | Difference in incremental error |
| $f_{V_1} - f_{M_1}$ | 13.3 | 9.5 | 10.9 | 12.0 | 8.3 | 10.8 | Incremental error |
| $f_{M_1} - f_{M_o}$ | 2.9 | 2.5 | 0.0 | -1.8 | 0.0 | 0.7 | Unlike velocities |
| $f_{V(10-0)} - f_{M(10-0)}$ | 6.6 | 1.6 | 6.4 | 5.1 | 4.7 | 4.9 | Difference in incremental errors |
| $f_{V(20-0)} - f_{M(20-0)}$ | 10.5 | 7.7 | 8.7 | 7.1 | 4.9 | 7.8 | Difference in incremental errors |
| $f_{V(30-0)} - f_{M(30-0)}$ | 12.7 | 6.6 | 6.5 | 9.4 | 5.3 | 8.1 | Difference in incremental errors |
| $f_{V(20-10)} - f_{M(20-10)}$ | 0.0 | 2.1 | 3.2 | 1.5 | 1.3 | 1.6 | Difference in incremental errors |
| $f_{V(30-20)} - f_{M(30-20)}$ | 0.0 | 0.0 | 1.9 | 0.0 | 1.4 | 0.9 | Difference in incremental errors |
| $f_{V(V_w-30)} - f_{M(V_w-30)}$ | -2.9 | -2.7 | 0.0 | 1.8 | 0.0 | -0.8 | Difference in incremental errors |
| $f_{V(V_w-10)} - f_{M(V_w-10)}$ | 2.8 | 0.0 | 1.8 | 3.5 | 1.4 | 1.9 | Difference in incremental errors |
| $f_{V(20-10)} - f_{D(15)}$ | 7.6 | 15.7 | 6.5 | 9.4 | 16.2 | 11.1 | Deceleration error |
| $f_{V(30-20)} - f_{D(25)}$ | 16.4 | 16.2 | 18.2 | 11.1 | 13.7 | 15.1 | Deceleration error |
| $f_{V(V_w-30)} - f_{D(35)}$ | — | 15.0 | 17.4 | 11.5 | 27.2 | 17.8 | Deceleration error |
| $f_{V_w} - f_{D_w}$ | 13.0 | 14.6 | 6.9 | 6.5 | 14.1 | 11.0 | Deceleration and incremental errors |

tests of low coefficient surfaces. Velocity and time were accurately measured in the velocity increments of 30 to 20 mph and 27.5 to 22.5 mph. The approximate coefficient at 25 mph was found to be about 1.8 percent less than $f_{V(30-20)}$. This difference reflects the "incremental" error which has been discussed elsewhere in the report. The incremental error which, also applied to coefficients $f_O$ and $f_M$, increases as the velocity increment widens and is dependent on the extent of the nonlinearity of the coefficient-velocity relationship. Particularly susceptible to this error are the coefficients $f_V$, as evidenced in the tabulation of percent differences between corresponding coefficients $f_M$ (Table 3).

A number of different measurements were made to determine skid-resistance values using the stopping-distance equation. The coefficient $f_{O_o}$, determined from the measurement of the observed stopping distance and observed velocity at brake application, was slightly higher than $f_{O_w}$, which was based on the actual velocity at wheel lock. This variation was caused by the difference between the observed velocity and velocity at wheel lock. The accuracy of the observed velocity, which was later checked on the velocity recording, was found to be biased. This was probably caused by the driver viewing the meter movement at an angle while carrying out other tasks during the test. The coefficients $f_{O_w}$ and $f_{M_w}$ should be identical since the same velocity measurement was used in their calculation; however, a difference of 3.1 percent resulted. This was attributed to error in the measurement of observed stopping distance, which was usually less than the actual skid distance. Because of this error, and inasmuch as

TABLE 4

STANDARD DEVIATIONS[a]

| Coefficients | Site 1 | Site 2 | Site 3 | Site 4 | Site 5 |
|---|---|---|---|---|---|
| $f_{O_o}$ | 0.016 | 0.012 | 0.025 | 0.025 | 0.016 |
| $f_{O_w}$ | 0.013 | 0.011 | 0.024 | 0.026 | 0.023 |
| $f_{M_o}$ | 0.015 | 0.010 | 0.018 | 0.015 | 0.011 |
| $f_{M_1}$ | 0.008 | 0.007 | 0.019 | 0.018 | 0.013 |
| $f_{M_w}$ | 0.007 | 0.010 | 0.025 | 0.013 | 0.016 |
| $f_{M(30-0)}$ | 0.009 | 0.010 | 0.029 | 0.021 | 0.018 |
| $f_{M(20-0)}$ | 0.014 | 0.014 | 0.046 | 0.022 | 0.039 |
| $f_{M(10-0)}$ | 0.047 | 0.041 | 0.075 | 0.055 | 0.042 |
| $f_{M(V_w-30)}$ | 0.030 | 0.017 | 0.040 | 0.029 | 0.055 |
| $f_{M(30-20)}$ | 0.010 | 0.016 | 0.033 | 0.021 | 0.023 |
| $f_{M(20-10)}$ | 0.015 | 0.015 | 0.050 | 0.020 | 0.051 |
| $f_{M(V_w-10)}$ | 0.012 | 0.009 | 0.026 | 0.012 | 0.018 |
| $f_{V_1}$ | 0.010 | 0.005 | 0.019 | 0.013 | 0.022 |
| $f_{V_w}$ | 0.006 | 0.009 | 0.020 | 0.012 | 0.023 |
| $f_{V(30-0)}$ | 0.010 | 0.011 | 0.030 | 0.009 | 0.022 |
| $f_{V(20-0)}$ | 0.012 | 0.014 | 0.037 | 0.016 | 0.033 |
| $f_{V(10-0)}$ | 0.024 | 0.018 | 0.044 | 0.030 | 0.035 |
| $f_{V(V_w-30)}$ | 0.031 | 0.012 | 0.034 | 0.027 | 0.062 |
| $f_{V(30-20)}$ | 0.010 | 0.015 | 0.031 | 0.012 | 0.024 |
| $f_{V(20-10)}$ | 0.010 | 0.016 | 0.038 | 0.017 | 0.044 |
| $f_{V(V_w-10)}$ | 0.009 | 0.013 | 0.021 | 0.012 | 0.025 |
| $f_{D_w}$ | 0.015 | 0.018 | 0.020 | 0.050 | 0.033 |
| $f_{D(15)}$ | 0.036 | 0.050 | 0.039 | 0.030 | 0.027 |
| $f_{D(25)}$ | 0.033 | 0.036 | 0.042 | 0.041 | 0.060 |
| $f_{D(35)}$ | — | 0.057 | 0.054 | 0.056 | 0.083 |

[a]Data from Rounds I and II.

TABLE 5

NUMBER OF TESTS REQUIRED FOR 5 PERCENT ERROR OR LESS

| Coefficients | Site 1 | Site 2 | Site 3 | Site 4 | Site 5 | Avg. |
|---|---|---|---|---|---|---|
| $f_{O_o}$ | 5 | 4 | 5 | 5 | 3 | 4 |
| $f_{O_w}$ | 4 | 3 | 5 | 6 | 4 | 4 |
| $f_{V_w}$ | 3 | 4 | 4 | 3 | 4 | 4 |
| $f_{M_o}$ | 5 | 4 | 6 | 4 | 3 | 4 |
| $f_{M_w}$ | 3 | 4 | 5 | 3 | 3 | 4 |
| $f_{M_1}$ | 3 | 3 | 6 | 4 | 4 | 4 |
| $f_{V(30-20)}$ | 4 | 5 | 7 | 3 | 4 | 5 |
| $f_{M(30-20)}$ | 4 | 5 | 7 | 5 | 5 | 5 |
| $f_{V(10-0)}$ | 5 | 4 | 7 | 5 | 6 | 6 |
| $f_{D_w}$ | 5 | 6 | 5 | 6 | 7 | 6 |
| $f_{D(25)}$ | 13 | 15 | 18 | 9 | 14 | 14 |

the velocity at brake application was used, $f_{O_o}$ was much larger than $f_{M_w}$, but $f_{M_w}$ represented the correct measurement of velocity and distance. Coefficients $f_{M_o}$ and $f_{M_1}$ were determined from the measurement of distance with the magnetic counter utilizing the observed velocity at brake application and the recorded velocity at the moment of brake light energization, respectively. The difference between these coefficients was quite small because the velocities were quite similar.

The repeatability of a particular skid-resistance measurement was judged largely on the basis of the standard deviation of the tests made in Round III. The pavement and the magnitude of the skid resistance, as well as instrumentation errors, influence the standard deviation; therefore, careful examination of the data in Table 4 is warranted. The influence of the pavement is evident on Site 3 where the standard deviation shows a significant deviation from the trend of the other sites. This pavement was extremely pitted, and the nonhomogeneous surface was the apparent cause of the deviation. The magnitude of the skid resistance affected the standard deviation; i.e., the standard deviation increased as skid resistance increased. The standard deviation was used to determine the number of tests required to achieve a desired degree of accuracy. The number of required tests for a few selected coefficients is presented in Table 5. The complete mathematical procedure used in the statistical analysis of the data is presented in the Appendix.

Further examination of the standard deviations reveals that the most repeatable test results were obtained when the largest velocity increment was chosen for the computation. There are three main reasons for this: first, the larger the velocity increment, the more accurate are the velocity, distance and time measurements; second, influences due to variability of skid resistance below 10 mph are minimized; third, errors due to premature or delayed front-wheel locking and errors in establishing the instant of rear-wheel locking are reduced. These latter errors were noted in the coefficients $f_V$ and $f_M$ for the velocity increment of $V_w$-30 mph.

The primary cause of poor repeatability of the coefficients in the 10-0 mph increment was the inability to steer the skidding vehicle in wheel tracks near the end of the skid. As the vehicle skids out of the wheel tracks, it encounters higher skid resistance; the degree of skid-out varied from test to test.

TABLE 6
CORRELATION EQUATIONS

| X | Y | Equation | R | $E_S$ |
|---|---|---|---|---|
| | | Good Correlation | | |
| $f_{O_0}$ | $f_{O_W}$ | Y = 0.024 + 0.909X | 1.000 | 0.004 |
| $f_{O_0}$ | $f_{M_0}$ | Y = 0.036 + 0.811X | 0.999 | 0.004 |
| $f_{V(30-20)}$ | $f_{V(20-10)}$ | Y = 0.058 + 1.067X | 1.000 | 0.006 |
| $f_{V(30-20)}$ | $f_{M(30-20)}$ | Y = 0.009 + 0.974X | 1.000 | 0.006 |
| $f_{V(30-20)}$ | $f_{V(V_W-10)}$ | Y = -0.031 + 1.084X | 0.998 | 0.006 |
| $f_{V_W}$ | $f_{V_1}$ | Y = 0.020 + 0.932X | 0.997 | 0.006 |
| $f_{V(30-20)}$ | $f_{M_W}$ | Y = -0.023 + 1.058X | 0.998 | 0.007 |
| $f_{V(30-20)}$ | $f_{V_1}$ | Y = 0.036 + 1.000X | 1.000 | 0.008 |
| $f_{O_0}$ | $f_{M_W}$ | Y = 0.036 + 0.857X | 0.999 | 0.008 |
| $f_{V_W}$ | $f_{M_W}$ | Y = -0.036 + 0.981X | 1.000 | 0.009 |
| $f_{V(30-20)}$ | $f_{V_W}$ | Y = 0.917 + 1.073X | 0.997 | 0.009 |
| $f_{V_W}$ | $f_{V(30-0)}$ | Y = 0.065 + 0.948X | 0.996 | 0.009 |
| | | Fair Correlation | | |
| $f_{V(30-20)}$ | $f_{M_0}$ | Y = -0.024 + 1.006X | 0.994 | 0.011 |
| $f_{V_W}$ | $f_{V(20-10)}$ | Y = 0.071 + 0.955X | 0.993 | 0.012 |
| $f_{V(30-20)}$ | $f_{V(30-0)}$ | Y = 0.082 + 1.012X | 0.992 | 0.012 |
| $f_{V_W}$ | $f_{V(V_W-10)}$ | Y = -0.045 + 1.005X | 0.996 | 0.013 |
| $f_{V(30-20)}$ | $f_{O_0}$ | Y = -0.074 + 1.242X | 0.995 | 0.014 |
| $f_{V(30-20)}$ | $f_{V(V_W-30)}$ | Y = -0.094 + 1.120X | 0.995 | 0.015 |
| $f_{V_W}$ | $f_{V(V_W-30)}$ | Y = -0.151 + 1.111X | 0.990 | 0.017 |
| $f_{V(30-20)}$ | $f_{V(20-0)}$ | Y = 0.184 + 0.944X | 0.988 | 0.017 |
| $f_{V_W}$ | $f_{D(25)}$ | Y = -0.070 + 0.889X | 0.971 | 0.017 |
| $f_{V(30-20)}$ | $f_{D(25)}$ | Y = -0.062 + 0.967X | 0.982 | 0.018 |
| | | Poor Correlation | | |
| $f_{V_W}$ | $f_{V(20-0)}$ | Y = 0.187 + 0.860X | 0.981 | 0.027 |
| $f_{V_W}$ | $f_{D_W}$ | Y = -0.054 + 0.973X | 0.981 | 0.029 |
| $f_{V_W}$ | $f_{V(10-0)}$ | Y = 0.336 + 0.735X | 0.938 | 0.029 |
| $f_{V(30-20)}$ | $f_{D_W}$ | Y = -0.027 + 1.024X | 0.964 | 0.032 |
| $f_{V(30-20)}$ | $f_{V(10-0)}$ | Y = 0.364 + 0.754X | 0.939 | 0.032 |

Velocity-time and velocity-distance coefficients in the 30-20 mph increment exhibited smaller deviations than the coefficients in the other 10-mph increments. This could be attributed to the higher velocity and therefore to longer skid intervals which permitted more accurate distance and time measurements. These measurements were not affected by differential wheel lock or by skid-out.

The measurement of deceleration yielded much lower coefficients than those obtained from measurement of other parameters for similar velocities. The conclusion is that the measurement of deceleration was in error because of improper correction for vehicle tilt. Even more significant was the fact that the coefficients $f_D$ had very poor repeatability, indicating that the method of holding the plate-mounted accelerometer was not satisfactory.

Data from the five test sites were used to correlate selected coefficients as given in Table 6. The results of these analyses were arbitrarily divided into three classifications on the basis of the standard error of estimate, $E_S$, and the correlation coefficient, R. The regression equations were linear, permitting simple conversion from one coefficient to another. This enabled a prediction of skid distance or duration of the skid without actually making the measurement. For example, by knowing $f_{V(30-20)}$, the coefficients $f_{V_W}$ and $f_{M_W}$ can be calculated from the appropriate regression equations. Then by using Eqs. 5 and 9 and the estimated velocity at wheel lock, the approximate skid distance and time in skid, from the moment of wheel lock, can be determined. The actual velocity at wheel lock can be closely estimated by subtracting one mph from the observed velocity. This method is applicable to the determination of the skid distance and skid duration at the velocity of 40 mph only.

Selection of a standard test was subjected to several criteria—accuracy, repeatability, rapid availability of test results, simplicity of measurement and minimum instrumentation. Several measurements fulfill most of these requirements. Coefficient $f_{M_0}$ in particular offers a number of advantages: the magnetic distance counter provides a simple and quick measurement of skid distance with little equipment, the velocity is obtained visually and the test results are highly repeatable. Coefficient $f_{O_0}$ provides highly repeatable test results and requires little or no equipment other than the test vehicle. However, the measurement of observed skid distance is cumbersome and requires additional personnel. Neither coefficient measures skid distance from the moment of wheel lock, and the velocity at brake application does not correspond to the beginning of either measurement of distance.

The measurement of time in the velocity increment of 30 to 20 mph, yielding coefficient $f_{V(30-20)}$, was selected as the standard for the following reasons:

1. Time can be measured accurately to ±1 percent;
2. Coefficient of friction in this velocity increment is nearly linear;
3. Good repeatability, requiring five tests for a 5 percent error or less;
4. Requires only one channel for recording purposes; and
5. Relative ease of chart interpretation.

Safety considerations prohibited the selection of a test which would require initiation of the skid above a speed of approximately 35 mph.

Coefficient $f_V(30\text{-}20)$ cannot be directly equated to a steady-state sliding coefficient of friction at 25 mph; this is due to the influence of air resistance and incremental error. The net effect of these influences is an increase in the magnitude of the coefficient. On the basis of this study, the increase, in terms of coefficient of friction, appeared to be about the same regardless of the skid resistance of the pavement—approximately 0.01.

## AFFECTING FACTORS

### Speed

The coefficient of friction between a tire and a road surface decreases as the velocity of the vehicle increases. No theory for this phenomena has met universal approval, but several have been offered. For some time, the reigning theory has been that higher speeds allow less time for penetration of the water film that covers the pavement. This is similar to hydroplaning in the sense that hydrodynamic lift is provided by the water film. It differs from hydroplaning because the tire is still deformed by the asperities and does not ride above them.

Obertop (5) presented a theory to show that the decrease in skid resistance is caused by the development of steam resulting from a transformation of energy. The kinetic energy of the moving vehicle is irreversibly converted into other types of energy, including heat created at the tire-pavement contact area. This heat raises the temperature of the water at this contact area to a point where the pressure exerted by the tire creates steam. When this occurs, adhesion becomes zero at the point of contact. As the speed of the vehicle increases, the amount of steam generated increases, and the average coefficient drops. Obertop further suggested a mathematical equation to define the coefficient at any speed after calculating the coefficient at any two speeds. A comparison of values obtained from this formula and observed values showed a maximum difference of 0.03 (5). Total hydroplaning results in almost complete loss of braking traction and cornering capability. Before total hydroplaning can occur, the depth of water must exceed the tread depth of the tire plus an amount necessary to submerge the asperities of the pavement. The latter depends on the texture of the pavement surface. For E 17 tires on a typical bituminous pavement, the minimum necessary depth is approximately 0.5 in. If this water condition exists, a formula using only the tire inflation pressure in psi as a parameter can be used to obtain the velocity in mph, $V_p$, at which total hydroplaning will occur ($V_p = 10.35\sqrt{p}$) (2). The normal operating tire pressure of 24 psi requires a minimum velocity of 51 mph to produce total hydroplaning.

While hydroplaning definitely does cause a decrease in the coefficient of friction with increased velocity when the depth of water exceeds about 0.15 in., evidence exists that on wet pavements where water depth is small, significant hydroplaning does not occur. The NASA Langley Research Center encountered no hydroplaning in wet runway tests (2). The authors also found that a 4-groove, rib tread passenger car tire, traveling 30 mph on a level, textured concrete runway surface covered with 0.04 in. of water, developed 88 percent of its dry-pavement cornering force. This loss of 12 percent is probably caused by loss of contact due to the presence of the lubricating film of water rather than by partial hydroplaning. When the velocity is greater than 50 mph, partial hydroplaning is small, but possibly not negligible. The degree of hydroplaning depends on the condition of the tire, the tire inflation pressure and the depth of the water.

Total hydroplaning can never result in complete loss of traction because of viscous friction. When a lubricating liquid causes loss of contact between two surfaces, the

friction depends on the viscosity of the liquid and hence on the temperature (7). When this friction is present, the force required to move the skidding tire at a constant rate, $F_v$, is given by (7)

$$F_v = \mu \frac{v}{h} A_c$$

where $\mu$ is the viscosity of the fluid, v is the velocity at which the tire is moving, h is the thickness of the water film and $A_c$ is the contact area of the tire. This formula indicates an increasing force with increasing velocity—causing a higher drag on the vehicle. This drag would decelerate the vehicle asymptotically if it were the only drag or resistance encountered.

The variation of coefficient of friction with velocity is shown in Figure 10 for a number of different types of pavements, including the five correlation study test sites.

## Air Resistance

Any object moving through a fluid encounters a resistance. When an automobile moves through air, this resistance in pounds, $R_a$, is given (14, pp. 304-305) by the equation

$$R_a = \frac{C_d v^2 A \gamma}{2g} \tag{13}$$

which is the general equation for drag. In this equation $C_d$ is a dimensionless drag coefficient, v is the velocity of the automobile in ft/sec, A is the projected frontal area of the vehicle in $ft^2$ and $\gamma$ is the unit weight of air in $lb/ft^3$. To make the equation dimensionally correct when V is in mph, it is necessary to use a conversion factor of $1.47^2$ to change mph to ft/sec. The result is then

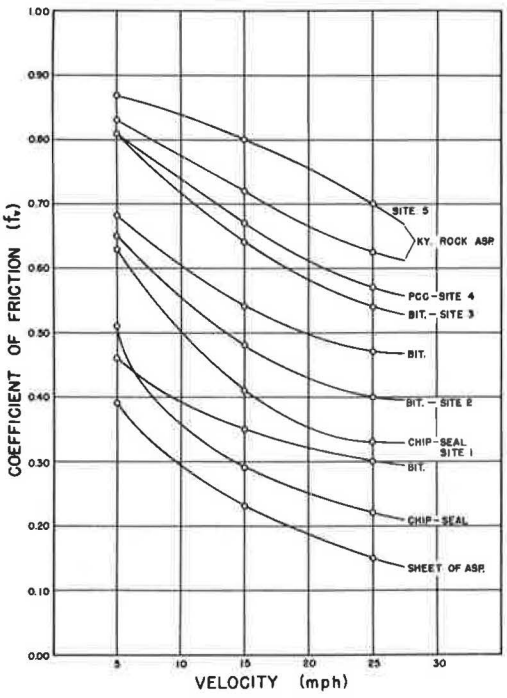


Figure 10. Coefficient of friction ($f_V$) vs velocity for a number of pavements.

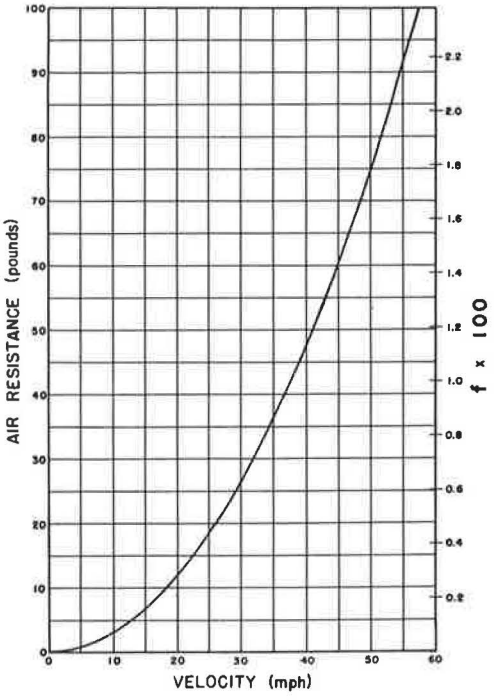


Figure 11. Air resistance and coefficient of friction vs velocity.

$$R_a = \frac{2.16\ C_d\ A\ V_a^2\ \gamma}{2g} \tag{14}$$

where $V_a$ is the velocity of the vehicle in mph, with respect to the air mass. The unit weight of air, $\gamma$, varies with temperature, T, and atmospheric pressure, p, according to the equation (14, p. 11)

$$\gamma = \frac{p}{53.3\ T} \tag{15}$$

Under normal atmospheric pressure and an ambient temperature of 85 F, $\gamma = 0.0732$ lb/ft$^3$.

The terms $C_d$ and A are constant for any given vehicle. For the test vehicle (information supplied by Ford Motor Company, Dearborn, Michigan) $C_d = 0.51$ and A = 24.1 sq ft.

Substituting these values and g = 32.2 ft/sec$^2$ into Eq. 14, $R_a$ can be plotted as a function of $V_a$, as shown in Figure 11. The equation is

$$R_a = 0.030176\ V_a^2 \tag{16}$$

Since air resistance is a force retarding a skidding vehicle, it can be considered as a portion of the total friction force—thereby affecting the computed coefficient of friction. The influence can be determined by substituting $R_a$ for the friction in Coulomb's equation, F = fN, or

$$R_a = fN \tag{17}$$

Using the value of $R_a$ from Eq. 16 and solving for f, Eq. 17 becomes

$$f = \frac{0.030176\ V_a^2}{N} \tag{18}$$

and by substituting the weight of the vehicle, 4,200 pounds, for the normal force, N,

$$f = 7.18 \times 10^{-6} V_a^2 \tag{19}$$

From the graph in Figure 11, f can be indicated opposite $R_a$ as a function of $V_a$.

The velocity $V_a$ is the sum of the vehicle velocity, $V_v$, and the wind velocity, $V_r$, or $V_a = V_r + V_v$. If wind velocity, $V_r$, is assumed to be zero, then $V_a = V_v$, or the vehicle speed. At 30 mph and 20 mph the air resistance is equivalent to f = 0.0065 and f = 0.0029, respectively. The calculated coefficient $f_{V(30-20)}$, therefore, is higher than the actual coefficient. This error is largest for low coefficient surfaces—approximately 2 percent for a coefficient of friction of 0.25.

## Vehicle Dynamics

The behavior of the vehicle body on its suspension system is referred to in this report as the vehicle dynamics. When brakes are rapidly applied to a moving vehicle, the body of the vehicle surges forward and oscillates in a pitching manner as shown by the deceleration recording in Figures 7 and 8. The motion of the body near the wheels is both vertical and horizontal and, to a large extent, is dampened out during the skid. The body tilt, however, continues to change with the change in skid resistance as the vehicle decelerates.

The vehicular dynamic behavior could affect a friction measurement as a result of weight transfer from rear to front or as a result of energy stored in the suspension system. To determine the extent of this influence, skid tests were conducted with the suspension system partially neutralized and with the suspension system acting freely. Rubber-cushioned wood blocks were constructed for this purpose and inserted near the suspension system components. A summary of the test results is given in Table 7.

TABLE 7
EFFECTS OF VEHICULAR DYNAMICS[a]

| Blocks | $V_l$ | $V_w$ | $S_m$ | $f_{V_w}$ | $f_{v(10-0)}$ |
|---|---|---|---|---|---|
| None | 44.5 | 43.0 | 117.5 | 0.64 | 0.80 |
| Front | 45.2 | 43.3 | 119.2 | 0.64 | 0.80 |
| Front and rear | 44.5 | 42.7 | 118.3 | 0.64 | 0.80 |

[a]All values are averages of ten tests conducted on Site 4.

In this investigation, the test results were not altered to a measurable degree by partially neutralizing the suspension system. From these results, it is surmised that the vehicle dynamics have insignificant effect on the skid distance or on the skid resistance at any given velocity during the skid.

It should be pointed out that the velocity increment measurements at velocities near the instant of wheel lock may be quite susceptible to error. This is due to the behavior of the vehicle body and the fact that the fifth wheel is attached to the body of the car rather than the rear axle. The velocity at wheel lock could be in error simply because the body of the car oscillates and momentarily increases or decreases the velocity of the fifth wheel. It becomes imperative then to provide the test automobile with a very stiff suspension so as to shorten the period of dynamic activity. While it is recognized that the vehicle continues to undergo a change in displacement with respect to the wheels and the chassis during skid, the resultant error in the measured velocity is assumed to be negligible.

### Tire Inflation Pressure

The influence of tire inflation pressure was observed in tests on all five test sites. Beginning at 32 psi, the tire pressure was decreased in 4-psi increments to 20 psi. Five tests were run at each tire pressure. The results of these tests showed a general decrease in the coefficient of friction with increase in tire pressure. The coefficient $f_{V(30-20)}$ has slightly less than a 5 percent decrease between 20 psi and 32 psi; therefore, a variation of 2 psi was considered insignificant.

## THE BRITISH PORTABLE TESTER

The British Portable Tester (BPT), shown in Figure 12, was employed by the Department of Highways in skid testing for three years, including 1964. The validity of the test results yielded by the tester for certain types of pavements has been in doubt for some time. Consequently,

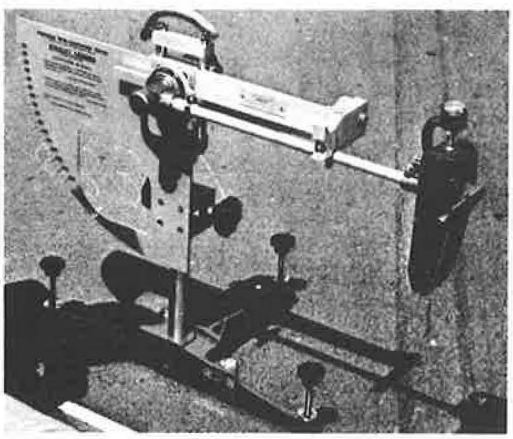

Figure 12. The British Portable Tester.

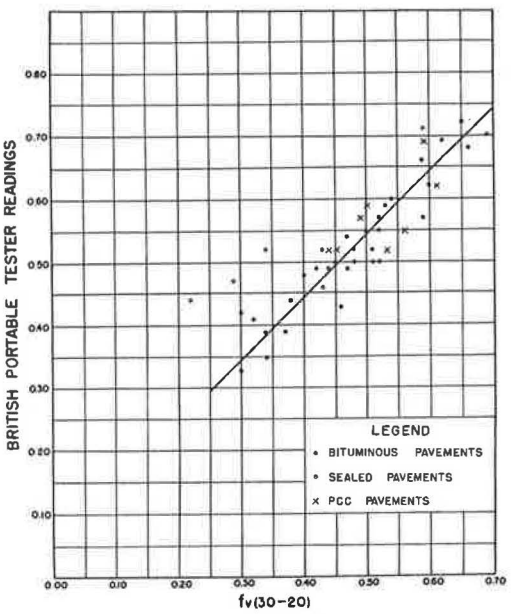


Figure 13. British Portable Tester readings vs coefficient $f_{V(30-20)}$.

TABLE 8

CORRELATION OF BPT AND $f_{V(30-20)}$

| Pavements | Equation[a] | R | $E_s$ |
|---|---|---|---|
| Combined | Y = 0.162 + 0.777X | 0.877 | 0.045 |
| Concrete and bituminous | Y = 0.066 + 0.957X | 0.928 | 0.036 |
| Bituminous | Y = 0.052 + 0.985X | 0.944 | 0.031 |

[a] Y = BPT reading.

a comparison was made between values obtained with this tester and $f_{V(30-20)}$. The surfaces tested were generally classified as bituminous, concrete and bituminous sealcoats. The results are shown in Figure 13.

Regression equations were found for data of several combinations of pavements, but only the equation for bituminous pavements was shown in Figure 13. The correlation of the BPT and $f_{V(30-20)}$ for various pavement surfaces is given in Table 8.

Obviously, a correlation exists between the two sets of values; but, on the basis of the criterion established for the correlation of the other coefficients in Table 5, the correlation is poor. The influence of sealed and concrete pavements is easily discernible (sealed pavements are included in the combined group in Table 8). On sealed surfaces, the BPT indicates much higher skid resistance, and a separate correlation would be warranted. Unfortunately, the number of these surfaces tested was insufficient to perform such a correlation.

## CONCLUSIONS

1. The measurement of time and velocity of a skidding automobile fulfills the requirement of an interim standard method of testing. The coefficient $f_{V(30-20)}$ was found to be a good indicator of pavement-tire friction but does not fully describe the frictional characteristics of the surface.
2. The use of an automobile as a regular pavement-slipperiness testing device is extremely unsatisfactory. The test interferes with traffic flow and is time-consuming, hazardous to testing personnel and expensive, since it requires the services of four technicians. The average cost of testing was $25.00 per site per lane.
3. Air resistance has little effect on the retardation of a skidding vehicle because of the low test velocities. The influence of vehicle dynamics was found to be negligible. Other test influences, such as speed and tire pressure, were determined and have been previously discussed. Much remains to be learned concerning the variation of skid resistance with seasons, temperature, and pavement washing.
4. The British Portable Tester results correlate poorly with coefficient $f_{V(30-20)}$, particularly when concrete and bituminous sealcoat surfaces are included. From the standpoint of safety, traffic interference, test personnel and time required to perform the test, the instrument offers little advantage over testing with an automobile. It does provide repeatable results and is quite useful in laboratory testing and in testing small areas and otherwise inaccessible locations.

## ACKNOWLEDGMENT

This report was prepared in cooperation with the U. S. Bureau of Public Roads. The opinions, findings, and conclusions in this report are not necessarily those of the Kentucky Department of Highways or of the Bureau of Public Roads.

## REFERENCES

1. Kummer, H. W., and Meyer, W. E. Rubber and Tire Friction. Bull. B-80, College of Engineering and Architecture, Penn. State Univ., Dec. 1960.
2. Horne, W. B., and Joyner, U. T. (NASA Langley Research Center). Pneumatic Tire Hydroplaning and Some Effects on Vehicle Performance. Booklet 970C, SAE, New York, Jan. 1965.
3. Bowden, F. P., and Tabor, D. The Friction and Lubrication of Solids. Oxford Univ. Press, London, 1950.
4. Moyer, R. A. A Review of the Variables Affecting Pavement Slipperiness. Proc. First Internat. Skid Prevention Conf., Virginia Council of Highway Investigation and Research, Univ. of Virginia, 1959, Part II, p. 411.

5. Obertop, D. H. F. Decrease of Skid-Resisting Properties of Wet Road Surfaces at High Speeds. ASTM Spec. Tech. Publ. 326, 1962.
6. Slocum, S. E. The Theory and Practice of Mechanics. Henry Holt and Co., New York, 1913, Chapter IV.
7. McGraw-Hill Encyclopedia of Science and Technology. New York, 1960, Vol. 5, p. 536.
8. Kummer, H. W., and Meyer, W. E. Measurement of Skid Resistance. ASTM Spec. Tech. Publ. 326, 1962.
9. Stutzenberger, W. J., and Havens, J. H. A Study of the Polishing Characteristics of Limestone and Sandstone Aggregates in Regard to Pavement Slipperiness. HRB Bull. 186, 1958, pp. 58-81.
10. Havens, J. H. Skid Prevention Studies in Kentucky. Proc. First Internat. Skid Prevention Conf., 1959, Part II, pp. 333-340.
11. Rizenbergs, R. L. Pavement Friction. Kentucky Engineer, May 1960.
12. Havens, J. H., and Rizenbergs, R. L. Pavement Slipperiness Studies. Intra-Departmental Rept., Kentucky Dept. of Highways, Feb. 1962 (Unpublished).
13. Richards, Sears, Wehr, and Zemansky. Modern University Physics. Addison-Wesley Publ. Co., Reading, Mass., 1960, p. 129.
14. King, A. W., Wisler, C. O., and Woodburn, J. G. Hydraulics. John Wiley and Sons, New York, 1958.

# *Appendix*

## STATISTICAL CALCULATIONS

### Regression Lines

All regression lines were of the form

$$Y = a + bX \tag{A1}$$

where

$$b = \frac{\eta(\Sigma XY) - (\Sigma X)(\Sigma Y)}{\eta(\Sigma X^2) - (\Sigma X)^2} \tag{A2}$$

$$a = \frac{\Sigma Y - b(\Sigma X)}{\eta} \tag{A3}$$

and

$\eta$ = number of observations
X and Y = observed values of data

### Coefficient of Correlation

$$R = \frac{\eta(\Sigma XY) - (\Sigma X)(\Sigma Y)}{\sqrt{\eta(\Sigma X^2) - (\Sigma X)^2}\sqrt{\eta(\Sigma Y)^2 - (\Sigma Y)^2}} \tag{A4}$$

### Standard Error of Estimate

$$E_S = \sqrt{\frac{\Sigma(Y - Y_1)^2}{\eta}} \tag{A5}$$

where

$Y_1$ = calculated values of Y for observed values of X

Standard Deviation

$$\sigma = \sqrt{\frac{\Sigma_1 \eta (X - \overline{X})^2}{\eta}} \tag{A6}$$

where

$\overline{X}$ = mean of $\eta$ number of X's

Required Number of Tests

$$N = \left(t \frac{\sigma}{E}\right)^2 \tag{A7}$$

where

t = student value
$\sigma$ = standard deviation, from Eq. A6
E = maximum allowable error, 5 percent

# Development of the PCA Road Meter: A Rapid Method for Measuring Slope Variance

M. P. BROKAW, Paving Engineer, Portland Cement Association, Madison, Wisconsin

Results of the AASHO Road Test were determined in part by measurements of variations in longitudinal slope of pavement surfaces as made by the AASHO Profilometer. Later, a device known as the CHLOE Profilometer was developed by members of the Road Test staff to afford a less expensive method for measuring slope variance. Both profilometers operate at a speed well below that of traffic. Highway tests can be made only with extreme precautions that are costly to the operating agency and traveling public. Furthermore, the devices require multiple operating personnel, are expensive to acquire or construct, and neither is able to survey large mileages of pavement in a short time.

The PCA Road Meter was developed to afford a rapid method for measuring slope variance. The method uses a simple electromechanical device, installed in a conventional passenger automobile, which measures the number and magnitude of road-car deviations. These are statistically summed and correlated with slope variance measured by the CHLOE Profilometer. The test automobile can be operated at speeds consistent with traffic and without extra personnel.

The PCA Road Meter is not difficult to construct, is inexpensive, and has been tested and compared during the period from June 1965 to July 1966 in thousands of miles of highway use. At present, it is being used in extensive studies of pavement performance for the Portland Cement Association.

In this paper, the basic mechanical and electrical features are described, results of correlative tests with the CHLOE Profilometer are presented, and physical limitations are defined and discussed.

•MEASUREMENTS of the condition of pavements in the AASHO Road Test were made by a device known as the AASHO Profilometer. This instrument provided a continuous analog of longitudinal slope of pavement surface in each wheelpath. These data were reduced to observations taken at 1-ft intervals, and statistical variance of slope was calculated and used as a partial measure of pavement serviceability.

The Road Test staff also developed a simplified profilometer, now known as the CHLOE Profilometer. This device moved in one wheelpath and measured longitudinal slope of pavement surface at 6-in. intervals. Statistical variance of slopes was computed and used as a partial measure of pavement serviceability.

Because of the short length of pavement sections in the Road Test, both profilometers were designed to operate at a speed of 5 mph. While this speed is not objectionable in a research project, it seriously limits the utility of the profilometers when tests are needed in many miles of highway carrying high-speed, mixed traffic.

Paper sponsored by Committee on Surface Properties—Vehicle Interaction.

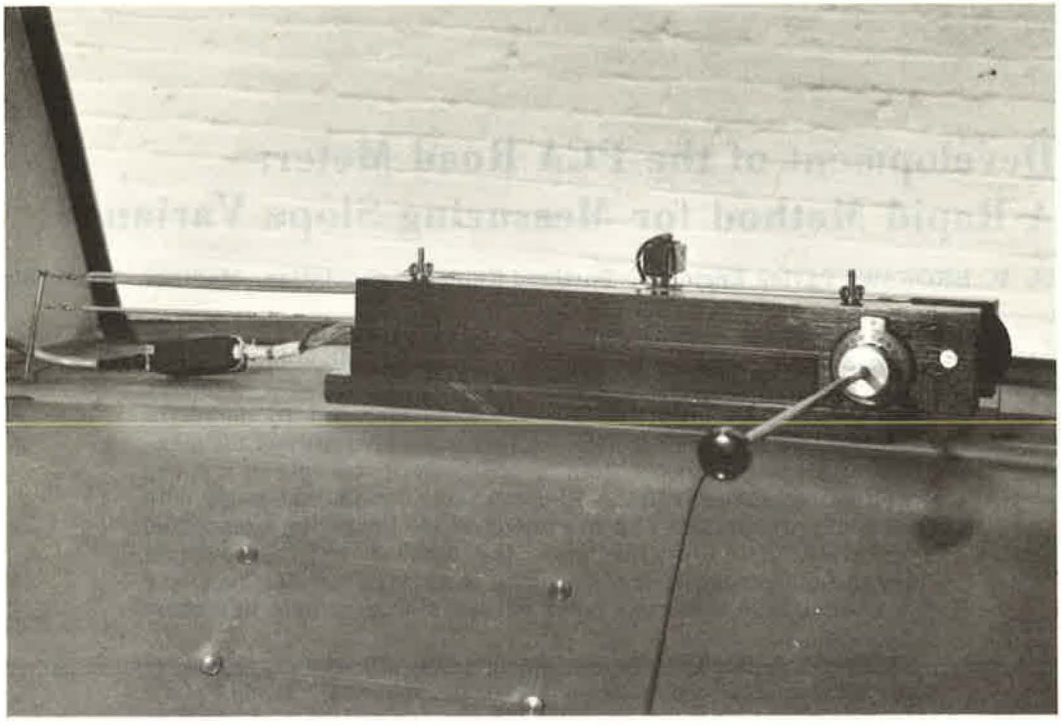

Figure 1. Switch assembly of Road Meter installed on rear package deck of automobile.

Recognizing this fact, the author has developed a simple, inexpensive device for installation in a conventional passenger automobile. The device measures the number and magnitude of vertical deviations per mile of road, between body of automobile and center of rear axle housing. From these measurements, sum of squares of road-car deviations can be calculated, and then correlated with slope variance from the CHLOE Profilometer.

The assumption was made that correlation coefficients include factors related to automobile suspension, shock absorbers, tires, speed of test, etc., and that while these factors remain reasonably constant, close estimates can be made of slope variance and serviceability. It was found that a satisfactory correlation with the CHLOE Profilometer can be achieved and that important variables can be evaluated.

Tests were conducted from June 1965 to July 1966. During this time, the Road Meter automobile was driven 40,000 miles and thousands of miles of highway were tested in Wisconsin and other areas. At the end of this period, the Road Meter was again compared with the CHLOE Profilometer with excellent results.

## DESCRIPTION OF PCA ROAD METER

The Road Meter is a simple electromechanical device, of durable construction, which can perform consistently with extremely low maintenance. Tests are made by the automobile driver without the need for traffic protection or extra personnel, and at a speed of 50 mph or more if required by the traffic stream.

The device consists of a flexible, nylon-covered, braided steel strand connected to the top center of the rear axle housing in a 1965 Ford Galaxie four-door sedan. The steel strand extends vertically through the trunk compartment and then through a small hole in the package deck just back of the rear seat. At this point, the strand passes over a transverse-mounted pulley, and is restrained by a tension spring attached to a small post on the package deck at a point near the right side of the body shell. Thus,

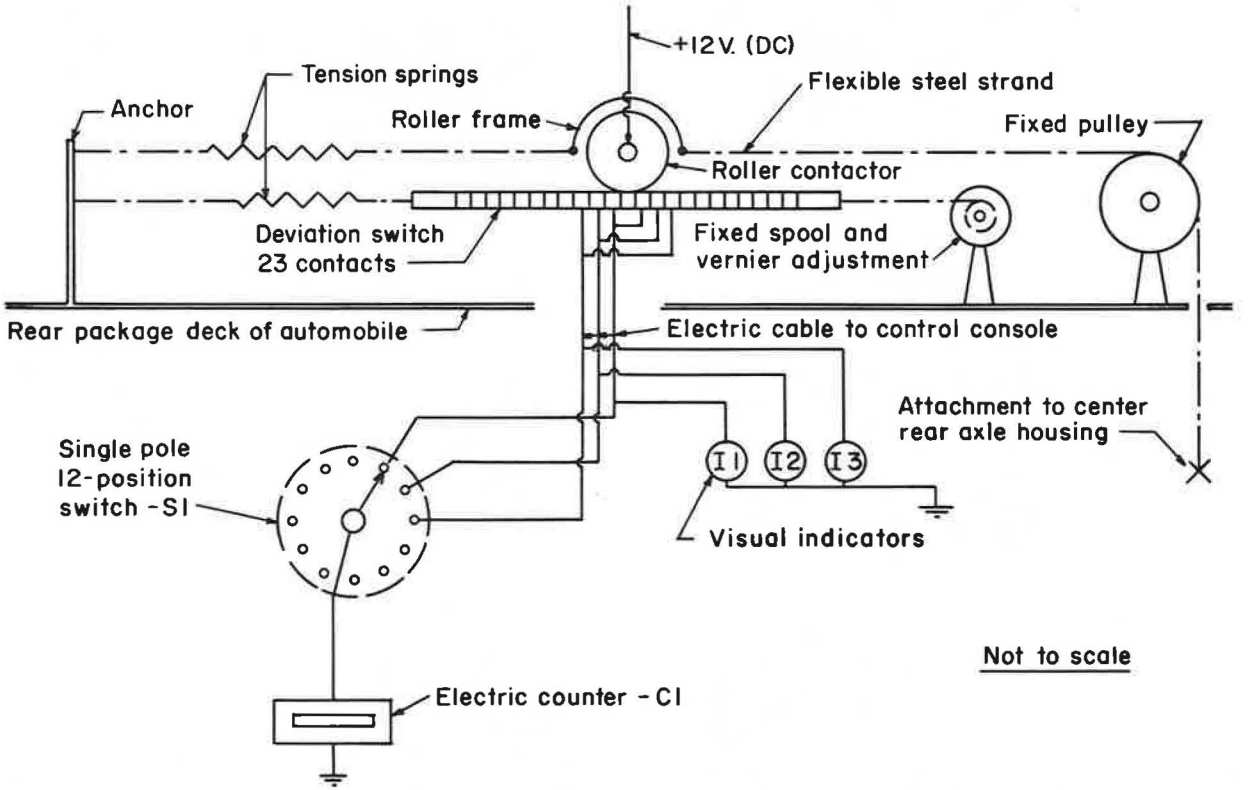


Figure 2. Diagram of mechanical and electrical features of the PCA Road Meter.

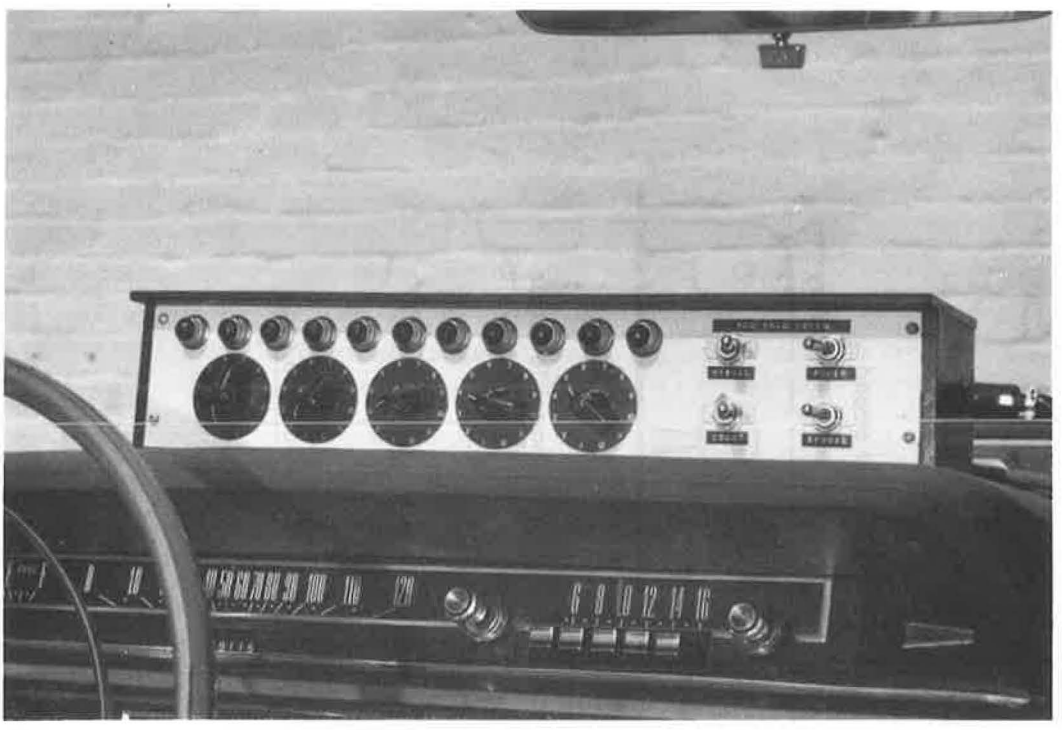

Figure 3. Road Meter control console, showing visual indicators and switches.

Figure 4. Electric counters mounted on separate chassis, resting on floor of automobile.

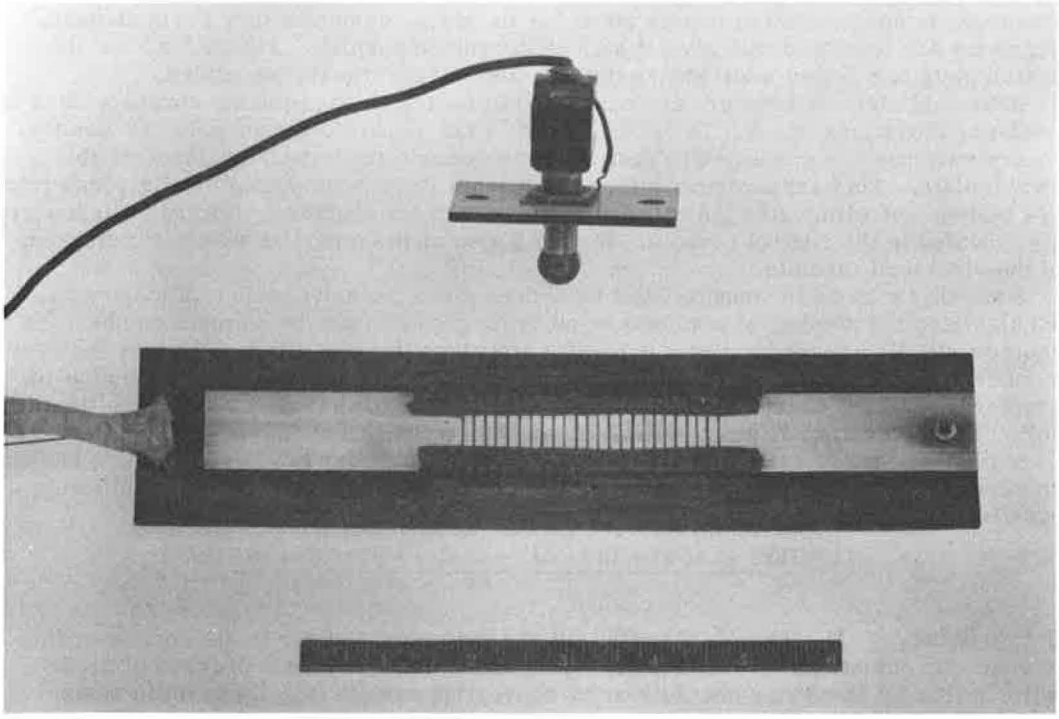

Figure 5. Disassembled switch plate and roller contactor.

vertical movement between the rear axle housing and the package deck is translated to horizontal movement of the strand.

Midway between the pulley and the tension spring, a roller microswitch (Minneapolis-Honeywell BZ-2RQ181-A2) is attached to the metal strand. The switch is mounted in a small rectangular Formica plate that slides in transverse metal guides. Figure 1 shows the switch assembly and tension spring installed on the package deck.

The microswitch roller impinges on a switch plate constructed so that transverse roller movements can be measured in $\frac{1}{8}$-in. increments, either plus or minus from a reference standing position of the automobile. The switch plate is also mounted in transverse metal guides. The transverse reference position of the switch plate can be adjusted under the roller to accommodate various static loads in the automobile. This adjustment is made by a separate tension-spring attachment and vernier control. Figure 2 is a schematic diagram of the mechanical features.

Automotive electrical power of 12 volts is inserted in the roller and switch plate system. Output is directed to visual indicators of road-car deviations, mounted in a console placed just above the automobile instrument panel. Control console and indicators are shown in Figure 3.

Output is also wired to high-speed electric counters capable of recording impulses having a "make" time of 0.03 second (ITT-General Controls CE-600). These sum the impulses received from each of the segments of the switch plate, according to the magnitude relative to road-car deviations. Electric counters are mounted on a separate chassis resting on the floor of the automobile (Fig. 4).

A roller microswitch is used because of its rugged construction and availability, and because it has an internal compression spring to force the roller against the switch plate. The switch is always in a partial compressed state, and electrical impulses are conducted through the roller and not by microswitch contacts.

The switch plate is divided into 23, $\frac{1}{8}$-in. segments. The center segment, used for initial static reference, has no electrical connection. The plate, which has never been

replaced, is constructed of copper about 1/32 in. thick, cemented to a Formica base. Segments are insulated with glyptal high-temperature varnish. Figure 5 shows the switch plate and roller microswitch disassembled from transverse guides.

Individual electric counters are connected to switch plate segments corresponding to road-car deviations of ± 1/8, 2/8, 3/8, 4/8, 5/8 and 6/8 in. Separate single-pole, 12-position rotary switches are connected to each electric counter and to each segment of the switch plate. This arrangement affords additional range when exceptionally rough roads are tested, and eliminates the expense of more than six counters. Rotary switches are also located in the control console. Figure 2 also shows a partial schematic diagram of the electrical circuits.

Methods for reducing counter data have been given intensive study. Each counter accumulates the number of impulses equal to or greater than its segment number. A counter will also record a double-count for impulses that are greater than its segment number. For example, a maximum road-car deviation of 4/8 in. will record twice on counters 1, 2, and 3, and once on counter 4. This is true because most of the time the roller will return to, or pass, its initial reference position at the end of a single impulse.

Mathematical deductions have shown that double-counts and total of impulses in each counter can be reduced to the sum of squares of road-car deviations by the following equation:

$$\Sigma(D^2) = \frac{(1 \times C1) + (2 \times C2) + (3 \times C3) + (4 \times C4) + (5 \times C5) + (6 \times C6) + \ldots}{64}$$

In this equation, C1, C2, C3, C4, C5, C6 are individual counter totals corresponding to road-car deviations of ± 1/8, 2/8, 3/8, 4/8, 5/8 and 6/8 in.; $\Sigma(D^2)$ is expressed per unit-mile, either by surveying one mile or by converting results to a single-mile basis. Development of the sum-of-squares equation is shown in the Appendix.

## CORRELATION OF CHLOE PROFILOMETER AND PCA ROAD METER

The sum of squares of road-car deviations measured by the Road Meter should be related in some way to slope variance measured by the CHLOE Profilometer. This is true because the CHLOE device detects incremental vertical deviations in longitudinal road profile in a 9-in. gage length, this being the distance between detecting wheels.

It can be shown (see Appendix) that the sum of squares of incremental vertical deviation per mile, measured by the CHLOE Profilometer, is related to slope variance. The equation for this relationship is CHLOE slope variance = 1.17 $\Sigma(d^2)$.

If passengers in an automobile can judge serviceability of a road, and serviceability rating can be partially related to slope variance, then there should be some mathematical connection between CHLOE slope variance, $\Sigma(d^2)$ and $\Sigma(D^2)$. A correlation of CHLOE slope variance and $\Sigma(D^2)$ should have the mathematical form

$$\text{CHLOE slope variance} = A \times \Sigma(D^2) \pm B$$

With the cooperation of the State Highway Commission of Wisconsin, correlative tests were made during June 1965. A wide variety of highways was tested. These included portland cement concrete, with and without granular subbase, bituminous pavements resting on granular base, and old resurfaced pavements of the two types.

The CHLOE Profilometer was operated according to instructions supplied by the U. S. Bureau of Public Roads. The PCA Road Meter was operated at 50 mph over the same road sections.

The regression equation, derived from results of 24 tests, is:

$$\text{CHLOE slope variance} = 0.68\ \Sigma(D^2) + 0.8$$

The practical significance of this regression is shown in Figure 6, where serviceability index of each pavement section, calculated with CHLOE slope variance, is compared with the serviceability index calculated with the slope variance given by the equation containing $\Sigma(D^2)$. Standard deviation of regression is 0.16.

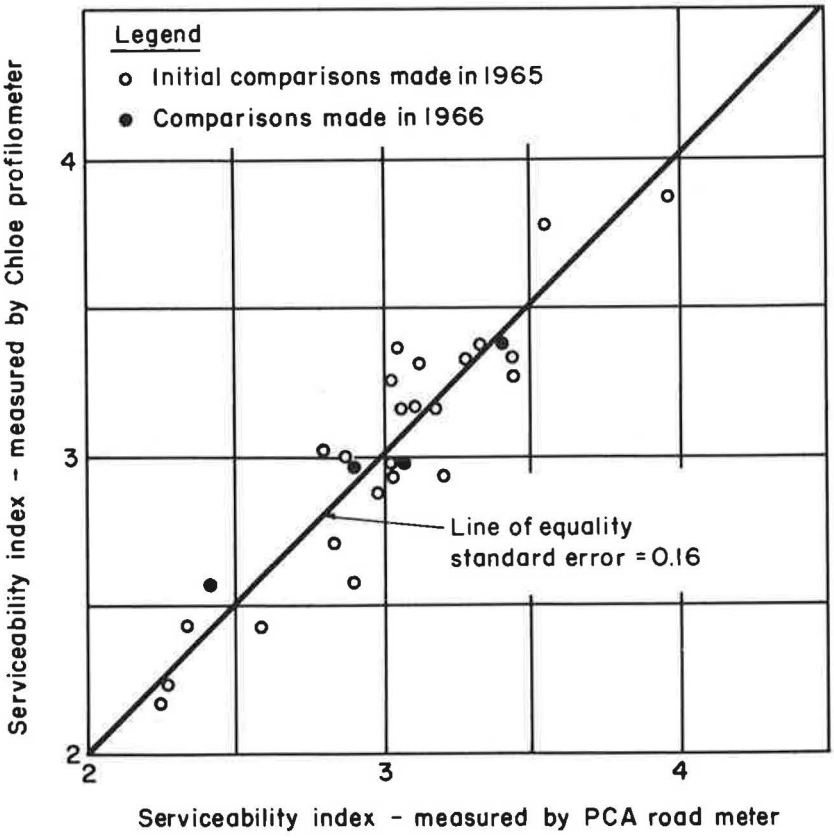


Figure 6. Comparison of serviceability index measured by the CHLOE Profilometer and by the PCA Road Meter.

## Investigation of Factors Affecting Road Meter Results

Soon after initial correlation tests were completed, the PCA Road Meter was used in five different road sites for the purpose of establishing references for future Road Meter performance and for immediate experimentation. These sites included substantially faulted undoweled rigid pavement having a 20-ft transverse joint spacing, undulating roadmix bituminous pavement on stage-constructed base, bituminous plant-mix pavement on crushed-stone base affected by sunken transverse sewer laterals, new portland cement concrete pavement, and frost-free pavement represented by the surface of structures spanning the Wisconsin river on I-90-94.

Experiments were made to assess the effects of changes in conditions that existed at the time of initial CHLOE-Road Meter tests. They are described in the following.

Type of Tire and Tire Pressure—Initial tests were made with standard 2-ply 7.7 × 15 tires inflated at a pressure of 25 psi. Later, rear tires were replaced by 4-ply nylon snow tires inflated at 25 psi. Tests in the experimental sites showed that snow tires did not significantly affect serviceability index. The mean difference for all sites was nearly zero.

Other tests with standard tires showed that pressure within the range of 24-26 psi (cool, static) had no significant effect on serviceability index.

Speed of Test Automobile—Initial tests were made with the Road Meter automobile operating at 50 mph. Additional tests in the experimental sites indicated that $\Sigma(D^2)$ varies with the speed of the automobile.

When tests must be made at a speed other than 50 mph, the following equation for CHLOE slope variance can be used with reasonable confidence, within the range of 30-65 mph:

$$\text{CHLOE slope variance} = (1.18 - 0.01 \text{ mph}) \Sigma(D^2) + 0.8$$

Load in Test Automobile—Initial tests were made with one person in the Road Meter automobile. Other tests of limited scope were made to determine the effect of additional weight of passengers. The driver and one passenger occupied the front seat and another passenger occupied the left rear seat. Results of this one test in six different roads showed that the serviceability index was increased 0.16. Other tests showed that a passenger in the front seat did not affect results.

These experiments were not continued because the purpose of the Road Meter is to make serviceability ratings with minimum personnel and expense.

Variable Air Temperature—One of the advantages of the Road Meter is that it can be operated throughout the year, provided roads are not covered by ice, snow, or water in wheelpath grooves. Effects of low temperature on mechanical and electrical components could be of concern.

Tests were made to evaluate this variable. It was found that the automobile should be driven for a period of time needed to warm electric counters and other components.

At air temperatures below 10 F, significant changes take place in road-car deviations. This is probably a result of changes in operating characteristics of shock absorbers and other automobile components, including tires. Therefore, tests are made only when the air temperature is above 10 to 15 F.

Variable Wind Velocity and Direction—Initial tests were made when wind velocity was low and not a matter of concern. Other tests have shown that wind velocity is not an important factor until it reaches about 15 mph. Crosswinds of that velocity create aerodynamic effects that disturb the automobile in motion and change the static reference position of the Road Meter roller contactor.

Tests should be made when wind velocity is less than the tolerable limit. Velocities are usually estimated from weather reports issued by local radio stations. Headwinds and tailwinds can be tolerated more than crosswinds. Data have not been collected to establish limits.

Deterioration of Automobile—Initial correlation of the PCA Road Meter and CHLOE Profilometer was made when the automobile had been driven about 20,000 miles. After that, the automobile was driven an additional 40,000 miles.

In July 1966, new comparisons were made with the CHLOE Profilometer to determine if wear in the automobile had affected the initial correlation made in June 1965. Tests were made in projects of portland cement concrete and bituminous-flexible pavement. Results were in agreement with the initial correlation (Fig. 6).

Type of Test Automobile—Another Road Meter, installed in a 1966 Ford 4-door sedan, has been operated about 8,000 miles. Comparison of test results between this and the original Road Meter showed no need to change the equation relating CHLOE slope variance and $\Sigma(D^2)$.

When a test automobile must be replaced, new comparisons should be made with the CHLOE Profilometer, or with ratings made of roads while using the old automobile.

## Application of the PCA Road Meter

During the first year of operation of the PCA Road Meter, the author completed an extensive design and serviceability study of 500 miles of non-reinforced concrete pavement. In an effort to assess resistance to frost and winter damage, work is under way to evaluate serviceability in 125 projects of rigid and bituminous pavement resting on treated and untreated base and subgrade soils. In addition, a large number of projects have been selected and tested in a continuing program to establish serviceability trends with weight of traffic and incremental age of pavement.

## CONCLUSIONS

The PCA Road Meter is a simple, durable, and economical device that can be constructed by anyone having ordinary mechanical aptitude and simple tools. Cost of the components is not excessive, and should not exceed $180, including electric counters and microswitch.

Results of tests have shown that the CHLOE Profilometer and PCA Road Meter can be correlated with satisfactory precision. The Road Meter affords a rapid method for measuring serviceability with minimum personnel, cost, and inconvenience to traffic. Where a CHLOE Profilometer is not available for comparison, locally acceptable estimates of serviceability rating can be correlated with $\Sigma(D^2)$.

## ACKNOWLEDGMENTS

For their cooperation in making possible the correlations with the CHLOE Profilometer, appreciation is expressed to the State Highway Commission of Wisconsin, and in particular to Karl Dunn, materials research engineer.

## REFERENCES

1. The AASHO Road Test: Report 5—Pavement Research. HRB Spec. Rept. 61E, 1962.
2. Carey, W. N., Jr., Huckins, H. C., and Leathers, R. C. Slope Variance as a Measure of Roughness and the CHLOE Profilometer. HRB Spec. Rept. 73, pp. 126-137, 1962.

# *Appendix*

## ROAD METER THEORY

The PCA Road Meter measures the number of road-car deviations in $\pm\frac{1}{8}$-in. increments referenced to the standing position of the automobile. Numbers are accumulated in electric counters. Sum of squares of deviations, $\Sigma(D^2)$, has been correlated with slope variance from the CHLOE Profilometer. The method for reducing Road Meter data is shown in the following.

### 1. Basic Data for Sum of Squares

Let a, b, c, d, e, f, ... = number of road-car deviations corresponding to $\pm 1$, 2, 3, 4, 5, 6, ... eighths of an inch, respectively. Then,

$$\Sigma(D^2) = (1a + 4b + 9c + 16d + 25e + 36f + \ldots)/64 \qquad (1)$$

### 2. Composition of Road Meter Counts

Because electric counters record once for a maximum deviation and twice for segment numbers less than the maximum, total recorded counts are

$$\begin{aligned}
\text{Counter 1 } (\tfrac{1}{8}\text{ in.}) &= a + 2b + 2c + 2d + 2e + 2f + \ldots \\
\text{Counter 2 } (\tfrac{2}{8}\text{ in.}) &= \quad b + 2c + 2d + 2e + 2f + \ldots \\
\text{Counter 3 } (\tfrac{3}{8}\text{ in.}) &= \quad\quad c + 2d + 2e + 2f + \ldots \\
\text{Counter 4 } (\tfrac{4}{8}\text{ in.}) &= \quad\quad\quad d + 2e + 2f + \ldots \\
\text{Counter 5 } (\tfrac{5}{8}\text{ in.}) &= \quad\quad\quad\quad e + 2f + \ldots \\
\text{Counter 6 } (\tfrac{6}{8}\text{ in.}) &= \quad\quad\quad\quad\quad f + \ldots
\end{aligned}$$

## 3. Reduction of Road Meter Counts to $\Sigma(D^2)$

If recordings shown in Road Meter counters 1, 2, 3, 4, 5, 6, ... are multiplied by the integers 1, 2, 3, 4, 5, 6, ..., respectively, the following reduction and summation can be made:

$$\begin{aligned}
\text{Counter 1} &= a + 2b + 2c + 2d + 2e + 2f + \ldots \\
\text{Counter 2} &= \quad 2b + 4c + 4d + 4e + 4f + \ldots \\
\text{Counter 3} &= \quad\quad 3c + 6d + 6e + 6f + \ldots \\
\text{Counter 4} &= \quad\quad\quad 4d + 8e + 8f + \ldots \\
\text{Counter 5} &= \quad\quad\quad\quad 5e + 10f + \ldots \\
\text{Counter 6} &= \quad\quad\quad\quad\quad 6f + \ldots \\
\hline
\Sigma(D^2) &= (a + 4b + 9c + 16d + 25e + 36f + \ldots)/64
\end{aligned} \qquad (2)$$

Eq. 2 = Eq. 1.

## 4. Sample Calculation

Road Meter count from one-mile survey of rigid pavement:

Counter 1 = 348
Counter 2 = 180
Counter 3 = 40
Counter 4 = 14
Counter 5 = 7
Counter 6 = 2
Counter 7 = 0 (extrapolated)

Composition of Road Meter count:

$\Sigma^{7}/_{8}$ in. deviations = 0
$\Sigma^{6}/_{8}$ in. deviations = 2 - (2 × 0) = 2
$\Sigma^{5}/_{8}$ in. deviations = 7 - (2 × 2) = 3
$\Sigma^{4}/_{8}$ in. deviations = 14 - (2 × 2) - (2 × 3) = 4
$\Sigma^{3}/_{8}$ in. deviations = 40 - (2 × 2) - (2 × 3) - (2 × 4) = 22
$\Sigma^{2}/_{8}$ in. deviations = 180 - (2 × 2) - (2 × 3) - (2 × 4) - (2 × 22) = 118
$\Sigma^{1}/_{8}$ in. deviations = 348 - (2 × 2) - (2 × 3) - (2 × 4) - (2 × 22) - (2 × 118) = 50

Sum of squares of deviations:

$$\begin{aligned}
\Sigma(^{6}/_{8})^2 &= 2 \times 36 = 72/64 \\
\Sigma(^{5}/_{8})^2 &= 3 \times 25 = 75/64 \\
\Sigma(^{4}/_{8})^2 &= 4 \times 16 = 64/64 \\
\Sigma(^{3}/_{8})^2 &= 22 \times 9 = 198/64 \\
\Sigma(^{2}/_{8})^2 &= 118 \times 4 = 472/64 \\
\Sigma(^{1}/_{8})^2 &= 50 \times 1 = 50/64 \\
\hline
\Sigma(D^2) &= 931/64 = 14.6
\end{aligned} \qquad (1)$$

Direct reduction of Road Meter counts:

Counter 1 = 348 × 1 = 348
Counter 2 = 180 × 2 = 360
Counter 3 = 40 × 3 = 120
Counter 4 = 14 × 4 = 56
Counter 5 = 7 × 5 = 35
Counter 6 = 2 × 6 = 12

$$\Sigma(D^2) = 931/64 = 14.6 \quad (2)$$

## 5. Typical Results From Road Meter Surveys

The following table shows a comparison of road-car deviations obtained from surveys in several different highways:

| Type of Pavement | Description | Road-Car Deviations/Mile (⅛ in.) | | | | | | $\Sigma(D^2)$ |
|---|---|---|---|---|---|---|---|---|
| | | 1 | 2 | 3 | 4 | 5 | 6 | |
| Rigid | In service for one year | 68 | 70 | 9 | 0 | 0 | 0 | 6.7 |
| Flexible | In service for one week | 90 | 56 | 8 | 1 | 0 | 0 | 6.2 |
| Rigid | Cracked and patched | 84 | 133 | 28 | 28 | 7 | 5 | 26.1 |
| Rigid | Undoweled joints (20 ft) faulted ¼ in. | 1 | 119 | 52 | 47 | 25 | 6 | 39.5 |
| Flexible | Scheduled for resurface | 31 | 104 | 37 | 20 | 23 | 2 | 27.3 |

## STATISTICAL SIMPLIFICATIONS IN THE ROAD METER

The unique Road Meter switch plate is the key to construction economy and ease of calculation of $\Sigma(D^2)$.

It was presumed that plus and minus road-car deviations, measured from a standing reference position of the automobile, are about equally distributed so that $\Sigma(\pm D) = 0$; or that the difference can be neglected in the calculation of variance and correct sum of squares.

Therefore, equivalent plus and minus segments are electrically interconnected within the switch plate, and outputs are summed in one counter instead of two (Fig. 2). The unconnected center segment serves as a reference for adjustment of plate under the roller contactor before tests are started.

This hypothesis was verified by tests in four different roads. Tests were made with a modified Road Meter switch plate capable of recording both plus and minus deviations. Results of the tests are given below.

### 1. New Rigid Pavement

Deviations per mile = 228
$\Sigma(D^2) = 5.8$
$\Sigma(D) = -6.8$

Simplified method:

CHLOE slope variance = 0.68 × 5.8 + 0.8 = 4.7
Serviceability index = 4.63

Correct method:

CHLOE slope variance = $0.68 \times 228 \times (5.8/228 - 6.8^2/228^2) + 0.8 = 4.6$
Serviceability index = 4.66

2. Rigid Pavement With Faulted Undoweled Joints at 20-foot Intervals

Deviations per mile = 348
$\Sigma(D^2)$ = 25.3
$\Sigma(D)$ = -16.4

Simplified method:

CHLOE slope variance = 0.68 × 25.3 + 0.8 = 18.0
Serviceability index = 3.23

Correct method:

CHLOE slope variance = $0.68 \times 348 \times (25.3/348 - 16.4^2/348^2) + 0.8 = 17.5$
Serviceability index = 3.27

3. Flexible Pavement Containing Sunken Transverse Sewers

Deviations per mile = 279
$\Sigma(D^2)$ = 23.0
$\Sigma(D)$ = +8.0

Simplified method:

CHLOE slope variance = 0.68 × 23.0 + 0.8 = 16.4
Serviceability index = 2.82

Correct method:

CHLOE slope variance = $0.68 \times 279 \times (23.0/279 - 8.0^2/279^2) + 0.8 = 16.3$
Serviceability index = 2.83

4. Flexible Pavement With Undulating Surface

Deviations per mile = 375
$\Sigma(D^2)$ = 11.1
$\Sigma(D)$ = -11.9

Simplified method:

CHLOE slope variance = 0.68 × 11.1 + 0.8 = 8.4
Serviceability index = 3.49

Correct method:

CHLOE slope variance = $0.68 \times 375 \times (11.1/375 - 11.9^2/375^2) + 0.8 = 8.1$
Serviceability index = 3.53

## INVESTIGATION OF REITERATIVE RESPONSE OF THE ROAD METER

Ability of the Road Meter to repeat measurements of $\Sigma(D^2)$, CHLOE slope variance, and serviceability index in a single test section was determined by multiple runs in two roads with widely different ratings. One was a new rigid pavement having a very good rating, and the other an old rigid pavement, severely cracked and patched, having a poor rating. Results of tests in the two roads were as follows:

| Site | Rating | Length of Test | No. of Tests | Average PSI | Standard Deviation | Range |
|---|---|---|---|---|---|---|
| New rigid | Very good | 0.90 mi | 8 | 4.56 | 0.07 | 4.45-4.64 |
| New rigid | Very good | 0.90 mi | 8 | 4.27 | 0.06 | 4.19-4.37 |
| Old rigid | Poor | 0.37 mi | 8 | 2.03 | 0.01 | 2.00-2.04 |

(Note: Pavement serviceability index does not include reductions for cracking and patching.)

## DERIVATION AND MODIFICATION OF CHLOE COMPUTING FORMULA SHOWING THE RELATION OF SLOPE VARIANCE AND SUM OF SQUARES OF CHLOE VERTICAL DEVIATIONS

Derivation of the CHLOE computing formula is outlined on page 136 of Highway Research Board Special Report 73. From it, Eq. 4b is restated as follows:

$$\text{CHLOE slope variance}/10^6 = (\tan 10')^2 \times \left[\frac{\Sigma Y^2}{N} - \left(\frac{\Sigma Y}{N}\right)^2\right]$$

Instead of computing slope variance of pavement surface, it is possible to calculate variance of vertical deviations (d) in a 9-in. gage length. Gage length is the distance between detecting wheels of the CHLOE Profilometer.

Then Eq. 4b can be modified:

$$\text{Variance of vertical deviations} = 81 \times \text{CHLOE slope variance}/10^6$$

Sum of squares of CHLOE vertical deviations per mile is equal to variance multiplied by the number (N) of observations taken at 6-in. intervals. Then,

$$\Sigma(d^2) = 10,560 \times 81 \times \text{CHLOE slope variance}/10^6$$

$$\Sigma(d^2) = 0.855 \times \text{CHLOE slope variance}$$

Therefore,

$$\text{CHLOE slope variance} = 1.17\ \Sigma(d^2)$$

# High-Speed Road Profile Equipment Evaluation

W. RONALD HUDSON, Center for Highway Research, University of Texas, Austin

The importance of evaluating the relative smoothness of pavements is well recognized in the highway profession, but such evaluation is largely a matter of qualitative judgment. These evaluations are useful in serviceability-performance studies and in studies of mechanistic evaluation of pavements for structural adequacy. Pavement surveys are used by maintenance engineers, design engineers, and highway administrators to help make many decisions with reference to the highway system.

This paper discusses the parameters affecting the measurement of roughness profiles, the evaluation of these parameters by various techniques, and the importance of measuring these profiles at high speeds. Several types of available equipment are discussed and associated data-processing techniques are described.

•HIGHWAY design speeds, which have increased steadily with the development of the automobile, demand that long, flowing ribbons of pavement be maintained in a very smooth condition so that the traveling public will be served adequately. Evaluation of the relative smoothness of pavements is largely a matter of qualitative judgment, but there is a recognized need for developing equipment capable of providing a quantitative measure of pavement smoothness for use in pavement evaluation studies such as those which are being conducted in Texas and which are expected to continue for the next several years.

Equipment available for measuring pavement roughness is limited in the accuracy with which the true road profile can be measured and in the speed with which measurements can be made. In general, the slower equipment gives greater accuracy; however, there is a need for a device capable of measuring road roughness more rapidly, as well as more accurately, than is now possible. Particular attention should be given to long-wavelength roughness (over 25 ft) because this characteristic is not presently being evaluated satisfactorily.

Recent developments in the electronics and directional control instrumentation field may help satisfy the need for faster and more accurate measurement, but no concerted effort has been made in the past to use these developments for highway pavement surface evaluation. The study discussed herein proposes to evaluate the feasibility of utilizing these developments and other recent technology in the development of high-speed road profile measuring equipment.

## PURPOSE OF PAVEMENT EVALUATION

Pavement condition is a subject of concern to highway engineers, including designers and maintenance personnel, but by far the largest interested group is composed of highway users. Each one seems to rate pavement condition either consciously or subconsciously every time he rides in a motor vehicle. There are a great many reasons for evaluating pavement condition, and even more ways of doing it. The names applied

Paper sponsored by Committee on Pavement Condition Evaluation and presented at the 46th Annual Meeting.

to the process are varied and many of the definitions are unclear. Terms like performance, serviceability index, condition survey, sufficiency rating, performance rating, and others are often bandied about by engineers and laymen alike. The definitions of such terms, however, are not precise and differ for the various interested parties.

## Philosophy of Pavement Evaluation

Two major categories of evaluation emerge: (a) serviceability-performance studies (functional behavior) and (b) mechanistic evaluation for structural adequacy. Regardless of the method used to make the evaluation, most studies can be listed in one of these two main categories.

In general, the serviceability-performance studies are concerned primarily with the overall behavior of the pavement, that is, how well it is performing its function as a riding surface for vehicular traffic. By and large this also seems to be the area of major concern to the highway user. Studies made at the AASHO Road Test (1) have shown that some 95 percent of the information about the serviceability of a pavement is contributed by the roughness of the surface profile. That is to say, the correlation coefficients in the present serviceability studies at the Road Test improved only about 5 percent when cracking and patching were added to the index equation.

The second category, mechanistic evaluation for structural adequacy, which is concerned with the evaluation of the load-carrying capacity of a small segment of pavement and the mechanics or method of carrying the load, is an important phase of pavement evaluation but will not be discussed in detail.

## Use of Pavement Roughness and Evaluation

Pavement condition and/or roughness profiles are studied for several reasons, a few of which can be stated from records of the Highway Research Board Committee on Pavement Condition Evaluation:

1. To measure acceptability for newly constructed pavements.
2. To assist the maintenance engineer and the highway administrator in the determination of optimum maintenance programs.
3. To aid in the establishment of priority for major maintenance, reconstruction and relocation. The object of this type of survey is to rank various pavement sections in terms of their importance and their current ability to serve traffic.
4. To furnish information needed for sufficiency ratings and needs studies. This involves a comprehensive study of pavement systems within a given area.
5. To assist in determination of the load carrying capacity of the pavement as to both volume of traffic and loads. This involves an evaluation of structural adequacy of the pavement structure, climatic effects, materials and drainage.
6. To aid the design engineer in determination of the degree of success with which his design has met the design criteria and to help him learn causes for failure.
7. To serve as a basis for new concepts and design.

This broad basis for use of pavement roughness information points to the need for better and faster methods of roughness measurement. All equipment in current use for the measurement of highway roughness suffers from limitations which need to be removed.

The evaluation of riding quality is complex, depending on three separate systems and the interactions between them; the highway user, the vehicle, and the pavement roughness are involved. Hutchinson (3) has described the problems associated with analyzing the subjective experience of highway users and deriving an absolute measure of pavement riding quality. These require (a) the development of a suitable mathematical model to characterize pavement roughness; (b) the development of a suitable mathematical model to describe the suspension characteristics of highway vehicles that may be used along with the roughness model to predict the dynamic responses of vehicles; and (c) a quantitative knowledge of the response of humans to motion.

This report is primarily concerned with the first factor but considers the others since the information required concerning roughness is dependent on the response of passengers and vehicles to the resulting motion. Consideration of roughness models emphasizes one important aspect of this study, the need to develop a method of measuring "true profile," meaning the faithful reproduction of the undulation of the pavement with respect to frequency, amplitude, slope and curvature at all points. No really good method for making such profiles exists and without one the progress in solving the overall problem will continue to be slow.

The second important aspect of the problem is more pragmatic. Based on data (1, 4, 7) which show that several different roughness parameters are highly correlated with riding comfort, the need for a better device for measuring present serviceability is apparent. In particular, an accurate device which travels at high speed is required.

The term "true profile" then can refer to an elevation profile, a slope profile or an acceleration profile. Any one of these is a "true profile" in a sense if it is a true representation of the factor it attempts to measure. It should be noted that most people are referring to an elevation profile when they refer to the "true profile." From our point of view, however, an instrument capable of reproducing any of these profiles faithfully could prove to be satisfactory. The desirability of a particular method depends on the purpose for which the data are to be used.

### Speed Aspects

It should be emphasized that the requirement to travel at high speed is inherent in this study. It is extremely important that the equipment be capable of traveling at least 30 mph, and speeds of 45 to 60 mph are definitely preferable, since they are closer to the current operating speeds on our freeways and would result in the least danger for personnel handling the equipment.

## PAVEMENT ROUGHNESS

The term "pavement roughness" is defined for this report as the distortion of the pavement surface which contributes to an undesirable or uncomfortable ride. In previous studies Hudson and Scrivner (2) have shown that variations in the surface less than ½-inch in length do not materially affect the riding quality and have been termed texture in lieu of roughness. The evaluation of this relationship between pavement roughness and passenger discomfort cannot be made until more is known about true profile, vehicle dynamics, and human response. For purposes of this report, however, the foregoing definition will suffice.

### Roughness Parameters

Four roughness factors are of general concern to highway engineers: (a) area roughness of the roadway, (b) transverse variations in profile, (c) longitudinal variations in profile, and (d) horizontal alignment of the roadway. In other words, any function of the roadway which imparts acceleration to the vehicle or to the passenger must be examined. More particularly of interest are those functions which influence the comfort or discomfort of the passenger. Previous study has shown that longitudinal roughness is probably the major contributing factor to undesirable vehicle forces (1), and the next greatest offender is transverse roughness, e.g., the roll component transmitted to the vehicle. The general curvature of the roadway which imparts yaw component to the vehicle is considered to be the least offensive and one which is normally handled by following good highway alignment practice. Whereas the total road roughness is certainly of importance because of normal variations in transverse vehicle placement, it is generally conceded that 70 percent of the vehicles travel in a well-defined wheelpath with their right wheels located 2½ to 3½ ft from the right-hand lane line. From this information we are tempted to conclude that measurements of longitudinal profile in the two respective wheelpaths, 6 ft apart, might provide the best sampling of roadway surface roughness. Furthermore, a comparison between the two wheelpaths can provide some measurement of the cross slope or transverse variations which are also important.

Data from existing instruments have not been totally adequate for evaluating even a longitudinal line profile of the roadway. However, if more proficient equipment could be developed, it should be merely a matter of duplicating the equipment to provide the comparison between the two wheelpaths. On the basis of these assumptions, immediate attention is directed to the development of adequate transducers and data processing equipment for recording a single line profile. This confines the problem to two distinct phases: (a) developing adequate transducers for measuring the roadway profile, and (b) developing adequate recording and data processing equipment capable of speedy and accurate data analysis to provide the necessary summary information.

## True Profile

In the past a great deal of effort has gone into measurements of pavement profiles. Cursory examination of the problem indicates that the profile is probably not the factor of major importance to the driver or passenger. Since there is no force associated with elevation or with velocity, the height of the passenger above sea level, i.e., his elevation, is of no great importance to him within normal ranges, nor is his vertical velocity or rate of change of elevation important. However, his vertical acceleration or rate of change of velocity (second derivative of elevation) becomes very important to him since it has a force associated with it which exerts desirable or undesirable pressures on his body and its components.

Other studies have shown that some passengers find undesirable characteristics to be associated with certain frequencies. The exact size and relationship of the effects remain to be studied.

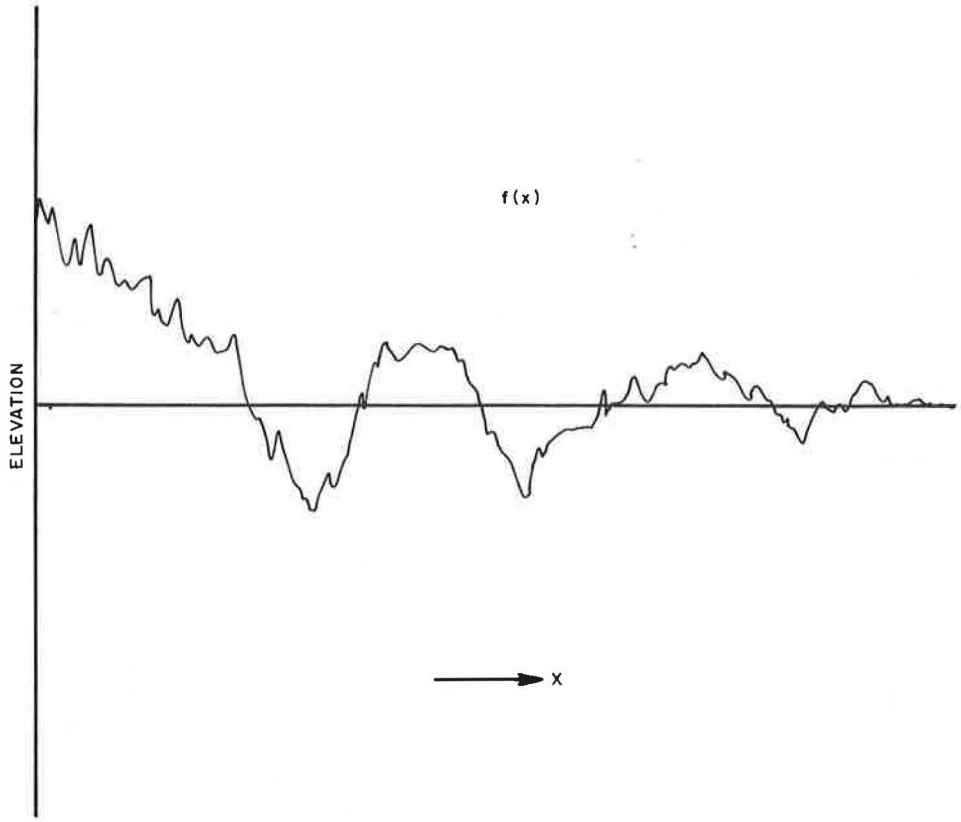


Figure 1. Plot of a random function.

In this regard, the characteristics of a typical random function (Fig. 1) are of interest. To define this function, in this instance an elevation profile, we are interested in (a) wavelength, (b) frequency, (c) surface slope, and (d) amplitude (elevation). On the other hand, some researchers record slope and plot a so-called slope profile, as was done on the AASHO Road Test with the AASHO slope profilometer (1). Finally, it is possible to record an acceleration profile by recording the analog trace output of a vertical accelerometer as done by the Kentucky Department of Highways (6).

A discussion of the various components of an elevation profile will be useful at this time, it being understood, however, that the recording of an elevation profile may not in the final analysis be of most interest. In order to consider this profile, the extremes covered in a roadway are of interest as is some estimate of the accuracy felt to be desirable because less accuracy than specified in the following will undoubtedly suffice if some sort of economic balance can be struck. These calculations describe the extremes of the parameters which have previously been measured in attempts to define this profile.

The parameters can be summarized as follows: wavelengths of interest—0.1 ft minimum, 500 ft maximum; frequency at 60 mph—range 0.17 cps to 1100 cps at 40 mph—0.1 cps to 700 cps; slope—dy/dx or dy/dt = ±18 deg. If a physical set of slope wheels with a finite wheelbase of 6 to 9 in. were used, it is probable that an angle of approximately ±10 deg or 0.166 radian would be all that could be obtained. This would be adequate to do the job.

Amplitudes of interest will depend on ability to measure wavelengths. For short-wavelength roughness, maximum amplitudes of ±6 in. will be desirable; however, for wavelengths up to 250 ft, amplitudes of 24 to 36 in. will be desirable. It is impractical to measure such amplitudes directly on an elevation profile and some compromise is therefore necessary in such cases. A General Motors Profilometer, for example, attenuates the signal based on frequency and wavelength to keep it on an analog chart.

## Accuracy

Accuracy is important in addition to the limitations suggested for measuring these parameters. This accuracy is improved by increased resolution in transducers and recording equipment. The values of resolution suggested below should be adequate for evaluating pavement roughness.

Amplitude or Elevation—Accuracy for amplitude or vertical displacement of 0.010 in. is desirable. This corresponds to 0.001 radian for a 9-in. wheelbase. Using a linear motion transducer covering a range of ±2 in. this requires a resolution of 400 units or 0.01 in.

Slope—For slope measurements a resolution of the total range into 100 units should be quite adequate.

Distance—The ability of any piece of equipment to measure distance accurately will decrease with speed. It is highly desirable, however, to be able to measure distance to the nearest ½ ft at 50 mph. It should be noted that all of the factors discussed herein are relative. The maximums or mimimums may not occur together. For example, a 6-in. deflection or elevation change is not of interest associated with a 2-in. wavelength.

## PROFILOMETER EQUIPMENT

Equipment capable of measuring pavement profiles at high speeds can be divided into two general categories. The first produces a summary statistic highly correlated with the present serviceability index of highway pavements. The second category is more sophisticated and consists of equipment capable of measuring a "true profile" of the pavement surface. With proper data recording and processing equipment, the second category of profilometer can also be used to provide the summary statistic. Visual analog profiles, however, are not satisfactory for this purpose.

A survey of existing equipment discloses three devices which purport to evaluate pavement profile at high speeds. These are (a) the Bureau of Public Roads Rough-

ometer, (b) the Kentucky Accelerometer, and (c) the GMR Road Profilometer. Other equipment currently used in the United States must be eliminated from this comparison because of speed characteristics. These include the AASHO Profilometer, the CHLOE Profilometer, and the Michigan-California Profilograph.

An evaluation of the measuring techniques used in the last three instruments indicates that it is not possible to use their principles at high speeds because of the mechanical problem of holding the recording wheel on the pavement. The Roughometer was also eliminated from consideration because its speed, while somewhat higher than most other equipment, is still not satisfactory for operation on modern highways. In addition, the ability of the Roughometer to measure serviceability of highway pavements consistently over a reasonable period of time is suspect because of temperature and moisture-associated variations which were observed at the AASHO Road Test (8) and which have been noted by the State of Illinois (9) with its equipment.

Two new pieces of equipment offer some possibility of development within the next two years. These are (a) a gyro-stabilized profilometer which uses a "true horizontal reference" and (b) a summary profiler being developed by Lane-Wells Corporation, Houston, Texas. The gyro-stabilized device offers possibilities of measuring true profile, while the Lane-Wells device is primarily intended as a device for measuring present serviceability index (PSI).

This then gives four types of equipment for primary consideration. Two of these offer possibilities of measuring true profile. The other equipment would be primarily useful for measuring PSI.

## Devices for Measuring True Profile

Gyro-Stabilized Profilometer—Since 1961 the Texas Highway Department and the Center for Highway Research of The University of Texas have been discussing the development of gyro-stabilized profilometers with various manufacturers of gyroscopes. Particular interest has been shown by Sperry Gyroscope Corporation and by

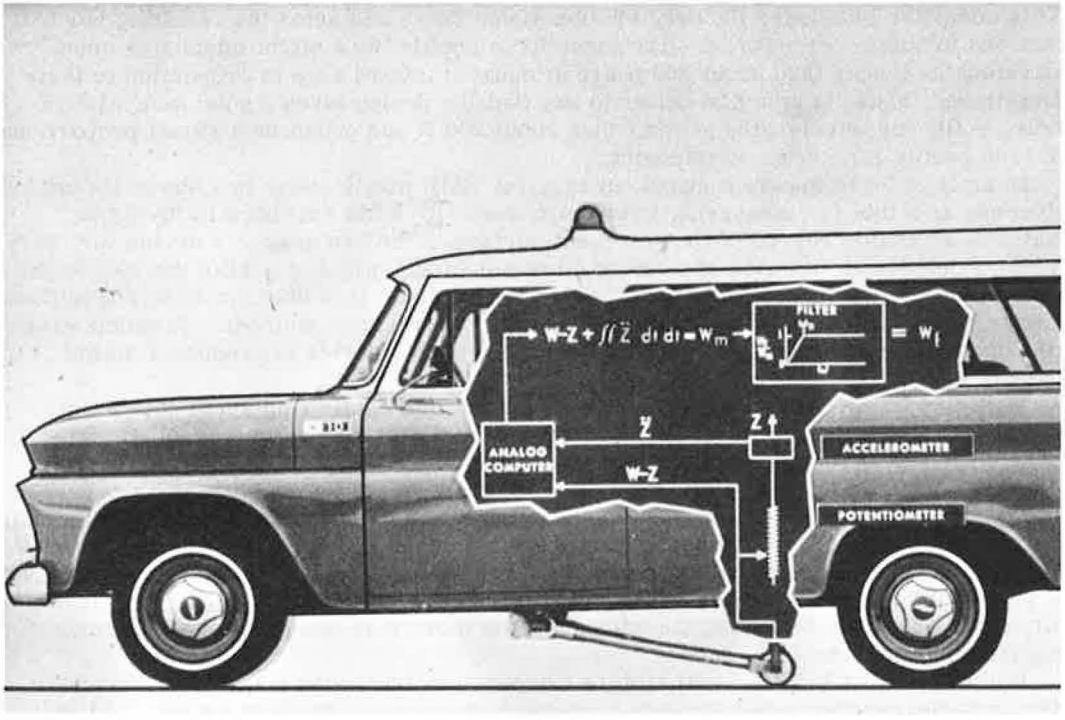


Figure 2. GMR road profilometer.

Minneapolis-Honeywell Corporation. The latter company at one time proposed to build for the Texas Highway Department a device stabilized by a single vertical gyro. However, experience at the AASHO Road Test has shown that a vertical gyro will not provide an accurate reference for measurement of profiles at high speeds. Large errors are introduced into the profile by precession of the gyro due to accelerations imparted by rough roads at high speeds. Further pursuit of this subject with commercial firms indicated that no stabilized platforms of the required accuracy were available at a cost of less than $100,000. A gyro-stabilized platform consists of three gyros mounted with their principal axes arranged orthogonally to each other to provide three-dimensional stability against rotation. Such a platform can be used as a very accurate indication of true horizontal. It appears that development costs for such a device would be approximately $100,000 if borne by an agency such as the Texas Highway Department or the Bureau of Public Roads.

Continued investigation into this subject, however, indicates that such a platform is being developed by a firm of physicists, LaCoste and Romberg, manufacturers of gravity meters, in Austin, Texas. They propose to use the platform as a base from which to measure very accurately small differences in the earth's magnetism or gravity. These differences are used to indicate ore deposits of various kinds. As soon as this platform is sufficiently operable, it will be tested as a possible road roughness profilometer.

GMR Road Profilometer—The only existing profilometer which appears capable of measuring true profile accurately is a device developed by the General Motors Research Laboratory, at Warren, Michigan (5). The device is small, compact, and relatively inexpensive (Fig. 2). The road wheel is mounted on a trailing arm underneath the measuring vehicle and is held in contact with the ground with a 300-lb spring force. The truck mass and truck suspension form a mechanical filter between the road and the accelerometer. The relative motion of a location on the vehicle body and the road wheel is measured with a potentiometer. The accelerometer is mounted on the vehicle body above the road-following wheel at a point where the potentiometer fastens to the body. Figure 3 is a diagram of these components. The signals from the accelerometer and the potentiometer are input into an analog computer which is carried in the vehicle. This computer integrates the acceleration signal twice and sums the resulting vertical motions to obtain true profile. The term "true profile" is a slight misnomer since wavelengths longer than about 200 ft are attenuated toward zero in proportion to their amplitude. Thus, it would be better to say that the device gives a good indication of true profile for wavelengths shorter than about 200 ft and produces a signal proportional to true profile for longer wavelengths.

In spite of these apparent shortcomings, the GMR profilometer has shown its effectiveness as a tool for measuring road roughness. Its main drawback is its output, which is an analog record of the pavement surface. The use of such a device for, say, 4 hours per day at 50 miles an hour could result in 200 miles of profile per day or the equivalent of 1000 road miles of profile per work week. It is uneconomical and almost humanly impossible to read such quantities of data with hand methods. It seems essential that electronic data processing be coupled with this device to produce a digital output.

With this in mind several efforts have been made to obtain equipment capable of converting the analog output of the GMR device to digital form. Two excellent proposals have been received. A summary of each proposal is included in the Appendix. These proposals were developed after several conferences between the Project Director and personnel from interested firms and, while not complete in all details, they should provide a good basis for estimating data processing needs and costs. In both cases it appears that the purchase price of such equipment is approximately $40,000 to $50,000. A large portion of this cost, however, can be saved by renting part of the equipment on a per-mile basis, or by using the equipment for more than one purpose, thus amortizing the cost more rapidly.

In the spring of 1966 General Motors Corporation announced plans to market their device to the general public through a licensed equipment manufacturer, K. J. Law Engineering Company, Detroit, Michigan. The device will be known as the Surface

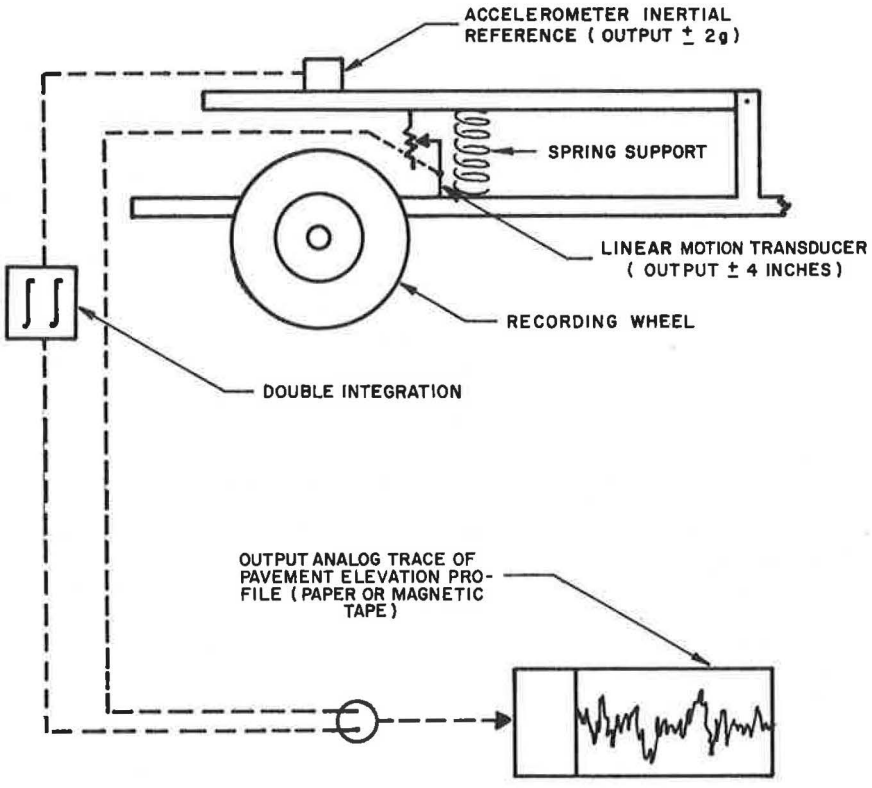


Figure 3. Schematic of GMR road profilometer.

Dynamics Road Profilometer. Unfortunately, the Center for Highway Research has not been able to obtain the use of a GMR device for evaluation. This has caused a delay in gaining information necessary to complete this project. A model of the new equipment was to be delivered to the Texas Highway Department early in 1967.

The Michigan Highway Department obtained a GMR profilometer from General Motors in 1964. A recent visit indicates that they now have the device working well. They have compared runs with the General Motors model and obtained excellent results. At the present time they use a simple vertical motion counter to summarize their data. They are working on development of power spectral techniques.

The many unknowns involved in this problem make it very difficult to establish accurate cost estimates, and, for that reason, no detailed cost breakdown is presented here. The best available information, however, indicates that a two-track GMR profilometer complete with towing vehicle will cost approximately $50,000. Data processing equipment will cost from $30,000 to $50,000, so that the total equipment package may cost approximately $80,000 to $100,000.

## Statistical Profilometers

In addition to a "true profile," an instrument capable of measuring roughness and summarizing it in the field is needed by highway departments for use in determining present serviceability index.

Evaluation of this problem has uncovered two types of equipment of potential usefulness for obtaining statistical summaries of pavement profiles, thus providing PSI in the field without the need for digital computers. One of these, the Kentucky Accelerometer, is presently in use in Kentucky and could be purchased and put into operation by others within six months. The other device is one being developed by the Lane-Wells Corporation.

The Kentucky Accelerometer—The Kentucky Department of Highways has available plans and specifications for accelerometer profile equipment which the Department developed. The equipment is not available commercially as yet. The parts and pieces for manufacturing such a device can be purchased for approximately $2,000. In addition the use of a standard automobile costing approximately $2,500 is required.

The Kentucky equipment has several distinct advantages but also several disadvantages. Data from the NCHRP study conducted at Purdue (7) indicate that the Kentucky device can measure PSI just as accurately as the CHLOE profilometer. Furthermore, it operates at speeds of 40-50 mph and therefore qualifies as a high-speed device. Finally, the equipment is already in existence and can be purchased without the delay of commercial developments.

The disadvantages of the equipment cannot, however, be neglected. As presently used by Kentucky the device involves the measurement of accelerations on a human body riding in a standard automobile. Cursory studies published by Kentucky indicate the effect of variations in the physical build of the subject and of the automobile is relatively minor. These factors do affect the profile to some extent; but the most important effect, as might be expected, is the quality of the automobile being used. A compact or "stripped, low-price car" gives relatively rough profiles when compared with those obtained from higher priced, luxury automobiles.

Lane-Wells Equipment—During recent years the Lane-Wells Corporation, a wholly owned subsidiary of Dresser Industries, has applied its technical knowledge to the improvement of equipment used in highway engineering. Their best-known developments include the nuclear road logger and a device for measuring deflections under dynamic load called a "Dynaflect." They have budgeted some $25,000 for the development of a prototype high-speed summarizing profilometer capable of providing PSI in the field without the requirement for digital computers. The pressure of other work, however, has delayed the development of this prototype.

## DATA PROCESSING AND ANALYSIS

An adequate physical description of pavement roughness is very complicated due to its multidimensional nature. Simplifications are required to describe roughness in terms meaningful to most engineers. The forces and movements to which the highway user is subjected by this pavement roughness are also very complex. As with many natural phenomena, man's efforts to describe pavement roughness and its effects have lead to empirical correlations, in this case between certain easily defined roughness parameters and the subjective rating of the riding quality of the pavement by the highway user. Such ratings have been termed present serviceability rating (PSR), and the resulting correlation based on certain measurable parameters, present serviceability index (PSI) (1).

The PSI concept has been very useful in recent years but the problem is by no means solved. Statistical evaluation of pavement ratings (1, 4, 7) indicates correlation coefficients for various roughness measurements to be in the range of 60 to 90 percent. Most of these correlations involve rather elementary use of longitudinal profile information. Better measurements should lead to better correlations. Continued study of human response to external stimuli and of roadway roughness parameters should lead to better ways of measuring pavement roughness and thus to better ways of characterizing the subjective serviceability rating of the highway user.

Most of the factors used in previous correlation work have been rather simple statistics, such as the summation of the deviations of the deflection profile from some mean value (Bureau of Public Roads Roughometer and the Michigan Profilograph). Other statistics include (a) the summation of the area under a continuous analog plot of vertical accelerations and (b) variance of slope measurements taken by a slope profilometer. In every case the development of these statistics has been governed by available economical data handling techniques.

Other more sophisticated data processing techniques have been developed. Coupled with the advent of better data recording equipment, these will undoubtedly make the use of the more sophisticated methods meaningful and desirable.

Two such useful data processing techniques are the harmonic analysis and the power spectral density analysis. In general, a harmonic analysis is useful for evaluating periodic or repetitive wave patterns. The power spectral density function on the other hand is most suitable for characterizing random functions. In one case the validity of the analysis depends on the assumption of periodicity; in the other on randomness.

Unfortunately, highway roughness is neither completely random nor especially periodic although periodic wave patterns often develop under repetitive traffic. Examples of periodic patterns include 15-ft joint spacing in concrete and washboarding associated with some classes of weaker flexible pavements. On the other hand, many pavements, particularly flexible pavements and continuously reinforced pavements, show no such periodic pattern.

Although the harmonic and power spectral analyses are rather complex, a practical method of performing them has been developed. Some of the best work available to date has been accomplished by Hutchinson (3). Other significant work has been done by Quinn (10). A complete discussion of these two methods does not seem to be appropriate here since only their use in analysis, evaluation, and correlation of ratings can provide an understanding of their suitability as pavement parameters.

Many other possible methods of analysis present themselves, such as an evaluation of body accelerations and the analysis of slope variance, as done at the AASHO Road Test. In such analyses, it is probable that some measure of frequency and wavelength should be considered along with amplitude.

The two types of profilometers of interest to the highway engineer have been discussed. One is the true profilometer, capable of giving rather exact reproduction of the pavement surface, and the other is the statistical summary profilometer, which coordinates data processing equipment in the field and produces a summary statistic which is correlated with riding quality. The development of the true profile equipment will facilitate research into the problem of correlating various roughness parameters with riding quality. The high-speed statistical profilometer is badly needed to provide highway engineers and researchers with rapid, efficient means of evaluating pavement serviceability in the field.

The equipment required for processing and analyzing data is even more diverse than the possible methods of recording the data because the output from each measuring method can be processed in many ways. In most instances it is desirable to discreetly sample a continuous analog output. Such a technique would be useful in sampling the output of the Kentucky accelerometer equipment and the GMR profilometer output. The proposals received describe equipment capable of performing this task and producing the output in a form compatible with high-speed digital computational equipment.

Equipment suitable for performing summary calculations and data processing in the field is highly dependent on the transducer and recording equipment. Many such techniques have been employed. These vary from the simple one-way clutch "integrater" used on the Bureau of Public Roads Roughometer, through the solenium electrochemical integrater used by the Kentucky device, to the compact special purpose digital computer developed and utilized with the CHLOE profilometer.

In summary, the data processing requirements can be stated as follows:

1. True profile information must be easily digitized for machine computations to be useful.
2. Summarizing-statistical profilometers should be equipped to do routine processing analysis in the field, but under certain circumstances digital output which can be processed by digital computers overnight could also be used very successfully.

## SUMMARY AND RECOMMENDATIONS

It is not possible nor desirable to make an exhaustive study of existing roughness equipment on a limited budget. Such a survey would require several studies the size of the NCHRP Study at Purdue (7). Furthermore, the instrument which should be evaluated, a GMR-type profiler coupled with automatic digital data processing equipment, does not exist. However, all other available information has been evaluated.

Consideration of all data now available indicates that the GMR profiler should be adapted for use by highway engineers. It is high-speed, far more accurate than other equipment available, and compact and efficient in operation. With the addition of proper digital data processing equipment the GMR device can serve not only as a basic tool for evaluating roadway profile parameters and their relationship to riding quality and ultimately to specifications for finished roadway surfaces, but can also serve as a summary profiler for evaluating serviceability (PSI) for pavements as desired by highway engineers and designers throughout the nation. Such a device would greatly facilitate the observation of selected experimental sections.

## ACKNOWLEDGMENTS

This is the first in a series of papers covering the findings of research conducted for the Texas Highway Department and U. S. Bureau of Public Roads. Thanks are due to B. F. McCullough and M. D. Shelby, Texas Highway Department, and to G. E. Price, U. S. Bureau of Public Roads, for their helpful advice and counsel in this research effort.

## REFERENCES

1. Carey, W. N., Jr., and Irick, P. E. The Pavement Serviceability-Performance Concept. HRB Bull. 250, 1960, pp. 40-58.
2. Scrivner, Frank H., and Hudson, W. Ronald. A Modification of the AASHO Road Test Serviceability Index Formula. Highway Research Record 46, 1964, pp. 71-87.
3. Hutchinson, B. G. Analysis of Road Roughness Records by Power Spectral Density Techniques. Final Report to Ontario Joint Highway Research Programme. Dept. of C. E., Univ. of Waterloo, Ont., January 1965.
4. Nakamura, Velma F., and Michael, Harold L. Serviceability Ratings of Highway Pavements. Highway Research Record 40, 1963, pp. 21-36.
5. Spangler, Elson B., and Kelly, William J. GMR Road Profilometer—A Method for Measuring Road Profile. Highway Research Record 121, 1966, pp. 27-54.
6. Rizenbergs, R. L., and Havens, J. H. Pavement Roughness Studies. Highway Research Lab, Kentucky Dept. of Highways, April 1962.
7. Yoder, Eldon J., and Milhouse, R. T. Comparison of Different Methods of Measuring Pavement Condition. NCHRP Rept. 7, 1964.
8. Hudson, W. Ronald, and Hain, Robert C. Calibration and Use of BPR Roughometer at the AASHO Road Test. HRB Spec. Rept. 66, 1961, pp. 19-38.
9. Hudson, W. Ronald. Determination of Present Serviceability Index with the Illinois Highway Roadometer. Spec. Rept., AASHO Road Test, 1960.
10. Quinn, B. E., and Zable, J. L. Evaluating Highway Elevation Power Spectra From Vehicle Performance. Highway Research Record 121, 1966, pp. 15-26.

# *Appendix*

## PROPOSAL FOR A ROAD-PROFILE DATA ACQUISITION AND PROCESSING SYSTEM

### FOREWORD

This proposal is submitted in response to a letter request-for-proposal dated February 26, 1965, from the Center for Highway Research, The University of Texas, Austin, Texas.

A Road Profile Data Acquisition and Processing System comprised of two subsystems is proposed. One subsystem consists of equipment to be installed in a truck, which is to be used in conjunction with a General Motors Corporation Road Profilometer to obtain and record road profile data in analog form. The other subsystem is an analog-to-digital tape conversion system to be installed in the laboratory, which converts the data on the analog tape to digital form. The digital tape produced by this subsystem contains the data in a format suitable for processing by the Control Data Corporation (CDC) Model 1604 Digital Computer presently installed at the Center.

### SUMMARY

It is proposed to furnish and install a Road Profile Data Acquisition and Processing System designed for use with a General Motors Corportation Road Profilometer. The

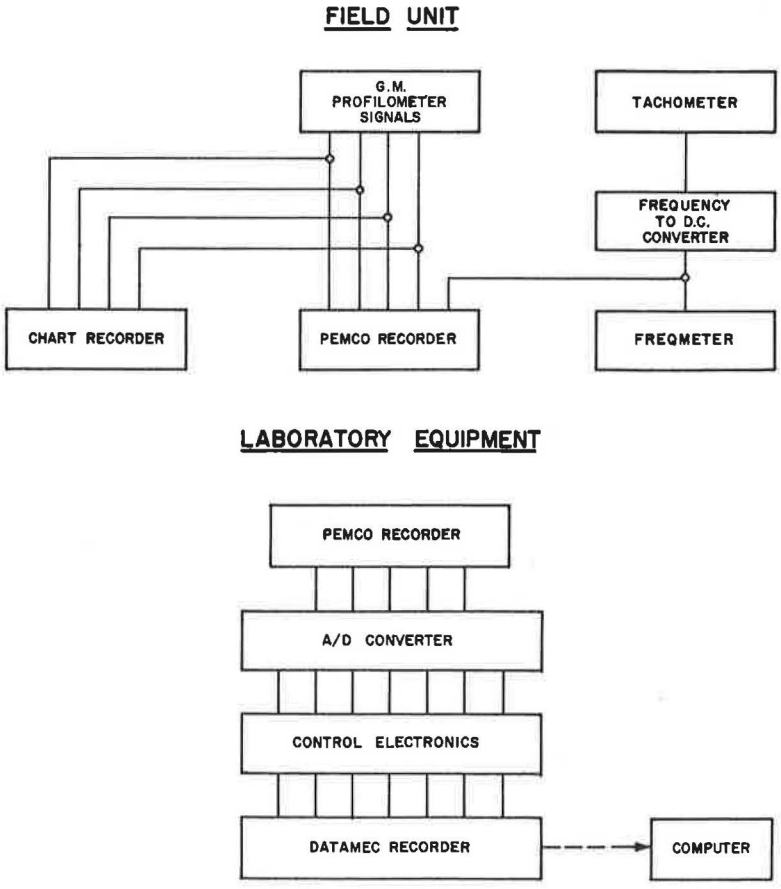


Figure A1. Proposal for a road profile data acquisition and processing system.

proposed equipment can record and process data from a vehicle containing two road profile transducer systems.

The proposed system is composed of two major assemblies; one is used for the acquisition of data, and the other for the conversion of the acquired data to a form suitable for processing by a digital computer. The data acquisition components are to be installed in a truck furnished by the customer. They supply reference data that augments the data obtained with the Road Profilometer. A portable, analog magnetic-tape recorder records the Road Profilometer and reference data as analog signals, and is used in the laboratory to play back the data into the conversion system. The analog-to-digital conversion components are to be installed in an equipment enclosure furnished by the contractor. This assembly converts the analog data to digital form on a computer-compatible tape.

The PEMCO Scientific Data Recorder used to record the data has a 1000-foot capacity, giving a recording duration of 26 minutes and, therefore, a recording distance of 26 miles when the truck is operated at the maximum acquisition speed of 60 mph. The accuracy of data conversion is 0.5 percent and the linear resolution is one inch when data is acquired at 60 mph.

A Thermal Writing Recorder is recommended as optional equipment for visually checking the analog data in the field. This chart recorder is not included in the contract price since it is not essential to system operation.

The price of the proposed system is $41,230. The Thermal Writing Chart Recorder can be furnished for an additional cost of $4,500. An inverter which will permit the Chart Recorder to operate from the truck's 12 volt battery is available at a price of $3000. The installation of the equipment in the truck will be performed by the contractor on a time and material basis. The contractor will guarantee freedom from defects in workmanship and materials for one year, exclusive of major assemblies of other than the contractor's manufacture. Delivery will be made within 120 days after receipt of a purchase order.

## PROPOSED MODIFICATION OF GMR ROAD PROFILOMETER TO FACILITATE AUTOMATIC DATA REDUCTION

A cost study has been made at the request of the Center for Highway Research to determine the approximate cost of a system to convert the output of the GMR Road Profilometer to a form easily acceptable by a computer. Two different cost estimates are shown below, one for leasing the equipment on an hourly basis and the other constructing a complete data conversion system. The cost shown below is not a firm quote, but is of the approximate value.

A block diagram of the proposed system is attached showing the recording system for the field equipment and the data conversion equipment. The analog data representing the road profile will be recorded on a portable FM magnetic tape recorder. Also the distance markers and voice will be recorded simultaneously on two channels of the recorder. A photocell pickup would have to be added to the GMR Profilometer to give better distance resolution. A tone generator could also be supplied to enable the operator to mark an event on the voice channel by simply pushing a button.

The same recorder could be used in the data conversion equipment for playback purposes. The analog profile data would by digitized by an analog to digital converter and sampled by the distance markers. These markers would probably be spaced every three (3) inches. After the profile data is digitized, it will be stored on digital magnetic tape in the form easily handled by available computers. Also a typewriter keyboard will be necessary to add header information on the magnetic tape and control the operation of the whole system. A breakdown of the costs follows.

| | |
|---|---|
| I. Portable Equipment | |
| Parts | $19,890 |
| Labor | 1,500 |
| | $21,390 |

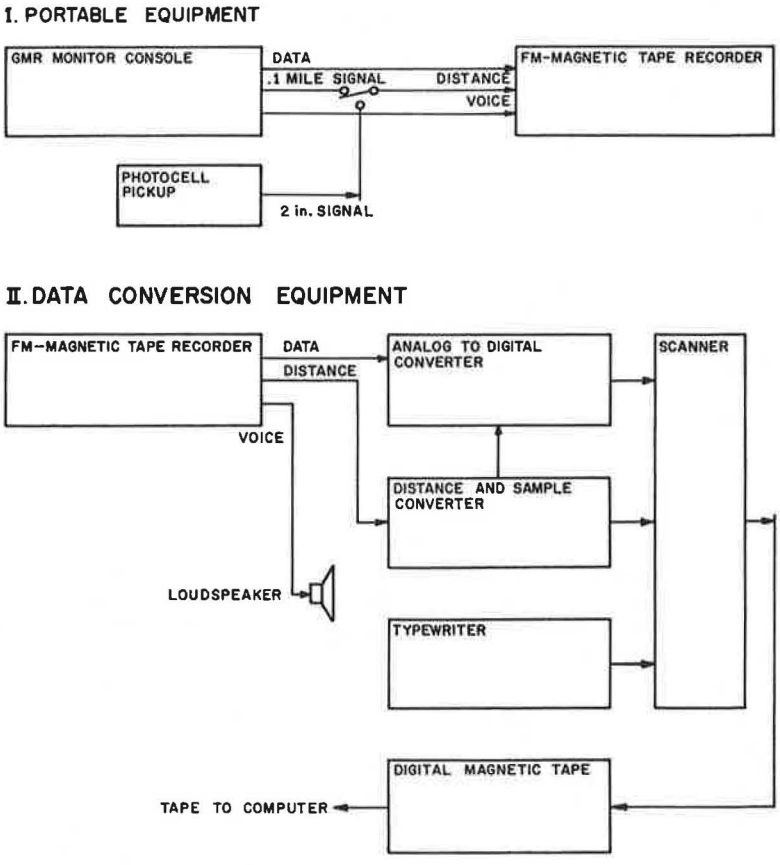


Figure A2. Proposed modification of GMR Road Profilometer to facilitate automatic data reduction.

| | | |
|---|---|---|
| II. | Data Conversion Equipment | |
| | Parts | $27,330 |
| | Labor | 4,500 |
| | | $31,830 |
| III. | Total Cost | |
| | Portable Equipment | $21,390 |
| | Data Conversion Equipment | 31,830 |
| | | $53,220 |

The other alternative of reducing the profile data is to record the data as before and lease time on existing equipment. This equipment can be leased locally at a rate of approximately $150.00 per hour. The analog data can be played back eight times faster than recorded. This would then cost $18.75 per hour of data. The cost of the portable equipment above would remain the same and the $31,830 would not be required. If the $31,830 was applied to lease the equipment and data were recorded at 25 miles per hour, approximately 42,300 miles of data could be converted.

The most economical method of converting the profile data will depend on the number of miles of data recorded and the maximum number of GMR Road Profilometers being serviced.

## *Discussion*

PAUL MILLIMAN, Supervisor, Instrumentation and Data Systems, Research Laboratory Division, Michigan Department of State Highways (Presented by E. A. Finney, Director, Research Laboratory Division, Michigan Department of State Highways)—Mr. Hudson has excellently summarized the field of highway profilometry, with emphasis on current systems—especially the system developed by General Motors Research. This brief supplemental discussion is in support of his comments relative to the GMR profilometer, and results from work performed with Michigan's GMR-type profilometer.

In 1962, the Michigan Department of State Highways teamed up with the General Motors Technical Center to determine the accuracy, reliability, and applicability of the GM rapid travel road profilometer to routine highway testing of road surfaces. This work, conducted in cooperation with the Bureau of Public Roads, had three principal objectives.

The first was to determine whether profiles reported by the GMR device were true profiles, using the term "true" in the same sense as Mr. Hudson, namely survey or elevation profile (of limited wavelength, of course). This was accomplished in the following manner:

1. The first step was to investigate the system's ability to reproduce dimensions and shapes of known pavement surface irregularities, and effects of various speeds on this ability. This was done by fabricating three steel obstacles, securing them to a pavement surface, and then profiling them at various speeds. The three shapes used were a semicircle, a triangle, and a rectangle, all of 1-in. amplitude. Shapes and dimensions reported by the profilometer were excellent at low speed (about 10 mph). Predictably, at higher speeds the large amplitude of these artificial bumps tended to throw the follower wheel away from the surface.
2. For the second verification method, nine test sections were selected, each representing a different construction method. They included six 1000-ft pavement sections and three bridge decks and approaches. On each of these test sections, elevations were taken with a precise level and target, at 1- to 5-ft intervals. Machine profiles were taken simultaneously with these elevation or "true" profiles. The results of this work were excellent. The machine profiles, taken at speeds up to 40 mph, duplicated the survey profiles for all practical purposes. After study of the data it was concluded that in those locations where the two profiles did exhibit minor differences, it was simply a matter of a continuous profile (machine) vs one made up of a series of connected straight lines (survey).

The second objective was to determine the correlation, if any, between the GMR profilometer and BPR-type roughometers, and between the profilometer and CHLOE-type slope variance devices. Successful correlation would allow replacement of both of these types of instruments with a superior device while not invalidating the massive body of important pavement data which they have accumulated over the years. In addition, it would permit determination of pavement serviceability indices with the profilometer.

Since both the roughometer and CHLOE produce a single accumulated numerical result for any surface measurement, it was necessary that a method be devised to digitize machine profiles prior to any correlation tests. Therefore, an electronic digitizer was designed and constructed. The output of this accumulator is the numerical sum, in inches, of all positive excursions of the profile being digitized.

Simultaneous runs were performed on 22 sections of flexible, overlay, and rigid pavement with the profilometer, Michigan's BPR-type roughometer, and a slope variance instrument furnished and operated by the Bureau.

Correlations resulting from these tests were all excellent and readily usable. They demonstrate that adoption of the new profilometer will not disrupt or invalidate pavement roughness histories and that pavement serviceability indices can be readily obtained.

The third and final objective was to determine whether the system was of such a nature and ruggedness as to be capable of the type of extensive, continuous use to which it would be subjected in highway work. It was decided that the only practical way to determine the durability and reliability of the system was to put it into service and see how it performed.

Before and after completion of the accuracy and correlation work, thousands of miles were logged with the system. It has been used on many projects, including bridge finishing studies, evaluation of blowup repair methods, performance of insulated flexible pavement, 24-hr observation of pavement slab action, joint spacing studies, continuously reinforced pavement evaluation, progress of joints constructed without load-transfer dowels, initial roughness surveys of new pavement projects (to be supplemented with 5-year measurements), as well as other miscellaneous applications.

Throughout all of this work, the system has performed admirably. The only malfunctions of any consequence to date have been in the system's magnetic tape recorder. These malfunctions, which were minor, have been isolated and corrected. The reliability and durability of the system have been demonstrated to be excellent—exceeding expectations.

Despite its complexity and the need for skilled operating personnel, the GMR Profilometer should ultimately prove to be of great value to highway engineers. In particular, it promises to be of great assistance to researchers studying over-the-road vehicle dynamics, and interactions of road and vehicle. It is being used for such purposes in a current research project in Michigan.

It is a device of great potential.

# Problems Encountered in Using Elevation Power Spectra as Criteria of Pavement Condition

B. E. QUINN, Professor of Mechanical Engineering, and
K. HAGEN, Graduate Student, Purdue University, Lafayette, Indiana

A power spectrum, calculated from highway elevation measurements, was used as a criterion for pavement condition. The criterion was influenced by the location, accuracy and spacing of the elevation measurements, and by the method used to determine pavement roughness from the variation in measurements. The influence of these factors on the resulting power spectrum was investigated, and the pavement condition criterion obtained from some of these spectra was compared with the corresponding BPR roughometer rating for certain highways.

The need is shown for a standardized procedure for obtaining elevation measurements and for making power spectrum calculations, if comparable criteria of pavement condition are to be obtained.

• UNDER NCHRP Project 1-2 a comparison was made of different devices for measuring pavement roughness (1). These included the BPR roughometer, the AASHO slope measuring equipment and other devices. In addition, it was possible to obtain elevation measurements for some of the pavement sections used in this investigation. By using these measurements it was possible to calculate elevation power spectra for some of the test sections.

This paper discusses the problems that are associated with the calculation of elevation power spectra, and indicates the need for a standardized procedure in making such calculations, if the results of different investigators are to serve as valid criteria of pavement condition. Many arbitrary decisions have to be made when elevation measurements are collected and when power spectra are calculated from these measurements. Consequently, there can be a wide difference in results obtained by different investigators using the same set of elevation measurements for a selected pavement. It is the purpose of this paper to indicate how this situation can occur.

## WHY CALCULATE AN ELEVATION POWER SPECTRUM?

Elevation measurements made with sufficient accuracy will reveal the roughness of a selected pavement section. If a power spectrum calculation is then performed using these measurements, a curve will be obtained similar to one of those shown in Figure 1. This curve will indicate pavement roughness and the extent to which various wavelengths in the pavement contribute to the roughness.

Roughness is indicated by the area under the curve. If the elevations are measured in feet, the area will have the units of feet squared. This is because the area represents the mean square value of the variation in the pavement profile.

The units associated with the horizontal and vertical axis of an elevation power spectrum curve require a brief explanation. Instead of plotting the values of wavelength in feet per cycle along the horizontal axis as might be expected, it is mathematically

Paper sponsored by Committee on Pavement Condition Evaluation.

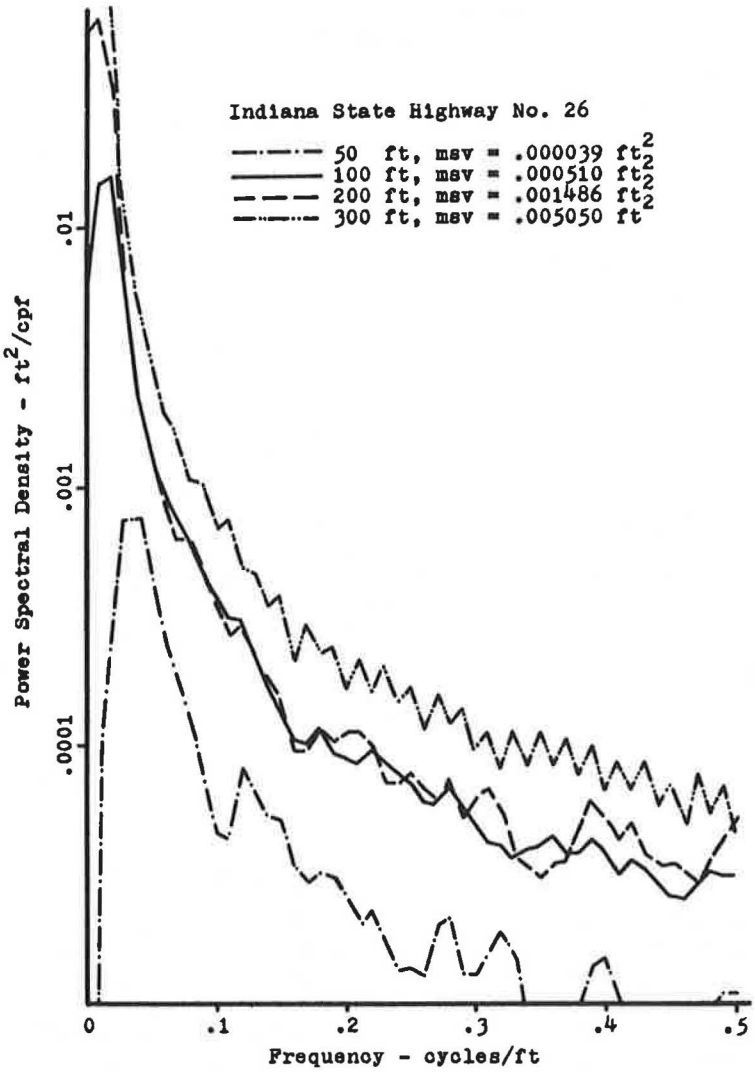


Figure 1. Illustration of elevation power spectra with different lengths of Secosq.

more convenient to plot the reciprocal of this quantity, which is a distance-based frequency having the units of cycles per foot. Long wavelengths are associated with low frequencies and are found close to the origin indicated on the curves. Short wavelengths are associated with high frequencies and are found further to the right. The units of the vertical axis are feet squared per cycle per foot. If any two arbitrary frequencies (or wavelengths) are selected, the area under the power spectrum bounded by these frequencies will represent the contribution to the total mean square roughness made by this range of frequencies. The power spectrum thus describes the condition of the pavement, and the pavement roughness indicated by the power spectrum should correlate highly with other indications of pavement roughness.

An elevation power spectrum has another property that makes it valuable to investigators. It is theoretically possible to use the power spectrum with appropriate vehicle characteristics to predict the performance of the vehicle on the highway. Therefore, it has been possible to predict the vertical acceleration of a vehicle moving over a selected highway as well as to predict the dynamic tire forces (2) generated between

the vehicle and the highway. Other investigators have described aircraft runway conditions in terms of elevation power spectra (3) and have predicted the behavior of aircraft (4) on these runways. The use of an elevation power spectrum as an input for predicting vehicle behavior makes it a very attractive highway characteristic.

If a highway elevation power spectrum is available, it would be possible to establish speed limits based on the maximum desired acceleration in the vehicle or on the maximum permitted forces between the wheels of the vehicle and the highway. Potentially, the elevation power spectrum is extremely useful.

## PROBLEMS IN CALCULATING AN ELEVATION POWER SPECTRUM

Although pavement roughness will be indicated by a variation in the elevation measurements, not all of the variation in the elevation measurements will be due to roughness. Elevation measurements made on a perfectly smooth highway having an inclined grade line will vary, but none of this variation can be attributed to pavement roughness. One of the most important fundamental problems encountered in calculating a highway elevation power spectrum from elevation measurements is that of determining the amount of variation in the elevation measurements that is due only to roughness in the pavement profile.

If the elevation power spectrum is a criterion of pavement condition, it must correlate highly with other criteria used for this purpose. Whatever procedure is used for calculating the elevation power spectrum should thus yield a result that will be closely related with any other valid measurement of pavement condition.

Another problem of considerable importance is that of determining the accuracy with which suitable elevation measurements must be made. In addition, the spacing of the elevation measurements along the highway will also influence the final results. Valid decisions must be made relative to the collection of the elevation measurements.

Because it is not possible to survey a highway for its entire length, it is necessary to select a representative section from which conclusions can be drawn concerning an appreciable length of the pavement. Another problem involves the statistical significance of the section of pavement that is measured relative to a much longer length of the same highway.

## DETERMINING PAVEMENT ROUGHNESS FROM ELEVATION MEASUREMENTS

Figure 2 indicates the original grade line of a highway and the present highway profile. Assuming that the original highway was perfectly smooth, Figure 2 indicates that a change has occurred in the highway profile. The effect of this change has been to increase the roughness of the pavement. A measure of the present highway roughness is indicated by the values $X_i$ which represent the deviation of the present highway profile from the original grade line. Unfortunately these values cannot be measured directly since an elevation survey would yield only the elevation measurements indicated by $Y_i$. The fundamental problem encountered is that of computing the deviations $X_i$ from the elevation measurements $Y_i$. It is here that the element of judgment is involved, and different investigators have approached this problem using different techniques. Because of this, different investigators may obtain different values of $X_i$ from the same set of elevation measurements. As a consequence, different power spectra will result even though the same set of elevation measurements is used at the beginning of the calculation.

One approach is to estimate the grade line of the highway from the elevation measurements, and to assume that deviations from this line are due to pavement roughness (Fig. 1). A 3000-ft length was surveyed by taking elevation measurements at 1-ft intervals. It was apparent from this survey that the grade line was not a simple curve.

Consequently, the highway was divided into 300-ft subsections. For each subsection, a second-order curve was fitted through the elevation measurements using a least-squares curve fitting technique. The grade line of the entire highway section was thus approximated by ten second-order curves. To obtain the deviations indicated by $X_i$ (Fig. 1), the corresponding ordinate of the second-order curve was subtracted from each elevation measurement.

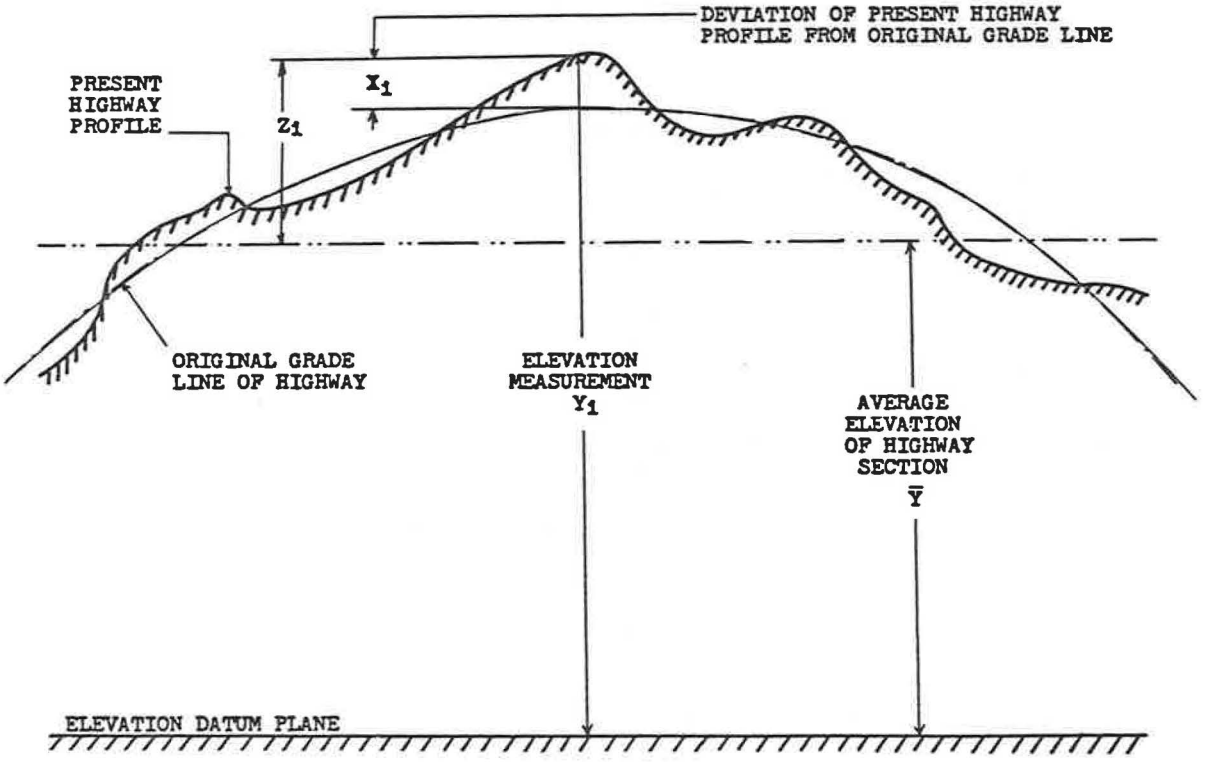


Figure 2. Relationship between elevation measurements and highway deviations.

A detailed procedure for calculating a power spectrum is given elsewhere (5) and will not be repeated here. When this procedure is used to calculate a power spectrum from the values of $X_i$ obtained using 300-ft highway subsections, the result is as shown in Figure 1. The area under the curve is indicated by the letters "msv" and is equal to 0.005050 ft squared. (In Figure 1 and subsequent figures, the term "Secosq" is an abbreviation for second-order curve fitted through elevation measurements using a least-squares curve fitting technique.)

If a larger number of smaller subsections is used, different values of $X_i$ will be obtained. The effect of using subsections varying from 50 ft to 300 ft in length is shown in Figure 1, together with the corresponding areas under the respective curves.

If the use of a second-order least squares curve is accepted for establishing the grade line of the highway from the existing elevation measurements, the problem of selecting a suitable subsection for establishing the grade lines still remains. Figure 1 shows that different subsection lengths will give different elevation power spectra. A highway that is 3,000 ft long will have a different elevation power spectrum if an analysis is based on 30 subsections of 100 ft each as compared to 10 subsections of 300 ft each. Using 50-ft subsections shows a marked difference when compared to 300-ft subsections.

Another technique for obtaining the deviations $X_i$ makes use of a running mean (6). Elevation measurements from $i-n$ to $i+n$ are averaged to obtain the mean value over the subsection established by n (usually 51 ft). This mean is subtracted from $Y_i$ to obtain $X_i$. The index i is increased by unity and the process is repeated, making use of a new elevation measurement and discarding one previously used.

Because this procedure for obtaining values of $X_i$ is considerably different from the procedure employing a second-order base line, different values of $X_i$ will be obtained for the same length of highway and a different power spectrum will be computed. For the same length of highway, Figure 3 shows the power spectrum using the two different methods for obtaining $X_i$. Different methods of processing the same elevation measurements yield different elevation power spectra for the same highway.

Because the area under an elevation power spectrum curve represents the mean square value of the roughness of a highway as measured by the deviations $X_i$, these areas for the same highway are compared using different lengths for both the running mean and the second-order base line. Figures 1 and 3 show that the greatest differences in the ordinates of these curves occur very close to the origin. This has prompted some investigators to suggest that the effect of the long wavelengths in the highway be omitted when a comparison of the areas under various elevation power spectrum curves is made (7). The magnitudes of the wavelengths thus eliminated in such a comparison are shown in Figure 3 by the distance from the origin indicated by the arrows as the first frequency band.

For the same highway, a series of elevation power spectra were calculated using different subsection lengths for both the running mean and the second-order base line to obtain sets of deviations. The areas under the corresponding power spectrum curves were then determined with and without the first frequency band (or the long wavelengths). The results of these calculations are shown in Figure 4. The second-order base line is indicated by Secosq and a running mean is indicated by "Rmean." If the total area under the respective curves is used, the symbol (0-M) is indicated, while the elimination of the first frequency band is indicated by (1-M). The four curves (Fig. 4) represent the corresponding areas under the respective elevation power spectrum curves using both the running mean and the second-order base line of different lengths, with and without the area contributed by the first frequency band.

If either procedure is used for determining deviations, different results will be obtained depending on the subsections of highway employed for the respective data processing procedures. Moreover, as would be expected, there is variation between the two procedures for the same subsection of highway. One notable exception occurs at a length of 50 ft, where essentially the same result is obtained whether a second-order least square base line is employed or whether a running mean is used.

These results indicate that different techniques for calculating the deviations $X_i$ will give different power spectra. Moreover, varying the subsection of the highway employed

when using either method will give a variation in the results. Figures 1, 3, and 4 thus show that a standardized procedure must be employed for computing the deviations if different investigators are to obtain the same results from the same set of elevation measurements.

## CORRELATION WITH OTHER CRITERIA OF PAVEMENT CONDITION

If the area under the elevation power spectrum curve represents the mean square roughness of the highway, it should correlate highly with other criteria of pavement

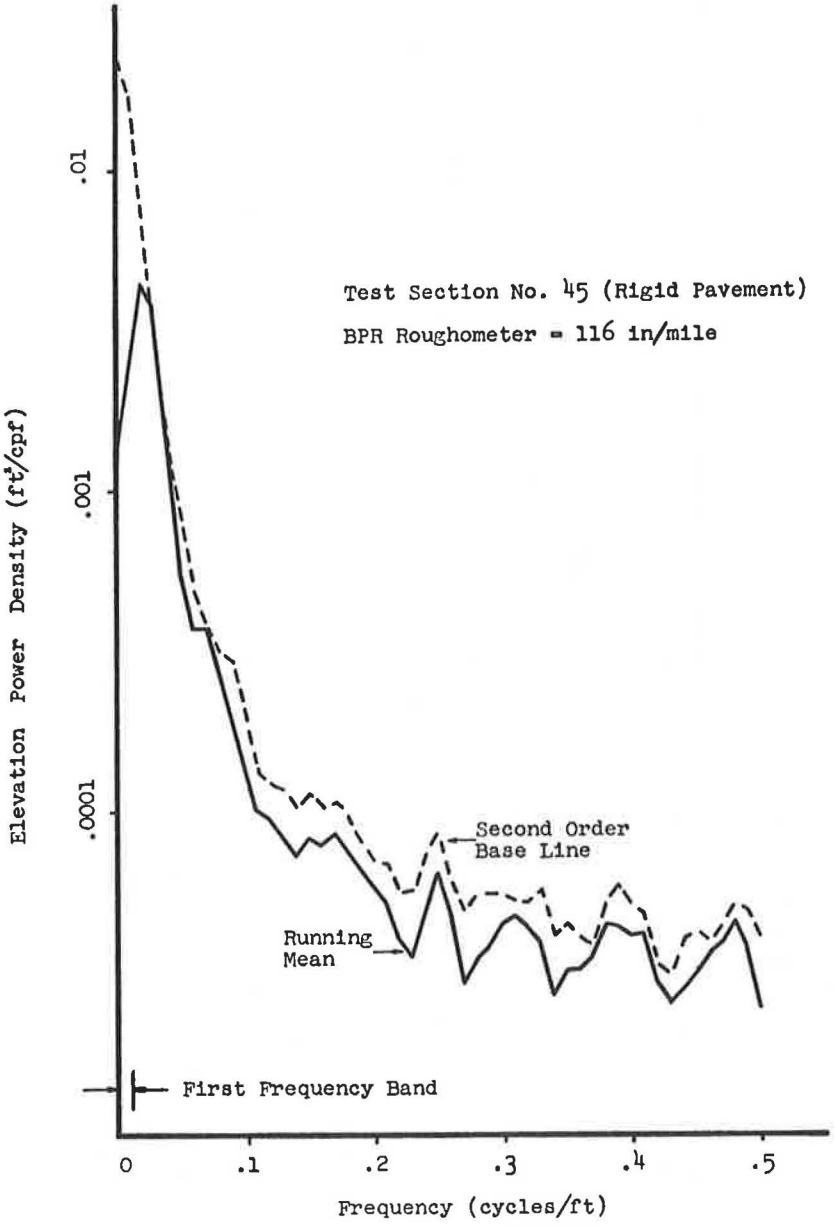


Figure 3. Highway elevation power spectra computed from elevation measurements.

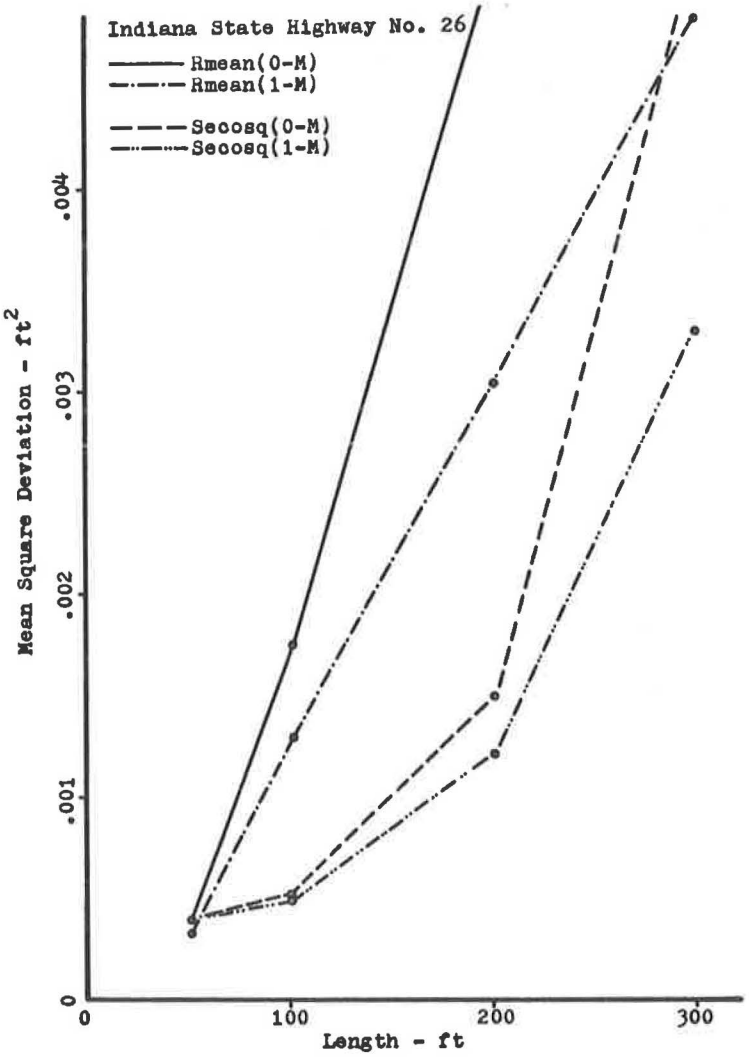


Figure 4. Comparison of mean square values.

condition. In other words, whatever procedure is used to obtain the deviations $X_i$ from elevation measurements should result in areas under the respective power spectrum curves that would be large for rough highways and small for smooth highways. Therefore, these areas are compared with the corresponding BPR roughometer readings for the highways in question.

In Figure 5, the roughometer ratings are indicated on the horizontal axis and the areas of the respective power spectrum curves are on the vertical axis. Five highway sections are included and for each section the elevation power spectrum was computed using both the running mean and the second-order least squares grade line to obtain the values of $X_i$. The corresponding areas were obtained under these curves with and without the contribution made by the first frequency band.

Figure 5 indicates that a reasonably good relationship exists between the area under the power spectrum curve and the corresponding roughometer rating when the running mean is employed. Unfortunately, this comparison is distorted because the results of using a 51-ft running mean are compared with those obtained using 300-ft subsections for the second-order grade line. The fact remains, however, that deviations computed

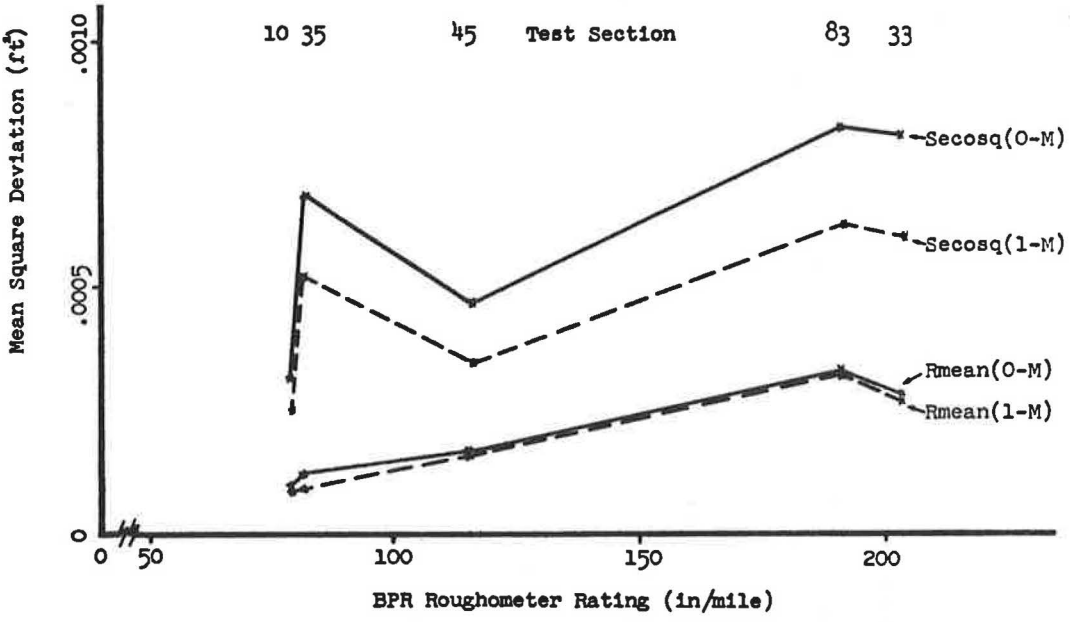


Figure 5. Mean square deviation vs BPR roughometer rating (rigid pavements).

using the shorter length of highway give better results. Including the effects of the first frequency band has relatively little effect.

As it was possible to measure the dynamic tire force of a passenger vehicle operated over the highway sections, the areas under the power spectrum curve were compared with the root mean square value of the dynamic tire force. It has been shown (8) that the dynamic tire force is related to the roughness of the pavement, and that under cer-

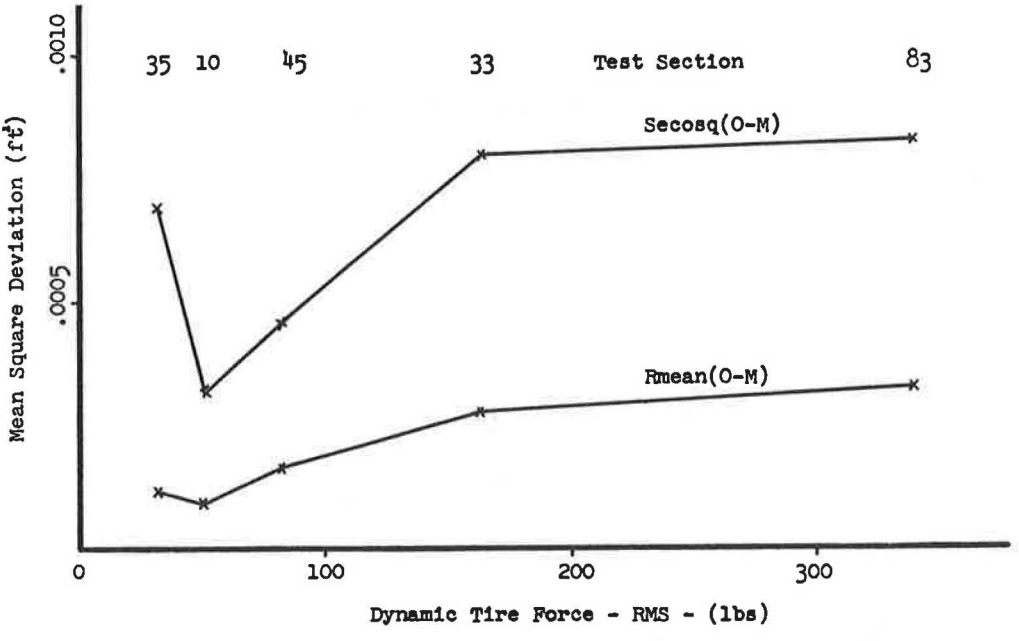


Figure 6. Mean square deviation vs dynamic tire force (rigid pavements).

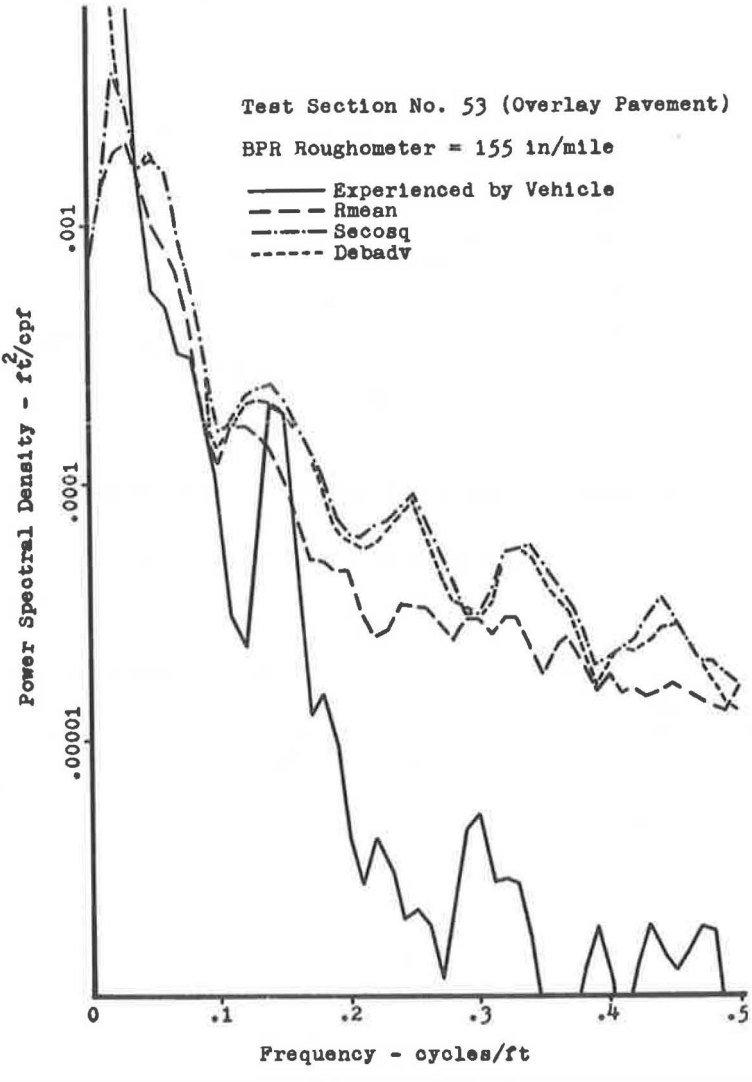


Figure 7. Comparison of elevation power spectra.

tain conditions the dynamic tire force and the roughometer ratings have a very high correlation.

Again using a 51-ft running mean gives a somewhat better relationship between the areas under the resulting power spectrum curves and the tire force measurements. Both curves in Figure 6 indicate that the area under the power spectrum curve is relatively insensitive to an increase in the dynamic tire forces at larger values of force. This is unsatisfactory, because generally a rough road will produce much higher forces than an average road.

If the appropriate vehicle characteristic is available, it is possible to take the dynamic tire forces and to work backward to determine the highway elevation power spectrum actually experienced by the vehicle. The technique (9) has been discussed previously and will not be repeated here. The result is to obtain a description of the highway as experienced by the vehicle. Therefore, this description is compared with the elevation power spectrum calculated from elevation measurements (Fig. 7). The

elevation power spectrum was calculated from a set of elevation measurements using three different procedures for determining the deviations, two of which have just been described. The elevation power spectrum experienced by the vehicle is also plotted as shown (Fig. 7). In making this calculation, it was necessary to apply the appropriate vehicle characteristic to the dynamic tire forces from which the experienced elevation power spectrum could be determined.

Figure 7 also indicates differences in the elevation power spectra computed from elevation measurements using the three different procedures. The big difference, however, is between these three curves and the elevation power spectrum experienced by the vehicle. All methods for computing the elevation power spectrum from elevation measurements consistently overestimate the contribution to the roughness made by shorter wavelengths in the highway.

Ideally, the elevation power spectrum computed from elevation measurements should be identical with the elevation power spectrum experienced by the vehicle. Figure 7 shows that this situation does not exist.

Actually the difference in the area in the high-frequency region between the three computed curves and the elevation power spectrum experienced by the vehicle is very small since a logarithmic plot is used for the ordinates. The difference is significant, however, if the elevation power spectrum, computed from elevation measurements, is used to predict the tire forces produced by the vehicle. This is because the vehicle is extremely sensitive to the shorter wavelengths (higher frequencies) and hence this difference is magnified when a power-spectrum curve determined from elevation measurements is used to predict vehicle performance.

## CONDUCTING HIGHWAY ELEVATION SURVEYS

When a highway-elevation survey is conducted, it is necessary to select the distance that will be used between adjacent elevation measurements. This distance influences the power spectrum calculations. The profile of the highway includes a wide range of wavelengths. To determine the effects of short wavelengths in the highway profile, it is necessary to have elevation measurements that are spaced relatively close together.

The effect of shorter wavelengths in the highway profile cannot be ignored by simply increasing the distance between adjacent values of elevation. If this is done, it will give rise to a condition known as "aliasing," in which the contribution to the roughness of the shorter wavelengths will be erroneously attributed to the longer wavelengths in the pavement profile (Fig. 8).

Figure 8 shows two power spectra. For both curves, the deviations $X_i$ were obtained by using a 51-ft running mean. The elevation power spectrum curve (solid line) indicates the results obtained when elevation measurements were made 1 ft apart. The other curve (broken line) is the power spectrum calculated from elevation measurements 2 ft apart on the same highway section.

The greater spacing of the elevation measurements did not make it possible to resolve the shorter wavelengths of the highway, and thus this curve does not extend as far along the horizontal axis as does the other. In many places the ordinates of the broken curve are larger than those of the solid curve, and the total area under the broken curve is considerably greater than that under the solid curve. By simply varying the distance between adjacent elevation measurements, a considerably different power spectrum is obtained for the same length of highway.

The accuracy with which the elevation measurements are made also influences the resulting power spectra (Fig. 9). Here "1 Significant Figure" indicates that the deviations were calculated to the closest tenth of a foot, while "2 Significant Figures" indicates that the deviations were calculated to the nearest hundredth of a foot. Figure 9 shows considerable difference between power spectra calculated from data accurate to a tenth of a foot and data accurate to a hundredth of a foot. The curve shows relatively little difference between data accurate to a hundredth of a foot and data accurate to a thousandth of a foot, but this is misleading. This slight difference is because it was not possible to obtain data that were accurate to within a thousandth of a foot due to the manner in which the elevation measurements were made. This curve indicates that an

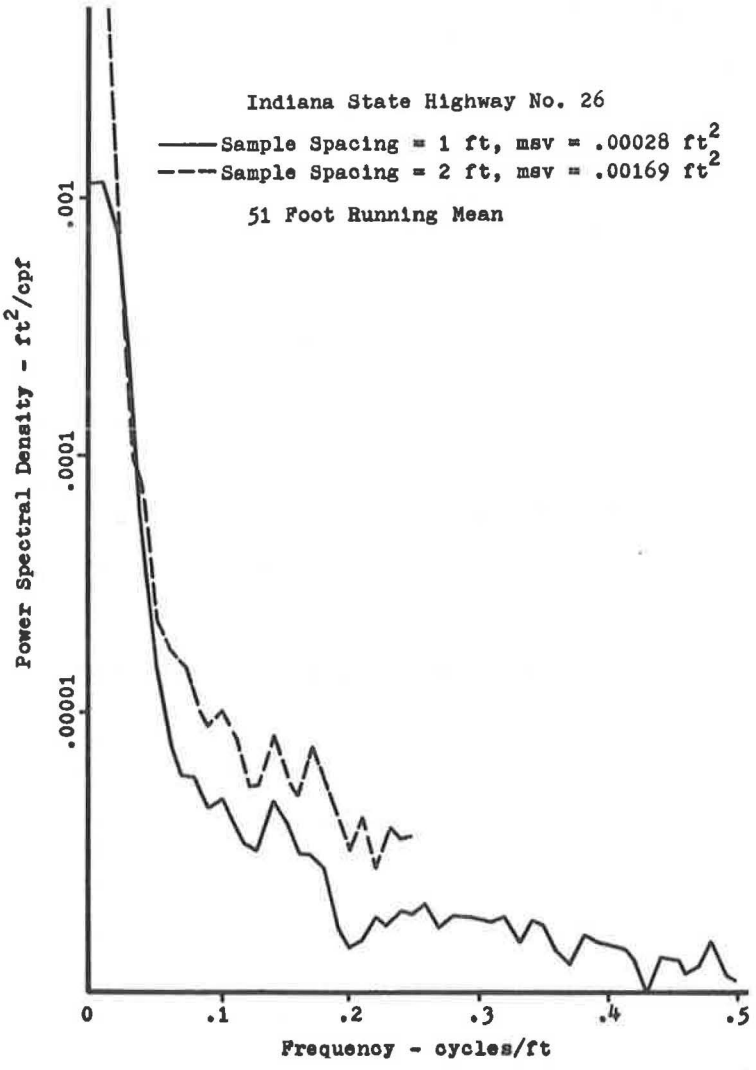


Figure 8. Illustration of aliasing.

appreciable difference in both the ordinates and the area of the power spectrum curves will occur for different degrees of accuracy employed in making elevation measurements.

When power spectrum calculations are made it is usually assumed that the data describe a stationary random process. In applying these calculations to highway elevation data this means that there should be no change in the statistical properties from one section of a highway to another. If this is so, the power spectrum calculated for the first half of a surveyed highway section should be identical with that calculated for the second half of the same section. In some cases this has been reasonably true, but this condition is not always satisfied.

For example, elevation measurements were taken at 1-ft intervals for a distance of 1,330 ft along a selected highway. Two elevation power spectra were calculated, one for the first half of the highway, the other for the second half (Fig. 10). There is considerable variation in the ordinates of these curves and a difference in area of approximately 3 to 1.

Figure 10 shows that a power spectrum calculated for the first half of a highway section will not always represent the second half. Inasmuch as it is impossible to

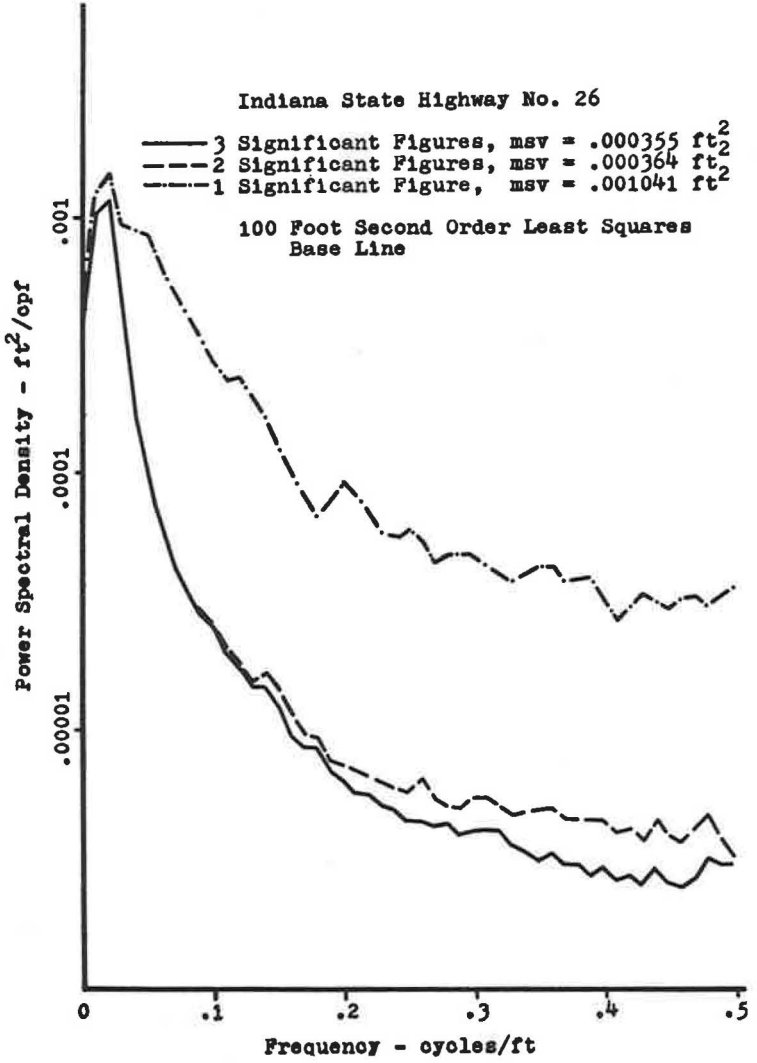


Figure 9. Illustration of elevation power spectra with different degrees of data accuracy.

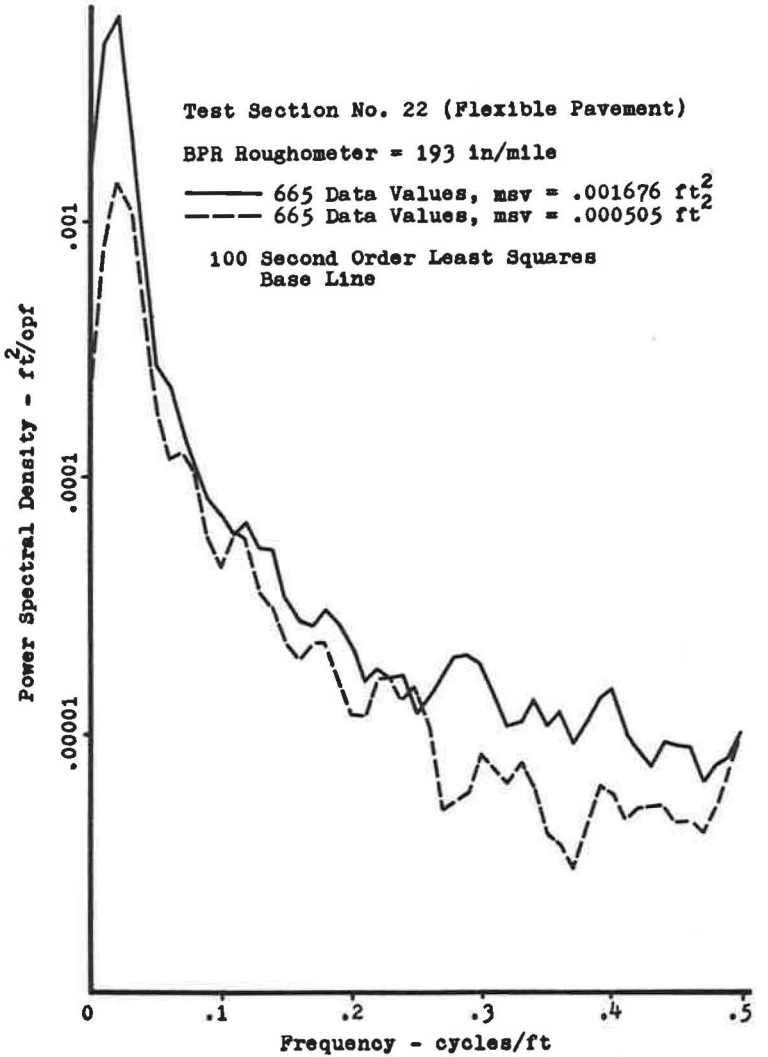


Figure 10. Illustration of non-stationary highway profile.

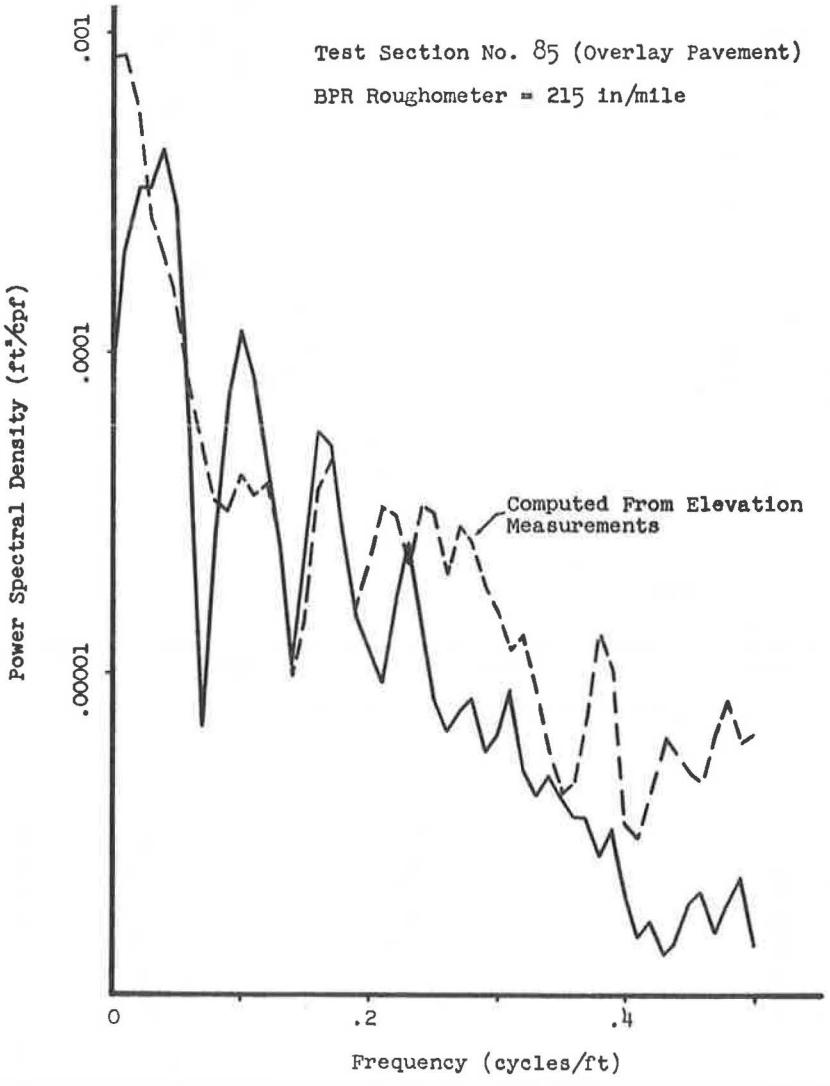


Figure 11. Power spectrum obtained from truck-mounted profilometer.

survey highways over their entire length, it is necessary to establish some type of averaging procedure which will yield statistically significant results for a long length of highway when a smaller length is taken as a representative sample.

## SIMILAR PROBLEMS WHEN SPECIAL INSTRUMENTS ARE USED

The problems of calculating elevation power spectra from elevation measurements obtained by rod and level surveys have been discussed. Similar problems are encountered, however, when special instruments are used to measure a highway profile. Although certain parameters are built into these instruments, this should not be allowed to obscure the still important problem of selecting appropriate values for these parameters.

A truck-mounted profilometer was operated over several test sections during this investigation. For one of these sections, the power spectrum was computed from elevation measurements using the techniques previously described. In addition, a power spectrum was calculated from the data obtained from the truck-mounted profilometer. Figure 11 compares these two power spectra.

A greater amount of periodicity is indicated in the power spectrum obtained from the profilometer than that calculated from elevation measurements. However, the data from the profilometer give a more accurate representation of the power in the shorter wavelengths when the power spectrum is compared with that experienced by the vehicle (on another highway) (see Fig. 7). It thus appears that in the high-frequency region, the data from the profilometer more accurately represent the highway profile as experienced by the vehicle than do the data from elevation measurements.

In addition to the truck-mounted profilometer, a special servo-seismic system using electronic means for measuring the highway profile was also operated over various

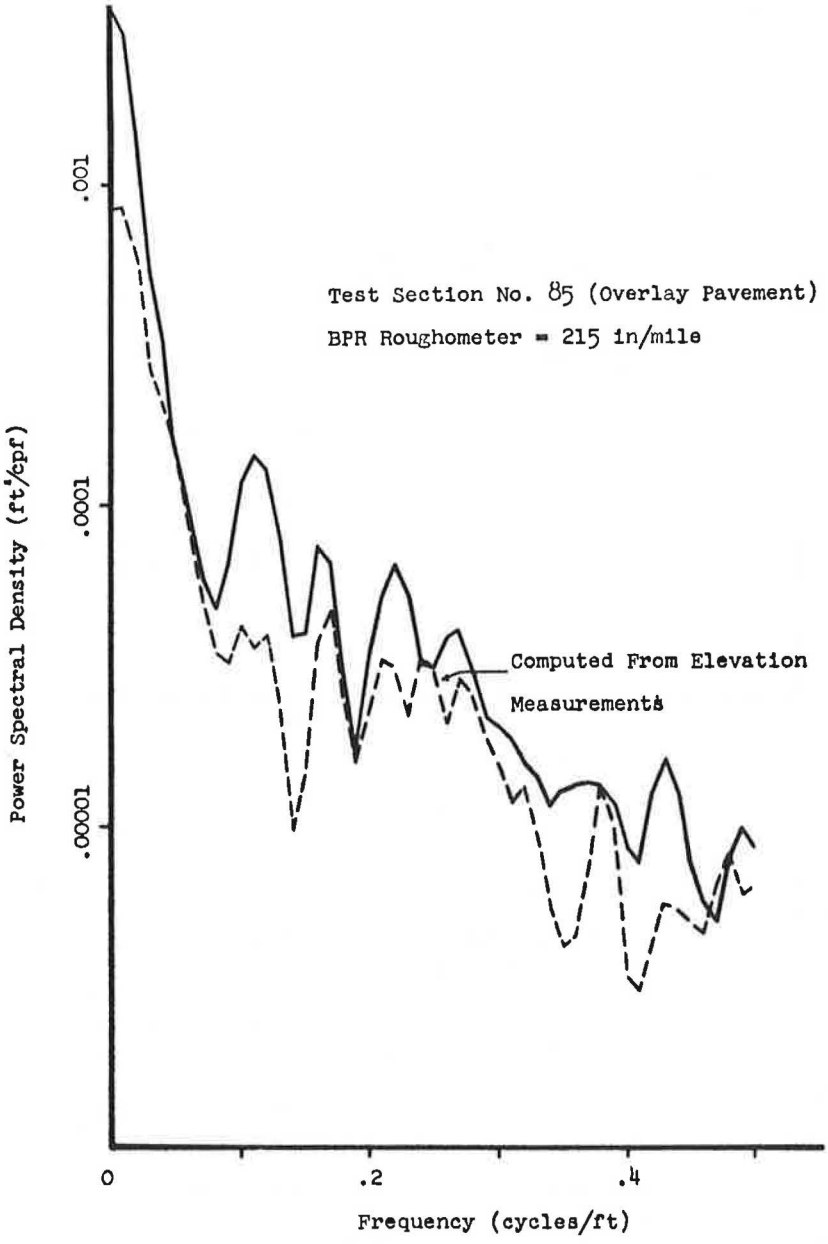


Figure 12. Power spectrum obtained from servo-seismic system (600-ft filter).

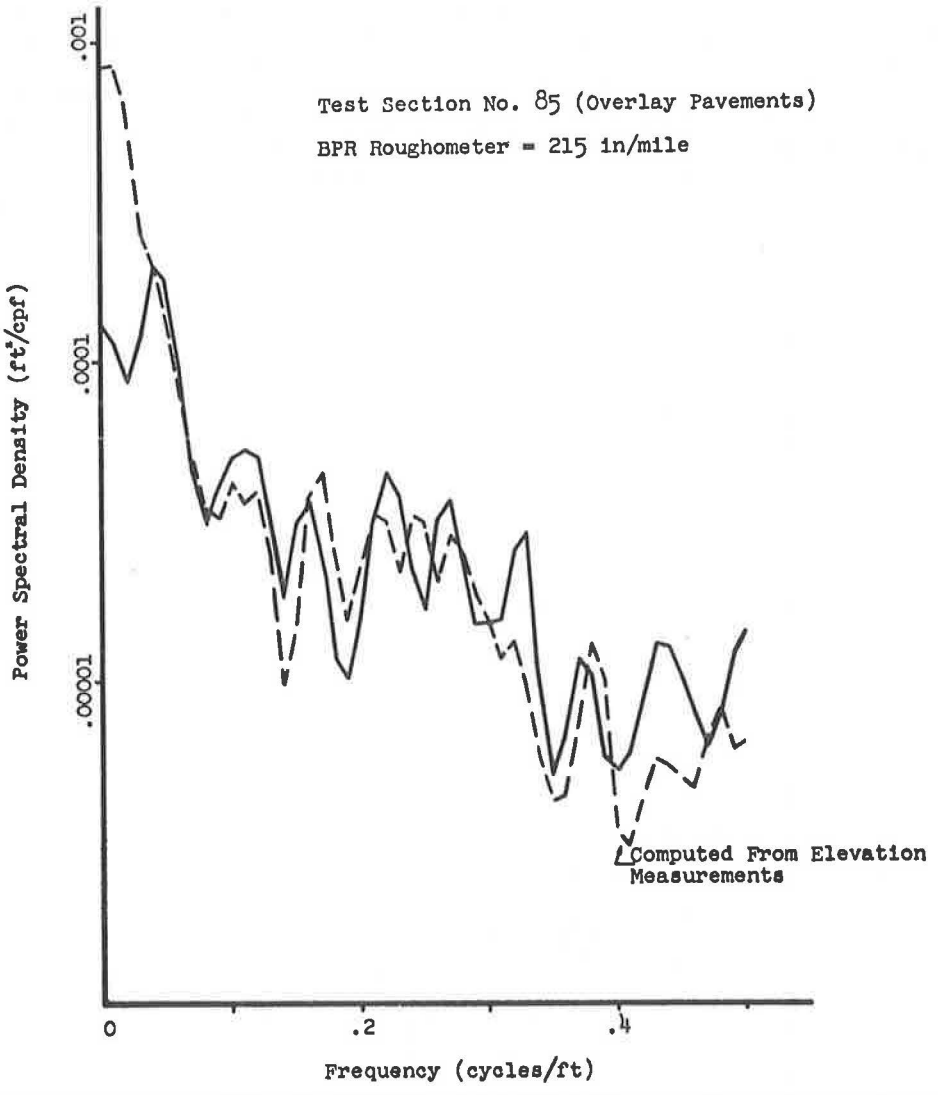


Figure 13. Power spectrum obtained from servo-seismic system (90-ft filter).

highway sections. It was possible to select the maximum wavelength that the system would include in the highway profile description.

Figure 12 compares the power spectrum calculated from elevation measurements with that calculated from data procured with the servo-seismic system with a 600-ft maximum wavelength. Because this wavelength was greater than that permitted in the calculation of the power spectrum from elevation measurements, there are correspondingly larger values for the ordinates of the power spectrum from the servo-seismic system in the long wavelength region.

The effect of varying the maximum permissible wavelength in the profile description is interesting. In Figure 13, the maximum wavelength was set at 90 ft; the corresponding power spectrum from this description is shown by the solid line. Here the ordinates in the long wavelength (low frequency) region are less than those computed from elevation measurements.

Figures 12 and 13 indicate the basic problem encountered whether elevation measurements or electronic devices are used to measure the highway profile. The results

depend on the arbitrary selection of the maximum wavelengths permitted in the description of the highway profile.

Describing a highway profile in terms of elevation measurements is an extremely time-consuming and costly process. It is encouraging to see a reasonably close approximation to the power spectrum obtained from elevation measurements, with the power spectrum obtained using either the truck-mounted profilometer or the servo-seismic system.

It appears as if an economical method for analyzing highway profiles must ultimately depend on some type of electronically instrumented procedure. In the design of such a system, however, many of the problems involved in calculating elevation power spectra from elevation measurements will still be encountered. A satisfactory design will require careful consideration of these problems.

## CONCLUSIONS

A power spectrum, calculated from elevation measurements, depends on the section of highway that is surveyed, the accuracy and spacing of the elevation measurements, and the method employed to determine the pavement roughness from these measurements.

A standardized procedure covering data collection and analysis must be used if the same criterion of pavement condition is to be obtained by different investigators studying the same pavement.

Those who are concerned with the spectral analysis of pavement profiles need to establish a suitable procedure that will give a valid criterion of pavement condition.

## ACKNOWLEDGMENTS

This investigation was conducted for the National Cooperative Highway Research Program (NCHRP Project 1-2) under the sponsorship of the American Association of State Highway Officials and with the full cooperation and support of the U. S. Bureau of Public Roads.

## REFERENCES

1. Yoder, E. J., and Milhous, R. T. Comparison of Different Methods of Measuring Pavement Condition: Interim Report. NCHRP Rept. 7, 1964.
2. Quinn, B. E., and Thompson, D. R. Effect of Pavement Condition on Dynamic Vehicle Reactions. HRB Bull. 328, pp. 24-32, 1962.
3. Houbolt, J. C. Runway Roughness Studies in the Aeronautical Field. Jour. Air Transport Div., ASCE Proc., Vol. 86, No. AT 1, March 1961.
4. Gunzler, G., and Case, E. R. A Statistical Approach to the Design of Aircraft Undercarriage Systems. Amer. Inst. Aeronautics and Astronautics, AIAA Paper No. 65-710, Oct. 1965.
5. Blackman, R. B., and Tukey, J. W. The Measurement of Power Spectra. Dover, 1958.
6. Walls, J. H., Houbolt, J. C., and Press, H. Some Measurements and Power Spectra of Runway Roughness. NACA TN 3305, 1954.
7. Thompson, W. E. Measurements and Power Spectra of Runway Roughness at Airports in Countries of the North Atlantic Treaty Organization. NACA TN 4303.
8. Quinn, B. E., and Wilson, C. C. Can Dynamic Tire Forces Be Used as a Criterion of Pavement Condition? Highway Research Record 46, pp. 88-100, 1964.
9. Quinn, B. E., and Zable, J. L. Evaluating Highway Elevation Power Spectra From Vehicle Performance. Highway Research Record 121, pp. 15-26, 1966.